SCUOLA DI DOTTORATO IN INGEGNERIA CIVILE E ARCHITETTURA
DOTTORATO IN INGEGNERIA STRUTTURALE E GEOTECNICA

Seismic vulnerability assessment of New Zealand unreinforced masonry churches

Alessandra Marotta

XXVIII Ciclo – A.A. 2015/2016

DIPARTIMENTO DI INGEGNERIA
STRUTTURALE E GEOTECNICA

SAPIENZA
UNIVERSITÀ DI ROMA

Abstract

Churches are an important part of the New Zealand historical and architectural heritage, and the extensive damage occurred to stone and clay-brick unreinforced masonry portfolio after the 2010-2011 Canterbury earthquakes emphasises the necessity to better understand this structural type. An effort was undertaken to identify the national stock of unreinforced masonry churches and to interpret the damage observed in the area affected by the earthquakes: of 309 religious buildings recognized and surveyed nationwide, a sample of 80 churches belonging to the Canterbury region is studied and their performance analysed statistically. Structural behaviour is described in terms of mechanisms affecting the so-called macro-elements, and discrete local damage levels are correlated firstly with macroseismic intensity through Damage Probability Matrices, computed for the whole building and for each mechanism. The results show that the severity of shaking alone is not capable to fully explain the damage, strongly influenced by structural details that can worsen the seismic performance or improve it through earthquake-resistant elements. Simple-linear regressions, correlating the mean damage of each mechanism with the macroseismic intensity, but neglecting the difference in the vulnerability of different churches subjected to the same level of shaking, are then improved through use of multiple-linear regressions accounting for vulnerability modifiers. Several statistical procedures are considered in order to select the best regression equation and to assess which parameters have closer relationships with damage. Results show good consistency between observed and expected damage, and the proposed regression models can be used as predictive tools to help determine appropriate seismic retrofit measure to be taken. The conclusions drawn for the Canterbury region are then extended to the whole national stock and a quantitative seismic risk assessment for existing unreinforced masonry churches in New Zealand is presented, using different intensity measures to model the seismic hazard. Seismic risk

is first computed mechanism by mechanism, highlighting how some mechanisms are more frequent than others, and that very large damage levels are expected for some New Zealand regions. Whereupon, an alternative synthetic damage index purely based on observed data is proposed to summarise damage related to several mechanisms and it is used to validate the choice of the best index for describing the global damage of a church when dealing with a territorial assessment. Territorial scale assessment of the seismic vulnerability of churches can assist emergency management efforts and facilitate the identification of priorities for more in-depth analysis of individual buildings. Finally, a preliminary attempt for dynamically characterize the response of unreinforced masonry church is conducted.

Acknowledgements

I wish to express my deepest gratitude to my supervisors, Dr. Luigi Sorrentino and Prof. Domenico Liberatore, for their wise guidance, constant support and inspiring suggestions during the whole research period.

I would like to greatly thank Prof. Jason Ingham, for coordinating the stimulating period at University of Auckland and for his crucial reviews, from which the present research has been significantly benefited. Prof. Sherif Beskhyroun is acknowledged for the assistance in performing the ambient vibration tests.

Special and affectionate thanks are owed to Prof. Luis D. Decanini, for conveying to me the passion for the discipline and for his precious and constant encouragement during my studies.

All the colleagues and members of the Department of Structural and Geotechnical Engineering in Rome are gratefully acknowledged for all the stimulating talks over the years, and, above all, for their sincere friendship.

A special thanks to my parents, Lucrezia e Matteo, and to my brother, Gianluca, for their invaluable support.

Finally, I have to deeply thank Stefano, without whom nothing would have been possible.

Table of Contents

List of figures

List of tables

Chapter 1

Introduction

The major physical consequences of an earthquake for human beings are, obviously, human casualties and damage caused to the built and natural environments. Both financially and technically, it is possible to reduce these consequences in view of future strong earthquakes, by minimizing the seismic risk of a territory. In order to predispose effective tools for planning and retrofitting, it is of paramount importance to evaluate the earthquake vulnerability of the built and natural environments, and this is pursuable by developing models calibrated on the damage observed in past earthquakes.

Among the building portfolio of a country, various earthquakes around the world have emphasized the high vulnerability of the monumental buildings, often the most heavily stricken by a seismic event. The uniqueness of each piece that is part of the cultural heritage, togheter with its historical, artistical, and societal values, does not allow applying the standardized procedures established for ordinary buildings. Within the invaluable buindings part of the cultural heritage of a nation, churches are of foundamental importance not only for historical and architectural reasons, but also for the symbolic significance they assume for the communities they belong to. For this reason, the analysis of their vulnerability has attracted strong interest after several major events throughout the world, when their worse performance compared to both ordinary and monumental buildings has highlighted their intrinsic structural vulnerability (Figure 1.1 and Figure 1.2). As the seismic vulnerability of a building is defined as its propensity to suffer certain damage when subjected to an earthquake, the aim of a seismic vulnerability assessment is to provide a measure of the tendency of a building to be damaged if hit by an earthquake, and operatively it consists in correlating the seismic hazard to the physical damage suffered.

Ribeirinha church, Faial Island, Azores (1998)
(photo from Guerreiro et al. 2000)

Santi Marciano e Nicandro, L'Aquila, Italy
(2006)

Basílica del Salvador, Santiago, Chile (2010)
(photo from Sorrentino et al. 2011)

San Lorenzo a Flaviano, Amatrice, Italy (2016)

Figure 1.1. Examples of damage caused to churches by recent earthquakes.

a)

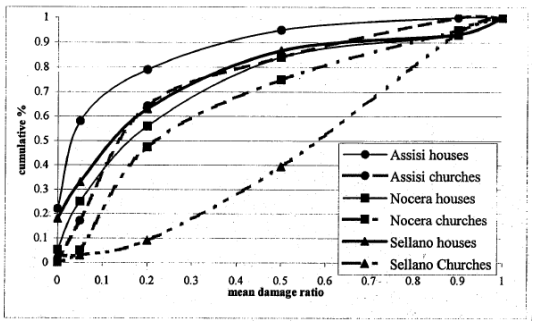

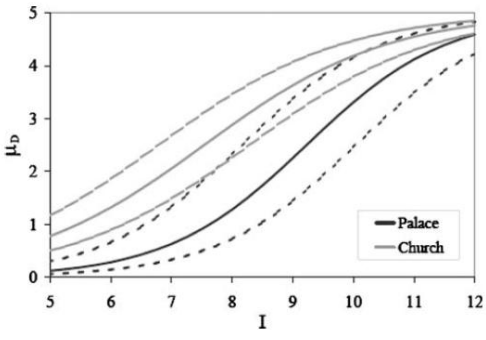

b)

Figure 1.2. a) Cumulative damage ratio distribution for houses and churches (D'Ayala, 1999); b) Vulnerability curves of palaces and churches (Lagomarsino, 2006). Data of both graphs are referred to the 1997 Umbria-Marche earthquake.

Urban and territorial scale vulnerability assessment methods have been developed from the early 1970's to the present time considering different approaches for the collection

and interpretation of data. These vulnerability assessment methods are classified as either empirical or analytical/mechanical. Empirical methods are based on selected parameters collected from in situ observation or expert judgement and are suited to identify the seismic vulnerability of a building stock. Analytical/mechanical methods are based on computational analysis defining a direct relationship amongst construction characteristics, structural response to seismic action, and damage effects. Obviously, the aforementioned approaches differ in computational burden and in the applicability at geographical scale: while the empirical methods are based on the collection of a small number of significant parameters and they are representative of the vulnerability of homogeneous typologies of buildings, the analytical methods require more specific information and are valid for a limited number of buildings. Both approaches are herein accounted in different proportion. Given the good amount of available information about the damage occurred to New Zealand churches during the 2010-2011 earthquake sequence and the extensive homogeneity of the buildings portfolio, an empirical approach is at first assumed for the analysis of New Zealand churches. According to such approach, observed vulnerabilities are based on statistical observations of recorded damage data as a function of the felt intensity, and the so-pursued seismic vulnerability assessment is spreadable at territorial scale. Large part of the vulnerability assessment of New Zealand unreinforced masonry churches herein conducted is based on such approach.

On the other hand, analytical methods tend to feature more detailed vulnerability assessment algorithms with direct physical meaning and they need experimental validation of the parameters used to define the vulnerability. As for historical churches, mechanical models have been widely adopted accounting for collapse mechanism analyses (refer, e.g., to Giovinazzi et al., 2006; Lagomarsino, 2006; Sorrentino et al., 2014a), based on acquired geometrical data. Less addressed, for the time being, is the issue related to the filter effect that the macro-elements of the building develop on the response of soaring elements. For this reason, a dynamic test campaign has been conducted on a number of representative New Zealand churches, whose results can provide information on modal parameters, and thus contribute to such estimation. A preliminary attempt in such direction is presented in the last part of this research.

1.1. Thesis format and chapter content

This manuscript is a "thesis by publications" wherein each chapter (plus seven Appendices) represents an article or combination of articles that have, at the time of thesis submission, been published, accepted, or submitted to a publisher for external peer review. Due to the "thesis by publications" format and the common motivations for the studies reported in the individual chapters, there is some unavoidable repetition of information throughout the manuscript. The following sub-sections include brief summaries of the studies pertaining to each chapter and references to the included publications. The referenced publications are typically journal or conference articles added to the thesis manuscript with slight changes to writing style and to in-text references made to other sections, figures, tables, or appendices within the thesis.

1.1.1. Chapter 2. An inventory of unreinforced masonry churches in New Zealand

An accurate documentation was undertaken in order to identify the New Zealand stock of unreinforced masonry churches, as a first step in understanding the relevance of the damage observed in the area affected by the Canterbury earthquakes and aimed to the subsequent implementation of effective conservation strategies. A country-wide inventory is then compiled based on bibliographic and archival investigation, and on a 10 000 km field trip, with estimated 297 unreinforced masonry churches currently present throughout New Zealand, excluding 12 churches already demolished in Christchurch because of heavy damage sustained during 2010-2011. The compiled database includes general information about the buildings, their architectural features and structural characteristics. Moreover, statistics about the occurrence of each feature are provided and preliminary interpretations of their role on seismic vulnerability are discussed.

Included publication:

Marotta, A., Goded, T., Giovinazzi, S., Lagomarsino, S., Liberatore, D., Sorrentino, L. and Ingham, J.M. (2015) An inventory of unreinforced masonry churches in New Zealand, *Bulletin of the New Zealand Society for Earthquake Engineering* 48(3), 170-189.

1.1.2. Chapter 3. Vulnerability assessment of unreinforced masonry churches following the 2010-2011 Canterbury earthquake sequence

Of 309 unreinforced masonry churches identified nationwide, including the 12 demolished in Christchurch, a sample of 80 buildings belonging to the affected region is studied and their performance analysed statistically. Structural behaviour of religious buildings is described in terms of mechanisms affecting the so-called macro-elements, being portions of the building behaving more or less independently. Discrete local damage levels are correlated with macroseismic shaking intensity through Damage Probability Matrices. Multiple-linear regressions are also considered, accounting for additional modifiers increasing/reducing the vulnerability of the macro-elements. Results show the relevance of the proposed multiple-linear regression models for the national heritage of churches and the advisability of extending mechanism-based regressions to other countries besides New Zealand.

Included publication:

Marotta, A., Sorrentino, L., Liberatore, D., and Ingham, J.M., 2016. Vulnerability assessment of unreinforced masonry churches following the 2010-2011 Canterbury earthquake sequence, *Journal of Earthquake Engineering*. DOI:10.1080/13632469.2016.1206761.

Marotta, A., Sorrentino, L., Liberatore, D., and Ingham, J.M., 2016. Statistical seismic vulnerability of New Zealand unreinforced masonry churches, in *Proceedings of the 10th International Conference on Structural Analysis of Historical Constructions*, 13-15 September, 2016, Leuven, Belgium, 1536 - 1543.

1.1.3. Chapter 4. Territorial seismic risk assessment of New Zealand unreinforced masonry churches

A quantitative seismic risk assessment for the existing unreinforced masonry churches in New Zealand is presented. Regression models correlating mean damage levels against ground-motion parameters are re-calibrated for all observed collapse mechanisms, accounting for different intensity measures. Due to the homogeneity of

New Zealand churches, the so-developed vulnerability models are extended to the whole national inventory. In order to summarise damage related to several mechanisms, different global damage indexes are accounted and an alternative synthetic damage index is proposed. The synthetic damage index has the advantage of not requiring a conventional estimation of the weights used in previous definitions of a global damage index and is entirely based on observed data. The computed damage indexes are then weighted on the foot-print area of each building and compared, and a risk level for unreinforced masonry churches is ascribed to the different New Zealand regions. Results can be used for the emergency management at regional scale in case of earthquake or for the identification of churches in need for more in-depth analysis in a preventive management of emergency.

Included publication:

Marotta, A., Sorrentino, L., Liberatore, D., and Ingham, J.M., 2017. Seismic risk assessment of New Zealand unreinforced masonry churches using statistical procedures, *International Journal of Architectural Heritage.* Accepted.

1.1.4. Chapter 5. Ambient vibration tests on New Zealand unreinforced masonry churches

Ambient vibration tests are carried out on a number of representative churches located in Auckland. Preliminary results from the dynamic tests are the base for future identification of the dynamic performance and construction weakness of different structural components, thus guiding the recognition of possible collapse mechanisms and estimating the filter effect that the building can develop on the response of soaring elements (e.g., gables, pinnacles).

Included publication:

Marotta, A., Beskhyroun, S., Sorrentino, L., Liberatore, D., and Ingham, J.M., 2017. Ambient vibration tests on New Zealand unreinforced masonry churches, *Proceedings of the 10th International Conference on Structural Dynamics - Eurodyn 2017,* 10-13 September, 2017, Rome, Italy. Abstract accepted.

Chapter 2

An inventory of unreinforced masonry churches in New Zealand

After a bibliographic and archival investigation, and a 10 000 km field trip, it is estimated that currently 297 unreinforced masonry churches are present throughout New Zealand, excluding 12 churches demolished in Christchurch because of heavy damage sustained during the Canterbury earthquake sequence. The compiled database includes general information about the buildings, their architectural features and structural characteristics, and any architectural and structural transformations that have occurred in the past. Statistics about the occurrence of each feature are provided and preliminary interpretations of their role on seismic vulnerability are discussed. The list of identified churches is reported in Appendix A, supporting their identification and providing their address.

2.1. Introduction

Unreinforced masonry (URM) is one of the construction materials that was most frequently used in New Zealand's early built heritage and URM churches represent a significant proportion of the heritage building stock of New Zealand. Churches, aside from having relevant historical and architectural value, often assume a symbolic significance for the communities that they belong to. The 2010-2011 Canterbury earthquakes had a dramatic impact on the community: 185 people died and many thousands were injured (Johnston et al., 2014), but also the extensive damage and collapse of churches deeply marked their communities, who placed a high value on

these heritage religious buildings, seen as an important part of the region's character and history (CEHBF, 2013). Therefore, the importance of preserving such buildings is a fundamental societal issue.

It is also widely known that URM churches frequently perform poorly even in moderate earthquakes, because of their intrinsic structural vulnerability (D'Ayala, 2000). URM churches are particularly vulnerable to earthquakes because of their open plan, large wall height-to-thickness and length-to-thickness ratios, and the use of thrusting horizontal structural elements for vaults and roofs. Their use of low strength materials often causes decay and damage due to poor maintenance, and the connections between the various structural components are often insufficient to resist loads generated during earthquakes (Ingham et al., 2012; Lagomarsino, 2012; Sorrentino et al., 2014). Additionally, damage is related to architectural types and construction details, which may vary from country to country. The 2010-2011 Canterbury earthquakes caused widespread damage to stone and clay-brick URM churches (Figure 2.1) (Leite et al., 2013). Hence, a research project was undertaken to identify the New Zealand stock of URM churches and to interpret the damage observed in the area affected by the Canterbury earthquakes (Cattari et al., 2015). An accurate documentation of architectural heritage is the first step in understanding the relevance of the damage observed and in the implementation of effective conservation strategies. Consequently, a national inventory of URM churches is presented, accounting for the geometry, construction details, building and transformation history, and the preservation state.

In the following section the inventory collection procedure is presented, and in the third section an outline of the history of URM churches in New Zealand is provided based on bibliographic and field research undertaken as part of this study. An overview of the characteristics of churches, with reference to geographical distribution, types, architectural features, and structural characteristics is given in the fourth section. Possible applications of the results of this research are given in the final notes. Almost three hundred URM churches are listed in Appendix A for each region of New Zealand.

2.2. Inventory collection procedure

For the purpose of understanding the scale and nature of the seismic risk of existing URM churches in New Zealand it is useful to investigate their number and national distribution. In the absence of a complete list of churches present across the country,

several reference sources were utilised, leading to the identification of 297 URM churches currently existing in New Zealand (Figure 2.2). This total does not account for 12 churches demolished in Christchurch because of heavy damage suffered during the Canterbury earthquake sequence.

The first identification source considered was the Heritage New Zealand List (HNZ, 2014), formerly referred to as the Register. Approximately half of the identified churches are recorded therein (Figure 2.3). Some of the non-registered buildings were identified through the online inventories of the different religious denominations in New Zealand, archive documentation, architectural books (Warren, 1957; Fearnley, 1977; Anonymous, 1979a and 1979b; Wells and Ward, 1987; Kidd, 1991; Knight, 1993; Donovan, 2002; Wells, 2003) and reports. Such research led to acquiring knowledge of churches constructed of all types of structural materials. Hence, a subsequent filtering was performed by preliminary observation using Google Street View. Finally, additional churches were identified during the field survey along the 10 000 km itinerary that was planned based on the previously identified sites. This field survey aimed to acquire technical information for all URM churches, and to appropriately identify numerous non-registered buildings considered to be potentially significant examples of early New Zealand architecture. Despite the care and effort put into the definition of this inventory, the existence of other churches along routes not explored during the field trip cannot be excluded.

The inventory database is subdivided into geographical regions and the information is gathered into three groups: (i) general data; (ii) architectural features; and (iii) structural characteristics. Table 2.1 shows the parameters considered for each main data group.

(a) St Peter's Church (1875), Christchurch (b) St Joseph’s Church (1921), Christchurch

Figure 2.1. Examples of damage caused by the 2010-2011 Canterbury earthquakes.

2.3. History of unreinforced masonry churches in New Zealand

As soon as settlers became established in New Zealand they started to build churches because of their strong Christian faith (Wells, 2003). The first churches were built mainly with timber, because of the ease of construction in terms of time and material availability (Tonks and Chapman, 2009). The architecture was in accordance with Early English style, familiar to both clergy and architects (Walden, 1961). Auckland and Wellington saw early examples of brick churches (respectively, St Paul's in 1841 and Wesley Chapel in 1844, the latter destroyed by the 1848 Marlborough earthquake (M_w 7.5)), both plastered to give an appearance of stone (Dowsett, 1985).

However, stone and clay-brick masonry buildings started being used largely from around 1880, when clay became readily available and prosperity increased. The 1931 Hawke's Bay earthquake (M_w 7.8) demonstrated the poor performance of URM and marked the beginning of the decline in use of URM (Dowrick, 1998; Reitherman, 2006). After the destruction caused by the Hawke's Bay earthquake, the New Zealand Standards Institute was formed to regulate building practice, and URM constructions were prohibited in 1965 (NZSI, 1965; Dowrick, 1998; Goodwin, 2009). After this ban, the use of reinforced concrete became predominant. However, the bibliographic and field research undertaken as part of this study has shown that reinforced-concrete construction was applied starting as early as the first quarter of the 20th century, either alone or together with masonry (e.g., reinforced-concrete frame + clay-brick infill, or reinforced masonry).

The period of construction has been determined for 86% of the masonry churches in the inventory, and in Figure 2.4 the churches of known construction date are grouped according to decade of construction. The majority of this building stock was established between the 1870s and 1931 (84%), with a few cases (13%) built between 1931 and 1965. The trend in age shows that most of the construction activity occurred between 1910 and 1940, with a peak around 1930. The age statistic confirms that New Zealand ecclesiastic masonry-construction heritage was built over a short time span, compared to other countries worldwide.

In New Zealand the majority of religious buildings are Christian churches. The religious history of the country after the arrival of the Europeans was characterised by significant missionary activity. The Anglican Church of England brought Christianity to New Zealand through the Church Missionary Society, while Presbyterianism and

Catholicism were respectively and largely brought by Scottish and French settlers (Davidson, 2004). Methodism arrived slightly later and the Baptist Church, which had grown rapidly in early 19th century in England, established its first congregations in New Zealand in about 1850 (Hearn, 2012). Later missionaries brought other religious denominations. With reference to the building inventory the four largest denominations are Anglican, Presbyterian, Catholic and Methodist (Figure 2.5a) and their churches can be found in all parts of the country. A much more limited number of buildings are, in decreasing order: Union parishes (grouping of Anglican, Presbyterian, Methodist and Congregationalist), Baptist, Congregationalist, Jewish, and Reformed.

Some of the ecclesiastic buildings are no longer used as was originally intended and are currently utilised for other functions, ranging from civic facilities to private usages. Both original and changed-use churches were included in the inventory. Figure 2.5b shows the proportion of URM buildings still used as originally intended (91%). The remainder of the inventory is made of buildings that have their use changed (7%), that are not in use (1%), or whose use could not be determined at the time of the survey (1%).

Table 2.1. Parameters considered in the inventory of New Zealand URM churches.

General Data
Name
Religious denomination
Location (region, city, suburb, street, #)
Former and current use
Construction date and architect
HNZ registered number
Phone contact and web-links
Architectural Features
Typological classification
Overall dimensions
Position (isolated or connected to other structures)
Plan and elevation regularity
Alterations / additions
Structural characteristics
Masonry type and quality
Wall texture and wall cross-section morphology
Type of roof
Presence of thrusting structures (e.g., arches, vaults, domes, roofs without bottom chord)
Additional vulnerability factors (e.g., soaring elements, large openings, heavy roof covers)
Additional strengthening factors (e.g., buttresses, tie-rods)
State of preservation

Figure 2.2. Distribution of URM churches in New Zealand.

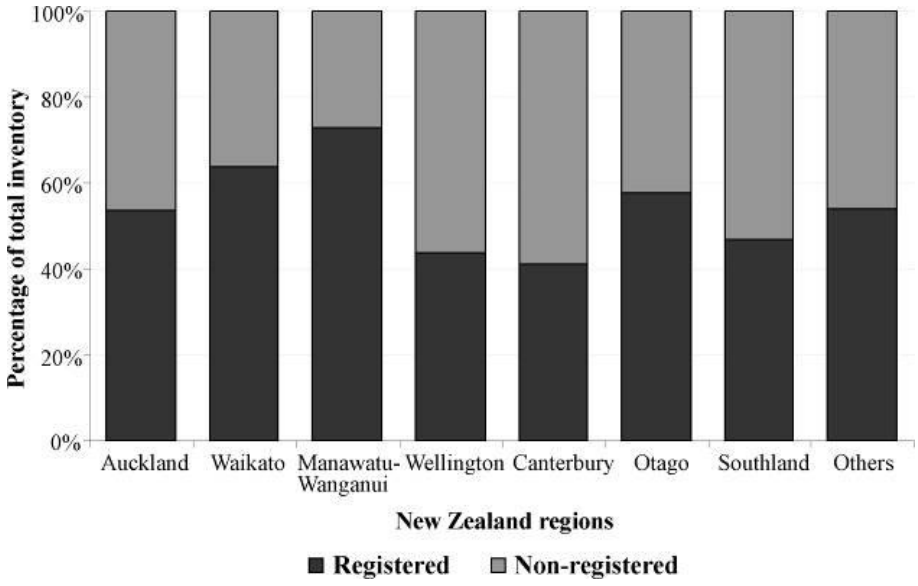

Figure 2.3. Percentage of existing URM churches registered within the New Zealand Heritage List (HNZ), grouped per region.

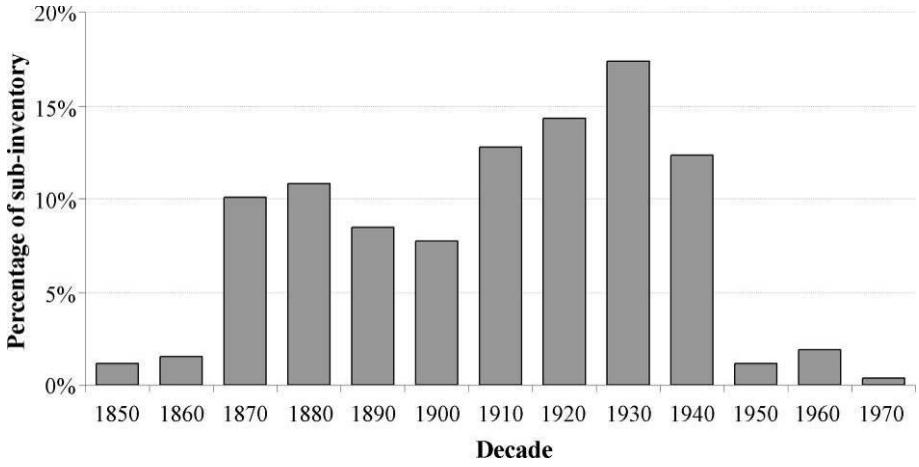

Figure 2.4. Percentage of URM churches according to construction period (for available date of construction).

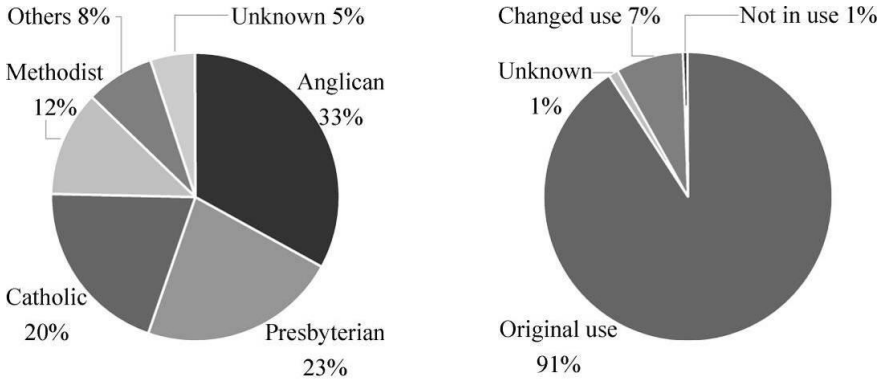

(a) Religious denomination (b) Current use

Figure 2.5. URM church denomination and use.

2.4. Churches characteristics

2.4.1. Geographical distribution

For the purpose of understanding the history of URM churches in New Zealand it is useful to consider their distribution nationally. Almost 70% of the inventory is concentrated in the South Island, with a prevalence of churches located in the Otago (30%) and Canterbury regions (29%), as shown in Figure 2.6.

The comparatively low proportion of buildings in the Auckland region (14%), despite the region having always been the most populated of New Zealand (STATS, 2013), can be explained because of the larger use of timber in construction. There are at least two

explanations for this fact. First, stone was less readily available in the area, whereas Kauri trees were common, especially on the Coromandel Peninsula and in northern areas (Orwin, 2012). Consequently most early constructions, including churches, were made with timber. For example, St Mary's in Parnell, Auckland, was originally designed in brick and stone masonry, but due to budget limitations was instead built in timber (Tonks and Chapman, 2009). Second, at the time of the 1848 Marlborough and 1855 Wairarapa (M_w 8.2) earthquakes, it was observed that masonry buildings were susceptible to destruction while wooden buildings appeared more able to withstand such forces (Schrader, 2013). In some cases, even wind induced damage in masonry churches. For example, St. Stephen's Chapel in Parnell, Auckland, was originally constructed in stone in 1844, but after being destroyed by a hurricane three years later was replaced in 1857 by the current timber building (Tonks and Chapman, 2009). Hence, timber ecclesiastic buildings became predominant in Auckland and acquired such a specific style as to be dubbed 'Selwyn churches', after the nation's first Anglican Bishop (1841-1867) George Augustus Selwyn (Sedcole and Crookes, 1930; Knight, 1972). Wooden churches, sometimes intended as temporary buildings, are in general still standing today and in good condition (Tonks and Chapman, 2009). This resilience was also proved by the Canterbury earthquakes, during which timber churches had the best overall performance, with no cases of structural damage (Leite et al., 2013). However, over time there was a change in building practice after several severe fires affected timber structures, and because masonry construction conveyed a sense of permanency, which was deemed to be a fundamental attribute for any church establishment in a new colony (Walden, 1964; Dowsett, 1985).

The Hawke's Bay region has a fairly low (1%) number of URM buildings, although many major churches were located in and around Napier up till 1931. In that year the M_w 7.8 Hawke's Bay earthquake and subsequent fire caused extensive damage and induced reconstruction with materials other than URM. The same reasoning can reliably be proposed for the Tasman, Nelson, and Marlborough regions, and for the upper portion of the West Coast region (combined 5%), which were strongly stricken by the 1929 Arthur's Pass (M_w 7.1) and 1929 Murchison (M_w 7.8) earthquakes (McSaveney, 2012). Similarly, it is worth mentioning that the upper portion of the Canterbury region has almost no URM churches.

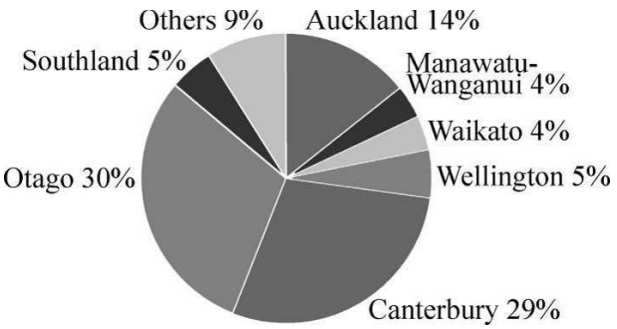

Figure 2.6. Estimated provincial percentage of existing URM churches.

The geographical distribution of URM churches was compared with the seismic hazard map of New Zealand, considering expected peak ground accelerations (PGAs) for a 475-year-return-period earthquake for shallow soils (Figure 2.7) (Stirling et al., 2012). The comparison was further explored by computation of the seismic hazard factor, *Z*, defined by New Zealand Standards (NZS 1170.5, 2004), where the hazard factor has been derived as 0.5 times the magnitude-weighted 5% damped response spectrum acceleration for 0.5 s period for site class C (shallow soils) with a return period of 500 years. This factor is determined through the Initial Evaluation Procedure (IEP) spreadsheet provided by the New Zealand Society for Earthquake Engineering (NZSEEG 2013). For church locations not listed in the IEP spreadsheet (about 20%), interpolation of the hazard factor was used. 27% of the inventory is located in zones with a hazard factor of $0.21 \leq Z \leq 0.30$, 10% in zones of $0.31 \leq Z \leq 0.40$ (Figure 2.8). A total of 13% of the inventory is located in high hazard areas, with a hazard factor greater than 0.30, being the current *Z* factor for Christchurch (raised from 0.22 by the Department of Building and Housing in May 2011 (McVerry et al., 2012)). This outcome confirms the relationship between the geographical distribution of currently existing URM churches and the seismic history of the country, and suggests that those churches located in the highest hazard zones should be investigated and possibly strengthened ahead of the remainder.

2.4.2. Typological classification

Within the characterisation of URM buildings, a very important classification is that concerning the overall building configuration. The seismic performance of a URM structure strongly depends on its general size and shape. Accordingly, a typological classification based on the plan and spatial features is developed, grouping structures

that may display a similar seismic behaviour. Six types are identified within the New Zealand URM church stock, as outlined in Figure 2.9 and Table 2.2. Photographic examples are given in Figure 2.10. The graph in Figure 2.11 shows the frequency of the types for the entire stock. Note that the majority of churches (58%) are part of the A type, underlining the simplicity of the architecture of New Zealand churches. The A_t type includes the presence of the transept and reaches 21%, such that the combined percentage of A and A_t types covers almost 80% of the analysed stock. Within the A type there is a group of small buildings, often officially denominated as chapels, that can be considered as votive churches, originally erected by wealthy families for devotion reasons or for celebrating a deceased. Generally, those churches are not part of a town centre, but are located in the countryside.

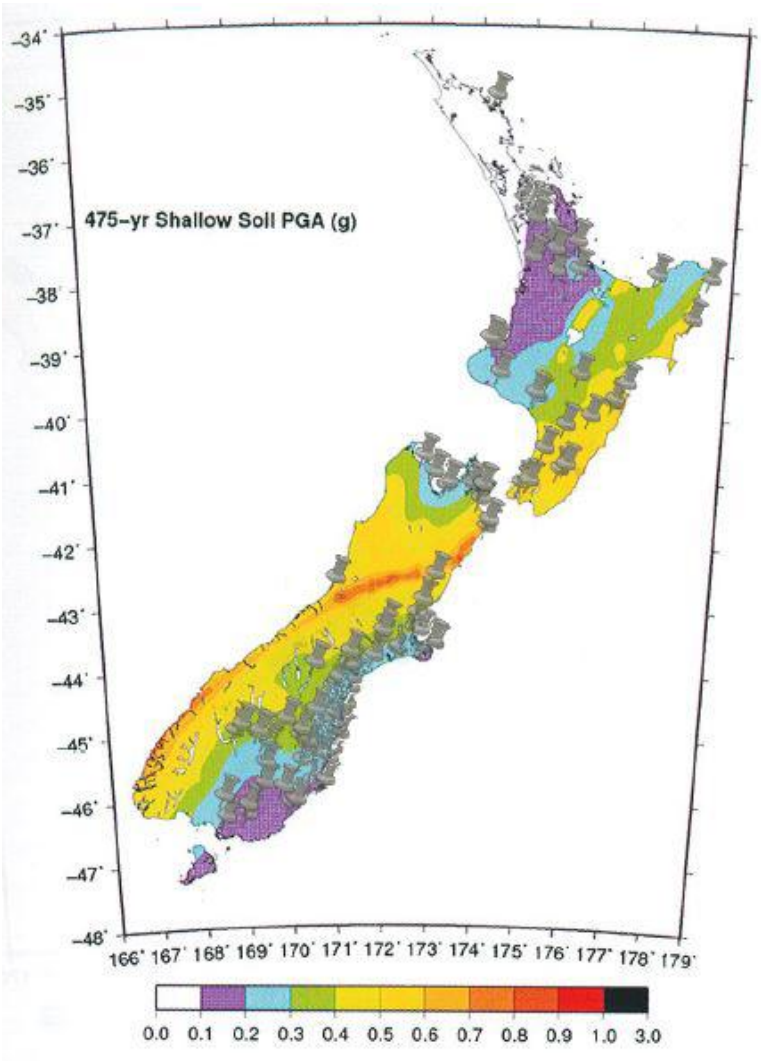

Figure 2.7. Distribution of URM churches compared with the New Zealand national seismic hazard model (Stirling et al., 2012).

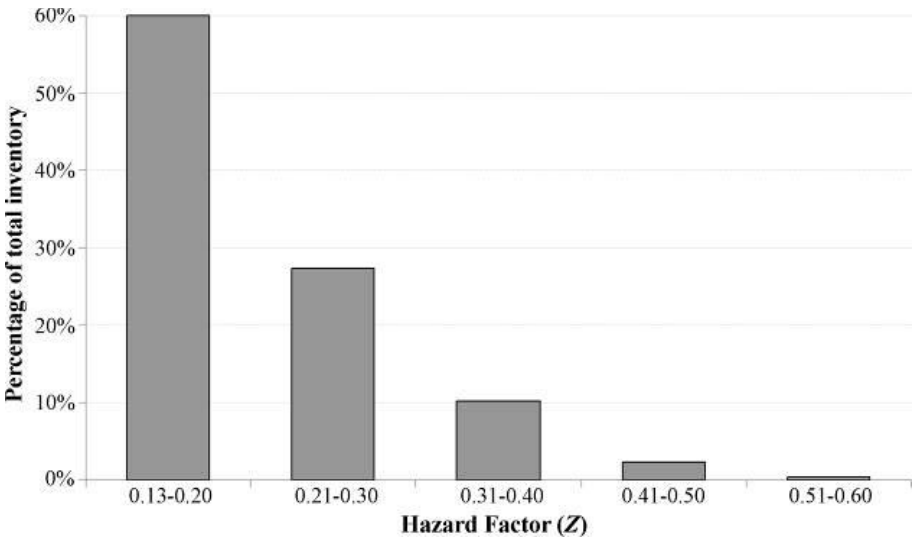

Figure 2.8. Percentage of URM churches according to hazard factor (*Z*).

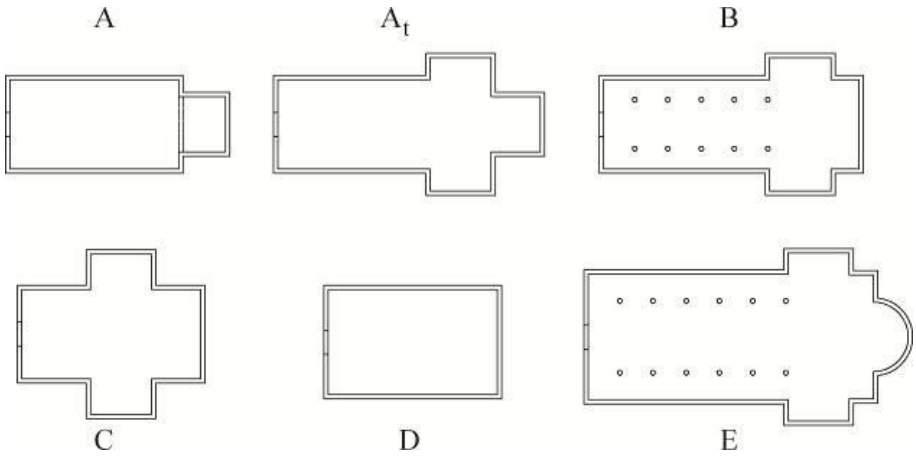

Figure 2.9. Typological classification of URM churches in New Zealand.

Table 2.2. Summary of typological classification of URM churches.

Type	Plan	No. of naves	Nave cover
A	Longitudinal	1	Roof
A_t*	Longitudinal	1	Roof
B	Longitudinal	3	Roof/Vaults
C	Central	1	Roof
D**	Central/ Longitudinal	1	Soffit
E***	Longitudinal	3 or more	Roof/Vaults

*A_t: one nave with transept;
**D: large hall without internal walls, with "box type" behaviour and exteriors as a building;
***E: Basilica, similar to B but much larger.

(a) St Andrew (1938), Maheno - A type

(b) All Saints' Church (1865), Dunedin - At type

(c) St Matthew's Church (1874), Dunedin - B type

(d) Trinity Church (now Fortune Theatre) (1869), Dunedin - C type

(e) Sacred Heart Cathedral (1899), Wellington - D type

(f) St Matthew in the City (1905), Auckland - E type

Figure 2.10. Examples of types of URM churches, based on plan and spatial configuration.

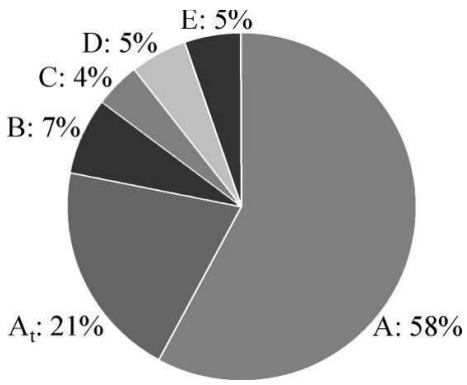

Figure 2.11. Recurring types of URM churches.

2.4.3. Architectural features

New Zealand URM churches tend to have similar characteristics, in terms of both architectural features and construction details. This similarity occurs because most of the structures were built over a relatively short time span, and were often designed by the same architects.

Focusing on the architectural characteristics of the churches, it has already been observed that the religious heritage is mainly represented by longitudinal plan churches, with a long nave eventually crossed by a transept (technical terminology is explained in Figure 2.12). The body of the building is arranged in naves. The main nave is at times flanked by lower aisles, and rows of piers or columns separate them. The main nave can end with a circular or polygonal apse.

Churches were first analysed according to their overall dimensions, noting geometric irregularities in plan and elevation (e.g., whether they are isolated or attached/connected to other buildings). The foot-print area data was sorted into five value ranges: 31% have an area ranging from 50 to 200 m^2, being mostly chapels and countryside churches, and 53% have an area ranging from 201 to 500 m^2 (Figure 2.13).

For churches where it was possible to identify the wall thickness, the mean ratio between the peak height (h_f) of the façade and its thickness (t_f) is 23.8, with a coefficient of variation equal to 7.8 (Figure 2.14a). In addition to the vertical slenderness, the horizontal slenderness was computed, with the average ratio between the length (l_f) and the thickness of the façade being 24.3, whereas the coefficient of variation is equal to 8.5 (Figure 2.14b). In the same way the ratio between the height (h_w) of the longitudinal walls and their thickness (t_w) was investigated (mean value and coefficient of variation

equal to 12.3 and 4.3, Figure 2.14c), as well as the ratio between their length (l_w) and thickness (mean value and coefficient of variation equal to 58.2 and 24.3, Figure 2.14d). These ratios can guide a preliminary vulnerability assessment, especially for those cases that show extreme values. Moreover, it would be interesting to compare New Zealand ratios with those from churches in other countries of both high and low seismic hazards, because existing data are limited and mostly restricted to ordinary buildings (Sorrentino 2014).

The presence of a porch/nartex (55%) is fairly widespread, being the church entrance. The porch/nartex is usually located facing the façade and opposite the church altar (37%), but sometimes is located on a side of the building, close to the corner of the façade (18%) (Figure 2.15).

A presbytery (refer to Figure 2.12) is also generally present (46%), while the apse is rarer (20%) and frequently polygonal (17%) rather than circular (3%). The apse is mainly present in three-nave churches and Basilicas.

Plan and elevation symmetry and regularity were also recorded. It can be observed that nearly 20% of churches are symmetrical and regular in both plan and elevation (Figure 2.16). Cases of asymmetry are often due to extensions in plan that occurred during the life of the building, or the presence of adjacent buildings and/or raised structural elements (Figure 2.17).

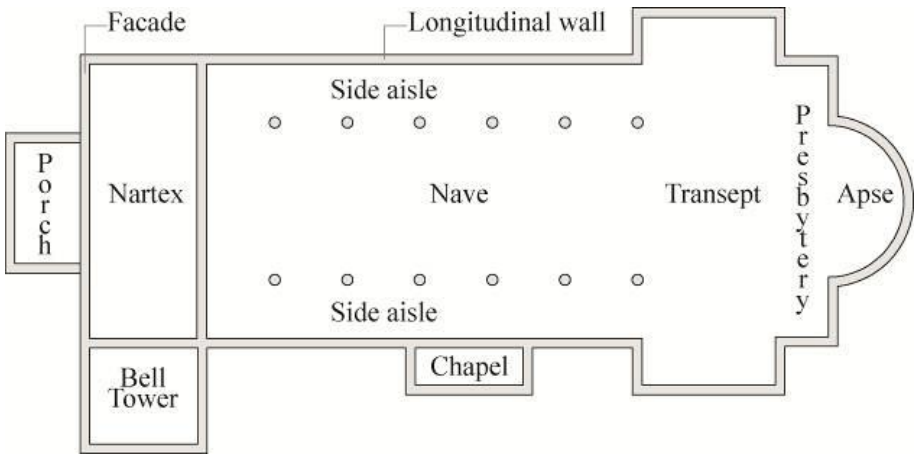

Figure 2.12. Schematic plan showing the common parts of a church.

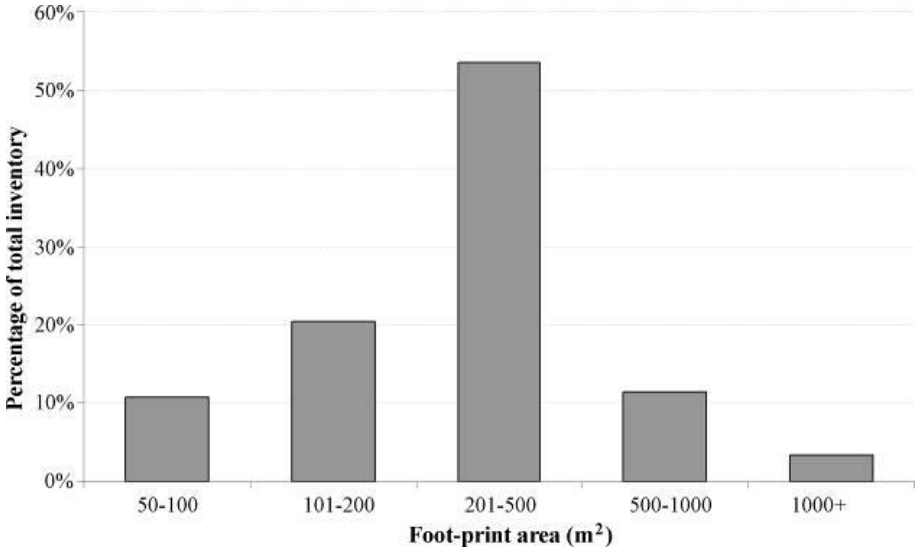

Figure 2.13. Approximate foot-print area.

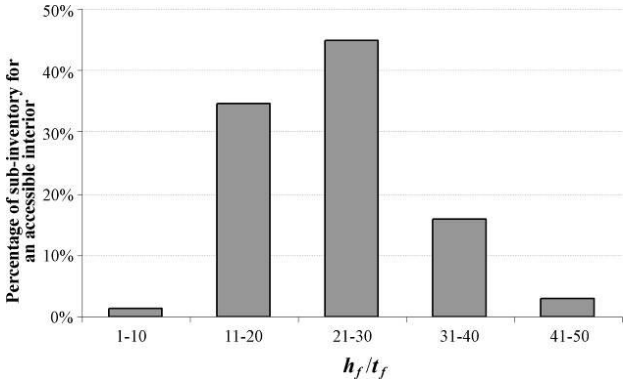

(a) Peak height/thickness ratio of the façade

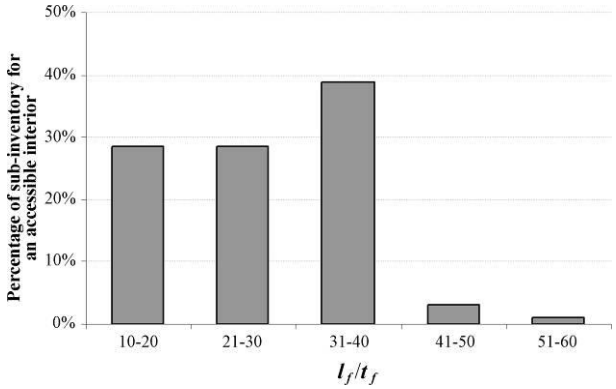

(b) Length/thickness ratio of the façade

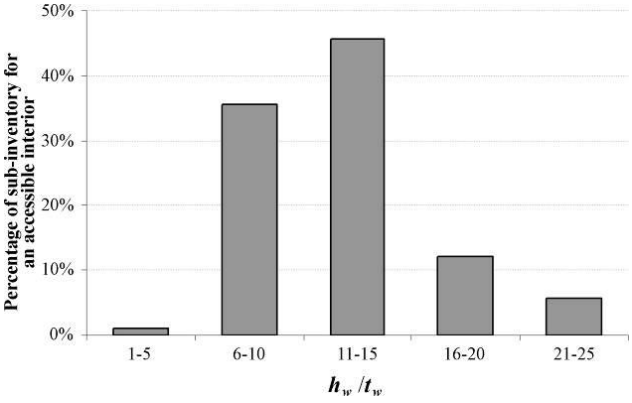

(c) Height/thickness ratio of longitudinal walls

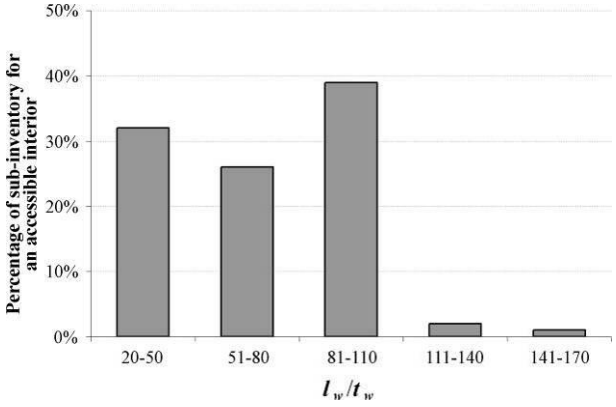

(d) Length/thickness ratio of longitudinal walls

Figure 2.14. Wall geometric ratios.

(a) St Johns (1922), Auckland - Porch facing the façade

(b) St Patrick Basilica (1894), Oamaru - Nartex

(c) St Oswald's Church (1914), Westmere - Porch on a side

Figure 2.15. Examples of porch/nartex.

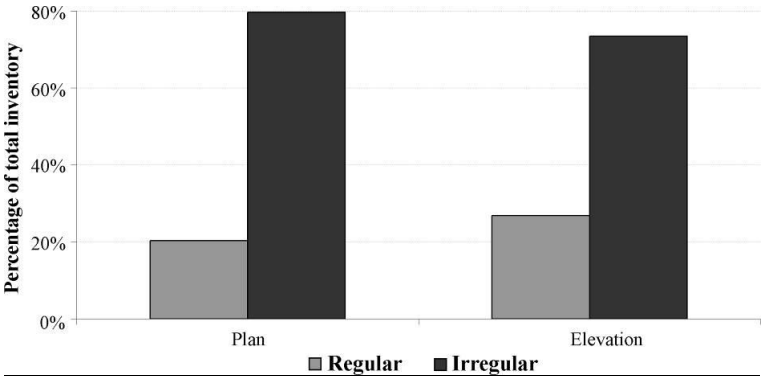

Figure 2.16. Regularity of URM churches, both in plan and in elevation.

(a) Holy Trinity (1898), Auckland - Extension in plan

(b) Wesley Broadway Methodist Church (1911), Palmerston North - Presence of adjacent buildings and raised element

Figure 2.17. Example of geometric irregularities in plan and elevation and position with respect to other buildings.

Raised elements can be domes and bell-towers, although the former is rarely present, and was found in only two churches of the inventory. Bell-towers are observed in 34% of the inventory, are always connected to the nave and can be the cause of vulnerability due to their different dynamic properties. In the majority of cases the bell-tower is flanked to the façade or along the longitudinal walls (80%), although sometimes it is included in the façade (20%) as seen in Figure 2.18. In 66% of cases bell-towers present buttresses and 53% have large openings up their height.

Chapels are present in 43% of the inventory, often not spread along the whole nave wall, and sometimes in an asymmetrical position with respect to the plan configuration (33%).

Sometimes the change from original use (refer to Figure 2.5b) caused alterations to the structure and/or configuration (Figure 2.19). These modifications could contribute to improve or worsen the earthquake performance of the building, e.g., depending on the addition of connections or the removal of structural elements and the increase of mass.

(a) St Mary's (1888), Pleasant Point - Bell tower included in the façade

(b) Sacred Heart (1926), Ranfurly - Bell tower flanked to the façade

(c) St Peter's (1932), Queenstown - Bell tower along the longitudinal walls

Figure 2.18. Examples of bell-tower included in the façade, flanked to the façade or along the longitudinal walls.

(a) Moray Place Congregational Church (1864), Dunedin - Residential apartments

(b) Hanover Street Baptist Church (1912), Dunedin - Bar

Figure 2.19. Examples of churches whose use has been changed.

2.4.4. Structural characteristics

As shown in Figure 2.20, 55% of the inventory is constructed of clay-brick URM (Figure 2.21a) and 39% is constructed of natural-stone URM (Figure 2.21b). In 3% of cases, building stones were limited to facings, basement walls, and the main façade, probably because stone was more expensive than clay brick. For the remainder of the inventory the presence of plaster hampered a positive identification of the masonry type, although the date of construction indicates a traditional building technique and response to simple percussion excludes the use of timber.

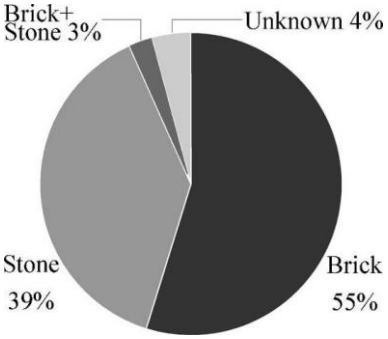

Figure 2.20. Masonry types of existing URM churches.

(a) St. Paul's church (1916), Auckland - Clay brick

(b) Caversham Church (1883), Dunedin - Natural stone

Figure 2.21. Examples of church construction materials.

The construction types were connected to local geology, with almost all stone URM buildings in New Zealand being constructed in areas where the material was available nearby from local quarries, fields and rivers (e.g., the volcanic rocks of Auckland, New Plymouth, Christchurch, Timaru and Dunedin, the limestone in Oamaru, and the schist in central Otago) (Nathan and Hayward, 2012). The natural-stone buildings are mostly concentrated in the South Island, in Canterbury and Otago regions (Figure 2.22), characterised by metamorphic rocks (such as schist, Figure 2.23a) and sedimentary rocks (such as limestone, Figure 2.23b), respectively. Igneous rocks are widely distributed throughout the country with a prevalence of basalt (Figure 2.23c) (Giaretton et al., 2013).

As already widely known, the quality of construction materials plays a key role in the response of URM buildings. Wall construction quality appears to have improved over the years, with early churches sometimes constructed using roughly shaped stone blocks with gaps filled with poor mortar. In Christchurch, in the aftermath of the Canterbury earthquakes, different levels of stone and mortar quality were detected in structures (Dizhur et al., 2011) and it was confirmed that the use of undressed stone units, in conjunction with low-strength lime mortar, often led to poor earthquake response (Figure 2.24).

Mortar is typically lime based, sometimes with a low compressive strength. In a few cases, modern cement mortar has been used to repoint existing masonry joints.

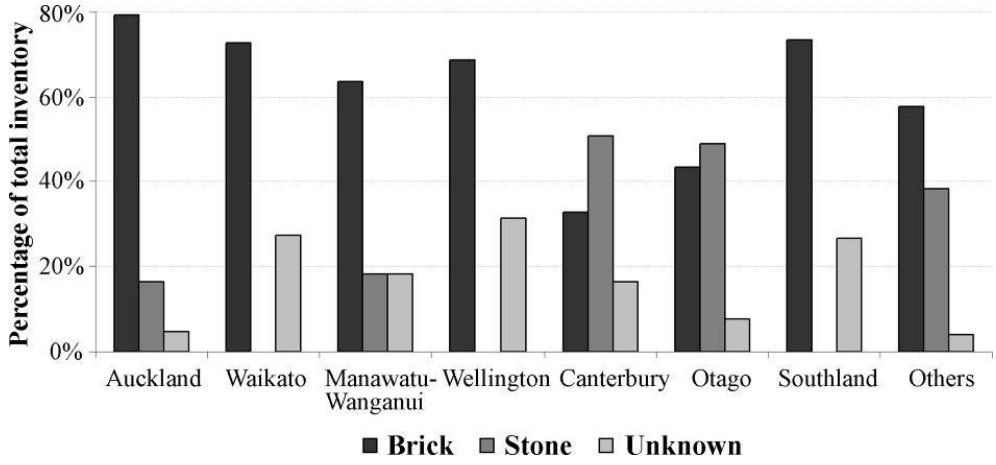

Figure 2.22. Masonry type distribution per region.

(a) St John's Church (1895), Middlemarch - Schist

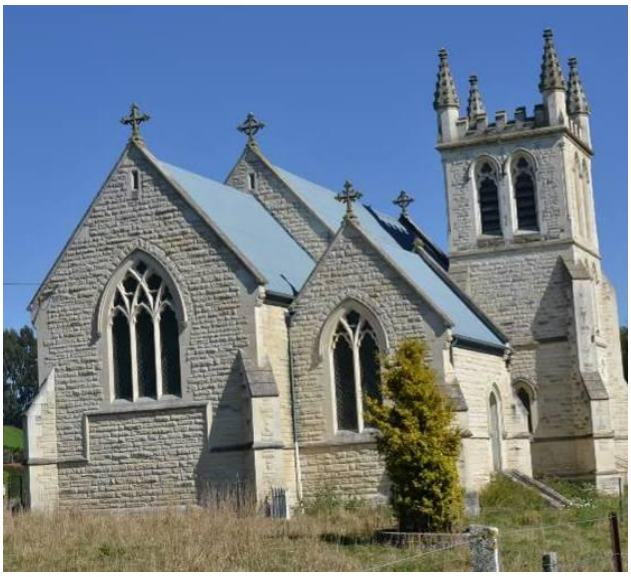

(b) St Martin's Church (1901), Duntroon - Limestone

(c) St Paul's Church (1895), Auckland - Basalt

Figure 2.23. Examples of stone types in New Zealand.

In the investigation of the wall cross-sections, 61% of the inventory (that was possible to survey) is made of single-material solid walls, while 39% of identifiable cases can be sorted into the following types showing:

- a cavity wall (presenting a continuous air gap separating wythes from one another), with either clay-brick (Figure 2.25a) or natural-stone (Figure 2.25b) leaves;
- a two-layer wall, with a stone external facing and one or two clay-brick leaves (Figure 2.25c).

Field observations have shown a rather high seismic vulnerability of non-solid walls, which are prone to failure of one or more leaves. Nonetheless, solid walls can also display inadequate performance, when the wythes are not properly connected and undressed units are used.

Unlike other countries, in New Zealand the nave cover is rarely a URM vault. Considering only those churches where a survey of the interior was possible, stone vaults are present in 7% of the cases, being just two type B and five type E churches. A sloping roof, visible from the nave, is registered in 77% of the subset of the churches surveyed internally (Figure 2.26a). In the remainder of cases the roof is concealed by a ceiling. In Britain and its colonies, trussed roofs started to be adopted in the 17th century and were developed up to the 19th century, initially hidden above the ceiling and later revealed as a visible feature of the buildings (Yeomans, 1992). As shown in Figure 2.27, there are four main statical schemes of sloping roofs in New Zealand:

1. king-post trusses (28% of visible roofs), with a bottom chord in just one case and a raised tie in the remainder 24 cases (Figure 2.28a);
2. queen-post trusses (4%), with one metal bottom tie, one bottom chord, and two raised ties (Figure 2.28b);
3. an elegant elaboration of timber truss consisting of a scissors roof (23%), with or without a raised tie (19% vs. 81%) (Figure 2.28c);
4. a rafter roof (19%), with a timber arch below the rafters in 83% of cases, and with or without a horizontal top beam, also dubbed collar (66% vs. 34%) (Figure 2.28d).

Roofs without a chord at support level develop a thrust that can worsen earthquake performance of the building (Sorrentino et al., 2008). The remaining 9% of the visible sloping roofs are partially hidden by a ceiling that prevents an assured classification (Figure 2.28e). As shown in Figure 2.26b the roof support is a corbel stone (60%), a timber beam (33%), or a reinforced-concrete beam (7%).

The occurrence of additional structural details, such as soaring elements, large openings and heavy roof covers, which might increase the vulnerability of the building, was also investigated. Soaring elements are recurrently present in New Zealand churches and in 62% of cases a pinnacle, a parapet-belfry, or a crenellation was encountered (Figure 2.29). Large openings on the longitudinal walls and rose windows on the façade are respectively present in 21% and 61% of cases. A heavy roof cover (e.g., thin stones) is present in 36% of the inventory.

St Cuthbert's Church (1860), Governors Bay

Figure 2.24. Example of bad masonry quality.

(a) St Joseph's Church (1921), Christchurch – Clay-brick cavity wall

(b) Trinity Congregational Church (1873), Christchurch – Natural-stone cavity wall

(c) St Peter's Church (1875), Christchurch (Photo courtesy of Joao Leite) - Two-layer wall

Figure 2.25. Examples of wall cross-sections.

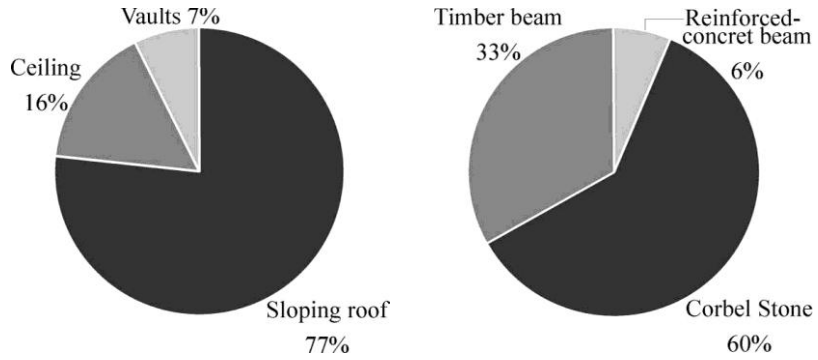

(a) Nave cover (b) Type of roof support

Figure 2.26. Type of nave cover and roof support (related to the sub-inventory for an accessible interior).

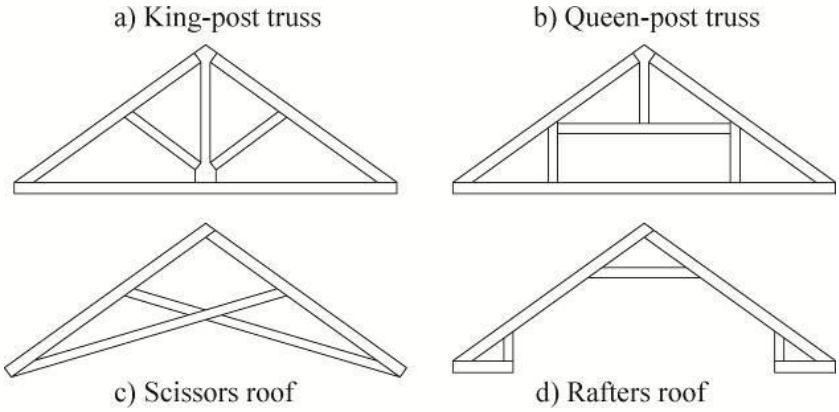

Figure 2.27. Statical schemes of New Zealand sloping roofs.

Different strengthening elements have been surveyed in the churches, with URM lateral buttresses observed in 82% of cases, whereas façade buttresses are present in 26% of the inventory. Tie rods are more rare, being used to eliminate the thrust of the roof in 24% of the surveyed cases (Figure 2.30a), or laid transversally and/or longitudinally in 18% of the sample (Figure 2.30b). Ring beams were detected in just two cases, but elsewhere they may be concealed by plaster or masonry facing.

A good state of preservation was encountered for 54% of the surveyed buildings in the inventory. However, the few churches not in use show some lack of maintenance in plaster and roof, and 27% show a limited number of small cracks or no more than two larger cracks induced by soil settlement and lack of connections (17 churches in Auckland, 10 in Dunedin, 5 in Wellington). Some churches (5%) show more relevant problems, presenting more than two large cracks, but the overall condition is still acceptable. Another 14% fall within Christchurch and have been damaged by the 2010-2011 Canterbury earthquakes.

St Gerard's Church (1908), Wellington - King-post truss

(b) St Joseph and St Joachim (1926), Auckland - Queen-post truss

Sacred Heart (1918), Takaka - Scissors roof

(d) All Saints (1913), Palmerston North - Rafters roof

(e) St Andrew’s Church (1914), Auckland - Roof partially hidden by ceiling

Figure 2.28. Examples of roof types.

(a) Garin Memorial Chapel (Wakapuaka Cemetery) (1890), Nelson - Parapet-belfry (on the left side)

(b) St Joseph's (1879), Temuka - Pinnacles

Figure 2.29. Examples of soaring elements.

(a) St Luke's (1908), Wellington - Tie rods in the roof

(b) St Magnus (1897), Duntroon - Tie rods connecting walls

Figure 2.30. Examples of presence of tie rods.

2.5. Conclusions

The 2010-2011 Canterbury earthquakes have again demonstrated the unsatisfactory earthquake performance of unstrengthened URM churches, with approximately 15% of the affected buildings demolished due to the heavy damage suffered. Due to the high seismicity of New Zealand, the large concentration of people that may occur in religious buildings, and the societal relevance of these structures for historical and symbolical reasons, assessment and mitigation of the earthquake vulnerability of URM churches are of paramount importance. Despite such prominence, a comprehensive list of New Zealand URM churches was not present at the beginning of this research. Hence, a

detailed inventory of URM churches throughout New Zealand was compiled, with a total of 297 buildings being located, excluding 12 buildings that were demolished after the Canterbury earthquakes. It is possible that additional churches are located across the country, along routes not explored during the 10 000 km field trip.

The analysis of the collected data led to the following considerations on the URM religious heritage buildings in existence in New Zealand:

- The buildings were constructed mainly between 1870 and 1940 and now approximately half of the entire inventory is registered with HNZ.
- The main religious denominations are: Anglican (33%), Presbyterian (23%), Catholic (20%) and Methodist (12%). Approximately ninety percent of churches are still used for their original function.
- The existing stock is concentrated in the Otago (30%), Canterbury (29%) and Auckland (14%) regions.
- A limited number of unreinforced masonry churches (13%) are located in high seismic hazard zones (*Z* hazard factor greater than 0.30).
- New Zealand churches usually have a simple layout when compared to European standards. 58% of the sampled buildings have a single nave, and in 21% of cases a transept is added to the nave. The most frequent gross foot-print area is larger than 200 m^2 and smaller than 500 m^2. Most of the buildings are not regular in plan or in elevation, due to the presence of added parts and connected bell-towers.
- In more than half of the inventory clay-brick masonry is used, while natural stone is slightly less common. Lime mortars are typically used. Masonry quality can vary significantly throughout New Zealand and it appears that the quality of construction improved over time. Cross-sections frequently show multiple leaves that are inadequately connected or even separated by cavities.
- The roof is usually sloping and has a raised tie in most cases, instead of a bottom chord. This detail can increase the vulnerability of the building due to exerted thrust. Vaults are rather seldom. In contrast, soaring elements (such as pinnacles, parapet-belfries and crenellations) are frequent.
- Buttresses are very frequent in New Zealand churches. In contrast, strengthening details such as tie rods are present in less than 20% of the cases. This absence of securing may be the result of the application of British construction practices, with a low awareness of detailing to safeguard against earthquakes.

- The state of preservation is usually good, although cracks can affect the buildings to a limited (27%) or moderate (5%) extent. The churches affected by the 2010-2011 Canterbury earthquakes, with varying degree of severity, are about 14% of the stock.

Further development will include in-depth analysis of the earthquake performance of the buildings affected by the 2010-2011 Canterbury earthquakes. Such analysis will address both the overall performance of the buildings and the response of their main elements (such as the façade, nave, apse, and transept). Knowledge of the behaviour of buildings with different structural features and geometric characteristics, as well as exposure to varying severity of shaking, will be helpful for the future seismic assessment of the national stock. The inventory reported in Appendix A will support the identification of buildings and provide their specific location. Moreover, it could be used for updating the HNZ Register. The overarching goal of this first part of the research was to support the conservation and protection of the religious heritage of New Zealand and the safety of people in and around these buildings.

2.6. References

Anonymous. (1979a). *Historic buildings of New Zealand – North Island*. Methuen Publications, Auckland, New Zealand, 271 pp.

Anonymous. (1979b). *Historic buildings of New Zealand – South Island*. Methuen Publications, Auckland, New Zealand, 264 pp.

Canterbury Earthquake Heritage Buildings Fund - CEHBF. http://www.savecanterburyheritage.org.nz/about/. (Accessed during December 2013).

Cattari, S., Ottonelli, D., Pinna, M., Lagomarsino, S., Clark, W., Giovinazzi, S., Ingham, J.M., Marotta, A., Liberatore, D., Sorrentino, L., Leite, J., Lourenco, P.B. and Goded, T. (2015). Preliminary results from damage and vulnerability analysis of URM churches after the Canterbury earthquake sequence 2010-2011. *New Zealand Society for Earthquake Engineering Technical Conference*, Rotorua, NZ, 10-12 April 2015.

Davidson, A. (2004). Christianity in Aotearoa: A History of Church and Society in New Zealand. Education for Ministry, Wellington, New Zealand, 16 pp.

D'Ayala, D.F. (2000). Establishing correlation between vulnerability and damage survey for churches, *12th World Conference on Earthquake Engineering*, Auckland, New Zealand, 30 January – 4 February 2000, Paper No 2237.

Dizhur, D., Ingham, J.M., Moon, L., Griffith, M., Schultz, A., Senaldi, I., Magenes, G., Dickie, J., Lissel, S., Centeno, J., Ventura, C., Leite, J. and Lourenco, P.B. (2011). Performance of masonry buildings and churches in the 22 February 2011 Christchurch earthquake. *Bulletin of the New Zealand Society For Earthquake Engineering.* **44**(4): 279-297.

Donovan, D. (2002). *Country churches of New Zealand*. London: New Holland, Auckland, New Zealand, 126 pp.

Dowsett, M. (1985). *The illusion of permanence: an investigation into 'timber-as-stone' architecture (non-domestic) of the colonial period*. Thesis for the degree of Bachelor of Architecture, University of Auckland.

Fearnley, C. (1977). *Early Wellington churches*. Millwood Press, Wellington, New Zealand, 224 pp.

Giaretton, M., Dizhur, D., da Porto, F. and Ingham, J.M. (2013). An inventory of unreinforced load-bearing stone masonry buildings in New Zealand. *Bulletin of the New Zealand Society for Earthquake Engineering.* **47**(2): 57 -74.

Goodwin, C.P. (2009). *Architectural considerations in the seismic retrofit of unreinforced masonry heritage buildings in New Zealand*. M.Arch-Thesis, School of Architecture and Planning, The University of Auckland, New Zealand.

Hearn, T. (2012). ”English - Religion” *Te Ara - the Encyclopedia of New Zealand*, updated 13rd July 2012. http://www.teara.govt.nz/en/english/page-11. (Accessed during December 2014).

Heritage New Zealand - Pouhere Taonga (2014). “The List - Rārangi Kōrero”. http://www.heritage.org.nz/the-list. (Accessed during December 2013 and January 2014).

Ingham, J.M., Lourenço, P.B., Leite, J., Castelino, S. and Colaco, E. (2012). Using simplified indices to forecast the seismic vulnerability of New Zealand unreinforced masonry churches. *Australian Earthquake Engineering Society 2012 Conference*, Gold Coast, Australia, 7-9 December 2012.

Johnston, D., Standring, S., Ronan, K., Lindell, M., Wilson, T., Cousins, J., Aldridge, E., Ardagh, M.W., Deely, J.M., Jensen, S., Kirsch, T. and Bissell R. (2014). The

2010/2011 Canterbury earthquakes: context and cause of injury. *Natural Hazards*, **73**: 627–637.

Kidd, J.H. (1991). *Some historic churches of Auckland*. The Club, Auckland, New Zealand, 15 pp.

Knight, C.R. (1972). *The Selwyn churches of Auckland*. A.H. & A.W. Reed, Wellington, New Zealand, 85 pp.

Knight, H. (1993). *Church building in Otago*. The University of Otago Printing Department, Dunedin, New Zealand, 345 pp.

Lagomarsino, S. (2012). Damage assessment of churches after L'Aquila earthquake (2009). *Bulletin of Earthquake Engineering*, **10**: 73–92.

Leite, J., Lourenco, P.B. and Ingham, J.M. (2013). Statistical assessment of damage to churches affected by the 2010–2011 Canterbury (New Zealand) earthquake sequence. *Journal of Earthquake Engineering*, **17**(1): 73–97.

McSaveney, E. (2012). Historic earthquakes - The 1929 Arthur's Pass and Murchison earthquakes, *Te Ara - the Encyclopedia of New Zealand*, updated 13rd July 2012. http://www.TeAra.govt.nz/en/historic-earthquakes/page-5. (Accessed during December 2014).

McVerry, G.H., Gerstenberger, M.C., Rhoades, D.A. and Stirling, M.W. (2012). Spectra and Pgas for the Assessment and Reconstruction of Christchurch. *New Zealand Society for Earthquake Engineering Conference*, Paper No 115.

Nathan, S. and Hayward, B. (2012). Building stone - Stone buildings in New Zealand. *Te Ara - the Encyclopedia of New Zealand*, updated 13rd July 2012. http://www.TeAra.govt.nz/en/building-stone/page-1. (Accessed during December 2014).

New Zealand Standards Institute - NZSI (1965). *NZSS 1900:1965. New Zealand Standard Model Building By-Law*. New Zealand Standards Institute, Wellington, New Zealand.

NZS 1170.5 (2004). *Structural design actions - Part 5: Earthquake actions*. New Zealand Commentary. Wellington, New Zealand.

New Zealand Society for Earthquake Engineering Guidelines - NZSEEG (2013). *Assessment and Improvement of the Structural Performance of Buildings in Earthquakes - Section 3 revision: Initial seismic assessment*. Wellington, New Zealand.

Orwin, J. (2012). "Kauri forest - How and where kauri grows", *Te Ara - the Encyclopedia of New Zealand*, updated 13rd July 2012, http://www.teara.govt.nz/en/kauri-forest/page-1. (Accessed during February 2015).

Reitherman, R. (2006). Earthquakes that have initiated the development of earthquake engineering. *Bulletin of the New Zealand Society for Earthquake Engineering*, **39**(3): 145-157.

Dowrick, D.J. (1998). Damage and intensities in the magnitude 7.8 1931 Hawke's Bay, New Zealand earthquake. *Bulletin of the New Zealand National Society for Earthquake Engineering*, **31**(3): 139-163.

Schrader, B. (2013). "Housing - Construction and materials", *Te Ara - the Encyclopedia of New Zealand*, updated 8th July 2013. http://www.teara.govt.nz/en/housing/page-5. (Accessed during February 2015).

Sedcole, A.J. and Crookes, S.I. (1930). *Early New Zealand ecclesiastical architecture*. Auckland University College, School of Architecture, Auckland, New Zealand, 17 pp.

Sorrentino, L., Bruccoleri, D. and Antonini, M. (2008). Structural interpretation of post-earthquake (19th century) retrofitting on the Santa Maria degli Angeli Basilica, Assisi, Italy. *6th International Conference on Structural Analysis of Historic Construction*, Bath, UK, 2-4 July 2008, 217-225.

Sorrentino, L. (2014). Reconstruction Plans After the 2009 L'Aquila Earthquake. From Building Performance to Historical Centre Performance. *9th International Conference on Structural Analysis of Historical Constructions*, Mexico City, Mexico, 14–17 October 2015, Paper No 11-006.

Sorrentino, L., Liberatore, L., Decanini, L.D. and Liberatore, D. (2014). The performance of churches in the 2012 Emilia earthquakes. *Bulletin of Earthquake Engineering*. **12**(5): 2299–2331.

Statistics New Zealand, Tatauranga Aotearoa - STATS (2013). *Digitised copies of Census of Population and Dwellings reports and results, from 1871 to 1911*. Published 21th August 2013. http://www.stats.govt.nz/browse_for_stats/snapshots-of-nz/digitised-collections/census-collection.aspx. (Accessed during February 2015).

Stirling, M.W., McVerry, G.H., Gerstenberger, M.C., Litchfield, N.J., Van Dissen, R.J., Berryman, K.R., Barnes, P., Wallace, L.M., Villamor, P., Langridge, R.M., Lamarche, G., Nodder, S., Reyners, M.E., Bradley, B., Rhoades, D.A., Smith, W.D., Nicol, A., Pettinga, J., Clark, K.J. and Jacobs, K. (2012). National seismic hazard

model for New Zealand: 2010 update. *Bulletin of the Seismological Society of America*, **102**(4): 1514-1542.

Tonks, G. and Chapman, J. (2009). Earthquake performance of historic timber buildings in New Zealand. *New Zealand timber design journal.* **17**(3): 3-9.

Walden, H.R. (1961). *A Study of Church Architecture*. Thesis for the degree of Bachelor of Architecture, University of New Zealand.

Walden, H.R. (1964). *New Zealand Anglican church architecture, 1814-1963*. Thesis for the degree of Master of Architecture, University of Auckland.

Warren, D. (1957). *Some Canterbury churches*. The Pegasus Press, Christchurch, New Zealand, 48 pp.

Wells, R. and Ward, T. (1987). *In a country churchyard*. The Caxton Press, Christchurch, New Zealand, 108 pp.

Wells, A. (2003). *Nelson historic country churches*. Nikau Press, Nelson, New Zealand, 176 pp.

Yeomans, D.T. (1992). *The trussed roof: its history and development*. Scolar Press, Aldershot, England, 221 pp.

Chapter 3

Vulnerability assessment of unreinforced masonry churches following the 2010-2011 Canterbury earthquake sequence

In this section, a sample of 80 affected buildings is analysed and their performance statistically interpreted. Structural behaviour is described in terms of mechanisms affecting the so-called macro-elements, and damage probability matrices are computed. Regression models correlating mean damage level against macroseismic intensity are also developed for all observed mechanisms, improving the initial simple-linear formulations through use of multiple-linear regressions accounting for vulnerability modifiers, whose influence is evaluated via statistical procedures. Results presented herein will support the future development of predictive tools for decision-makers, also contributing to seismic vulnerability mitigation at a territorial scale.

3.1. Introduction

The extensive damage that occurred to unreinforced stone and clay brick masonry (URM) churches after the 2010-2011 seismic swarm in the Canterbury region emphasises the need to better understand the vulnerability of this structural type and to determine appropriate seismic retrofit measures. Churches frequently display a seismic vulnerability higher than ordinary buildings (D'Ayala, 1999), especially at larger intensities of ground shaking, that in recent years has led to studies at a territorial scale after several major earthquakes (Montilla et al., 1996; Guerreiro et al., 2000; Guevara and Sanchez-Ramirez, 2005; Lagomarsino and Podestà, 2004a; Lagomarsino, 2012; da Porto et al., 2012; Sorrentino et al., 2014a) and to structural assessment of their

vulnerability (Sofronie, 1982; Elton and Marciano, 1990; Rivera De Uzcategui and Torres, 1997; Stiros et al., 2006; Gonzalez Ballesteros et al., 2012; Sorrentino et al., 2014b).

At least 297 URM churches are present in New Zealand, as shown in the inventory reported in Appendix A, and several assessments of the performance of New Zealand URM churches have been carried out recently (Anagnostopoulou et al., 2010; Leite et al., 2013; Lester et al., 2013; Lourenço et al., 2013; Senaldi et al., 2014). To improve the understanding of the seismic response of ecclesiastic buildings during the Canterbury earthquake sequence the existing observations were reanalysed and additional surveys were performed, resulting in an increased sample of 80 URM church buildings. The damage, contrary to the common practice in use for other building types, has been described both at global and local levels and damage degrees have been defined according to the European Macroseismic Scale (EMS-98; Grünthal, 1998).

Existing unreinforced masonry buildings frequently suffer damages concentrated in the weakest elements (e.g., D'Ayala and Speranza, 2003; Sorrentino et al., 2014c). This behaviour is even more pronounced in churches that, because of their architectural characteristics (large horizontal and vertical spans), usually do not show an overall behaviour but instead local mechanisms generally occur. This specific feature was recognised by Giuffrè (1988) and systematically used by Doglioni et al. (1994) with the definition of the macro-element, which is an architectural component whose seismic behaviour is only weakly coupled to that of the rest of the structure. According to such an approach Lagomarsino (1998) and Lagomarsino et al. (2004) proposed a damage survey form with 28 local mechanisms identified in its latest official version (PCM-DPC MiBAC, 2006), and this Italian survey form was used to assess the 80 URM churches of the Canterbury area.

Several seismic vulnerability assessment methods have been developed from the early 1970's to the present time considering different approaches for the collection and interpretation of data, both at urban and territorial scale. These vulnerability assessment methods are classified as either empirical or analytical/mechanical methods. Empirical methods are based on directly observed vulnerability or expert judgement (ATC 1985-Report 13), are developed based on knowledge of selected parameters collected from in situ observation, and are suited to identification of the seismic vulnerability of a building stock. There are three main types of empirical methods: damage probability matrices (DPMs), which express in a discrete form the conditional probability of

obtaining a damage level due to a ground motion of given intensity (Whitman et al. 1973); the vulnerability index method (VIM), based on the summation of parameters that can influence the vulnerability (Benedetti et al. 1988); and continuous vulnerability functions, which express the probability of exceeding a damage state, given a function of the earthquake intensity (Spence et al., 1992; Sabetta et al., 1998). Analytical/mechanical methods are based on computational analysis defining a direct relationship among construction characteristics, structural response to seismic action and damage effects. Because these methods need more detailed information, they can be applied to a limited number of buildings. Analytical methods produce more detailed algorithms with physical meaning, and their development has been strongly influenced by the growth of attenuation equations for specific seismic regions and corresponding derivation of seismic hazard maps in terms of spectral ordinates (D'Ayala, 2013). They can be classified according to three categories: analytically-derived vulnerability curves and DPMs methods (Singhal and Kiremidjian, 1996), collapse-mechanism methods (Bernardini el at., 1990), and capacity-spectrum-based methods (Kircher et al., 1997; Calvi, 1999). Finally, methods using features belonging to both previous methods, combining post-earthquake damage statistics with analytical damage statistics, are named hybrid methods (refer, e.g., to Barbat et al., 1996; Kappos et al., 1998). Because analytical methods need detailed information, they can be applied to a limited number of buildings.

Given the available information and the interest associated with "experimental" data, an empirical approach was assumed for the analyses of earthquake damage to New Zealand URM churches, by opting for the computation of damage probability matrices (DPMs). Although ecclesiastical buildings have sometimes been treated as individual structures because of their specific architecture, several studies have previously been undertaken in order to statistically characterize churches at territorial level (e.g. Lagomarsino and Podestà, 2004b; Lagomarsino, 2006; da Porto et al., 2012). Moreover, New Zealand URM churches tend to have similar characteristics, in terms of both architectural features and construction details, because of a relatively short time span of construction and because they were often designed by the same architects, leading to a reasonably homogeneous set of buildings (refer to §2.4). According to the predominant literature, the first and foremost parameter considered for explaining damage is the severity of shaking, and macroseismic intensity is herein used as the intensity measure (IM) of ground motion.

3.2. Seismic event

The Canterbury region of New Zealand experienced an extensive earthquake sequence during 2010-2011 with more than 10 000 seismic shocks since the Darfield earthquake on 4 September 2010 that had moment magnitude (M_w) 7.1. The most severe event, in terms of damage, occurred on 22 February 2011 with M_w 6.3 and an epicentre located 10 km south-east of Christchurch, which is the second largest city in New Zealand. Additional information about the seismic sequence can be found in Bannister and Gledhill (2012) and in Bradley et al. (2014). The earthquake sequence caused extreme disruption, with damage to Christchurch architectural heritage being particularly extensive (Moon et al., 2014). With reference to churches, the Darfield earthquake caused limited damage compared to the February event (Anagnostopoulou et al., 2010), after which more than 80% of the URM churches were classified as unsafe or temporarily restricted for access (Leite et al., 2013).

Goded et al. (2014a) assigned a macroseismic intensity to each district of Christchurch and to peripheral areas stricken by the February event, using the New Zealand Modified Mercalli (NZMM) intensity scale. In New Zealand, felt intensities have been assigned using this scale since the 1960s (Eiby, 1966), when the MM scale was revised in order to be directly applicable to the national stock of structures. A second revision was performed in 1992 (Study Group of the NZSEE, 1992), and the current version was developed just a few years later (Dowrick, 1996). The MM scale presents just four construction types, all made of masonry, whereas the current NZMM scale accounts for six different construction types and involves a more detailed damage description for grades larger than 7, including references to specific construction dates related to significant changes in structural codes. According to Dowrick (1996), the NZMM scale is broadly similar to the EMS, and minor differences can be recognised only for intensities 11 and 12. For the sites of 57 churches the intensities in Goded et al. (2014b) have been used, and the distribution of the most probable NZMMI for the Christchurch districts is summarised in Figure 3.1. For the remaining 23 churches, all located south of Ashburton (which is a town located 89 km to the south west of central Christchurch), the same lowest intensity (NZMMI = 4) was assumed, in accordance with the damage observed.

3.3. Damage and vulnerability assessment

3.3.1. The sample of churches and the data collected

New Zealand became a British colony following the signing of the Treaty of Waitangi in 1840. As a consequence, New Zealand colonial settlements were modelled on British society and as parishes became established, churches were built in English forms with which the clergy and architects were familiar (refer to §2, and references therein). The first churches were built mainly with timber because of the simplicity and speed of construction, and material availability, but with growing prosperity stone and clay brick masonry buildings became popular until 1931, when the Hawke's Bay earthquake (M_w 7.8) proved the poor earthquake performance of those materials. The use of URM was explicitly outlawed in 1965 in most areas of New Zealand (NZSI, 1965), such that almost all unreinforced masonry churches in New Zealand were constructed between the late 1840s and 1931, with a few cases of construction until 1965, being a short time span compared to other countries worldwide.

Nationwide 297 URM churches have been recognized and surveyed, and data on structural details and geometric characteristics have been collected (§2). 80 URM churches have been identified in the area of the Canterbury region affected by the earthquakes, with 42 being in Christchurch city and an additional 12 having been demolished because of the heavy damage suffered (CERA, 2014). About 38% of the 80 URM churches are made of natural-stone URM (Figure 3.2a), 51% are made of clay-brick URM (Figure 3.2b) and the remaining 11% have a brick structure with a stone veneer. These percentages closely match the nationwide inventory, where 39% are constructed of natural-stone URM and 55% are made of clay-brick URM, showing the good representativeness of the Canterbury sample compared to the national portfolio. As for the entire New Zealand inventory, in the area affected by the earthquake wall cross-section morphologies can be delineated among single-material solid walls, cavity walls (presenting a continuous air gap separating wythes from one another) with either clay-brick or natural-stone leaves, and two-layer walls with a stone external facing and one or two clay-brick leaves. Among the structural characteristics examined, the British-derived trussed roofs were particularly interesting as in New Zealand there common statical schemes do not present a chord at the support level.

Regarding the typological classes identified nationwide according to the plan and spatial features of the buildings (§2.4.2), most of the churches present in the Canterbury region (85%) fall into the combined A (one nave without transept, 62%) and A_t (one nave with transept, 23%) types, confirming the simplicity of their architecture. These percentages are once again close to those for the entire national stock, where respectively 58% and 21% of churches belong to A and A_t types. Similar agreements also apply to the four remaining and less common types.

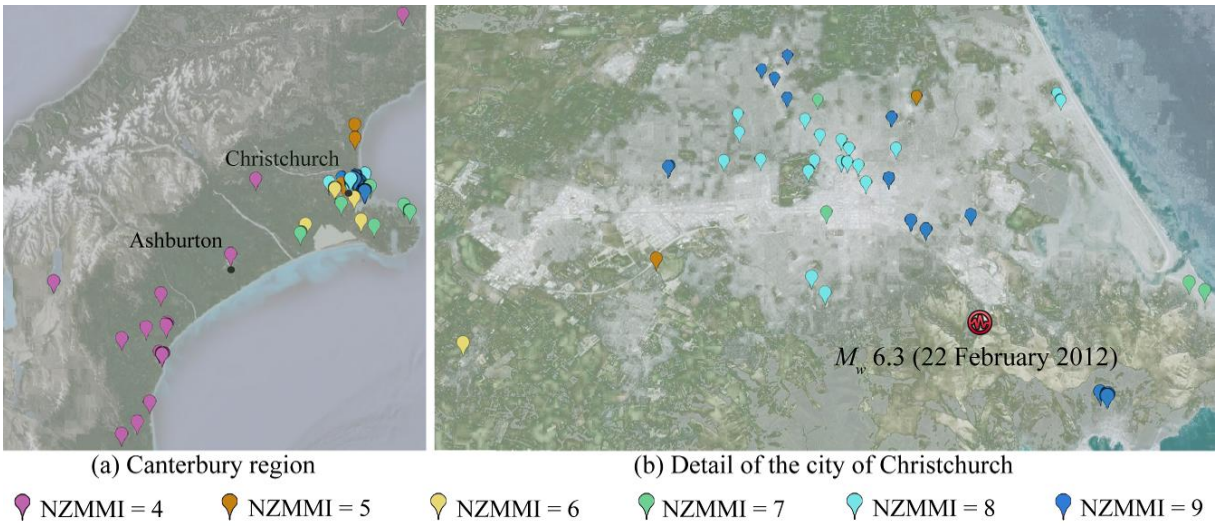

Figure 3.1. Locations of the 80 URM churches with their NZMMI assignments

Figure 3.2. Examples of building materials of the URM churches in the Canterbury region. Photo (b) is courtesy of João Leite.

3.3.2. Damage classification

Data concerning the damage suffered by ecclesiastic buildings in the Canterbury earthquakes were collected during 2014 and compared to the results of the surveys carried out in 2011, immediately after the major events (Leite et al., 2013). This earlier 2011 survey is the only source of information about the damage to the 12 churches demolished before 2014. The analysis procedure was the one currently adopted in Italy for post-earthquake assessment (PCM-DPC MiBAC, 2006), involving the evaluation of 28 possible collapse mechanisms (Figure 3.3), which is a more detailed approach when compared to the straightforward assignment of a global damage level, as is customary for other building types (Benedetti and Petrini, 1984; Erberik, 2008). When a single building is under investigation, quantitative procedures relying on detailed surveys through dense point clouds acquisition can be used to identify collapse mechanisms (Andreotti et al., 2014). When, as for the Canterbury earthquakes, a large sample of buildings is analysed, qualitative judgment, based on the observation of macroscopic cracks and deformations, is the most suitable possibility. Six damage levels, d_k, were assigned for each mechanism, according to the approach of the EMS-98 scale: 0 - No damage; 1 - Negligible to slight damage; 2 - Moderate damage; 3 - Substantial to heavy damage; 4 - Very heavy damage; 5 - Destruction. In Figure 3.4 examples of damage ascription for one mechanism are reported.

The percentages of mechanisms whose activation is possible are presented in Figure 3.5, alongside a ratio of activated-over-possible mechanisms. The first parameter highlights the simplicity of the architecture of New Zealand URM churches (as already pointed out in §2). One macro-element, vaults in the chapels (related mechanism: #24) is not present at all, some other mechanisms (12, 14-15) showed systematic activation but their macro-elements, vaults, domes and roof lanterns, are present in just one or two buildings. Because of their rather poor sample size, these mechanisms, together with 7-9 and 18, are not further discussed in the following. Within the 20 remaining mechanisms, the most vulnerable one is the shear response of the longitudinal walls (#6, Figure 3.6a), activated in 80% of possible cases. Overturning (#10, Figure 3.6b) and shear (#11) in the transept present the same activation rate (73%). Sixty-eight % of projections (#26, Figure 3.6) and triumphal arches (#13) were damaged, whereas interactions between nave and its roof (#19, Figure 3.6d) and damages in the porch (#4) were observed in 67% of cases.

Figure 3.3. Collapse mechanisms in the Italian survey form for churches (PCM-DPC MiBAC 2006).

Figure 3.4. Examples of damage ascription for mechanism no. 2 (gable mechanisms). Photo (b) is courtesy of João Leite.

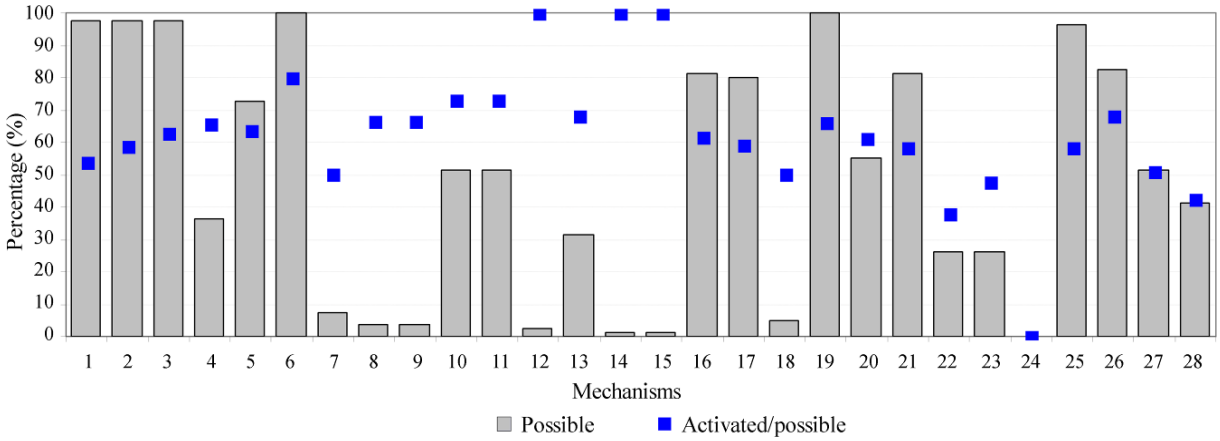

Figure 3.5. Percentage of possible (over the sample of 80 churches) and activated (over the sample of possible) mechanisms depicted in Figure 3.3.

In Figure 3.7 the mean damage of each mechanism is plotted. Their comparison is meaningful provided that the distribution of buildings across felt intensities is comparable, which is not the case for some macro-elements that are rarely present (e.g., vaults in the naves, related to mechanism #9; vaults in the transept, #12; dome and roof lantern, #14-15), belonging to buildings located in the centre of Christchurch and displaying very high mean damage. Damage in the triumphal arch (#13) shows an average value of about 2.2, being slightly higher than for shear in longitudinal walls (#6), while mechanisms regarding damage in the porch (#4), overturning and shear in the transept (#10-11), interactions between the nave and its roof (#19), and damage in projections (#26) display a mean damage between 1.6 and 1.8.

Figure 3.6. Examples of some of the most activated mechanisms. Photo (a) is courtesy of João Leite.

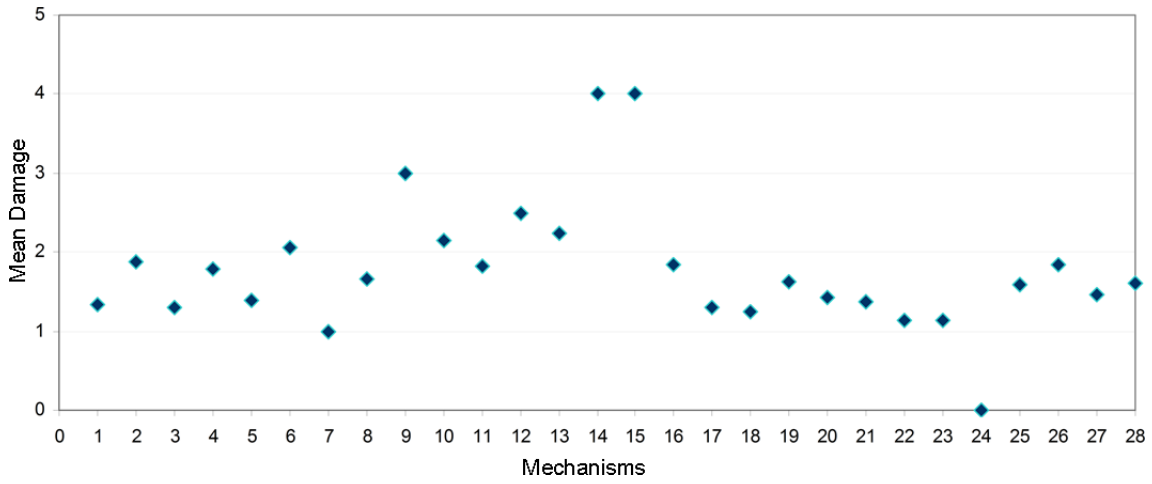

Figure 3.7. Mean damage for the 28 mechanisms.

3.4. Damage probability matrices

3.4.1. Damage probability matrices for global damage

The DPM approach is an empirical method originally proposed by Whitman et al. (1973) after the 1971 San Fernando earthquake and subsequently applied in Europe by several authors (Braga et al., 1982; Lagomarsino, 1998; Dolce et al., 2003; Lagomarsino et al., 2004; Di Pasquale et al., 2005; Liberatore et al., 2006; Vicente et al., 2011). Despite shortcomings associated with discrete definition of the damage and the strong dependence on direct damage data (Calvi et al., 2006; D'Ayala, 2013), this method is one of the most suitable at territorial level, allowing the estimation of vulnerability on the basis of a limited number of structural and architectural characteristics. DPMs express the probability P of reaching a damage state ($D = D_i$) due to a ground motion level (I):

$$DPM_{I,D} = P\left(D = D_i \mid I\right) \tag{1}$$

Given the intensity of the earthquake shaking, the damage is described by a distribution of a discrete damage variable D.

In literature DPMs have generally been proposed for the global performance of a church, being computed from a global damage index, i_d, representative of the damage that occurred to the church, calculated by means of a weighted mean of the damage scores assigned to each collapse mechanism:

$$i_d = \frac{1}{5} \frac{\sum_{k=1}^{N} \rho_k \, d_k}{\sum_{k=1}^{N} \rho_k} \tag{2}$$

where ρ_k is a weight score ranging between 0 and 1, based on the influence of the considered mechanism on the global response of the structure; d_k is the damage score concerning the k-th mechanism, ranging between 0 and 5; and N is the number of mechanisms that can be activated ($N \leqslant 28$).

The damage index, originally proposed in Lagomarsino et al. (1997) and revised in Lagomarsino et al. (2004), is a synthetic parameter that allows comparison between the level of damage to churches of different typologies, sizes and shapes recognising that the seismic performance of a URM structure strongly depends on the overall building configuration. This is not a main issue in the present case, considering the already highlighted homogeneity of the ecclesiastical New Zealand stock. The damage indices for the 80 churches are plotted in Figure 3.8, showing a trending increase with felt intensity, but with significant scatter. This phenomenon means that macroseismic intensity alone cannot fully explain the damage.

In order to express global damage in levels (D_j) comparable with those of EMS98, the previously calculated damage index, i_d, was transformed into a discrete variable, using the correlation suggested by Lagomarsino and Podestà (2004b) (Table 3.1). In the damage distribution (Figure 3.9) slight damage (D_1) is prevalent (29%), followed by substantial (D_3), moderate (D_2) and null damage (D_0), each of about 19%, followed by heavy damage (D_4, 13%) and destruction (D_5, 4%).

The interpretation of the damage observed after the 2011 seismic event was undertaken by fitting the obtained frequencies with a binomial distribution (Braga et al., 1982), according to the following equation:

$$p_i = \frac{5!}{i!(5-i)!}\left(\frac{\mu_D}{5}\right)^i\left(1-\frac{\mu_D}{5}\right)^{5-i} \tag{3}$$

where p_i is the probability of having a damage of level i (i = 0, 1, 2, 3, 4, 5) and μ_D is the mean damage defined as:

$$\mu_D = \frac{\sum_{j=1}^{n_I} D_j}{n_I} \tag{4}$$

where n_I is the number of churches suffering the same NZMM intensity.

Table 3.1. Correlation between damage index, i_d, and damage level, D_j.

D_j	i_d	Description
0	$i_d \leq 0.05$	No damage: light damage only in one or two mechanism
1	$0.05 < i_d \leq 0.25$	Negligible to slight damage: light damage in some mechanisms
2	$0.25 < i_d \leq 0.4$	Moderate damage: light damage in many mechanisms, with one or two mechanisms activated at medium level
3	$0.4 < i_d \leq 0.6$	Substantial to heavy damage: many mechanisms have been activated at medium level, with severe damage in some mechanisms
4	$0.6 < i_d \leq 0.8$	Very heavy damage: severe damage in many mechanisms, with the collapse of some macroelements of the church
5	$i_d > 0.8$	Destruction: at least 2/3 of the mechanisms exhibit severe damage

In order to develop the DPM the sample was split according to felt macroseismic intensities (Figure 3.1) and the DPM was defined according to the percentage of occurrence of damage for each intensity. Because a small number of churches are present at some intensities, namely NZMMI = 5 and 6, a linear variation of mean damage is assumed over intensity, i.e.:

$$\mu_D = a + b\ NZMMI \tag{5}$$

The parameters a and b have been estimated over the whole sample of 80 churches according to the maximum-likelihood criterion.

In Figure 3.10 the histograms of damage, and their binomial fitting, are presented for each macroseismic intensity, where the binomial distribution appears effective for some intensities (4, 7, 9) but less so for others (5, 6, 8). These results highlight that the macroseismic intensity alone is not able to fully explain the damage, which can be increased or reduced by vulnerability factors that have not yet been considered.

For each intensity a goodness-of-fit test (Benjamin and Cornell, 1970) was performed on the corresponding damage probability distribution by calculating the statistic, S:

$$S = \sum_{i=0}^{5} \frac{\left(N_i - n_I\ p_i\right)^2}{n_I\ p_i} \tag{6}$$

where N_i is the number of churches with damage level i, p_i is the corresponding probability and n_I is the total number of churches which underwent that intensity.

Because the terms in the summation have the probability p_i in the denominator, large values of S occur for outliers, i.e. churches which have a damage level with small probability. The observed values of the statistic S are reported in Figure 3.11, along with the individual contributions to the summation of the different damage levels.

In order to establish if the binomial distribution is adequate, for each intensity 50 000 samples were generated by the Monte Carlo method (the small size of the samples makes the χ^2 distribution unsuitable for the statistic S) and the resulting critical values for the significance level at 5%, denoted as $S_{0.05}$, were computed (Figure 3.11). Values of S less than $S_{0.05}$ (as happens for NZMMI = 7, 8, 9) lead to acceptance of the probability distribution, while values greater than the significance level imply rejection of the distribution (as happens for NZMMI = 4, 5, 6). Apart from the scarcity of data for some intensities, it can be noticed that high values are mainly determined by outliers corresponding to substantial or high damage for low intensities. Conversely, cases where low damage occurred in conjunction with high intensities produce comparatively high values of S. These results confirm that vulnerability factors need to be considered, by applying suitable regression models to the response of local mechanisms.

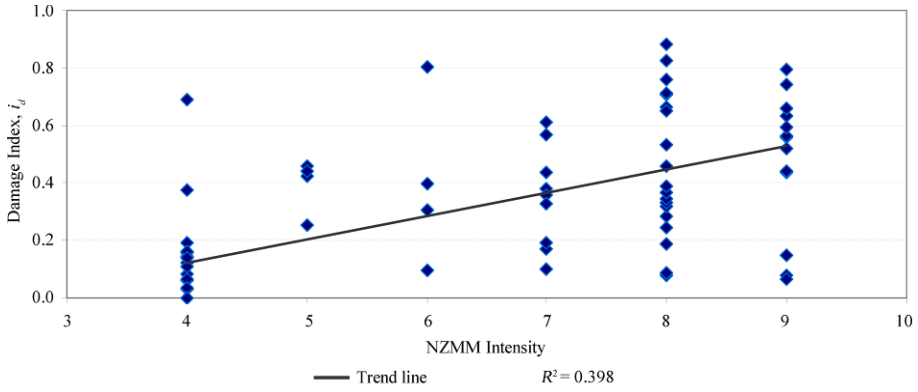

Figure 3.8. Distribution of the damage index, i_d, with NZMM intensity.

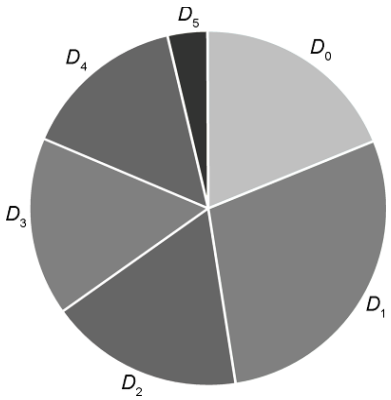

Figure 3.9. Percentage of the damage level (D_i) for the 80 observed churches.

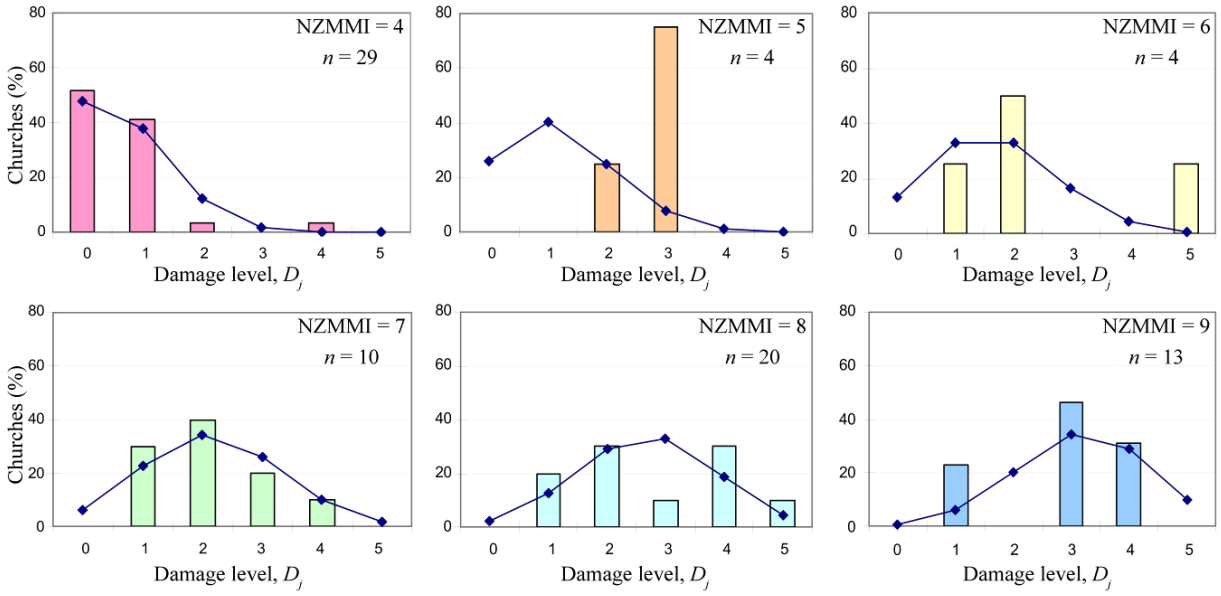

Figure 3.10. Damage Probability Matrices and binomial distribution of the 80 observed churches for given intensities.

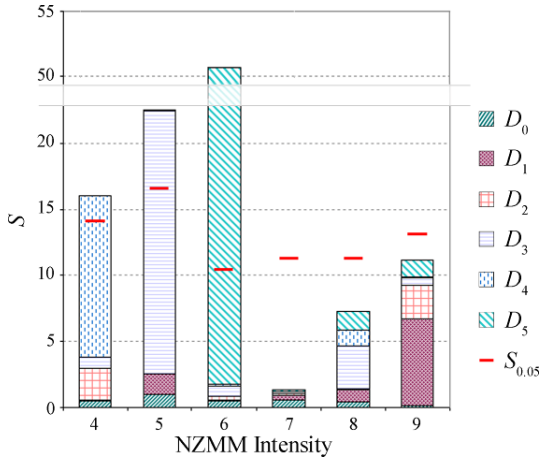

Figure 3.11. Goodness-of-fit test of the 80 observed churches for given intensities. The contribution of each damage level to the statistic *S*, Eq. (6), is reported. The ordinate values are cut between approximately 25 and 50.

3.4.2. Damage probability matrices for local damage

Because local collapse mechanisms are identifiable in autonomous structural parts of churches, an individual analysis of each mechanism is here developed. This approach was explored by Liberatore et al. (2009) on 86 churches and by De Matteis et al. (2014) for groups of mechanisms on a sample of 26 three-nave churches.

Here the damage histograms and the binomial fitting are computed for all the relevant mechanisms based on direct observations. The mean damage, μ_D, is now computed according to:

$$\mu_D = \frac{\sum_{j=1}^{n_I} d_j}{n_I} \tag{7}$$

where d_j is the damage score assigned to the mechanism, ranging again between 0 and 5. A selection of the outcomes is presented in Figure 3.12 while all 20 cases are showed in Appendix B, showing that for some mechanisms the probabilistic approach is improved compared to the DPMs proposed for the global performance of churches (Figure 3.10). The underperformance of the global damage levels, D_j, can be interpreted as the effect of the summation of diverse mechanism damage scores, d_k, for the same macroseismic intensity. In some of the DPMs proposed for local mechanisms (see Figure 3.12) it is possible to observe a flatness in the damage distribution, even for increasing intensity, suggesting that heavy damage for medium intensities shows a high vulnerability of some macro-element, whereas little or no damage in churches strongly shaken indicates a successful design.

In order to verify if a better correlation occurs between the observed damage and a different statistical distribution, a beta distribution is also used to fit the empirical data (Giovinazzi and Lagomarsino, 2005; Lallemant and Kiremidjian, 2015). The beta distribution is a family of continuous probability distributions defined on the interval [0, 1] and parametrized by two positive parameters, α and β, that are the exponents of the random variable controlling the shape of the distribution.

$$p(d_j) = \frac{d_j^{\alpha-1}(1-d_j)^{\beta-1}}{B(\alpha-\beta)} \tag{8}$$

where $B(\alpha, \beta)$ is the beta function and α, β are > 0 and computed through the Maximum Likelihood Estimation method (the small size of the samples makes the method of moments unsuitable for the computation of the parameters α and β).

Although the beta distribution can model various shapes of damage distribution, similar results are obtained with respect to the binomial distribution (Figure 3.13), confirming discrepancies between the statistical distributions and the probabilistic functions. These

observations are probably due to the paucity of data, especially for some intensities, and to the fact that the intensity measure alone is not adequate in explaining the damage.

Similarly to the procedure employed to assess global damage, the goodness-of-fit test was performed for each mechanism of the corresponding damage probability binomial distribution by calculating the statistic *S*, Eq. (6), and its distribution. Figure 3.14 shows the observed values of the statistic for the same two mechanisms addressed in Figure 3.12 and the comparison with the critical values for the significance level $S_{0.05}$. The goodness-of-fit test of all mechanisms is presented in Appendix C, and it appears that the DPM approach works well for some mechanisms, but is less effective for those mechanisms where there are no substantial differences compared to the global analysis. Once again the results confirm that the macroseismic intensity alone is not able to fully explain the observed damage, and that vulnerability factors need to be accounted for.

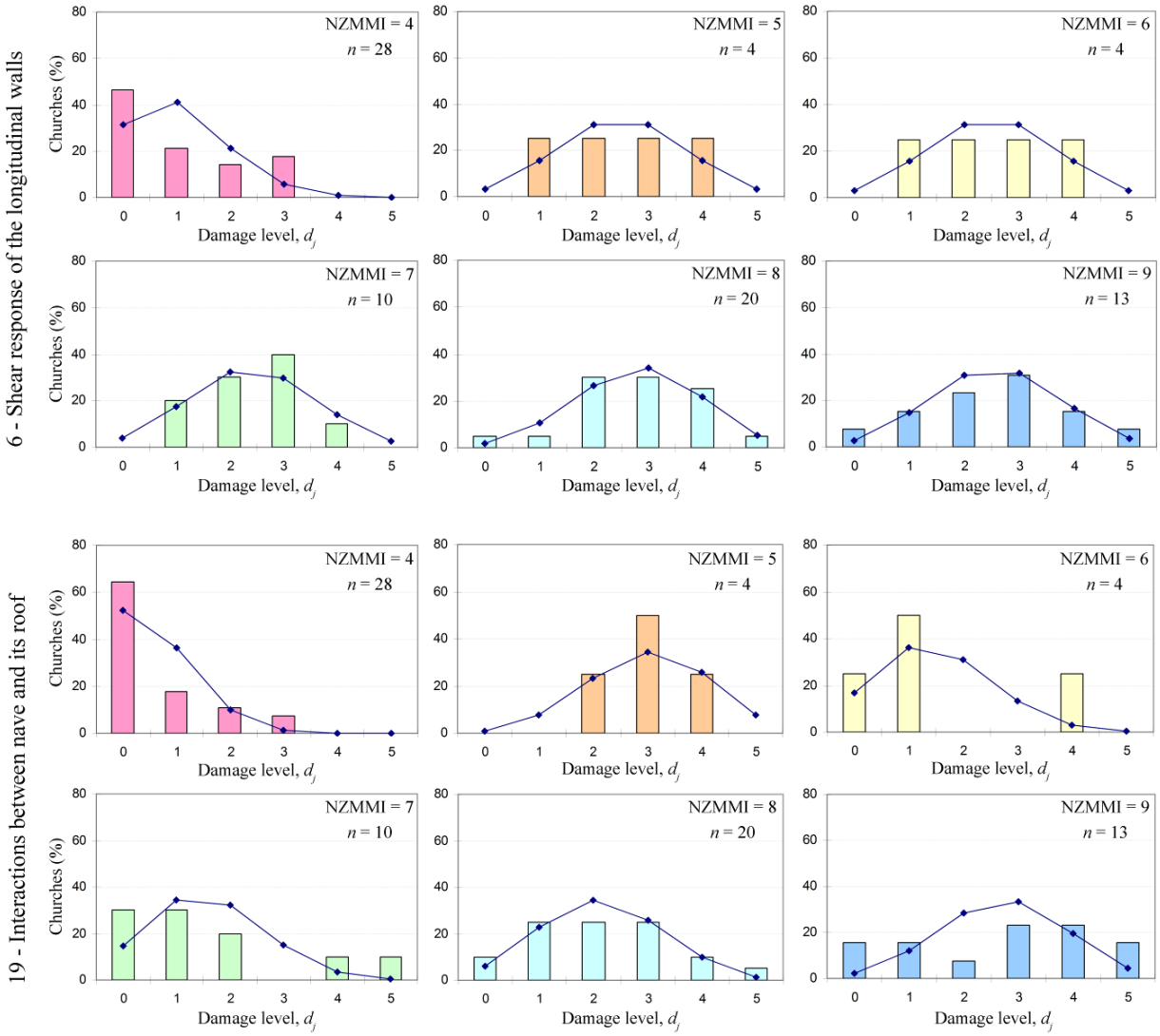

Figure 3.12. Damage Probability Matrix and binomial distribution for two of the 20 considered mechanisms (refer to Figure 3.3).

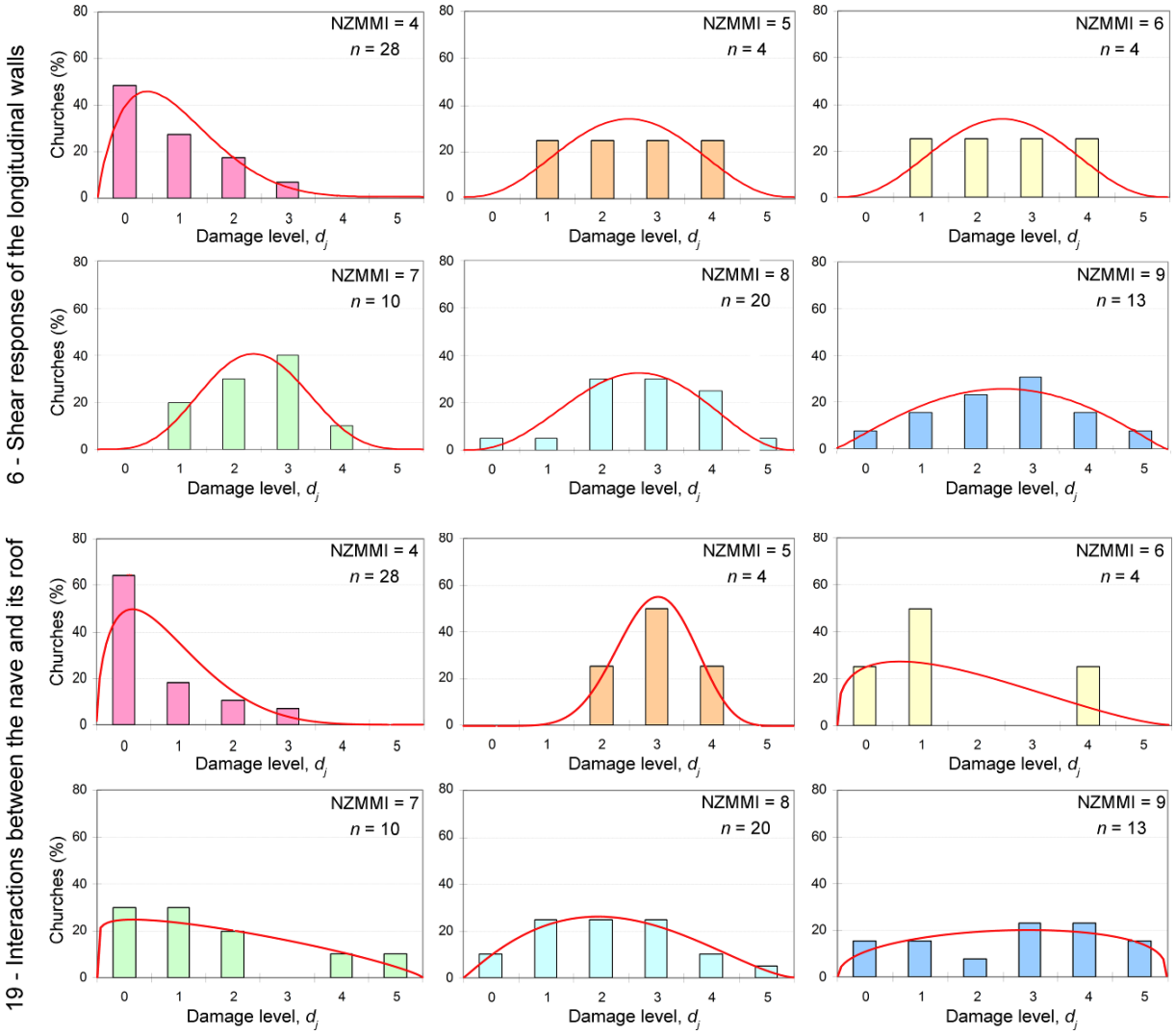

Figure 3.13. Damage Probability Matrix and beta distribution for two of the 20 considered mechanisms (refer to Figure 3.3).

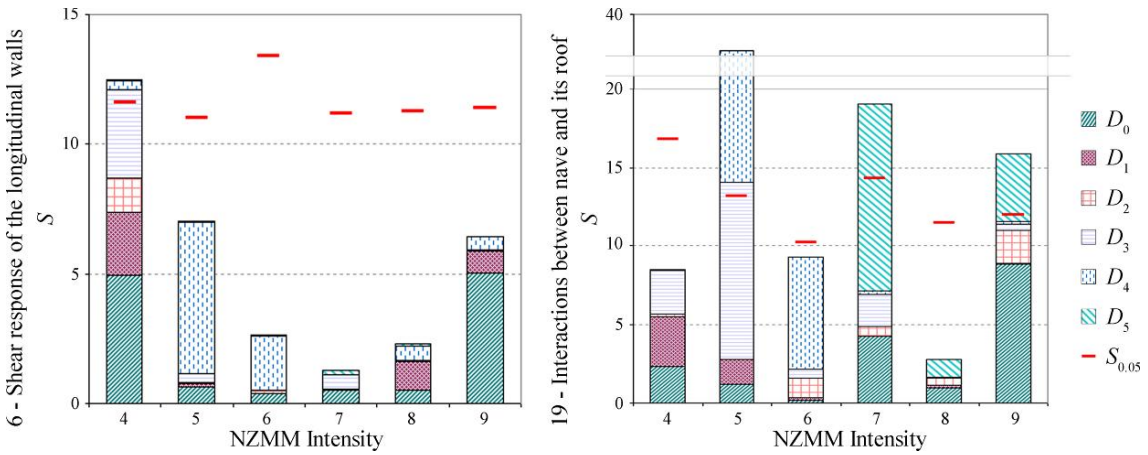

Figure 3.14. Goodness-of-fit test for two of the 20 considered mechanisms.

3.5. Correlation between mechanisms

Additional attempts were made considering groups of mechanisms and groups of intensities, as also suggested in De Matteis et al. (2014). In the first case out-of-plane mechanisms (#1-10-16), façade mechanisms (#2-3-4), lateral walls mechanisms (#6-11-17), roof mechanisms (#19-20-21), and bell tower mechanisms (#27-28) were collectively considered, whereas in the second case intensities were merged according to the following scheme: 4-5 NZMMI, 6-7 NZMMI, 8-9 NZMMI. Neither attempts markedly improved the agreement between statistical and binomial distributions, compared to those previously presented. A possible correlation between the considered mechanisms was investigated through the computation of the Pearson coefficient, measuring the linear correlation between two variables, and ranging between -1, when there is a perfect negative correlation, 0, when there is no correlation, and 1, when there is a perfect positive correlation. The Pearson coefficient, $R_{c,r}$, is defined as the covariance of the two variables considered (d_c, d_r) divided by the product of their standard deviations:

$$R_{c,r} = \frac{\sigma_{d_c,d_r}}{\sigma_{d_c}\sigma_{d_r}} = \frac{\sum_{i=1}^{n}\left(d_{c,i} - \overline{d_c}\right)\left(d_{r,i} - \overline{d_r}\right)}{\sqrt{\sum_{i=1}^{n}\left(d_{c,i} - \overline{d_c}\right)^2 \sum_{i=1}^{n}\left(d_{r,i} - \overline{d_r}\right)^2}} \tag{9}$$

where $d_{c,i}$ and $d_{r,i}$ = damage level of two mechanisms c and r of the i-th church out of n; σ_{d_c,d_r} = covariance; σ_{d_c} and σ_{d_r} = standard deviations; $\overline{d}_c$ and $\overline{d}_r$ = mean values.

The correlation coefficients between mechanisms (Figure 3.15) are fairly various, ranging between 0.29 and 0.95, but mainly rather high (> 0.5), not disproving the hypothesis of an autonomous response of each macro-element, because the most correlated mechanisms concern structural responses activated by parallel seismic actions (e.g., transversal response of the nave, #5, and behaviour of the triumphal arch, #13; shear mechanism of the longitudinal walls, #6 and overturning of the apse, #16). The lowest values of correlation ($R_{c,r}$ = 0.29) are found for mechanisms related to projections (#26) and triumphal arch (#13) and to the transversal response of the nave (#5) and the bell tower (#27), which is a reasonable result considering that an undamaged bell tower, located on one side of the church, benefits the nave of a transversal restraint. The highest value of the Pearson coefficient concerns the

overturning of transept (#10) and chapels (#22), which once again is a reliable outcome when recognising how two structural parts of the church respond to seismic action oriented transverse to the nave. Figure 17 can thus guide possible merging of different but correlated mechanisms.

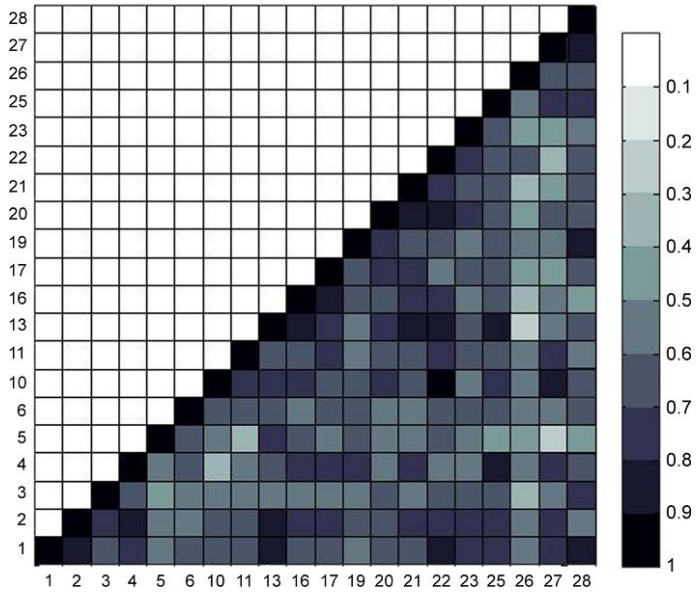

Figure 3.15. Correlation between mechanisms: 1 implies a total positive correlation.

3.6. Regression models

3.6.1. Simple-linear regressions

Similarly to the procedure for the global damage index, i_d, linear regression between the mean damage of each mechanism and the macroseismic intensity was investigated to evaluate their straight-line relationships according to the equation:

$$y_{pred} = b + mx + \varepsilon \tag{10}$$

where y_{pred} is the predicted value of damage for a given x that represents the NZMM intensity, b is the intercept, m is the regression coefficient and ε is the error term.

Sample regressions are presented in Figure 3.16, where a bubble chart is assumed to emphasise the different occurrence of damage levels and where a weak correlation can be graphically observed. Bubble charts of all 20 mechanisms are reported in Appendix D.

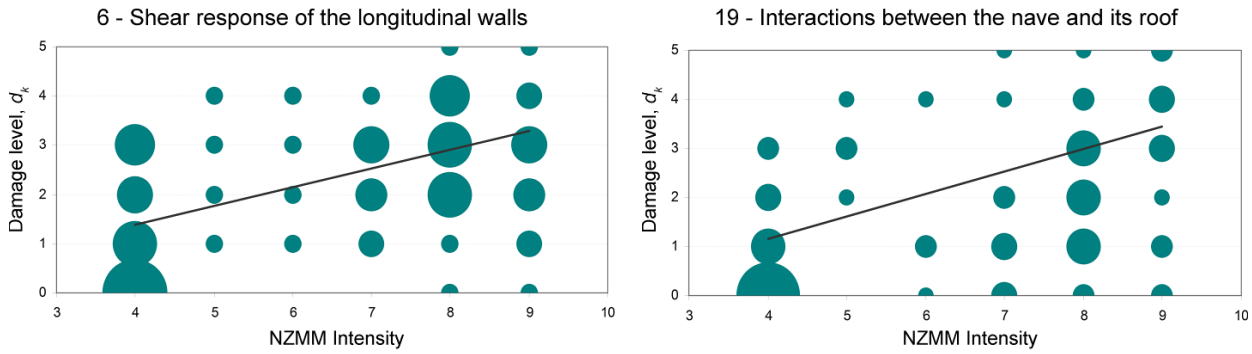

Figure 3.16. Linear regressions between occurred damage levels and macroseismic intensity for sample mechanisms.

The goodness of fit of the model can be quantitatively evaluated through the coefficient of determination, R^2, reported in Figure 3.20 (left-most column for each mechanisms), where low values occurring in most cases indicate that simple-linear regression is not sufficient to explain damage occurrence.

3.6.2. Multiple-linear regressions

Although referring to single mechanisms, simple regressions neglect the difference in the vulnerability of different churches subjected to the same level of shaking. As shown in Figure 3.17, vulnerability depends on structural details that can worsen the seismic performance (e.g., poor masonry quality, large openings, thrusting structures) or improve seismic performance through earthquake-resistant elements (e.g., connections between walls and to horizontal structures, buttresses, tie rods). For this reason, such vulnerability modifiers were included in the survey, as already envisaged by the Italian simplified procedure for seismic vulnerability assessment of churches (DPCM, 2011). The Italian procedure is based on previous research by Lagomarsino et al. (2004), who used modifiers to obtain a global vulnerability index. In the following the influence of each vulnerability modifier on each mechanism is addressed in a disaggregated fashion and the corresponding equations are derived. Moreover, the Italian procedure suggests a limited number of modifiers for each mechanism, without differentiating between the relevance of each modifier with respect to the others, whereas hereinafter all applicable modifiers are considered for all mechanisms, and their influence is quantified.

In order to consider more than one predictor variable, in the computation of the expected damage and in addition to the macroseismic intensity, the vulnerability level of each mechanism of each church was evaluated by resorting to multiple-linear

regressions. The accounted for v explanatory variables, x_v, and the response, y_{pred}, are fitted by a linear formulation, according to the following equation:

$$y_{pred} = b + m_1 x_1 + m_2 x_2 + ... + m_v x_v + \varepsilon \quad (11)$$

where x_1 represents at all times the NZMM intensity and x_2, x_3 … x_v are the vulnerability modifiers considered, m_1, m_2, …m_v are the regression coefficients, b is the intercept and ε is the error term. For each mechanism all relevant modifiers were considered, but the absence of some modifiers (e.g., tie rods in the triumphal arch mechanism) has resulted in a different set of modifiers for each of the 20 mechanisms analysed.

(a) St. John of God Chapel, Halswell, Christchurch

(b) St. Barnabas', Fendalton, Christchurch

(c) St. Andrew the Apostle, Geraldine

(d) Christchurch North Methodist, Papanui, Christchurch

Figure 3.17. Examples of vulnerability modifiers: (a-b) presence/lack of buttresses; (c-d) presence/lack of a horizontal element able to absorb the thrust of the roof.

Given the uncertainties in the estimation of the vulnerability modifiers, initially they are assumed as dichotomous variables, often called “dummy” variables. These variables work as qualitative indicators of either the absence or presence of a characteristic, scoring 1 if a fragility increaser is present or if an earthquake-resistant element is absent and scoring 0 otherwise. Besides predicting the value of the damage in a more accurate way, multiple-linear regression analyses allow the strength of the relationship between damage and vulnerability modifiers to be quantified. In fact, the regression coefficients represent the rate of change of the response y_{pred} as a function of changes in the other x_v variables and are computed using the least squares method (Benjamin and Cornell, 1970).

The customary statistical checking tests carried out for each regression model were detection of multicollinearity, test of significance, and examination of residuals. Such examinations are useful for confirming the reliability of the models, selecting the best regression equation and assessing which parameters have closer relationships with damage. Multicollinearity is defined as high correlation between the predictor variables (in our case the vulnerability modifiers), so that one of them can be linearly predicted from the others. The detection of multicollinearity was performed by means of the variance inflation factor (VIF_j), which provides an index that measures how much the variance is increased because of collinearity and is computed according to the following equation:

$$VIF_j = \frac{1}{1 - R_j^2} \tag{12}$$

where R^2_j = coefficient of determination of the regression equation with x_j dependent variable and all other variables included in the model. Following Snee (1973), multicollinearity was excluded for $VIF_j < 5$, and in the case at hand this value was never exceeded (Table 3.2).

Another issue to be investigated in a regression analysis concerns the test of significance, which excludes a relationship (null hypothesis) between the dependent variable, y_{pred}, and the i-th independent variable, x_i, included in the regression model. To perform the test of significance it is necessary to preliminarily carry out the z-test, according to the distribution of the data under the null hypothesis can be approximated

by a normal distribution (with mean = 0 and standard deviation = 1), and the test statistic, z_0, can be defined as:

$$z_0 = \frac{\bar{y} - \bar{y}_{pred}}{\sigma / \sqrt{n}} \tag{13}$$

where $\bar{y}$ = observed mean; $\bar{y}_{pred}$ = predicted mean; and $\sigma/\sqrt{n}$ = standard error, being the ratio between the standard deviation (σ) and the square root of the sample size (n).

The test statistic, z_0, is used to check the null hypothesis through the so-called *P*-value:

$$P\text{-value} = P\left(z < -|z_0| \; or \; z > |z_0|\right) \tag{14}$$

The smaller the *P*-value, the greater the evidence against the null hypothesis. Following Fisher (1925), the null hypothesis was rejected whenever *P*-value < 0.05. In Table 3.3 an example of the computation of the *P*-value is given for mechanism 1: it is possible to observe a lack of dependency between damage and buttresses, tie rods, top beam and lateral restraint. These results are related to specific features of New Zealand churches, which frequently have ties that are spaced too far apart, small wall anchors and buttresses, and poor quality masonry. Top beams are seldom present, whereas lateral restraints are usually small compared to the façade, and hence do not influence the regressions. After the test of significance some modifiers were removed from the multiple linear regressions.

The last check performed was the analysis of residuals, defined as the differences between the observed values and the values estimated by the regression. The usual assumption when performing a regression analysis is that residuals are independent, have zero mean, constant variance and follow a normal distribution, and if the predictive model is correct then the residuals should exhibit trends that do not contradict the above-mentioned assumptions. Therefore, the residual plots were analysed for each independent variable involved in the regressions, confirming the reliability of the model when the plot gives the overall impression of an approximately horizontal band. This requirement was met for almost all of the vulnerability modifiers considered here, except for those present in very few buildings (Figure 3.18).

The examination of the relationship between damage observed and damage predicted confirms that multiple regression models, accounting for vulnerability modifiers, allow better forecasting of the damage, as shown in Figure 3.19 for some of the mechanisms,

while the whole portfolio in reported in Appendix E. This trend confirms that the intensity measure alone is not sufficient for a reliable estimation of the expected damage, whereas construction details and materials are fundamental to understanding the seismic behaviour of historical buildings.

Table 3.2. Coefficients R^2_j and VIF_j of the x_j dependent variable of mechanism no.1.

	R^2_j	VIF_j
x_1 and other x	0.114	1.247
x_2 and other x	-0.020	1.082
x_3 and other x	0.273	1.519
x_4 and other x	0.058	1.172
x_5 and other x	-0.024	1.078
x_6 and other x	-0.036	1.065
x_7 and other x	0.015	1.121
x_8 and other x	0.122	1.258

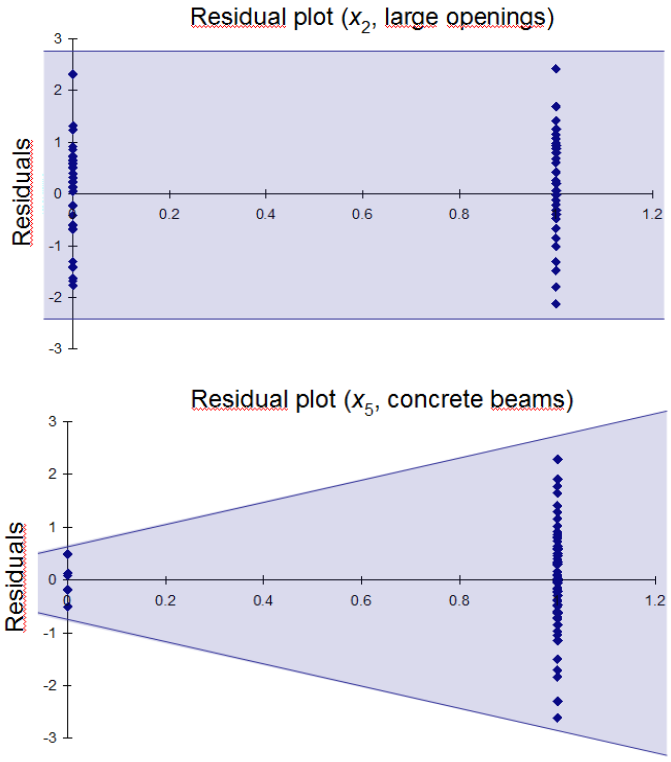

Figure 3.18. Analysis of residuals for two of the variables accounted for in mechanism no. 1.

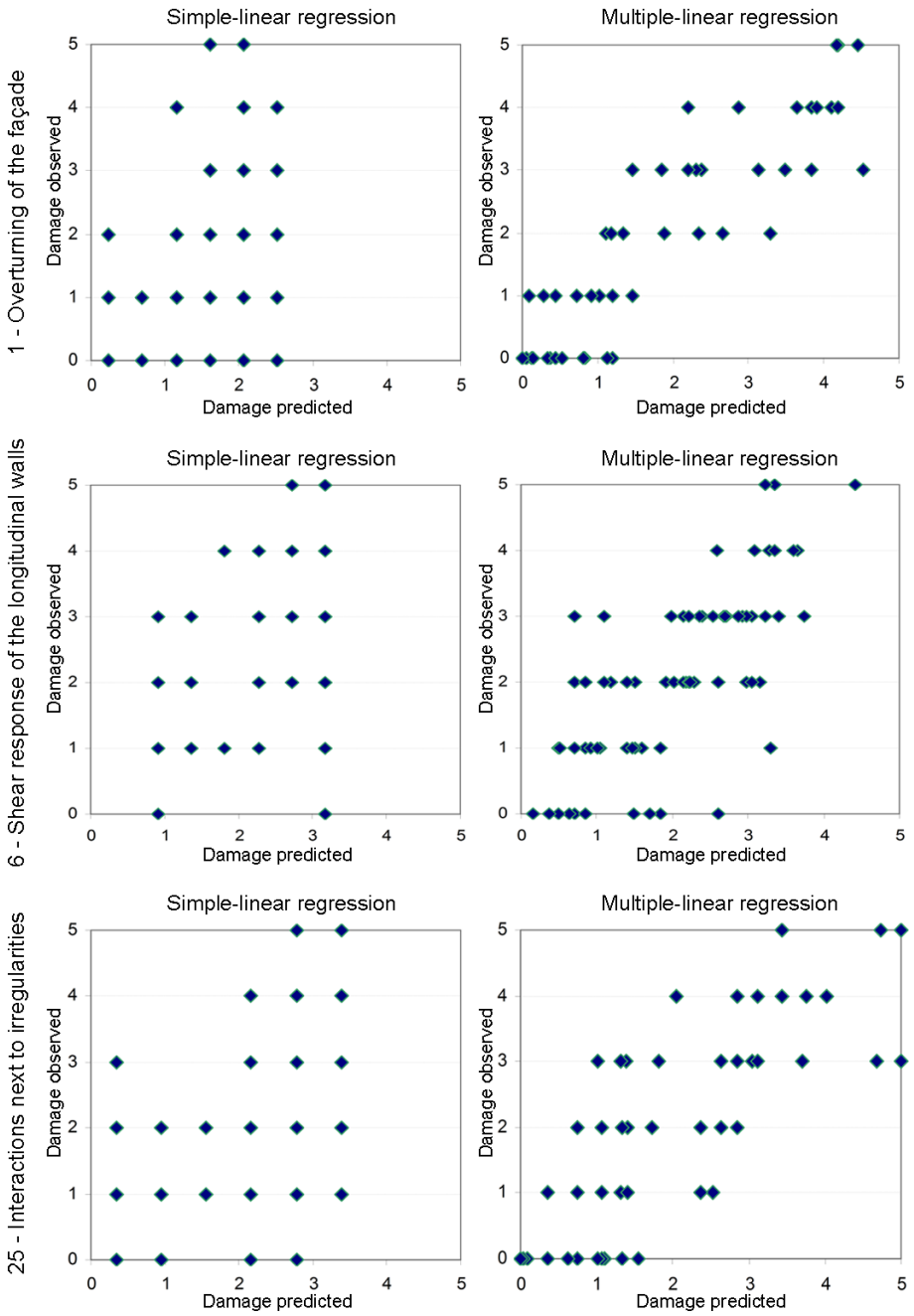

Figure 3.19. Comparison in the correlation between damage observed and damage predicted using simple- or multiple-linear regression models for sample mechanisms.

More accurate statistical are used in the following to identify those parameters that can be neglected, while providing a better damage prediction. The *stepwise* selection method allows the determination of the variables that generate the most efficient predictive model, involving the inserting of variables in turn until the regression equation is satisfactory (Draper and Smith, 1981). The *best subsets* procedure selects the subset of parameters optimising an objective criterion, such as having the largest coefficient of determination R^2.

Table 3.3. Coefficients *m* and *P*-value of the multiple-linear regression of mechanism no.1.

	m	***P*-value**
x_1 (NZMMI)	0.349	0.000
x_2 (Connections)	0.865	0.033
x_3 (Buttresses)	-0.078	0.676
x_4 (Tie rods)	-0.010	0.982
x_5 (Thrusting elements)	1.689	0.003
x_6 (Large openings)	0.538	0.011
x_7 (Top beam)	0.132	0.738
x_8 (Lateral restraint)	-0.279	0.171
x_9 (Poor quality masonry)	1.011	0.000
x_{10} (Slenderness)	0.852	0.008

Table 3.4. Comparison between the R^2 for the simple-linear regression and R^2_{adj} for all multiple-linear regression of all the considered mechanisms (SR = Simple-linear regression; MR = Multiple-linear regression; S = *Stepwise* procedure; BS = *Best Subsets* procedure).

Mech. no.	R^2	R^2_{adj}			**Mech. no.**	R^2	R^2_{adj}		
	SR	***MR***	***S***	***BS***		***SR***	***MR***	***S***	***BS***
1	0.461	0.829	0.829	0.837	***17***	0.260	0.539	0.543	0.556
2	0.456	0.751	0.757	0.766	***19***	0.308	0.537	0.516	0.555
3	0.344	0.549	0.557	0.567	***20***	0.096	0.292	0.442	0.442
4	0.320	0.835	0.828	0.841	***21***	0.220	0.613	0.694	0.694
5	0.386	0.674	0.670	0.682	***22***	0.485	0.706	0.726	0.728
6	0.430	0.530	0.542	0.546	***23***	0.517	0.672	0.670	0.694
10	0.348	0.801	0.820	0.820	***25***	0.417	0.689	0.670	0.690
11	0.330	0.382	0.455	0.455	***26***	0.287	0.445	0.330	0.445
13	0.520	0.884	0.881	0.884	***27***	0.562	0.745	0.734	0.765
16	0.371	0.790	0.780	0.797	***28***	0.394	0.777	0.816	0.816

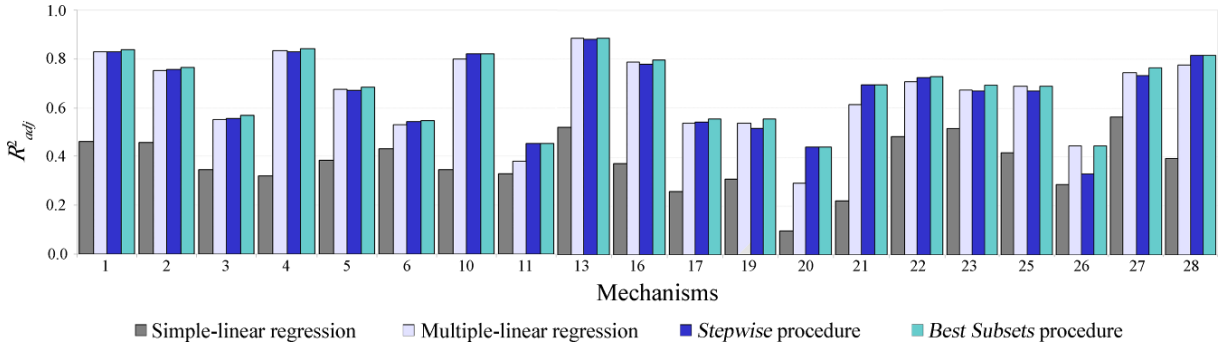

Figure 3.20. Comparison between the R^2_{adj} for all regression models (for the simple-linear regression, it is the value of R^2).

The coefficient of determination R^2 was computed for all regression models, indicating how well the statistical model fits the data. Because when more than one variable is considered R^2 automatically increases, for multiple linear regressions the adjusted coefficient of determination, R^2_{adj}, has been used:

$$R^2_{adj} = 1 - \left[\left(1 - R^2\right) \frac{n-1}{n-v} \right] \tag{15}$$

where v is the number of considered vulnerability modifiers. In Figure 3.20 and Table 3.4 it can be noted that for any of the three multiple regressions a systematic increase in the value of the adjusted coefficient of determination R^2_{adj} is observed with respect to the coefficient of determination R^2 computed for the simple-linear regressions. The average increase of the three multiple-linear regressions is about 90%, with a very marked improvement for mechanisms #20 and #21 (interaction between transept or apse and their roof), #16-17 (apse, out-of- and in-plane), and #28 (belfry). This trend confirms that the intensity measure alone is not sufficient for a reliable estimation of the expected damage, whereas construction details and materials are fundamental to understanding the seismic behaviour of historical buildings.

Modifiers can be compared against each other (Figure 3.21 and Table 3.5), in order to recognise those modifiers that are most relevant. Poor quality masonry was introduced in the regressions as a unity value for the case of undressed natural stone units or the presence of cavity walls (Figure 3.22), and was found to be crucial for at least ten mechanisms (#1, #4, #13, #19-22, and #25-28). It is notable that the Italian procedure does not suggest this modifier for mechanisms #1, #4, #19-22, #25, and #28. High slenderness noticeably influenced seven mechanisms (#2, #3, #11, #16, #17, #23, and #28). This modifier was implemented when the estimated height/thickness ratio of the façade exceeded a value of 25, and when the ratio between the height of the longitudinal walls and their thickness exceeded 15, where both limiting values were higher than the average ratio identified by §2.4.3 for New Zealand churches. Again, it is noted that the Italian procedure does not suggest this modifier for mechanism #16. Connections, introduced in the regressions both in the case of interlocking between orthogonal walls and of wall anchors linked to the horizontal structures, were found to markedly affect six mechanisms (#2, #4, #5, #10, #16, and #27), and again the Italian procedure does not suggest this modifier for mechanisms #4, #5, and #16. Other parameters, such as thrusting elements (e.g., roofs without a bottom chord or arches), large openings (whose

combined length exceeds 1/3 of the wall length), heterogeneous materials (both in two adjacent architectural parts and within a single structural element) and top ring beams, are relevant for specific mechanisms.

Unexpectedly, it was found that buttresses, which are present in most New Zealand churches, only slightly influenced the predicted damage. This observation can be explained by the significant spacing usually observed between buttresses (Figure 3.23a), their small depth compared to the wall thickness (Figure 3.23b), the poor quality of their masonry (Figure 3.23c), or failure of the poor quality masonry walls that they were meant to strengthen (Figure 3.23d). As already shown, for several mechanisms the poor quality masonry parameter was the most important in the regression. Similarly to buttresses, tie rods appear to have a rather limited relevance on earthquake performance, although they were present in only five buildings. This limited effectiveness of tie appears to be associated with the use of small wall anchors positioned close to the wall top (Figure 3.23e) or because the tie rods were spaced too far apart (Figure 3.23f). Hence, this observation is not meant to discourage future use of tie rods, but rather to point out that their presence will not automatically improve the seismic performance of a church. Modifiers that do not have a strong influence on the regressions are the presence of a lateral restraint (such as an adjacent building or a bell tower), asymmetry conditions (e.g., due to eccentricity of a projection with respect to the underlying masonry, or due to juxtaposition of a new extension), and braced roof pitches.

Finally, the comparison between the three multiple regressions shows that in all cases the *best subsets* has an R^2_{adj} value substantially larger than that of the multiple-linear regression and marginally larger than that of the *stepwise* regression. Nonetheless, the *stepwise* regression considers a smaller, or occasionally an equal, number of predictor variables, suggesting its selection for a faster territorial scale vulnerability assessment. In Table 3.6 the coefficients defining the multiple-linear regressions of the 20 considered mechanisms computed through the *stepwise* procedure are numerically presented. The modifiers added with respect to those suggested by the DPCM February, 9 2011 (DPCM, 2011) are also highlighted therein boldface. The derived equations can be consequently used in future risk assessments, provided that the expected NZMM intensities for specific locations are available. Such hazard information is currently not available for New Zealand, whereas Peak Ground Acceleration (PGA) hazard maps have been published in recent years (Stirling et al., 2012). Hence, at least as a preliminary attempt, a correlation law between ground-motion parameters and

macroseismic intensity could be used, e.g., referring to Anbazhagan et al. (2015). Alternatively, the same method presented here can be used to derive multiple-linear regressions, with the selected intensity measure being a ground-motion parameter for which hazard maps are available.

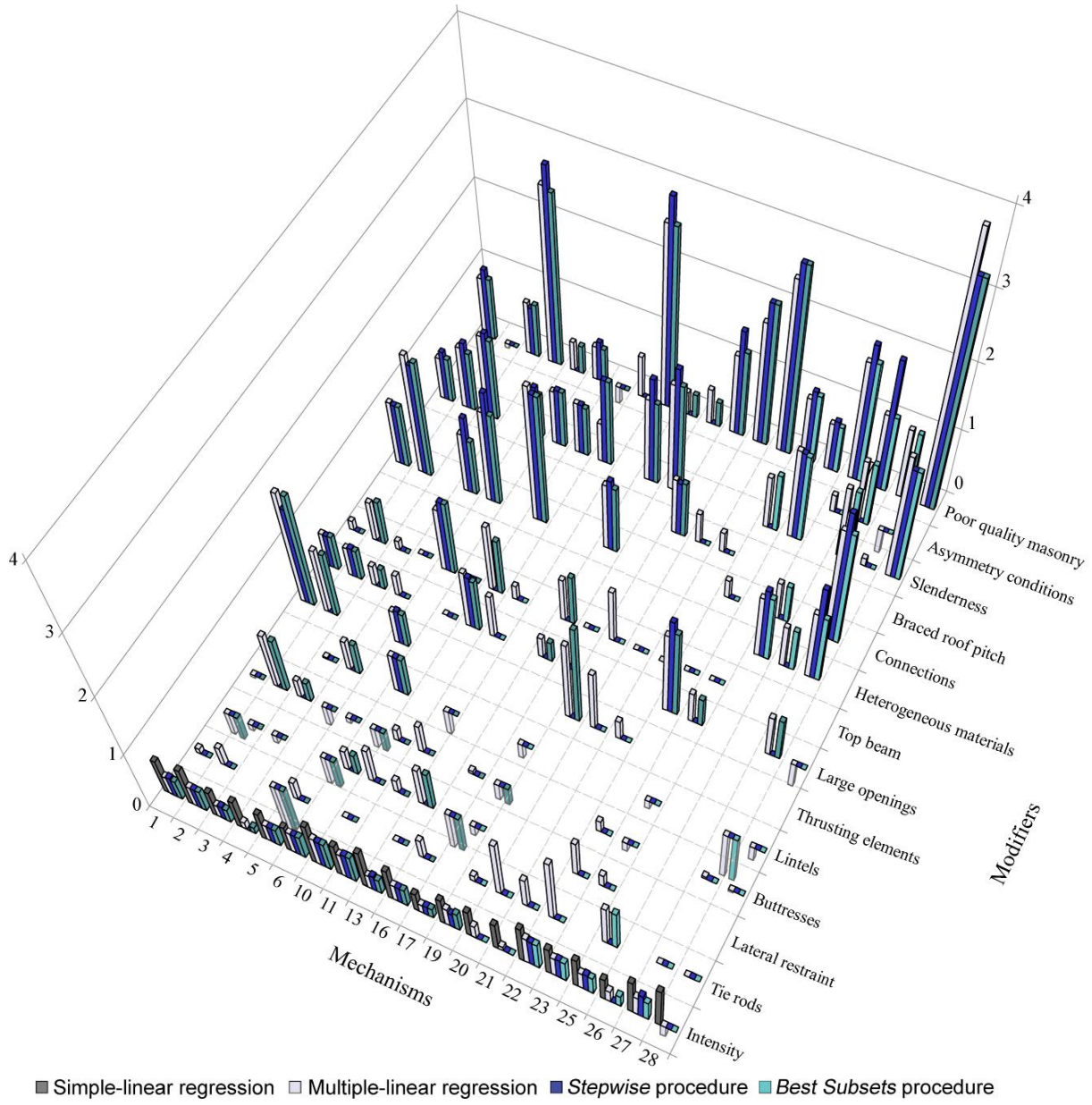

Figure 3.21. Comparison between the regression coefficients for all the regression models among all the considered mechanisms (refer to Figure 3.3).

Table 3.5. Comparison between the regression coefficients for all the regression models. (SR: simple-linear regression, MR: multiple-linear regression, S: *Stepwise* procedure, BS: *Best Subsets* Procedure).

Mech. no.		*SR*	*MR*	*S*	*BS*
1	*b* (intercept)	-2.347	-1.700	-1.836	-1.482
	Intensity measure	0.590	0.326	0.352	0.323
	Tie rods		0.088		
	Lateral restraint		-0.385		-0.402
	Buttresses		-0.045		
	Thrusting elements		1.775	1.545	1.784
	Large openings		0.530	0.524	0.539
	Top beam		0.150		
	Heterogeneous material		0.436		0.427
	Connections		0.953	0.938	0.940
	Slenderness		0.624	0.741	0.652
	Poor quality masonry		0.880	1.026	0.901
2	*b* (intercept)	-2.201	-3.122	-1.558	-2.989
	Intensity	0.637	0.354	0.356	0.360
	Tie rods		0.313		
	Lateral restraint		-0.106		
	Buttresses		0.894		0.871
	Thrusting elements		1.026		1.021
	Large openings		0.459	0.482	0.469
	Top beam		0.617		0.683
	Heterogeneous material		0.926	1.012	0.875
	Connections		1.803	1.681	1.741
	Slenderness		-0.007		
	Poor quality masonry		-0.062		
3	*b* (intercept)	-1.331	-0.927	-0.673	-0.924
	Intensity	0.434	0.225	0.243	0.228
	Lateral restraint		-0.134		
	Buttresses		0.294		0.314
	Lintels		0.019		
	Large openings		0.322		0.327
	Top beam		0.137		
	Slenderness		1.223	1.296	1.202
	Poor quality masonry		0.775	0.716	0.779
4	*b* (intercept)	-1.745	0.769	0.109	0.710
	Intensity	0.487	0.125		0.108
	Tie rods		-1.358		-1.215
	Buttresses		-0.334		
	Lintels		0.491		0.501
	Large openings		0.334		
	Connections		0.907	1.185	0.841
	Poor quality masonry		2.534	2.809	2.478
5	*b* (intercept)	-1.658	-2.903	-2.270	-2.757
	Intensity	0.475	0.296	0.297	0.297
	Tie rods		0.307		
	Lateral restraint		0.504		0.494
	Buttresses		-0.086		
	Thrusting elements		0.543	0.573	0.546
	Top beam		0.991	1.138	1.133
	Connections		1.397	1.708	1.390
	Slenderness		0.636	0.756	0.656
	Poor quality masonry		0.434		0.419

Table 3.5. Comparison between the regression coefficients for all the regression models. (SR: simple-linear regression, MR: multiple-linear regression, S: Stepwise procedure, BS: Best *Subsets* Procedure). (continued)

Mech. no.		*SR*	*MR*	*S*	*BS*
6	*b* (intercept)	-0.899	-0.919	-0.801	-1.013
	Intensity	0.453	0.386	0.381	0.387
	Lateral restraint		0.339		0.334
	Buttresses		-0.348		-0.338
	Lintels		0.628	0.631	0.619
	Large openings		0.010		
	Top beam		-0.107		
	Poor quality masonry		0.502	0.591	0.501
10	*b* (intercept)	-2.752	-4.322	-2.616	-3.407
	Intensity	0.711	0.508	0.488	0.487
	Tie rods		0.000		
	Lateral restraint		0.570		
	Buttresses		0.193		
	Large openings		0.909	0.858	0.818
	Top beam		1.045		0.869
	Connections		2.064	1.968	1.961
	Slenderness		-0.025		
	Poor quality masonry		-0.254		
11	*b* (intercept)	-2.233	-2.733	-2.113	-2.113
	Intensity	0.564	0.436	0.469	0.469
	Lateral restraint		0.214		
	Buttresses		0.468		
	Lintels		-0.419		
	Large openings		0.683		
	Top beam		0.221		
	Slenderness		0.600	1.290	1.290
	Poor quality masonry		0.619		
13	*b* (intercept)	-2.865	-1.101	-1.250	-1.101
	Intensity	0.676	0.256	0.292	0.256
	Tie rods		0.000		
	Lateral restraint		0.638		0.638
	Poor quality masonry		2.638	3.000	2.638
16	*b* (intercept)	-1.906	-1.752	-1.158	-1.533
	Intensity	0.559	0.307	0.313	0.311
	Tie rods		0.330		
	Lateral restraint		-0.670		-0.651
	Buttresses		0.057		
	Large openings		0.322		0.314
	Top beam		0.679		0.785
	Connections		1.029	1.121	1.020
	Slenderness		1.263	1.589	1.245
	Poor quality masonry		0.343		0.346
17	*b* (intercept)	-1.021	-0.113	-0.391	-0.288
	Intensity	0.338	0.158	0.168	0.170
	Lateral restraint		-0.179		
	Buttresses		-0.285		-0.301
	Lintels		-0.255		
	Large openings		0.106		
	Slenderness		1.627	1.878	1.648
	Poor quality masonry		0.522		0.366

Table 3.5. Comparison between the regression coefficients for all the regression models. (SR: simple-linear regression, MR: multiple-linear regression, S: Stepwise procedure, BS: Best *Subsets* Procedure). (continued)

Mech. no.		*SR*	*MR*	*S*	*BS*
19	*b* (intercept)	-0.867	-2.935	-0.656	-2.372
	Intensity	0.475	0.332	0.275	0.326
	Tie rods		0.101		
	Thrusting elements		1.264		1.597
	Top beam		0.832		
	Braced roof pitch		0.863	0.826	0.853
	Poor quality masonry		1.189	1.567	1.274
20	*b* (intercept)	-1.573	-2.595	1.000	1.000
	Intensity	0.490	0.234		
	Tie rods		0.974		
	Thrusting elements		0.957		
	Braced roof pitch		0.462		
	Poor quality masonry		1.802	2.100	2.100
21	*b* (intercept)	-1.576	-0.805	0.444	0.444
	Intensity	0.492	0.071		
	Tie rods		0.521		
	Thrusting elements		0.309		
	Braced roof pitch		0.313		
	Poor quality masonry		2.528	2.756	2.756
22	*b* (intercept)	-2.866	-4.427	-2.545	-2.513
	Intensity	0.682	0.517	0.493	0.491
	Tie rods		1.113		
	Lateral restraint		0.613		
	Buttresses		0.194		
	Large openings		1.317	1.576	1.403
	Connections		0.284		
	Slenderness		0.805		0.887
	Poor quality masonry		0.962	1.091	1.043
23	*b* (intercept)	-1.921	-2.661	-1.555	-2.640
	Intensity	0.512	0.372	0.386	0.377
	Lateral restraint		0.214		
	Buttresses		-0.159		
	Lintels		-0.145		
	Large openings		0.495		0.461
	Top beam		1.150		1.098
	Slenderness		1.380	1.364	1.334
	Poor quality masonry		0.715	0.773	0.703
25	*b* (intercept)	-1.921	-2.661	-1.555	-2.640
	Intensity	0.512	0.372	0.386	0.377
	Lateral restraint		0.214		
	Buttresses		-0.159		
	Lintels		-0.145		
	Large openings		0.495		0.461
	Top beam		1.150		1.098
26	*b* (intercept)	-0.683	-0.702	1.333	-0.702
	Intensity	0.428	0.213		0.213
	Heterogeneous material		0.665		0.665
	Slenderness		1.106		1.106
	Asymmetry		0.966		0.966
	Poor quality masonry		1.150	1.974	1.150

Table 3.5. Comparison between the regression coefficients for all the regression models. (SR: simple-linear regression, MR: multiple-linear regression, S: Stepwise procedure, BS: Best *Subsets* Procedure). (continued)

Mech. no.		*SR*	*MR*	*S*	*BS*
27	*b* (intercept)	-2.410	-1.374	-1.633	-1.334
	Intensity	0.654	0.367	0.461	0.362
	Buttresses		0.037		
	Lintels		-0.858		-0.857
	Large openings		0.669		0.682
	Connections		1.794	2.085	1.781
	Heterogeneous material		1.078	1.520	1.057
	Slenderness		0.117		
	Poor quality masonry		1.064		1.047
28	*b* (intercept)	-2.304	1.699	0.380	0.380
	Intensity	0.757	-0.223		
	Buttresses		-0.031		
	Lintels		-0.252		
	Large openings		-0.409		
	Slenderness		1.902	1.718	1.718
	Poor quality masonry		3.925	3.352	3.352

(a) St. Cuthbert's, Governors Bay

(b) Holy Trinity, Lyttleton (demolished)

(c) Church of the Good Shepherd, Phillipstown, Christchurch (demolished)

(d) St. Luke's, Central Christchurch (demolished)

Figure 3.22. Examples of poor quality masonry: (a-b) undressed natural stone units; (c-d) cavity walls. Photos (b-c-d) are courtesy of João Leite.

(a) St. Cuthbert's, Governors Bay

(b) Christchurch North Methodist, Papanui, Christchurch

(c) ChristChurch Cathedral, Central Christchurch

(d) Lyttelton Union, Lyttelton (demolished)

(e) New Brighton Union, New Brighton, Christchurch (demolished)

(f) St. John the Evangelist, Okains Bay

Figure 3.23. Examples of limited effectiveness of earthquake-resistant elements: (a-b-c-d) buttresses; (e-f) tie rods. Photos (d-e) are courtesy of João Leite.

Table 3.6. Regression coefficients of the *stepwise* models. Modifiers added with respect to the DPCM February, 9 2011 are boldface.

Mechanism no. / Variable	*1*	*2*	*3*	*4*	*5*	*6*	*10*	*11*	*13*	*16*
Intensity measure	0.352	0.356	0.243	N/A	0.297	0.381	0.488	0.469	0.292	0.313
Tie rods	N/A	N/A	N/A	N/A	N/A	N/A	N/A	N/A	N/A	N/A
Lateral restraint	N/A	N/A	N/A	N/A	N/A	N/A	N/A	N/A	N/A	N/A
Buttresses	N/A	N/A	N/A	N/A	N/A	N/A	N/A	N/A	N/A	N/A
Lintels	N/A	N/A	N/A	N/A	N/A	0.631	N/A	N/A	N/A	N/A
Thrusting elements	1.545	N/A	N/A	N/A	**0.573**	N/A	N/A	N/A	N/A	N/A
Large openings	0.524	0.482	N/A	N/A	N/A	N/A	0.858	N/A	N/A	N/A
Top beam	N/A	N/A	N/A	N/A	**1.138**	N/A	N/A	N/A	N/A	N/A
Heterogeneous materials	N/A	N/A	N/A	N/A	N/A	N/A	N/A	N/A	N/A	N/A
Connections	0.938	1.681	N/A	**1.185**	**1.708**	N/A	1.968	N/A	N/A	**1.121**
Braced roof pitch	N/A	N/A	N/A	N/A	N/A	N/A	N/A	N/A	N/A	N/A
Slenderness	**0.741**	1.012	1.296	N/A	0.756	N/A	**0.773**	1.290	N/A	**1.589**
Asymmetry conditions	N/A	N/A	N/A	N/A	N/A	N/A	N/A	N/A	N/A	N/A
Poor quality masonry	**1.026**	N/A	**0.716**	**2.809**	N/A	0.591	N/A	N/A	3.000	N/A
b (intercept)	-1.836	-1.558	-0.673	0.109	-2.270	-0.801	-2.616	-2.113	-1.250	-1.158

Mechanism no. / Variable	*17*	*19*	*20*	*21*	*22*	*23*	*25*	*26*	*27*	*28*
Intensity measure	0.168	0.275	N/A	N/A	0.493	0.386	0.341	N/A	0.461	N/A
Tie rods	N/A	N/A	N/A	N/A	N/A	N/A	N/A	N/A	N/A	N/A
Lateral restraint	N/A	N/A	N/A	N/A	N/A	N/A	N/A	N/A	N/A	N/A
Buttresses	N/A	N/A	N/A	N/A	N/A	N/A	N/A	N/A	N/A	N/A
Lintels	N/A	N/A	N/A	N/A	N/A	N/A	N/A	N/A	N/A	N/A
Thrusting elements	N/A	N/A	N/A	N/A	N/A	N/A	N/A	N/A	N/A	N/A
Large openings	N/A	N/A	N/A	N/A	1.576	N/A	N/A	N/A	N/A	N/A
Top beam	N/A	N/A	N/A	N/A	N/A	N/A	N/A	N/A	N/A	N/A
Heterogeneous materials	N/A	N/A	N/A	N/A	N/A	N/A	1.136	N/A	**1.520**	N/A
Connections	N/A	N/A	N/A	N/A	N/A	N/A	N/A	N/A	2.085	N/A
Braced roof pitch	N/A	0.826	N/A	N/A	N/A	N/A	N/A	N/A	N/A	N/A
Slenderness	1.878	N/A	N/A	N/A	N/A	1.364	N/A	N/A	N/A	1.718
Asymmetry conditions	N/A	N/A	N/A	N/A	N/A	N/A	N/A	N/A	N/A	N/A
Poor quality masonry	N/A	**1.567**	**2.100**	**2.756**	**1.091**	0.773	**2.049**	1.974	N/A	**3.352**
b (intercept)	-0.391	-0.656	1.000	0.444	-2.545	-1.555	-1.598	1.333	-1.633	0.380

3.7. Conclusions

The 2010-2011 Canterbury earthquakes affected at least 80 unreinforced masonry churches, 12 of which were demolished due to the suffered damage, demonstrating the inadequate seismic performance of churches due to their intrinsic structural fragility. Considering the high seismicity of New Zealand, the high exposure of human lives, and the societal significance of ecclesiastic buildings, for both historical and symbolic reasons, the reduction of the vulnerability of unreinforced masonry churches is a fundamental issue. In order to understand which churches are most vulnerable, the analysis and the interpretation of their observed performance is of great interest. Moreover, considering the homogeneity of churches across New Zealand, the

conclusions drawn for the Canterbury region can be reasonably extended to the whole national stock.

Because URM churches respond to earthquakes as a composition of macro-elements, the damage that occurred to the churches of the Canterbury region has been surveyed by accounting for 28 possible local collapse mechanisms. Only 20 of these mechanisms were developed in a statistically relevant number of churches, due to the comparatively simple architectural layout of New Zealand churches. Damage data has been interpreted mechanism by mechanism, and firstly analysed using Damage Probability Matrices (DPMs) that correlate discrete damage levels with shaking intensity. DPMs were also fitted with a binomial distribution, and reasonable agreement was observed in a few cases indicating the weakness of the basic assumption that damage can be explained by the severity of shaking alone, neglecting any difference in vulnerability. Consequently, additional modifiers that increase/reduce the vulnerability of the macro-elements were systematically introduced as "dummy" variables in multiple-linear regressions. Several statistical models were considered, in order to obtain the model having the largest coefficient of determination, together with the smallest number of relevant modifiers for a faster territorial scale application. The coefficients defining the multiple-linear regressions of 20 mechanisms were computed and among structural details, poor quality masonry, connections, and slenderness have the largest influence on damage. Once associated with the appropriate hazard scenario, the proposed regressions can deliver relevant information for the future assessment at territorial scale of the seismic vulnerability, for the emergency management and for the prioritisation of more in-depth analysis of individual buildings, both in New Zealand and in other regions possessing a similar churches stock.

Further development will involve the introduction of vulnerability modifiers in regressions accounting for their effectiveness, releasing the 0/1 alternative. Moreover, the regression equations will be re-evaluated with alternative intensity measures.

3.8. References

Anagnostopoulou, M., Bruneau, M. and Gavin, H. P. (2010). Performance of churches during the Darfield earthquake of September 4, 2010, *Bulletin of the New Zealand Society for Earthquake Engineering* 43(4), 374–381.

Anbazhagan, P., Sreenivas, M., Ketan, B., Moustafa, S.S. and Al-Arifi, N.S.N. (2015). Selection of Ground Motion Prediction Equations for Seismic Hazard Analysis of Peninsular India, *Journal of Earthquake Engineering*, doi: 10.1080/13632469.2015.1104747. In press.

Andreotti, C., Liberatore, D. and Sorrentino L. (2015). Identifying seismic local collapse mechanisms in unreinforced masonry buildings through 3D laser scanning, *Key Engineering Materials* 628, 79-84. doi:10.4028/www.scientific.net/KEM.628.79.

ATC - American Technology Council (1985). *Earthquake damage evaluation data for California*, Report 13, Redwood City, California.

Bannister, S. and Gledhill, K. (2012). Evolution of the 2010–2012 Canterbury earthquake sequence, *New Zealand Journal of Geology and Geophysics* 55(3), 295-304.

Benedetti, D. and Petrini, V. (1984). Sulla vulnerabilità sismica degli edifici in muratura: un metodo di valutazione, *L'Industria delle Costruzioni* 149, 66-74. In Italian.

Benedetti, D., Benzoni, G. and Parisi, M.A. (1988). Seismic vulnerability and risk evaluation for old urban nuclei, *Earthquake Engineering & Structural Dynamics* 16, 183–201. doi: 10.1002/eqe.4290160203.

Benjamin, J.R. and Cornell, C.A. (1970). *Probability, statistics and decision for civil engineers*, McGraw-Hill, New York.

Bernardini, A., Gori, R. and Modena, C. (1990). Application of coupled analytical models and experimental knowledge to seismic vulnerability analyses of masonry buildings, in *Engineering Damage Evaluation and Vulnerability Analysis of Building Structures*, ed A. Koridze (Omega Scientific, Oxon, U.K), pp. 161-180.

Bradley, B.A., Quigley, M.C., Van Dissen, R.J. and Litchfield, N.J. (2014). Ground motion and seismic source aspects of the Canterbury earthquake sequence, *Earthquake Spectra* 30(1), 1–15.

Braga, F., Dolce, M. and Liberatore, D. (1982). A statistical study on damaged buildings and an ensuing review of MSK-76 Scale, *Proc of the 7th European Conference on Earthquake Engineering*, Athens, Greece, pp. 431–450.

Calvi, G.M., Pinho, R., Magenes, G., Bommer, J.J., Restrepo-Vélez, L.F. and Crowley, H. (2006). Development of seismic vulnerability assessment methodologies over the past 30 years, *ISET Journal of Earthquake Technology* 43(3), 75-104.

CERA - Canterbury Earthquake Recovery Authority (2014) “Demolitions List“. http://cera.govt.nz/demolitions/list. Accessed 05 November 2014

da Porto, F., Silva, B., Costa, C. and Modena, C. (2012). Macro-scale analysis of damage to churches after earthquake in Abruzzo (Italy) on April 6, 2009, *Journal of Earthquake Engineering* 16(6), 739-758. doi: 10.1080/13632469.2012.685207.

D’Ayala, D. (1999). Correlation of seismic vulnerability and damage between classes of buildings: Churches and houses, in *Seismic damage to masonry buildings: proceedings of the International Workshop on Measures of Seismic Damage to Masonry Buildings*, ed. A. Bernardini (Taylor & Francis, Balkerna, Rotterdam), pp. 41-58.

D'Ayala, D. and Speranza, E. (2003). Definition of Collapse Mechanisms and Seismic Vulnerability of Historic Masonry Buildings, *Earthquake Spectra* 19(3), 479–509. doi: 10.1193/1.1599896.

D’Ayala, D. (2013). Assessing the seismic vulnerability of masonry buildings, in *Handbook of seismic risk analysis and management of civil infrastructure systems*, ed. S. Tesfamariam and K. Goda (Woodhead publishing, Sawston, Cambridge), pp 334-365.

De Matteis, G., Criber, E. and Brando, G. (2014). Damage Evaluation On Churches Belonging To The Sulmona-Valva Diocese After The 2009 L’Aquila Earthquake, *Proc of the 2nd International Conference on Protection of Historical Constructions*, Antalya, Turkey.

Di Pasquale, G., Orsini, G. and Romeo, R.W. (2005). New developments in seismic risk assessment in Italy, *Bulletin of Earthquake Engineering* 3(1), 101-128. doi: 10.1007/s10518-005-0202-1.

Doglioni, F., Moretti, A. and Petrini, V. (ed) (1994). *Le chiese e il terremoto. Dalla vulnerabilità constatata nel terremoto del Friuli al miglioramento antisismico nel restauro, verso una politica di prevenzione*, Ed. LINT, Trieste. In Italian.

Dolce, M., Masi, A., Marino M. and Vona, M. (2003). Earthquake damage scenarios of the building stock of Potenza (Southern Italy) Including Site Effects, Bulletin *of Earthquake Engineering* 1(1), 115-140. doi: 10.1023/A:1024809511362.

Dowrick, D.J. (1996). The Modified Mercalli earthquake intensity scale; revisions arising from recent studies of New Zealand earthquakes, *Bulletin of the New Zealand National Society for Earthquake Engineering* 29, 92-106.

DPCM (Direttiva del Presidente del Consiglio dei Ministri) 9 febbraio 2011. "Valutazione e riduzione del rischio sismico del patrimonio culturale con riferimento alle Norme tecniche per le costruzioni di cui al DM 14 gennaio 2008," Gazzetta Ufficiale della Repubblica Italiana n. 47 del 26 febbraio 2009, Supplemento Ordinario n. 54. In Italian.

Draper, N. and Smith, H. (1981). *Applied Regression Analysis*, John Wiley & Sons, New York.

Eiby, G.A. (1966). The Modified Mercalli scale of earthquake intensity and its use in New Zealand, *New Zealand Journal of Geology and Geophysics* 9, 122-129.

Elton, D.J. and Marciano, E.A. (1990). Ground acceleration near St Michael's Church during the 1886 Charleston, SC, Earthquake, *Earthquake Spectra* 6, 81-103. doi: 10.1193/1.1585559.

Erberik, M.A. (2008). Generation of fragility curves for Turkish masonry buildings considering in-plane failure modes, *Earthquake Engineering and Structural Dynamics* 37(3), 387-405. doi: 10.1002/eqe.760.

Giovinazzi, S, Lagomarsino, S. (2005). Fuzzy-random approach for a seismic vulnerability model. In: *Proc. ICOSSAR2005 safety and reliability of engineering systems and structures*. Rome, Italy, pp 2879–2887

Giuffrè, A. (1988). Restauro e sicurezza sismica. La cattedrale di S. Angelo dei Lombardi, *Palladio, nuova serie* 1, 95-120. In Italian.

Goded, T., Cousins, W.J. and Fenaughty, K.F. (2014a). Analysis of the Severe-Damage Online Felt Reports for the Canterbury (New Zealand) 2011 Aftershocks on 22 February Mw 6.2, 13 June Mw 6.0, and 23 December Mw 6.0, *Seismological Research Letters* 85(3), 678-691. doi: 10.1785/0220130198.

Goded, T., Ingham, J.M., Giovinazzi, S., Lagomarsino, S., Clark, W, Cattari, S., Ottonelli, D., Marotta, A., Lourenço, P.B. and McClean, R. (2014b). *Results on most probable MMI values for Christchurch URM churches*, Report part of the EQC Project 14/660 Vulnerability analysis of unreinforced masonry churches.

González Ballesteros, J.Á., Gallardo Carrillo, J. and López Aguilera, V. (2012) Afecciones ocasionadas por el terremoto en el conjunto de panteones históricos del cementerio de San Clemente, iglesia de Santa María, iglesia de San Pedro y la Fuente del Oro de Lorca, Murcia, *Boletin Geologico y Minero* 123, 537–548. In Spanish.

Grünthal, G., Musson, R.M.W., Schwartz, J. and Stucky, M. (1998) *European Macroseismic Scale 1998 (EMS-98)*, European Seismological Commission, Working Group Macroseismic Scales, Luxembourg.

Guerreiro, L., Azevedo, J., Proença, J., Bento, R. and Lopes, M. (2000). Damage in ancient churches during the 9th of July 1998 Azores earthquake, *Proc. of the 12th World Conference on Earthquake Engineering*, Auckland, New Zealand, paper 780.

Guevara, P.L.T. and Sanchez-Ramirez, A.R. (2005). Los sismos de Enero y Febrero de 2001 en El Salvador y su impacto en las iglesias del patrimonio cultural, *Boletin Tecnico, Instituto de Materiales y Modelos Estructurales* 43, 28–57. In Spanish.

Kircher, C.A., Nassar, A.A., Kustu, O. and Holmes, W.T. (1997). Development of Building Damage Functions for Earthquake Loss Estimation, *Earthquake Spectra* 13(4), 663-682. doi: 10.1193/1.1585974.

Lagomarsino, S. (1998). A new methodology for the post-earthquake investigation of ancient churches, *Proc. of the 11th European Conference on Earthquake Engineering*, Paris, France, paper LAGNMF.

Lagomarsino, S. and Podestà, S. (2004a). Damage and vulnerability assessment of churches after the 2002 Molise, Italy, earthquake, *Earthquake Spectra* 20(S1), 271–283. doi: 10.1193/1.1767161.

Lagomarsino, S. and Podestà, S. (2004b). Seismic vulnerability of ancient churches: II. Statistical Analysis of Surveyed Data and Methods for Risk Analysis, *Earthquake Spectra* 20(2), 395-412. doi: 10.1193/1.1737736.

Lagomarsino, S., Podestà, S., Cifani, G. and Lemme, A. (2004). The 31st October 2002 earthquake in Molise (Italy): a new Methodology for the damage and seismic vulnerability survey of churches, *Proc. of the 13th World Conference on Earthquake Engineering*, Vancouver, B.C., Canada, paper 1366.

Lagomarsino, S. (2006). On the vulnerability assessment of monumental buildings, *Bulletin of Earthquake Engineering* 4, 445-463. doi: 10.1007/s10518-006-9025-y.

Lagomarsino, S. (2012). Damage assessment of churches after L'Aquila earthquake (2009), *Bulletin of Earthquake Engineering* 10, 73–92. doi: 10.1007/s10518-011-9307-x.

Lallemant, D., and Kiremidjian, A. (2015). A Beta Distribution Model for Characterizing Earthquake Damage State Distribution, *Earthquake Spectra* 31, 1337-1352.

Lang, K. (2002). *Seismic vulnerability of existing buildings*, Institute of Structural Engineering (IBK), ETH Zurich, Report No. 273, vdf Hochschulverlag, Zurich.

Leite, J., Lourenço, P.B. and Ingham, J.M. (2013). Statistical assessment of damage to churches affected by the 2010–2011 Canterbury (New Zealand) earthquake sequence, *Journal of Earthquake Engineering* 17(1), 73-97. doi: 10.1080/13632469.2012.713562.

Lester, J.R., Brown, A.G. and Ingham, J.M. (2013). Stabilisation of the Cathedral of the Blessed Sacrament following the Canterbury earthquakes, *Engineering Failure Analysis*, 34, 648-669. doi: 10.1016/j.engfailanal.2013.01.041.

Liberatore, D., Spera, G. and Pacifico, S. (2006). Damage probability matrices of the architectural heritage of Basilicata (Italy), *Proc. of the 1st European Conference on Earthquake Engineering and seismology*, Geneva, Switzerland, paper 1550.

Liberatore, D., Martino, D. and D'Orsi, L. (2009). Valutazione della vulnerabilità e stima del danno atteso di edifici ecclesiastici della Basilicata, *XIII Convegno dell'Associazione Nazionale Italiana di Ingegneria Sismica (ANIDIS) L'Ingegneria Sismica in Italia*, Bologna, ref. S14.19. In Italian.

Lourenço, P.B., Oliveira, D.V., Leite, J.C., Ingham, J.M., Modena, C. and da Porto, F. (2013). Simplified indexes for the seismic assessment of masonry buildings: International database and validation, *Engineering Failure Analysis* 34, 585-605. doi: 10.1016/j.engfailanal.2013.02.014.

Marotta, A., Goded, T., Giovinazzi, S., Lagomarsino, S., Liberatore, D., Sorrentino, L. and Ingham, J.M. (2015). An inventory of unreinforced masonry churches in New Zealand, *Bulletin of the New Zealand Society for Earthquake Engineering* 48(3), 170-189.

Montilla, P.J., Uzcategui, A.I. and Hernandez, S.M. (1996). Damages occurred to churches due to the earthquake of February 8, 1995 in Pereira, Colombia, *Proc. of the 11th World Conference on Earthquake Engineering*, Acapulco, Mexico, paper 963.

Moon, L., Dizhur, D., Senaldi, I., Derakhshan, H., Griffith, M., Magenes, G. and Ingham, J.M. (2014). The demise of the URM building stock in Christchurch during the 2010/2011 Canterbury earthquake sequence, *Earthquake Spectra*, 30(1), 253-276. doi: 10.1193/022113EQS044M.

NZSI (New Zealand Standards Institute) (1965) "New Zealand Standard Model Building By-Law," New Zealand Standards Institute, Wellington, New Zealand.

PCM-DPC MiBAC (Presidenza Consiglio dei Ministri—Dipartimento della Protezione Civile Ministero Beni e Attività Culturali) (2006) “Model A-DC Scheda per il rilievo del danno ai beni culturali—Chiese,” http://www.protezionecivile.gov.it/resources/cms/documents/MOD_SCHEDA_DANNO_CHIESE_2006.pdf. In Italian.

Rivera De Uzcàtegui, A.I. and Torres B.R.A. (1997). Estudio de danos originados a las iglesias de la ciudad de Merida por la accion de los terremotos de 1812 y 1894, *Boletin Tecnico, Instituto de Materiales y Modelos Estructurales* 35, 10–21. In Spanish.

Sabetta, F., Goretti, A. and Lucantoni, A. (1998). Empirical Fragility Curves from Damage Surveys and Estimated Strong Ground Motion, *Proc. of the 11th European Conference on Earthquake Engineering*, Paris, France.

Senaldi, I., Magenes, G. and Ingham, J.M. (2014). Damage assessment of unreinforced stone masonry buildings after the 2010-2011 Canterbury earthquakes, *International Journal of Architectural Heritage Conservation, Analysis, and Restoration*, 9(5), 605-627. doi: 10.1080/15583058.2013.840688

Singhal, A. and Kiremidjian, A.S. (1996). Method for probabilistic evaluation of seismic structural damage, *Journal of Structural Engineering* 122(12), 1459-1467. doi: 10.1061/(ASCE)0733-9445(1996)122:12(1459).

Sofronie, R. (1982). Behaviour of eastern churches in earthquakes, *Proc. of the 7th European Conference on Earthquake Engineering*, Vol. 3, Athens, Greece, pp. 287–294.

Sorrentino, L., Liberatore, L., Decanini, L.D. and Liberatore, D. (2014a). The performance of churches in the 2012 Emilia earthquakes, *Bulletin of Earthquake Engineering* 12, 2299–2331. doi: 10.1007/s10518-013-9519-3.

Sorrentino, L., Alshawa, O. and Liberatore, D. (2014b). Observations of out-of-plane rocking in the Oratory of San Giuseppe dei Minimi during the 2009 L'Aquila earthquake, *Applied Mechanics and Materials* 621, 101-106. doi: 10.4028/www.scientific.net/AMM.621.101.

Sorrentino, L., Liberatore, L., Liberatore, D. and Masiani, R. (2014c). The behaviour of vernacular buildings in the 2012 Emilia earthquakes, *Bulletin of Earthquake Engineering* 12(5), 2367-2382. doi: 10.1007/s10518-013-9455-2.

Stirling, M.W., McVerry, G.H., Gerstenberger, M.C., Litchfield, N.J., Van Dissen, R.J., Berryman, K.R., Barnes, P., Wallace, L.M., Villamor, P., Langridge, R.M.,

Lamarche, G., Nodder, S., Reyners, M.E., Bradley, B., Rhoades, D.A., Smith, W.D., Nicol, A., Pettinga, J., Clark, K.J. and Jacobs, K. (2012). National Seismic Hazard Model for New Zealand: 2010 Update, *Bulletin of the Seismological Society of America* 102(4), 1514-1542.

Stiros, S., Papageorgiou, S., Kontogianni, V. and Psimoulis, P. (2006). Church repair swarms and earthquakes in Rhodes Island, Greece, *Journal of Seismology* 10, 527–537. doi: 10.1007/s10950-006-9035-x.

Study Group of the NZSEE (1992) A revision of the Modified Mercalli seismic intensity scale, *New Zealand National Society for Earthquake Engineering* 25(4), 345-357.

Vicente, R., Parodi, S., Lagomarsino, S., Varum, H. and Silva J.A.R.M. (2011). Seismic vulnerability and risk assessment: Case study of the historic city centre of Coimbra, Portugal, *Bulletin of Earthquake Engineering* 9(4), 1067-1096. doi: 10.1007/s10518-010-9233-3.

Whitman, R.V., Reed, J.W. and Hong, S.T. (1973). Earthquake damage probability matrices, *Proc. of the 5th World Conference on Earthquake Engineering*, Vol. 2, Rome, Italy, pp. 2531-2540.

Chapter 4

Territorial seismic risk assessment of New Zealand unreinforced masonry churches

Given the high seismicity of the country, the exposure of human lives and the societal significance of ecclesiastic buildings, for both historical and religious reasons, the reduction in seismic vulnerability of this building type is of primary importance. By analysing the seismic performance of a sample of 80 affected buildings, regression models correlating mean damage levels against ground-motion parameters were developed for observed collapse mechanisms, accounting for vulnerability modifiers whose influence was estimated via statistical procedures. Considering the homogeneity of New Zealand URM churches, the vulnerability models developed for the Canterbury region were extended to the whole country inventory, and a synthetic index was proposed to summarise damage related to several mechanisms. Territorial scale assessment of the seismic vulnerability of churches can assist emergency management efforts and facilitate the identification of priorities for more in-depth analysis of individual buildings. After proper calibration, the proposed approach can be applied to other countries with similar building heritage.

4.1. Introduction

New Zealand is subject to frequent seismic activity, being located along a zone of contact between the Pacific and the Australian tectonic plates, on the so-called “Ring of Fire”. The country has experienced several major earthquakes, at times very destructive, as in 1929 (Arthur’s Pass M_w 7.1, Murchison M_w 7.8) and in 1931 (Hawke’s Bay M_w 7.8). During 2010-2011 the Canterbury region was stricken by an extensive earthquake

sequence, with the most severe event in terms of damage occurring on 22 February 2011 (M_w 6.3). Unreinforced masonry (URM) buildings form a significant component of the national building stock dating prior to the 1965 Model Building Code (Russell and Ingham, 2010) and represent an inestimable portion of the national architectural heritage, whilst during the Canterbury earthquakes this building type was particularly severely affected (Moon et al., 2014). The seismic sequence also had an impressive impact on the religious community, given the societal relevance of New Zealand churches (Marotta et al., 2015). Moreover, it is widely known that churches frequently exhibit a seismic vulnerability higher than ordinary buildings (D'Ayala, 2000), because of their open plan, large wall height-to-thickness and length-to-thickness ratios, and the use of thrusting horizontal structural elements for vaults and roofs (Sorrentino et al., 2014a, b). Therefore, it is relevant to assess the seismic risk of New Zealand churches.

Seismic risk models constitute important tools for framing public policies toward land-use planning and emergency management, and a reliable estimation of seismic risk can minimize social and economic losses caused by earthquakes. For these reasons, seismic risk assessment has attracted strong interest in seismic areas, at both urban (e.g., Faccioli et al., 1999; Dolce et al., 2006; Kappos et al., 2008; Erberik, 2010; Marulanda et al., 2013; Cardona et al., 2014; Toma-Danila et al., 2015) and territorial scales (e.g., Rota et al., 2011; Chrysostomou et al., 2014; Dunand et al., 2014; Eleftheriadou et al., 2014; Chaulagain et al., 2015; Siddique and Schwarz, 2015).

The study reported here investigates the structural vulnerability of New Zealand unreinforced masonry churches, and the associated seismic risk, as an outcome of seismic hazard, building vulnerability and exposure (Dowrick, 2003). Exposure refers to the national inventory of URM churches described in Marotta et al. (2015), compiled after an extensive survey that for each building provided information about location, geometry, and construction techniques. Marotta et al. (2015) have shown the homogeneity of the building portfolio in terms of both architectural features and construction details. For example, 79% of the URM churches nationwide are single-nave buildings, compared to 85% of those affected by the 2010-2011 Canterbury earthquakes. Similarly 39% of New Zealand URM churches are made of natural-stone masonry, compared to 38% of the Canterbury set (Marotta et al., 2016). The observed vulnerability of Canterbury URM churches during 2010-2011 has already been analysed according to statistical procedures in Marotta et al. (2016), assuming the New Zealand Modified Mercalli macroseismic intensity (NZMMI) as the ground motion parameter.

Hereinafter, different intensity measures are considered, with the most robust measure used to model seismic hazard, and consequently damage data is reinterpreted. Given the homogeneity of the national inventory, fragility curves derived from Canterbury data are applied to all of New Zealand to obtain seismic risk estimates.

4.2. Ground motion intensity measures

Selecting appropriate ground motion parameters is of fundamental importance in the definition of fragility curves that are used to correlate building damage against intensity measures and subsequently used to forecast the seismic risk within a specific region. The most frequently used parameter when dealing with observed vulnerabilities is the macroseismic intensity, which is attributed based on effects on the built and natural environment. Use of the macroseismic intensity, whilst common in literature (for example: Dolce et al., 2006; Chrysostomou et al., 2014; Vicente et al., 2014; Cherif et al., 2015), presents some disadvantages, such as its conventional nature and the use of discrete values. Additionally, when damage forecast is of interest, rather than observed damage interpretation, the inclusion of site effects typical of macroseismic intensity is a limitation if just one expected intensity should be applied to a territory where different local amplifications are likely. Finally, seismic hazard is described in terms of expected macroseismic intensities only in regions where catalogues date back an adequate timespan. Therefore, different ground motion descriptors are considered herein, computed from the records of the 22 February 2011 Christchurch earthquake. All intensity measures are vector sums relative to their two orthogonal components, and the two intensity measures at each church location are extracted by means of a triangulation-based linear 2-D interpolation of the ground-motion records at the scattered accelerometric stations.

Peak Ground Acceleration (PGA) and Peak Ground Velocity (PGV) are selected as ground motion parameters because they are the most commonly used intensity measures and because they are familiar to technical practitioners. Recorded PGA values vary between 0.01 g and 1.34 g, with an average of 0.36 g, whereas PGV values vary between 0.004 m/s and 1.15 m/s, with an average of 0.27 m/s.

Arias Intensity, I_A, is selected as a ground motion descriptor because it captures the potential destructiveness of an earthquake as the integral of the square of the

acceleration-time history (Travasarou et al., 2003) and because it has been demonstrated to be an effective predictor of the likelihood of damage to short-period structures (Stafford et al., 2009). As defined by Arias (1970), I_A is the total energy per unit weight absorbed by a set of undamped single-degree-of-freedom oscillators at the end of an earthquake, calculated as follows:

$$I_A = \frac{\pi}{2g}\int_0^{\infty} a^2(t)dt \tag{16}$$

where a is the acceleration as a function of time t, in units of g, the acceleration due to gravity. I_A varies between 0.0002 m/s and 17.08 m/s, with an average of 1.12 m/s.

Housner Intensity (Housner, 1959), I_H, is selected because it captures important aspects of the amplitude and frequency content of a record over a range of primary importance for many structures (Kramer, 1996), and is defined as:

$$I_H = \int_{0.1}^{2.5} S_v(T,\xi)dT \tag{17}$$

where the integral refers to the area under the pseudo-velocity response spectrum, S_v, over the period T ranging between 0.1 and 2.5 s, and where ξ is the damping ratio of the structure. Moreover, some studies (for example: Decanini et al., 2002; Masi et al., 2011; Chiauzzi et al., 2012; Mouyiannou et al., 2014) have demonstrated that I_H can be a valid alternative to other seismic peak parameters. Recorded I_H varies between 0.02 m and 4.30 m, with an average of 1.02 m.

To better account for the global response of ordinary masonry structures, whose effective fundamental period is rarely beyond 0.5 s, a modified Housner Intensity, mI_H, has been proposed by Mouyiannou et al. (2014):

$$mI_H = \int_{0.1}^{0.5} S_v(T,\xi)dT \tag{18}$$

Recorded mI_H varies between 0.001 m and 0.77 m, with an average of 0.09 m.

Cross-validation is used to estimate how accurate the interpolations are, by removing each accelerometric station one at a time and predicting the associated intensity measure value using the remaining data. The comparison between predicted and recorded values of each omitted point shows a fairly low correlation for I_A (R^2 = 0.45), a reasonable agreement for mI_H and PGA (coefficient of determination, respectively, equal to 0.61 and 0.66), and a very good correlation for PGV and I_H (R^2 = 0.89 and R^2 = 0.91, respectively).

4.3. Vulnerability calibration of local mechanisms

The aim of a seismic vulnerability assessment is to provide a measure of the tendency of a set of buildings to suffer certain damage when subjected to earthquake ground shaking. The physical damage suffered by 80 URM churches following the 22 February 2011 Christchurch earthquake (§3.3) is herein correlated to the five aforementioned intensity measures. The earthquake response of historical URM constructions, and particularly churches, can be described by identifying separate macro-elements, which are specific architectural parts whose seismic behaviour is only slightly linked to adjacent parts (e.g., D'Ayala and Speranza, 2003; Gizzi et al., 2014; Sorrentino et al., 2014c). Consequently, the damage survey and interpretation of Canterbury URM churches were undertaken based on 28 local mechanisms (Lagomarsino et al., 2004), as currently adopted in Italy for post-earthquake assessment of churches (De Matteis et al., 2016). Six levels of damage were assigned to each mechanism on the basis of a qualitative judgment, ranging between 0 (no damage) to 5 (total collapse), according to the approach of the European Macroseismic Scale (Grünthal, 1998). When a single building is under investigation, or in the case of moderate to low shaking, advanced survey techniques can be used to identify collapse mechanisms, for example through dense point cloud acquisition (Andreotti et al., 2015).

Because some of the 28 mechanisms in the Italian form are rarely observed in New Zealand as they are related to macro-elements that are seldom present (e.g., columns between the naves, vaults, chapels, domes), eight mechanisms were eliminated and the remaining twenty mechanisms were analysed in the vulnerability assessment (Table 4.1).

Table 4.1. List of the damage mechanisms observed in Canterbury churches. Numbering refers to the 28 mechanisms in the Italian form (Lagomarsino et al. 2004).

Ref. no.	Description	Ref. no.	Description
1	Overturning of the façade	***17***	Shear in the apse
2	Gable mechanisms	***19***	Interactions between the nave and its roof
3	Shear in the façade	***20***	Interactions between the transept and its roof
4	Damage in the porch	***21***	Interactions between the apse and its roof
5	Transversal response of the nave	***22***	Overturning of the chapels
6	Shear in longitudinal walls	***23***	Shear in the chapels
10	Overturning of the transept	***25***	Interactions next to irregularities
11	Shear in the transept	***26***	Projections
13	Triumphal arch	***27***	Bell tower
16	Overturning of the apse	***28***	Belfry

As already pointed out in §3.6.2, the seismic vulnerability of URM churches is strongly modified by structural details that can worsen the seismic performance, such as large openings, thrusting structures, or poor masonry quality (Liberatore et al., 2016) or improve seismic performance through the presence of earthquake-resistant elements, such as connections between walls and to horizontal structures, top ring beams, or tie rods.

Consequently, the vulnerability of each mechanism was evaluated by multiple-linear regressions, in which the accounted v explanatory variables, x_v, and the response, d, representing the damage that occurred, were fitted by a linear formulation, according to:

$$d = m_1 x_1 + m_2 x_2 + ... + m_v x_v + b + \varepsilon \tag{19}$$

where x_1 represented the ground motion severity (macroseismic intensity was used in §3.6.2), x_2, x_3, … x_v are the vulnerability modifiers considered, m_1, m_2, …m_v are the regression coefficients, b is the intercept and ϵ is the error term. For each mechanism a different set of modifiers was considered. In §3.6.2 the vulnerability modifiers were assumed equal to either 0 or 1, working as indicators of either the absence or presence of a characteristic and its effectiveness, scoring 1 if either a fragility increaser was present or if an earthquake-resistant element was absent, or scoring 0 if a fragility increaser was absent or if an earthquake-resistant element was present and effective. Herein the vulnerability modifiers can score between the limits of 0 and 1, dependent on whether a fragility increaser was partially present (e.g., a trussed roof without a bottom

chord but with a raised tie) or if an earthquake-resistant element was present but ineffective (e.g., buttresses not connected to the walls that they are meant to strengthen). In the following evaluations the discrete values of 0.33 and 0.67 have been used on the basis of expert judgment. An example of the use of these variables is presented in §4.7. Two statistical procedures, namely Stepwise and Best Subsets (Draper and Smith, 1981), were used to determine the variables that generated the most efficient predictive model. The Stepwise selection method allows the determination of the variables that generate the most efficient predictive model, involving the inserting of variables in turn until the regression equation is satisfactory. The Best Subsets procedure selects the subset of parameters that optimise an objective criterion, such as having the largest coefficient of determination.

Differently from §3.6.2, Eq. (19) is hereinafter used assuming that x_1 may be either PGA, PGV, I_A, I_H, or mI_H. The effectiveness of each intensity measure is then evaluated with reference to the regression (Eq. (19)) of the twenty mechanisms. Because several variables contribute to Eq. (19), R^2 will automatically increase when compared to a monoparametric regression (Draper and Smith, 1981). Consequently, it is appropriate to use the adjusted coefficient of determination R^2_{adj}:

$$R^2_{adj} = 1 - \left[\left(1 - R^2\right) \frac{n-1}{n-v} \right] \tag{20}$$

where n is the sample size and v is the number of considered vulnerability modifiers. As for R^2, $R^2_{adj} \leq 1$ and the higher R^2_{adj} the better the correlation.

R^2_{adj} is computed for both Stepwise and Best Subsets regression models, and the one presenting the highest R^2_{adj} is used. In the case of equivalence between the two R^2_{adj}, the regression model that considered a smaller number of predictor variables is chosen in order to achieve a faster territorial scale vulnerability assessment. The regression models accounting for the different intensity measures do not differ greatly in terms of the vulnerability modifiers that need to be taken into account (Appendix F). In Figure 4.1 the intensity measures are compared in terms of R^2_{adj}, by varying the mechanisms reported in Table 4.1. PGA, PGV and I_H have practically the same mean R^2_{adj}, with I_H having a fairly lower scatter. NZMMI has a slightly higher average value but much larger scatter compared to I_H. I_A and mI_H have fairly lower average values and larger scatter.

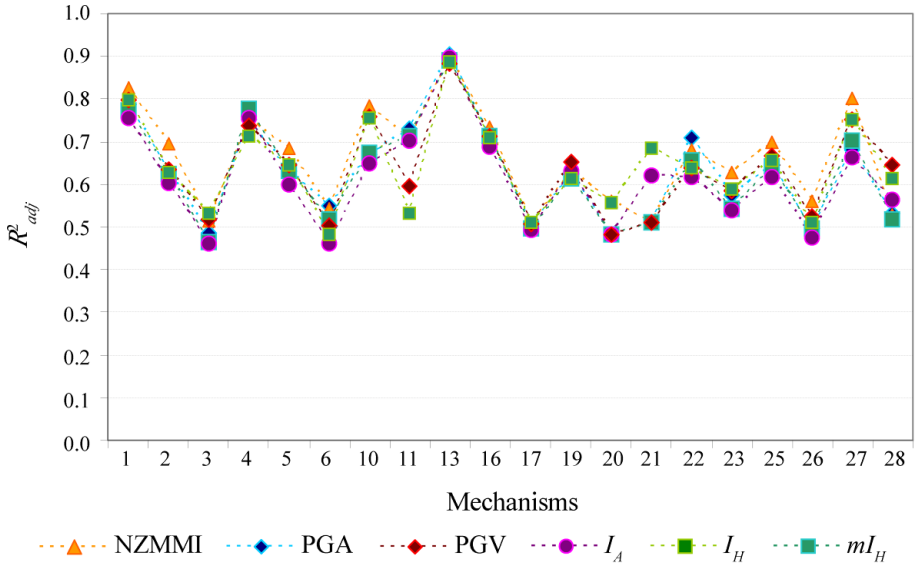

Figure 4.1. Comparison between adjusted coefficients of determination, R^2_{adj}, for different intensity measures based on mechanisms reported in Table 4.1. NZMMI data after §3.2.

Table 4.2. Comparison between adjusted coefficients of determination, R^2_{adj}, for different intensity measures based on mechanisms reported in Table 4.1.

Mech. no.	NZMMI	PGA	PGV	I_A	I_H	mI_H
1	0.827	0.787	0.799	0.756	0.797	0.771
2	0.697	0.630	0.636	0.603	0.628	0.625
3	0.514	0.486	0.519	0.462	0.533	0.464
4	0.753	0.753	0.739	0.756	0.713	0.777
5	0.683	0.630	0.645	0.601	0.645	0.631
6	0.543	0.550	0.505	0.459	0.483	0.516
10	0.784	0.671	0.758	0.648	0.754	0.675
11	0.704	0.731	0.596	0.702	0.530	0.713
13	0.896	0.903	0.884	0.897	0.885	0.891
16	0.735	0.707	0.711	0.688	0.710	0.714
17	0.511	0.509	0.508	0.493	0.511	0.495
19	0.630	0.625	0.654	0.631	0.614	0.615
20	0.561	0.483	0.483	0.483	0.555	0.483
21	0.511	0.511	0.511	0.621	0.683	0.511
22	0.683	0.709	0.638	0.619	0.637	0.655
23	0.629	0.576	0.585	0.540	0.588	0.543
25	0.697	0.646	0.667	0.616	0.655	0.640
26	0.559	0.495	0.523	0.475	0.511	0.495
27	0.803	0.679	0.753	0.661	0.752	0.704
28	0.530	0.533	0.645	0.565	0.614	0.517
mean	0.662	0.631	0.638	0.614	0.640	0.622
standard dev.	0.117	0.115	0.112	0.113	0.106	0.118

According to this comparison, although peak ground measures are more straightforward parameters, I_H is the preferred intensity measure for use in the following computations because it exhibits similar reliability of PGV in the interpolation of ground motion at the sites of the churches but better results to both PGA and PGV in terms of effectiveness in damage regressions.

For the twenty mechanisms considered here, the coefficients defining the selected multiple-linear regressions of Eq. (19) are presented in Table 4.3.

Among the modifiers accounted for, tie rods have no influence on the regressions of any mechanism, confirming the observation reported in §3.6.2. Their inadequate effectiveness can be associated with the use of small wall anchors and with their placement being too far apart along the wall, together with their rather limited presence among the sample. It is expected that their appropriate use in strengthening interventions will markedly improve church earthquake performance.

Table 4.3. Computed coefficients of the regression models (Eq. (19)) for I_H as intensity measure

Mechanism no. / Variable	*1*	*2*	*3*	*4*	*5*	*6*	*10*	*11*	*13*	*16*
Intensity measure (m^{-1})	0.376	0.353	0.358	0.156	0.267	0.516	0.565	0.594	0.042	0.352
Lateral restraint	N/A	N/A	N/A	N/A	N/A	0.706	N/A	N/A	0.468	N/A
Buttresses	N/A	1.428	N/A	0.870	N/A	N/A	N/A	N/A	N/A	N/A
Lintels	N/A	N/A	N/A	1.289	N/A	0.666	N/A	N/A	N/A	N/A
Thrusting elements	1.713	N/A	N/A	N/A	0.614	N/A	N/A	N/A	N/A	N/A
Large openings	0.479	N/A	N/A	N/A	N/A	N/A	1.072	N/A	N/A	N/A
Top beam	N/A	N/A	N/A	N/A	N/A	N/A	3.215	N/A	N/A	N/A
Heterogeneous materials	N/A	N/A	N/A	N/A	N/A	N/A	N/A	N/A	N/A	N/A
Connections	1.368	2.023	N/A	1.488	2.306	N/A	2.156	N/A	N/A	1.206
Slenderness	0.875	0.745	1.626	N/A	0.654	N/A	N/A	1.485	N/A	2.044
Asymmetry conditions	N/A	N/A	N/A	N/A	N/A	N/A	N/A	N/A	N/A	N/A
Poor quality masonry	0.987	N/A	0.424	1.848	N/A	0.886	N/A	N/A	4.179	N/A
b (intercept)	-0.458	-0.935	0.241	-1.470	0.180	-0.454	-3.305	0.117	0.062	0.335
σ (residual standard error)	0.778	1.135	1.001	0.966	0.932	1.033	0.955	1.163	0.351	0.954

Mechanism no. / Variable	*17*	*19*	*20*	*21*	*22*	*23*	*25*	*26*	*27*	*28*
Intensity measure (m^{-1})	0.236	0.417	0.365	0.384	0.472	0.361	0.422	0.452	0.638	0.943
Lateral restraint	N/A	N/A	N/A	N/A	N/A	N/A	N/A	N/A	N/A	N/A
Buttresses	N/A	N/A	N/A	N/A	N/A	N/A	N/A	N/A	N/A	N/A
Lintels	N/A	N/A	N/A	N/A	N/A	N/A	N/A	N/A	N/A	N/A
Thrusting elements	N/A	3.266	1.663	1.673	N/A	N/A	N/A	N/A	N/A	N/A
Large openings	N/A	N/A	N/A	N/A	N/A	0.574	N/A	N/A	N/A	N/A
Top beam	N/A	N/A	N/A	N/A	N/A	N/A	N/A	N/A	N/A	N/A
Heterogeneous materials	N/A	N/A	N/A	N/A	N/A	N/A	0.904	N/A	N/A	N/A
Connections	N/A	N/A	N/A	N/A	2.053	N/A	0.990	N/A	2.092	N/A
Slenderness	1.728	N/A	N/A	N/A	N/A	1.599	N/A	2.388	N/A	N/A
Asymmetry conditions	N/A	N/A	N/A	N/A	N/A	N/A	N/A	1.170	N/A	N/A
Poor quality masonry	N/A	1.055	3.094	1.510	1.316	0.855	1.543	1.089	0.919	2.028
b (intercept)	0.298	-1.925	-2.210	-0.367	-0.243	0.046	-0.337	-0.436	-0.009	-0.174
σ (residual standard error)	0.904	1.020	1.371	0.960	1.152	0.893	1.024	1.265	0.915	1.554

The damage predicted by Eq. (19) using the modifiers in Table 4.3, which is the basis of the following risk analysis, is a mean value. However, in the same table the residual standard error, σ (Draper and Smith, 1981), is computed for each mechanism showing mean and standard deviation equal to 1.024 and 0.262, respectively. A residual standard error of approximately unity is not negligible, but needs to be compared to a damage value as large as 5, and is smaller than the residual standard error of the simple-linear regressions accounting for intensity measure alone (mean = 1.367, standard deviation = 0.253).

The so-computed coefficients of the regression models are consequently used to derive equations for the following territorial seismic risk assessment. An overview of the estimated total number of damaged churches, disaggregated in terms of damage levels, is presented in Figure 4.2 for the considered mechanisms. Histograms refer to New Zealand regions, with the least populated regions being grouped. Some mechanisms can occur in more churches than can others (#1-3, #5-6, #16-17) because they are related to the most commonly present macro-elements. Damage level usually is up to d_3 (substantial to heavy damage), with the few exceptions occurring mostly in Auckland, Canterbury and Otago regions (d_5 in mechanisms #2, #13, #27-28). Because the overall dimensions of the buildings are relevant in a seismic risk analysis (Dolce et al. 2006), on the right axes of Figure 4.2 a regional mean damage, weighted on foot-print area and normalised by the maximum value in the accounted mechanisms, is also presented. The comparison between these two damage measures highlights how the simple reference to number of buildings can be over simplistic.

4.4. Vulnerability calibration of global response

In buildings with multiple mechanisms it is important to define a synthetic index expressing the overall severity of damage. For a risk analysis it would be ideal to have reparation costs related to each mechanism, but unfortunately such information is currently not available for New Zealand. However, part of the reparation cost estimation entails accounting for the geometrical size of the macro-elements. For this reason, following Cattari et al. (2015), the damage of each mechanism can also be weighted based on the surface area of the associated macro-element when compared to the church surface area (Figure 4.3).

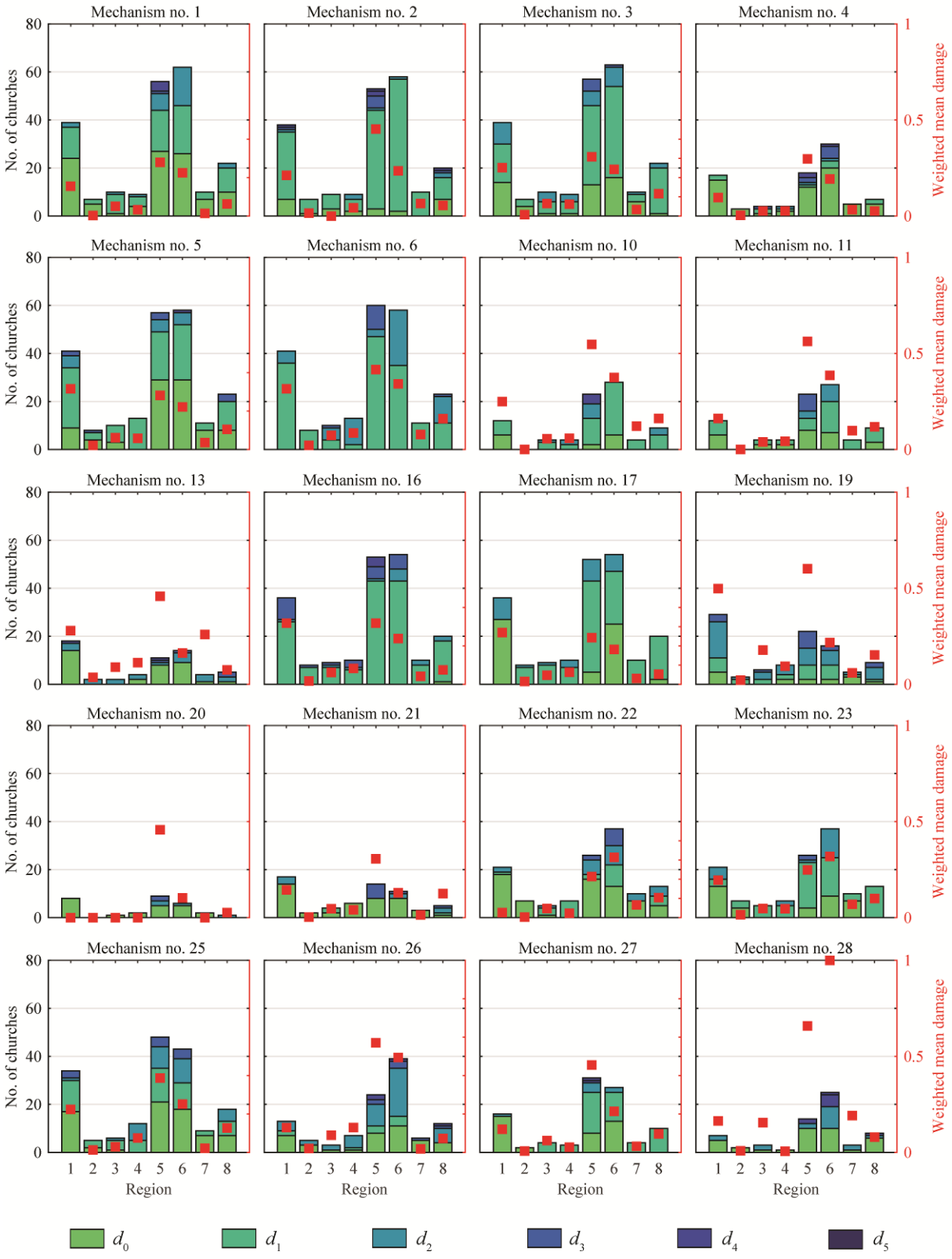

Figure 4.2. Expected regional damage. Left axis: number of damaged churches, disaggregated in terms of damage levels. Right axis: normalised mean damage, weighted on building foot-print area. Regions: 1 = Auckland, 2 = Waikato, 3 = Manawatu-Wanganui, 4 = Wellington, 5 = Canterbury, 6 = Otago, 7 = Southland, 8 = others (Northland, Bay of Plenty, Gisborne, Hawke's Bay, Taranaki, Marlborough, Nelson, Tasman, West Coast). Mechanism description given in Table 4.1.

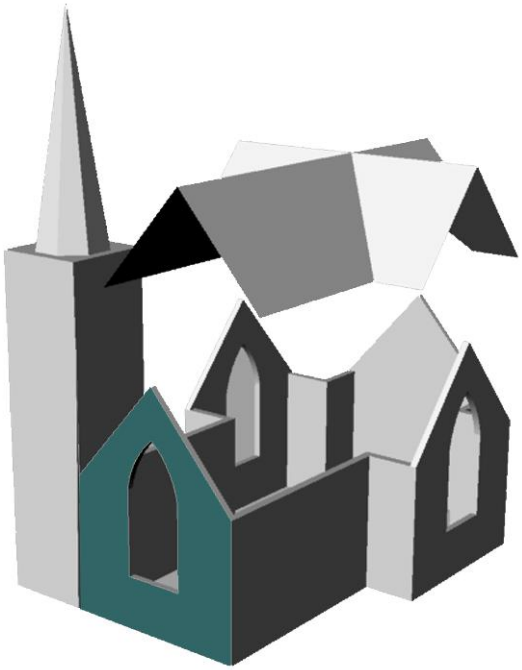

Figure 4.3. Surface area of the façade macroelement (associated to mechanisms #1 and #3) and church total surface area.

A possible alternative is given by the normalized average, i_d, proposed by Lagomarsino et al. (2004), as the mean of the damage scores, d_k, assigned to each of the N collapse mechanisms, multiplied by the weights ρ_k:

$$i_d = \frac{1}{5} \frac{\sum_{k=1}^{N} \rho_k \, d_k}{\sum_{k=1}^{N} \rho_k} \tag{21}$$

Equation (21) has the drawback of requiring an expert judgement estimation of the weights ρ_k. The normalised average, i_d, can be transformed into a discrete variable, varying from 0 to 5, using the correlation suggested by Lagomarsino and Podestà (2004). In the following, the weighted mean damage, D, is continuous over a 0-5 scale and is defined simply as:

$$D = 5\, i_d = \frac{\sum_{k=1}^{N} \rho_k \, d_k}{\sum_{k=1}^{N} \rho_k} \tag{22}$$

By assigning unitary values to the weights ρ_k the arithmetic mean is obtained.

In order to avoid a conventional estimation of the ρ_k weights, an alternative synthetic damage index can be defined. Given the damage observed in Canterbury churches, Eq. (19) can be re-expressed in vector form as:

$$\mathbf{d} = \mathbf{m}_1 x_1 + \mathbf{c} + \mathbf{b} + \boldsymbol{\varepsilon} \tag{23}$$

where **d** represents the vector of observed damage, $\mathbf{m}_1$ is the vector of the regression coefficients of the intensity measure x_1, vector **c** groups the regression modifiers associated with the twenty mechanisms (e.g., for the *j*-th mechanism: $c_j = m_{j2}x_{j2} + ... + m_{jv}x_{jv}$), **b** is the vector of intercepts and **ε** is the vector of error terms. In the case of New Zealand URM churches, regression coefficients $m_{j,i}$ and intercepts b_j can be found in Table 4.3.

The ground motion parameter x_1 that best fits the observed damage by minimizing the sum of squares of the error terms can then be established as:

$$\frac{d}{dx_1}\boldsymbol{\varepsilon}^T\boldsymbol{\varepsilon} = 0 \tag{24}$$

Whereas Eq. (19) was obtained by minimizing the error on a mechanism-by-mechanism basis with x_1 being a known parameter, the formulation may be re-considered where x_1 is a ground motion parameter that fits data of all considered mechanisms at one time. From Eqs. (23) and (24) x_1 can be expressed as:

$$x_1 = \frac{\mathbf{m}_1^T(\mathbf{d} - \mathbf{b} - \mathbf{c})}{\mathbf{m}_1^T\mathbf{m}_1} \tag{25}$$

that can be rearranged as:

$$x_1 = \frac{\mathbf{m}_1^T(\mathbf{d} - \mathbf{b})}{\mathbf{m}_1^T\mathbf{m}_1} - \frac{\mathbf{m}_1^T\mathbf{c}}{\mathbf{m}_1^T\mathbf{m}_1} \tag{26}$$

The sought after ground motion parameter x_1 is equal to the difference of two terms, where the first term depends on observed damage (including intercepts) and is here defined as the synthetic damage index, D_s:

$$D_s = \frac{\mathbf{m}_1^T(\mathbf{d} - \mathbf{b})}{\mathbf{m}_1^T\mathbf{m}_1} \tag{27}$$

The second term depends on the vulnerability modifiers alone, and is here defined as the vulnerability index, *V*:

$$V = \frac{\mathbf{m}_1^T \mathbf{c}}{\mathbf{m}_1^T \mathbf{m}_1} \tag{28}$$

Accordingly, Eq. (26) can be rewritten as:

$$x_1 = D_s - V \tag{29}$$

or:

$$D_s = x_1 + V \tag{30}$$

A simple additive model is therefore established, where the synthetic damage index, D_s, is calculated as the sum of the ground motion parameter, x_1, and the vulnerability index, V, and all quantities share the same unit of measure. Because the elements of vectors $\mathbf{m}_1$, **b**, and **c** were derived herein as regressions with I_H as the intensity measure, it follows that the damage, the ground motion parameter and the vulnerability in Eq. (30) are all measured in metre units. The observed variable x_1 was computed for each church and a mean value of 1.68 m was obtained. The Housner Intensity associated with the records of the February event was similarly estimated for each church site as explained in the previous section, and a comparable mean value of 1.57 m was obtained.

By comparing Eq. (26) with Eq. (27) it follows that D_s can be interpreted as the ground motion x_1 causing damage **d** in a building having null modifiers (**c** = **0**). It also follows that this ground motion is higher than the value required to induce the same damage to a building with non-zero vulnerability modifiers. Accordingly, based on Eq. (29), V can be interpreted as the reduction of the ground motion parameter x_1 necessary to induce the same damage **d** to the actual building. The higher the building vulnerability, the lower the necessary ground motion x_1.

The synthetic damage of Eq. (27) is an *observed* damage, which can be used for comparisons and model validation. An alternative interpretation of synthetic damage can be established by means of Eq. (30), defining x_1 as being the ground motion parameter either interpolated from accelerograms recorded during the earthquake or as determined from hazard studies. In this way, D_s is a *predicted* damage, given the intensity measure at the site, for a building with vulnerability V computed using Eq. (28).

Both definitions of synthetic damage are scalar measures computed from the damage associated with the mechanisms that are possible in the analysed church, but these synthetic indexes avoid the conventional definition of the weights present in Eq. (22).

An example of the computation of *predicted* D_s is given in §4.7. It is also worth mentioning that the vulnerability V does not provide the intensity measure that a building will resist but, when added to the expected intensity measure at the site, will forecast the predicted damage.

As Equation (30) establishes a relationship between three quantities, it follows that when any two quantities are known it is possible to obtain the third. Specifically, once damage and vulnerability are known (e.g. after an earthquake) it is possible to estimate the ground motion severity, gaining a quantitative alternative to the conventional macroseismic intensity, which enables a qualitative estimate of ground motion severity based upon the effects on buildings accounting for their vulnerability. Alternatively, when the expected ground motion and vulnerability are provided (e.g. in a risk analysis), the forecast damage can be established.

A comparison of the *observed* synthetic damage index with the *classical* weighted mean damage D, computed for Canterbury churches according to Eq. (22) and assuming ρ_k = 1, is provided in Figure 4.4a to illustrate the application of a damage index expressed in terms of a ground motion unit of measure. An extremely good correlation is achieved, confirming the efficacy of the proposed synthetic damage index.

Given the relationship between the *predicted* synthetic damage index D_s and the weighted mean damage D observed for the Canterbury sample (Figure 4.4b), a constant equal to 2.5 m can be used to obtain a non-dimensional damage, $\overline{D_s}$, in a 0-5 scale:

$$\overline{D_s} = \frac{D_s}{2.5} \tag{31}$$

The minimum and maximum values of V recorded in the inventory were 0.16 m and 7.63 m. The highest level of damage (d_5) is obtained considering a value of x_1 equal to 4.87 m: (7.63 + 4.87) / 2.5 = 5. Considering that the maximum value of expected I_H is 6.41 m for the case of soil class E (very soft soil), hazard factor equal to 0.60 (the maximum value in NZS 2004), and a return period factor of 1.80 (2500 years), the maximum value that the non-dimensional parameter $\overline{D_s}$ can assume in the worst case scenario is: (7.63 + 6.41) / 2.5 = 5.62, which slightly exceeds d_5. Conversely, the smallest value of expected I_H is equal to 0.08 m, for soil A (strong rock), a hazard factor equal to 0.13 (the minimum value in NZS 2004), and a return period factor 0.20 (20

years). This minimum value is still larger than the smallest I_H = 0.03 m interpolated from the 2011 Canterbury earthquake, for which Eq. (30) was calibrated.

The *predicted* synthetic damage index computed following Eq. (30) and the weighted mean damage D have the same general trend, as proven by an R^2 = 0.80 (Figure 4.4b). It is also worth mentioning that the normalized average damage of Eq.(21), for the inventory considered here, differs from the simpler arithmetic mean (ρ_k = 1) in only eight cases for the whole stock, with a difference of approximately 1% in the mean value. Moreover, because the synthetic damage index D_s has the units of a ground motion intensity measure, the weighted mean damage D could be correlated directly with a customary intensity measure, e.g. PGA or I_H. When this exercise is undertaken a coefficient of determination equal to 0.73 or 0.71, respectively, is achieved, which is significantly smaller than that provided in Figure 4.4b.

Finally, another advantage of the proposed damage index which is a combination of a ground motion intensity measure and building vulnerability, is the ability to use a simple plot (Figure 4.5) to illustrate the contribution of each component. By reporting the intensity measure on the horizontal axis and the vulnerability on the vertical axis, the global damage index of a single building can be read on the bisector, in intensity measure dimension scale (by a factor $1/\sqrt{2}$) or in a non-dimensional 0-5 scale. Different combinations of intensity measure and vulnerability can deliver the same damage (Figure 4.5a-b), whereas for the same building (equal vulnerability) different return period events (entailing different values of x_1) will cause different levels of damage (Figure 4.5b-c).

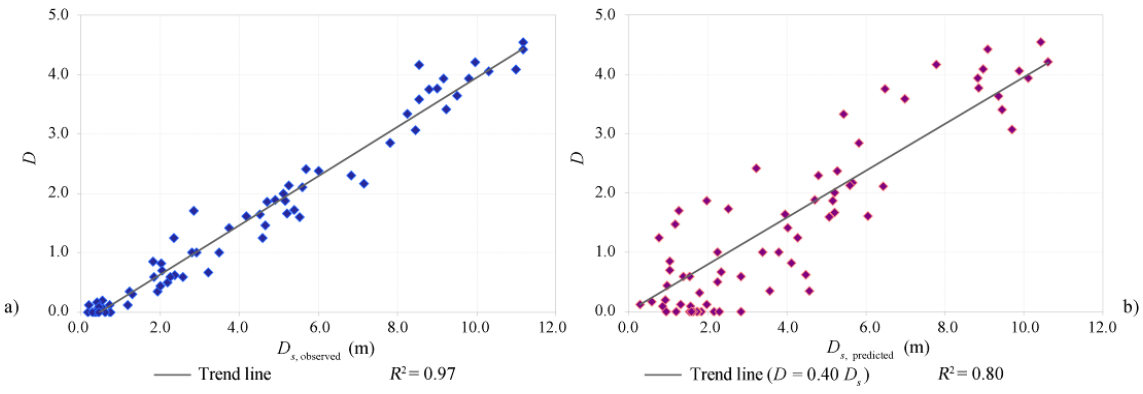

Figure 4.4. Correlation between weighted mean damage, *D*, observed in the Canterbury churches (Eq. (22), ρ_k = 1) and: a) observed synthetic damage index (Eq. (27)); b) predicted synthetic damage index (Eq. (30)).

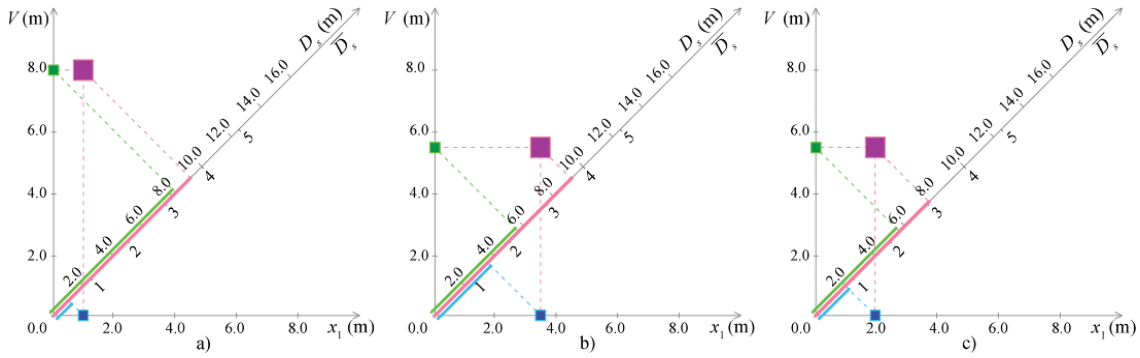

Figure 4.5. Global damage index, D_s, as a combination of hazard, x_1, and vulnerability, V: a) church with high V and low x_1; b) church with same D_s as in a) but higher x_1 and lower V; c) church with same V as in b) but lower x_1 (shorter event return period).

4.4.1. Estimation of the global damage index of churches with limited access

In the aftermath of an earthquake the collection of damage data can be hampered by the partial accessibility of churches due to safety restriction. In order to find a method for the expeditious assessment of churches for which some of the macro-elements are not visible, the correlation between the damage of the observed mechanisms, investigated through the computation of the Pearson coefficient in §3.5, is used.

Figure 3.15 provides guidance on the selection of the most correlated mechanisms, for which simple-linear regressions can be used to estimate the damage of macro-elements that cannot be inspected by means of the damage ascribed to observed macro-elements (e.g. estimating the damage in mechanism #13 based on the damage due to mechanism #1). The assumption underlying the selection of the mechanisms to be used in the regression models is that usually at least one side of the inspected church is visible, as are mechanisms that are related to lateral walls, projections and belfries (#5, #6, #26, #28). According to this hypothesis, only one regression coefficient is given for mechanisms concerning the main macro-elements that are visible from outside (façade, #1-4, apse, #16-17, and transept, #10-11), while more than one regression coefficient is proposed for mechanisms that can be inspected from inside (triumphal arch, #13, and roofs, #19-21) and for macro-elements that can be located alternatively along different sides of the church, such as chapels and bell tower (#22-27) (Table 4.4). Even if more than one regression coefficient is given, the procedure entails the use a monoparametric regression such that if both independent variables are available then the mechanism involving the highest coefficient of correlation is recommended for use and

consequently is printed in boldface in Table 4.4. In this specific case, the use of bilinear regressions involves a negligible increase of the adjusted coefficient of determination with respect to the monoparametric regressions. The computed regression coefficients are applied to the Canterbury sample in order to verify the reliability of the proposed method, assuming churches to be visible only from outside and excluding the mechanisms not visible from the street. Good agreement is achieved between the weighted mean damage observed in the Canterbury churches, D, and the damage computed applying the coefficients in Table 4.4, D_c, as proven by an $R^2 = 0.96$ (Figure 4.6). Nonetheless, in the following, the complete set of observed damages is used.

Table 4.4. Estimation of damage in churches with partial accessibility, through simple-linear regressions. The columns report mechanisms with inspected damage; the rows report mechanisms that cannot be inspected. When more than one independent variable is present the highest R^2 value is shown in boldface.

x / *y*	***1***	***2***	***10***	***16***	***17***	***28***
1					0.901	
2					1.233	
3					1.257	
4					1.165	
10	1.021					
11	0.824					
13	1.145			0.869		**0.718**
16		0.830				
17		0.603				
19		**0.720**			1.031	
20		0.587			**0.942**	
21		0.647			**0.946**	
22	**0.907**			0.719		
23	**0.744**			0.578		
25	**0.993**		0.853	0.770		
27		**0.944**		0.823		

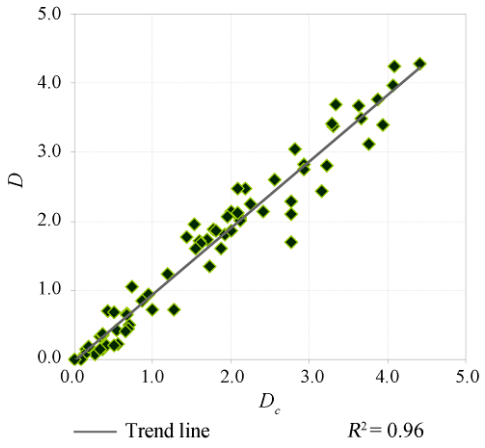

Figure 4.6. Correlation between mean damage, D, observed in the Canterbury churches and the damage computed applying the coefficients in Table 4.4, D_c.

4.5. Seismic risk

The territorial seismic risk of New Zealand churches is herein computed accounting for the previously defined intensity measure and vulnerability, and for exposure as surveyed in §2. As for the seismic hazard, the expected I_H values can be derived on the basis of the site hazard spectra calculated according to the New Zealand Loadings Standard, by multiplying the spectral shape factor for site classes by the hazard factor. Once the elastic site spectrum for horizontal loading has been obtained, I_H can be computed as the area under the pseudo-velocity spectrum for a 5% damping ratio (Eq. (17)). To account for site response, subsoil classes have been identified according to the georeferenced database released by GNS Science. This database has been developed using the New Zealand 1:250 000 scale digital geological map, and suggests ranges of shear-wave velocity values for various geological formations, based on direct measurements in boreholes or derived from geophysical methods coupled with the available subsurface data (Perrin et al., 2015). I_Hs are computed using the site subsoil class coefficients provided in NZS (2004) for the modal response spectrum and the numerical integration time history methods.

The four aforementioned global damage indexes (mean damage weighted based on the geometrical surface area, weighted mean damage, simple mean damage, and synthetic damage index) are computed for each building, given the expected I_H at their site. Figure 4.7 shows the computations carried out according to Eq. (30) for three example regions. The four global damage indexes are multiplied by the corresponding foot-print area and summed up over the relevant territory. In the case of a scenario analysis, the territory is that affected by the earthquake. For example, Table 4.5 presents the scenario related to the 2011 February event and computes the total loss, where the loss is thus the damage times the foot-print area, that an insurance company could take into account for re-insurance purposes.

The four aforementioned indexes can be also used for the computation of the Expected Annual Loss of different regions (Table 4.6), where the loss is computed as previously defined, and could be used for the allocation of a national budget for risk reduction or as part of the computation of an insurance premium. Results relative to the weighted mean damage, the simple mean damage and the synthetic damage index are very similar.

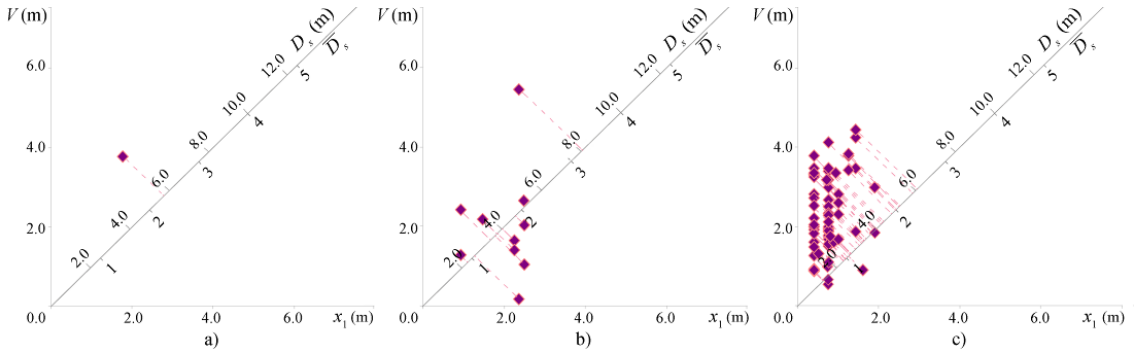

Figure 4.7. Predicted synthetic damage index, D_s, computed according to Eq (30), for churches belonging to different regions: a) Bay of Plenty; b) Manawatu-Wanganui; c) Otago.

The weighted mean damage has average deviation with respect to the simple mean not exceeding 2%, therefore it is confirmed that the ρ_k weights do not deliver a significant contribution, as observed in Figure 4.4. On the contrary, although the mean damage weighted on the geometrical size of the macro-elements presents lower values, the percentages for the allocation of a national budget among regions are very similar to that of the simple mean. Because the synthetic damage index has been derived without any a-priori assumption about the weights of the mechanisms, this index can be used as validation for the arithmetic mean as a more straightforward tool.

A map with risk values per region, based on the simple mean damage index (Eq. (22) with ρ_k = 1) is presented in Figure 4.8. In order to better understand the results, Figure 4.8 also shows for each region average values of damage index, D, and total foot-print area. Although the damage index D, being computed according to Eqs (19) and (22), already encloses for hazard and vulnerability, Figure 4.8 also shows expected Housner Intensity I_H, and surveyed vulnerability V (Eq. (28)), where these values are averages of the individual values computed for each church. It is clear that the highest risks are expected in the Canterbury and Otago regions. Despite the similar exposure, Canterbury has a higher hazard and a smaller vulnerability than Otago. The higher risk of these two regions is due to the very large size of building portfolios compared to all other regions, with the exception of Auckland. On the contrary, Wellington has a significantly larger hazard than the previously mentioned regions, but smaller vulnerability and exposure. The very large hazard of West Coast and Gisborne is more than compensated for by the rather low combined size of URM buildings, as a result of the 1929 and 1931 earthquakes (§2.3). In contrast, the highest average vulnerability is observed in the Northland region, but low hazard and the presence of only one small URM church make

the risk comparatively small. In these regions, as well as in the Bay of Plenty, Hawke's Bay, Taranaki, Tasman, and Waikato, the risk level is bracketed between 180 m^2 and 1993 m^2 because of limited exposure and a combination of low hazard and vulnerability, as compared to the value of 28 520 m^2 reached in Canterbury.

Table 4.5. Scenario analysis of the 2011 February event for the Canterbury region, according with the different global damage

	Mean damage weighted on the geometrical size	Weighted mean damage	Mean damage	Synthetic damage index
Canterbury	19 367.00 m^2	27 881.00 m^2	28 531.00 m^2	27 901.24 m^2

Table 4.6. Expected Annual Loss of New Zealand regions, according with the different global damage

	Mean damage weighted on the geometrical size	Weighted mean damage	Arithmetic mean damage	Synthetic damage index
Auckland	38.31 m^2	41.87 m^2	42.09 m^2	35.89 m^2
Bay of Plenty	0.36 m^2	0.36 m^2	0.36 m^2	0.25 m^2
Canterbury	39.67 m^2	59.93 m^2	57.04 m^2	55.11 m^2
Gisborne	2.02 m^2	2.02 m^2	2.02 m^2	1.75 m^2
Hawke's Bay	0.38 m^2	0.38 m^2	0.38 m^2	0.39 m^2
Manawatu-Wanganui	7.84 m^2	8.46 m^2	7.60 m^2	11.51 m^2
Marlborough	3.28 m^2	3.72 m^2	3.72 m^2	4.34 m^2
Nelson	2.76 m^2	3.60 m^2	3.60 m^2	4.47 m^2
Northland	0.30 m^2	0.60 m^2	0.60 m^2	0.51 m^2
Otago	38.71 m^2	47.49 m^2	47.73 m^2	42.59 m^2
Southland	7.50 m^2	8.69 m^2	8.69 m^2	8.14 m^2
Taranaki	2.65 m^2	3.99 m^2	3.99 m^2	3.48 m^2
Tasman	1.08 m^2	1.08 m^2	1.08 m^2	1.82 m^2
Waikato	3.13 m^2	3.13 m^2	3.13 m^2	2.55 m^2
Wellington	9.22 m^2	10.33 m^2	10.33 m^2	12.85 m^2
West Coast	1.62 m^2	1.62 m^2	1.62 m^2	2.23 m^2

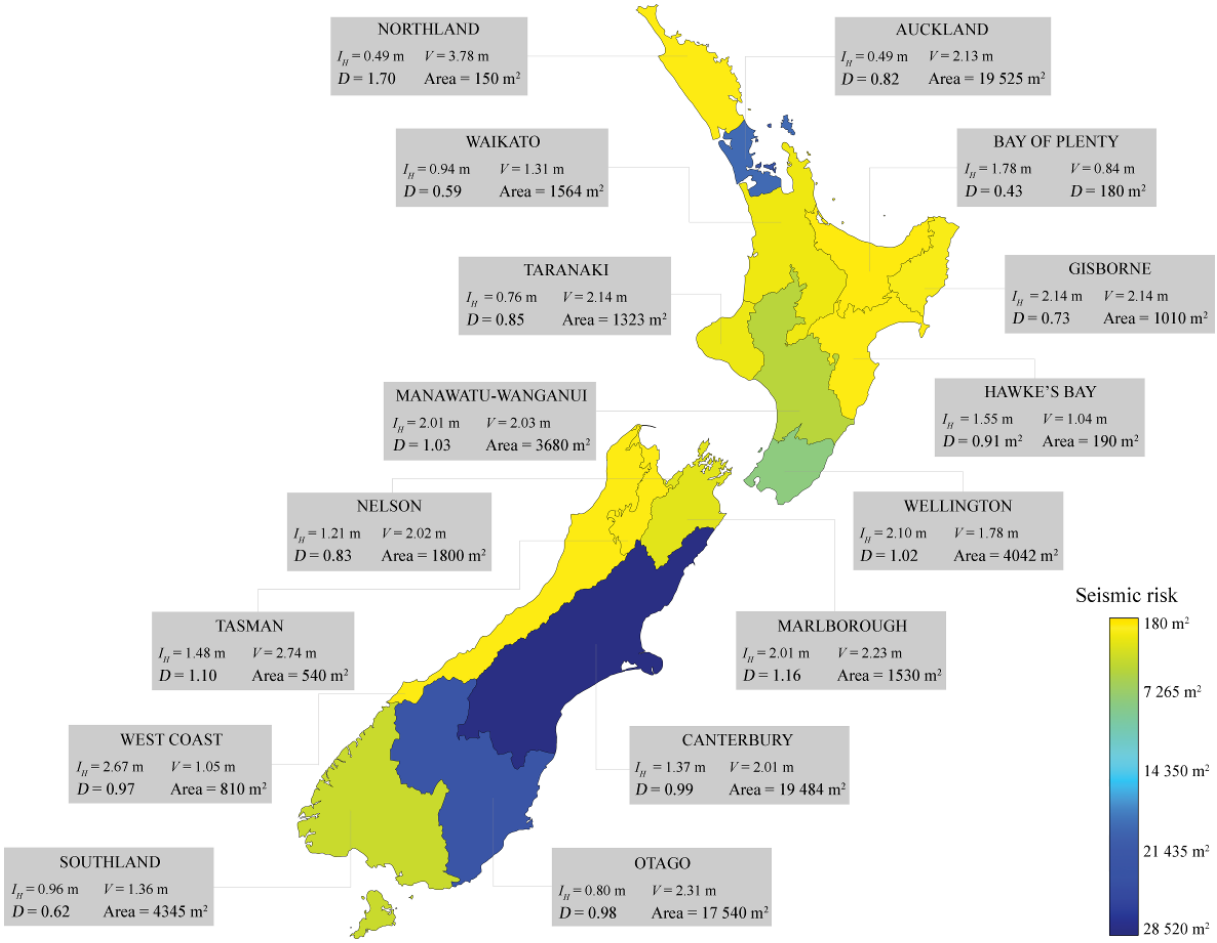

Figure 4.8. Seismic risk values of New Zealand regions computed with the churches individual values of damage, *D*, and foot-print area. Values in boxes are regional averages of *D*, I_H, and *V*, and regional total of foot-print area.

4.6. Conclusions

A quantitative seismic risk assessment for existing unreinforced masonry churches in New Zealand has been presented, based on a national inventory previously surveyed. Hazard has been estimated based on code defined bedrock acceleration expected for a return period of 500 years and literature available regarding site subsoil classes. Several ground motion parameters have been considered as intensity measures, and physical damage suffered by 80 URM churches following the 22 February 2011 event has been correlated to these descriptors. For twenty local mechanisms the vulnerability is expressed as a linear regression of intensity measure and modifiers worsening or improving the seismic response. The considered intensity measures show a similar correlation to damage, but the Housner Intensity can be interpolated more robustly from recorded data and consequently is used for the following analyses. The most efficient

correlation is evaluated for each mechanism according to Stepwise and Best Subsets statistical procedures, and corresponding coefficients are provided.

Seismic risk is first computed mechanism by mechanism, highlighting how some mechanisms are more frequently encountered than are others, and that very large damage levels are expected in a few cases for some regions only. The findings of the analyses also emphasise how results can vary significantly if the number of buildings or their size is considered when expressing exposure. Because reparation cost information is not available, an alternative synthetic damage index is proposed as a ground motion parameter, by minimizing the sum of squares of the difference between expected and observed damage. The proposed index does not require a conventional estimation of the weights used in previous definitions of a global damage index and is purely based on observed data.

Different global damage indexes have been computed and then compared through the computation of the Expected Annual Loss of different regions. Because results are very similar, the synthetic damage index, that has the advantage of being derived without any a-priori assumption about the weights of the mechanisms, can be used as validation for the arithmetic mean as a more straightforward tool. Finally, risk values for each New Zealand region have been presented. Maximum values are expected in the Canterbury and Otago regions, where exposure is very large and offsets the higher vulnerability or hazard observed in other regions. A method for the expeditious assessment of churches with partial accessibility is also proposed, by means of the correlation between observed mechanisms. Territorial scale assessment of church seismic risk can be used for emergency management at regional scale in the case of occurrence of an earthquake, allowing an estimate of the required resources to be deployed and possible scenarios, given the recorded ground motion. In a preventive framework, such a risk assessment serves to identify priorities for more in-depth analysis of individual buildings, to evaluate the impact of possible retrofitting by accounting for modifiers not previously present in the building, and could be used for the assignment of a national budget among regions or for the computation of an insurance premium. The method proposed can be applied elsewhere, provided that enough observation damage data is available to calibrate the vulnerability regressions, or can be used for a rough preliminary assessment in countries with a similar built heritage.

4.7. Calculation section

As a practical development from the theoretical basis presented above, a worked example of an existing URM church is reported herein. The building under consideration is a stone masonry church located on the foreshore of Lake Tekapo, in the Canterbury region (Figure 4.9). Only 9 mechanisms out of 20 are possible, because the porch, transept, triumphal arch, chapels, and bell tower (mechanisms #4, #10-11, #13, #20-23, #25, #27-28) are not present.

Figure 4.9. Church of the Good Shepherd (Lake Tekapo): a) external view from the street; b) internal view.

4.7.1. Computation of the synthetic damage index

In Table 4.7 an overview of the modifier attribution is reported, varying between 0 and 1 depending on the presence and effectiveness of fragility increasers or earthquake-resistant elements. For the sake of conciseness only some modifiers are discussed in detail, whereas a full explanation of all modifiers is given in §3.6.2. E.g., because the façade does not present buttresses whatsoever, a unity value (absent earthquake resistant element) is attributed to the corresponding modifiers of mechanism #2. Likewise, a unity value is introduced to account for the poor quality masonry modifier (fragility increaser), because of the presence of undressed natural stone units (mechanisms #1, #3, #6, #19, #26). The nave cover is a sloping roof without a chord at support level (thrusting element, i.e. fragility increaser), but with a raised tie, which contributes to the thrust reduction (as shown in Sorrentino et al., 2008) thus scoring a 0.33 score in mechanisms #5 and #19. In contrast, no thrusts are applied to the façade, leading to zero scores for mechanism #1. Finally, in the last line of Table 4.7 the elements of vector **c**

are computed as column-wise sums, whereas in Table 4.8 the reported data are the vector $\mathbf{m}_1$ of the regression coefficients of the intensity measure.

Accordingly, the vulnerability index, *V*, is computed as:

$$V = \frac{\mathbf{m}_1^T \mathbf{c}}{\mathbf{m}_1^T \mathbf{m}_1} = 3.93 \text{ m} \tag{32}$$

From the hazard analysis the expected I_H in Lake Tekapo is 1.60 m such that the *predicted* non-dimensional synthetic damage index can be obtained as:

$$\overline{D_s} = \frac{1.60 + 3.93}{2.5} = \frac{5.53}{2.5} = 2.21 \tag{33}$$

corresponding to a moderate damage d_2.

4.7.2. Computation of the mean damage considering the church as partially accessible

In order to fully illustrate how the proposed procedure works, let us initially assume that the apse is not visible, whereas the façade is. Consequently, according to Table 4.4:

$$d_{16} = 0.830 \times d_2 \tag{34}$$

$$d_{17} = 0.603 \times d_2 \tag{35}$$

As for mechanism #19, related to the interactions between the nave and its roof, there are three possible cases. If only the façade is visible:

$$d_{19} = 0.729 \times d_2 \tag{36}$$

If only the apse is visible:

$$d_{19} = 1.031 \times d_{17} \tag{37}$$

If both façade and apse are visible, Eq. (36) has to be used, because associated to the highest R^2, as highlighted in Table 4.4 through boldface.

Table 4.7. Modifier attribution and computed vector c for each mechanism of the sample church.

Mechanism no. / Variable	*1*	*2*	*3*	*5*	*6*	*16*	*17*	*19*	*26*
Lateral restraint	N/A	N/A	N/A	N/A	1×0.706	N/A	N/A	N/A	N/A
Buttresses	N/A	1×1.428	N/A	N/A	N/A	N/A	N/A	N/A	N/A
Lintels	N/A	N/A	N/A	N/A	1×0.666	N/A	N/A	N/A	N/A
Thrusting elements	0×1.713	N/A	N/A	0.33×0.614	N/A	N/A	N/A	0.33×3.266	N/A
Large openings	0×0.479	N/A	N/A	N/A	N/A	N/A	N/A	N/A	N/A
Top beam	N/A	N/A	N/A	N/A	N/A	N/A	N/A	N/A	N/A
Heterogeneous materials	N/A	N/A	N/A	N/A	N/A	N/A	N/A	N/A	N/A
Connections	0×1.368	0×2.023	N/A	0.33×2.306	N/A	0×1.206	N/A	N/A	N/A
Slenderness	0×0.875	0×0.745	0×1.626	0×0.654	N/A	0×2.044	0×1.728	N/A	0×2.388
Asymmetry conditions	N/A	N/A	N/A	N/A	N/A	N/A	N/A	N/A	0.67×1.170
Poor quality masonry	1×0.987	N/A	1×0.424	N/A	1×0.886	N/A	N/A	1×1.055	1×1.089
c	0.987	1.428	0.424	0.964	2.258	0.000	0.000	2.133	1.861

Table 4.8. Coefficients of the intensity measure.

Mechanism no. / Variable	*1*	*2*	*3*	*5*	*6*	*16*	*17*	*19*	*26*
$\mathbf{m_1}$ (m^{-1})	0.376	0.353	0.358	0.267	0.516	0.352	0.236	0.417	0.452

4.8. References

Andreotti, C., Liberatore, D., and Sorrentino, L., 2015. Identifying seismic local collapse mechanisms in unreinforced masonry buildings through 3D laser scanning, *Key Engineering Materials* 628, 79-84.

Arias, A. 1970. A measure of earthquake intensity. In *Seismic Design for Nuclear Power Plants*. Edited by R. J. Hansen. Cambridge, MA: MIT Press.

Cardona, O. D., Salgado, M. A., Carreño, M. L., Bernal, G. A., Villegas, C. P., and Barbat, A. H., 2014. Urban seismic risk assessment of Santo Domingo: a probabilistic and holistic approach, in *Proceedings, 10th U.S. National Conference*

on Earthquake Engineering: Frontiers of Earthquake Engineering, 21-25 July, 2014, Anchorage, Alaska.

Cattari, S., Ottonelli D., Pinna M., Lagomarsino S., Clark W., Giovinazzi S., Ingham J., Marotta A., Liberatore D., Sorrentino L., Leite J., Lourenco P.B., and Goded T., 2015. Preliminary results from damage and vulnerability analysis of URM churches after the Canterbury earthquake sequence 2010-2011, in *Proceedings*, *New Zealand Society for Earthquake Engineering Technical Conference,* 10-13 April, 2015, Rotorua, New Zealand, paper O-36.

Chaulagain, H., Rodrigues, H., Silva, V., Spacone, E., and Varum, H., 2015. Seismic risk assessment and hazard mapping in Nepal, *Natural Hazards* 78, 583–602.

Cherif, S., Chourak, M., and Abed, M., 2015. Seismic risk assessment of the city of Al Hoceima (North of Morocco) using the RISK-UE vulnerability index method, in *Proceedings, 50th International Conference on Earthquake Engineering and Seismology*, 12-16 May, 2015, Kiel, Germany.

Chiauzzi, L., Masi, A., Mucciarelli, M., Vona, M., Pacor, F., Cultrera, G., Gallovič, F., and Emolo, A., 2012. Building damage scenarios based on exploitation of Housner intensity derived from finite faults ground motion simulations, *Bulletin of Earthquake Engineering* 10, 517–545.

Chrysostomou, C. Z, Kyriakides, N., and Çağnan, Z., 2014. Scenario-based seismic risk assessment for the Cyprus region, in *Proceedings*, *2th European Conference on Earthquake Engineering and Seismology*, 25-29 August, 2014, Istanbul, Turkey.

D'Ayala, D., 2000. Establishing Correlation between Vulnerability and Damage Survey for Churches, Paper No 2237, in *Proceedings, 12th World Conference on Earthquake Engineering*, 30 January – 4 February, 2000, Auckland, New Zealand.

D'Ayala, D., and Speranza, E., 2003. Definition of Collapse Mechanisms and Seismic Vulnerability of Historic Masonry Buildings, *Earthquake Spectra* 19, 479–509.

Decanini, L., Mollaioli, F., and Oliveto, G., 2002. Structural and seismological implications of the 1997 seismic sequence in Umbria and Marche, Italy, in *Innovative approaches to earthquake engineering* (G. Oliveto, ed.), WIT Press, Southampton, 229–323.

De Matteis, G., Criber, E., and Brando, G., 2016. Damage Probability Matrices for Three-Nave Masonry Churches in Abruzzi After the 2009 L'Aquila Earthquake, *International Journal of Architectural Heritage* 10, 120–145.

Draper, N. and Smith, H., 1981. *Applied Regression Analysis*, John Wiley & Sons, New York, USA, 736 pp.

Dolce, M., Kappos, A., Masi, A., Penelis, G., and Vona, M., 2006. Vulnerability assessment and earthquake damage scenarios of the building stock of Potenza (Southern Italy) using Italian and Greek methodologies, *Engineering Structures* 28, 357–371.

Dowrick D.J., 2003. *Earthquake risk reduction*, John Wiley & Sons, Chichester, UK, 506 pp.

Dunand, F., Nicol, J., Moutou Pitti, R., Fournely, E., and Toussaint, E., 2014. Seismic risk quantification in France: probabilistic evaluation, in *Proceedings, 2th European Conference on Earthquake Engineering and Seismology*, 25-29 August, 2014, Istanbul, Turkey.

Eleftheriadou, A. K., Baltzopoulou, A. D., and Karabinis, A. I., 2014. Seismic risk assessment of buildings in the extended urban region of Athens and comparison with the repair cost, *Open Journal of Earthquake Research* 3, 115-134.

Erberik, M. A., 2010. Seismic risk assessment of masonry buildings in Istanbul for effective risk mitigation, *Earthquake Spectra* 26, 967–982.

Faccioli, E., Pessina, V., Calvi, G. M., and Borzi, B., 1999. A study on damage scenarios for residential buildings in Catania city, *Journal of Seismology* 3, 327–343.

Gizzi, F. T., Masini, N., Sileo, M., Zotta, C., Scavone, M., Liberatore, D., Sorrentino, L., and Bruno, M., 2014. Building features and safeguard of church towers in Basilicata (Southern Italy), in *Science, Tecnology and Cultural Heritage* (M. A. Rogerio-Candelera, ed.), CRC Press, 369-374.

Grünthal, G. (ed.), 1998. *European Macroseismic Scale 1998 (EMS-98)*, Centre Europèen de Géodynamique et de Séismologie, Luxembourg.

Housner, G. W., 1959. Behaviour of structures during earthquakes, *Journal of the Engineering Mechanics Division* 85, 109-129.

Kappos, A. J., Panagopoulos, G., and Penelis, G. G., 2008. Development of a seismic damage and loss scenario for contemporary and historical buildings in Thessaloniki, Greece, *Soil Dynamics and Earthquake Engineering* 28, 836-850.

Kramer, S. L., 1996. *Geothecnical earthquake engineering*, Prentice Hall, Upper Saddle River, NJ, 653 pp.

Lagomarsino, S., and Podestà, S., 2004. Seismic vulnerability of ancient churches: II. Statistical Analysis of Surveyed Data and Methods for Risk Analysis, *Earthquake Spectra* 20, 395-412.

Lagomarsino, S., Podestà, S., Cifani, G., and Lemme, A., 2004. The 31st October 2002 earthquake in Molise (Italy): a new methodology for the damage and seismic vulnerability survey of churches, paper 1366, in *Proceedings*, *13th World Conference on Earthquake Engineering*, 1-6 August, 2004, Vancouver, Canada.

Liberatore, D., Masini, N., Sorrentino, L., Racina, V., Sileo, M., AlShawa, O., Frezza, L., 2016. Static penetration test for historical masonry mortar, *Construction and Building Materials*, in press. DOI:10.1016/j.conbuildmat.2016.07.097.

Marotta, A., Goded, T., Giovinazzi, S., Lagomarsino, S., Liberatore, D., Sorrentino, L., and Ingham, J. M., 2015. An inventory of unreinforced masonry churches in New Zealand, *Bulletin of the New Zealand Society for Earthquake Engineering* 48, 170-189.

Marotta, A., Sorrentino, L., Liberatore, D., and Ingham J. M., 2016. Vulnerability assessment of unreinforced masonry churches following the 2010-2011 Canterbury (New Zealand) earthquake sequence, *Journal of Earthquake Engineering*, in press. DOI:10.1080/13632469.2016.1206761.

Marulanda, M. C., Carreño, M. L., Cardona, O. D., Ordaz, M. G., and Barbat, A. H., 2013. Probabilistic earthquake risk assessment using CAPRA: application to the city of Barcelona, Spain, *Natural Hazards* 69, 59–84.

Masi, A., Chiauzzi, L., Braga, F., Mucciarelli, M., Vona, M., and Ditommaso, R., 2011. Peak and integral seismic parameters of L'Aquila 2009 ground motions: observed versus code provision values, *Bulletin of Earthquake Engineering* 9, 139–156.

Moon, L., Dizhur, D., Senaldi, I., Derakhshan, H., Griffith, M., Magenes, G. and Ingham, J. M., 2014. The demise of the URM building stock in Christchurch during the 2010/2011 Canterbury earthquake sequence, *Earthquake Spectra* 30, 253-276.

Mouyiannou, A., Penna, A., Rota, M., Graziotti, F., Magenes, G., 2014. Implications of cumulated seismic damage on the seismic performance of unreinforced masonry buildings, *Bulletin of the New Zealand Society for Earthquake Engineering* 47, 157-170.

New Zealand Standard (NZS), 2004. *Structural Design Actions - Part 5: Earthquake Actions*, NZS 1170.5:2004, Wellington, New Zealand.

Perrin, N. D., Heron, D., Kaiser, A., and Van Houtte, C., 2015. VS30 and NZS 1170.5 site class maps of New Zealand, Paper No. O-07, in *Proceedings, New Zealand Society for Earthquake Engineering (NZSEE) Annual Technical Conference*, 10-12 April, 2015, Rotorua, New Zealand.

Ragone, A., Ippolito, A., Liberatore, D., and Sorrentino, L., 2016. Emerging Technologies for the Seismic Assessment of Historical Churches: The Case of the Bell Tower of the Cathedral of Matera, Southern Italy, in *Handbook of Research on Emerging Technologies for Architectural and Archaeological Heritage* (A. Ippolito, ed.), IGI Global, Hershey, Pennsylvania, 163-200. DOI: http://doi.org/10.4018/978-1-5225-0675-1.ch006.

Rota, M., Penna, A., Strobbia, C., and Magenes G., 2011. Typological seismic risk maps for Italy, *Earthquake Spectra* 27, 907-916.

Russell, A. P., and Ingham, J. M., 2010. Prevalence of New Zealand's unreinforced masonry buildings, *Bulletin of the New Zealand Society for Earthquake Engineering* 43, 182-201.

Siddique, M. S., and Schwarz, J., 2015. Elaboration of multi-hazard zoning and qualitative risk maps of Pakistan, *Earthquake Spectra* 31(3), 1371–1395.

Sorrentino, L., Bruccoleri, D., and Antonini, M., 2008. Structural interpretation of post-earthquake (19th century) retrofitting on the Santa Maria degli Angeli Basilica, Assisi, Italy. *Proceedings, 6th International Conference on Structural Analysis of Historical Constructions,* 2-4 July, 2008, Bath, United Kingdom.

Sorrentino, L., Liberatore, L., Decanini, L. D., and Liberatore, D., 2014a. The performance of churches in the 2012 Emilia earthquakes, *Bulletin of Earthquake Engineering* 12, 2299–2331.

Sorrentino, L., Alshawa, O., and Liberatore, D., 2014b. Observations of out-of-plane rocking in the Oratory of San Giuseppe dei Minimi during the 2009 L'Aquila earthquake, *Applied Mechanics and Materials* 621, 101-106.

Sorrentino, L., Liberatore, L., Liberatore, D., and Masiani, R., 2014c. The behaviour of vernacular buildings in the 2012 Emilia earthquakes, *Bulletin of Earthquake Engineering* 12, 2367-2382.

Stafford P.J.,·Berrill J.B., Pettinga J.R. 2009. New predictive equations for Arias intensity from crustal earthquakes in New Zealand. J Seismol (2009) 13:31–52.

Toma-Danila, D., Zulfikar, C., Manea, E. F., and Cioflan, C. O., 2015. Improved seismic risk estimation for Bucharest, based on multiple hazard scenarios and analytical methods, *Soil Dynamics and Earthquake Engineering* 73, 1–16.

Travasarou T, Bray JD, Abrahamson NA (2003) Empirical attenuation relationship for Arias intensity. Earthq Eng Struct Dyn 32(7):1133–1155.

Vicente, R., Ferreira, T., and Maio, R., 2014. Seismic risk at the urban scale: assessment, mapping and planning, in *Proceedings, 4th International Conference on Building Resilience*, *Building Resilience*, 8-10 September, 2014, Salford Quays, United kingdom.

Chapter 5

Ambient vibration tests on New Zealand unreinforced masonry churches

The extensive damage observed in stone and clay brick unreinforced masonry churches after the 2010-2011 Canterbury earthquakes has highlighted the need to appropriately describe their dynamic features. Dealing with historical structures, characterized by a high level of uncertainty affecting both material properties and structural schemes, and given the paramount need of non-destructive investigation techniques, ambient vibration tests can be considered an effective tool. A test campaign has been conducted on four churches located in Auckland and deemed to be representative of the New Zealand portfolio, being both in stone and clay brick unreinforced masonry, single- or multiple-nave buildings with or without bell towers, with naves covered by a sloping timber roof or vaults. The structures have been instrumented with tri-axial digital wireless accelerometer sensors. The sensor setup has been arranged following both vertical and horizontal alignments, recording with a sampling rate of 128 Hz and a sampling time ranging between 10 to 60 mins. Results of the dynamic tests can guide the identification of possible collapse mechanisms, can provide information on modal parameters, and contribute to estimate the filter effect that the macro-elements of the building develop on the response of soaring elements, such as gables, pinnacles and crenellations.

5.1. Introduction

A great deal of knowledge about the dynamic performance associated with existing structures can be generated by experimentally evaluating the structures' dynamic properties. In general, such tests provide true forms of many complex phenomena such as soil-structure interaction, nonlinearities in stiffness, non-structural components and energy dissipation mechanisms. Thus, in-situ test results can be considered as the true base for advanced assessment of structural integrity, damage detection and validation of design assumptions. Nevertheless, in case of historical structures characterized by a high level of uncertainty affecting both material properties and structural schemes and given the paramount need of a non-destructive approach, ambient vibration tests can be considered an effective tool for assessing their dynamic behaviour (Rainieri and Fabbrocino, 2011).

Several studies based on ambient vibration tests have already been carried out on historical structures (Gentile and Saisi, 2007; Bayraktar et al., 2009; Aras et al., 2011; Osmancikli et al., 2012; Karatzetzou et al., 2015; Nohutcu et al., 2015) and specifically on churches (Jaishi et al., 2003; Baptista et al., 2005; Casarin and Modena, 2007; Tashkov et al., 2010; Votsis et al., 2012; Ramos et al., 2013; Gizzi et al., 2014).

The study reported here investigates the dynamic behaviour of New Zealand unreinforced masonry churches by means of the results of an ambient vibration campaign carried on four buildings, representative of the national inventory (§ 2). In fact, it is widely known that URM churches frequently perform poorly even in moderate earthquakes, because of their intrinsic structural vulnerability due to their open plan, large wall height-to-thickness and length-to-thickness ratios, and the use of thrusting horizontal structural elements for vaults and roofs. Moreover, their use of low strength materials and a poor maintenance often causes decay, and the connections between the various structural components are often insufficient to resist loads generated during earthquakes (Sorrentino et al. 2008). Additionally, damage is related to architectural types and construction details, which may vary from country to country (§ 3). The 2010-2011 Canterbury earthquakes have again demonstrated the unsatisfactory earthquake performance of unstrengthened URM churches with damage occurred being particularly extensive. For this reason to properly describe the dynamic characteristics of this structural type is of paramount importance.

Modal identification is based on operational modal analysis (OMA) techniques, also called output-only modal analysis, which use structural response measurements from ambient excitation to extract modal characteristics of a structure in terms of eigenfrequencies, damping and mode shapes. The main assumption at the base of OMA methods is that the ambient excitation input, represented by wind, traffic and human activities, is a Gaussian white noise characterized by a flat spectrum in the frequency range of interest. Unlike experimental modal analysis (EMA), where the structure is excited by a controlled and measured signal and thus developed in a deterministic framework, the output-only modal analysis, being based on random responses, follows a stochastic approach and is used for modal identification under actual operating conditions, and in situations where it is difficult or impossible to artificially excite the structure, as in the case of historical buildings. Nevertheless, due to the random nature of the excitation, the response includes not only the modal contributions of the ambient forces and the structural system but also the contribution of noise signals from undesired sources.

Such dynamic tests, aside from guiding the identification of possible collapse mechanisms in historical structures as unreinforced masonry churches, can contribute to estimate the filter effect that the macro-elements of the building develop on the response of soaring elements, such as gables, pinnacles and crenellations. The Italian Building Code (DMI 2008) provides simplified formulas for modal shapes and participation factors when dealing with the verification of portion of buildings at a given height above ground, but only in the case of ordinary buildings and no calibration is set for such factors in case of churches.

5.2. Local mechanisms analysis according to the Italian Building Code

Existing masonry buildings are prone to suffer earthquake induced local collapse mechanisms, that can be assessed using limit analysis of equilibrium according to the kinematic approach, aiming to estimate the horizontal action activating the kinematism. The seismic capacity can be evaluated in terms of strength or displacement, and the considered macro-element is transformed into a single-degree-of-freedom system, identified as a rigid body. Considering a virtual rotation θ_k, it is possible to determine the generalised displacement of the body (centre and angle of rotation) and the displacement components of the points in which forces are applied.

According to the strength-based linear kinematic analysis, the horizontal load multiplier, α_0, that activates the local mechanism is obtained solving the Equation of Virtual Works, written in the form of virtual displacements:

$$\alpha_0 \left(\sum_{i=1}^{n} P_i \delta_{x,i} + \sum_{j=n+1}^{n+m} P_j \delta_{x,j} \right) - \sum_{i=1}^{n} P_i \delta_{y,i} - \sum_{h=1}^{o} F_h \delta_h = L_{fi} \qquad (38)$$

where P_i is the generic gravity load (self-weight of the body, applied in the centroid, or other loads on the body); P_j is the generic gravity load not directly sustained by the bodies of the kinematic chain, but whose mass, as a consequence of the earthquake, if not appropriately transferred to other parts of the building, generates an horizontal force on the bodies of the mechanism; $\delta_{x,i}$ is the virtual horizontal displacement of the point of application of the *i*-th weight P_i, and $\delta_{x,j}$ is the virtual horizontal displacement of the point of application of the *j*-th weight P_j,; $\delta_{y,i}$ is the virtual vertical displacement of the point of application of the *i*-th weight P_i; F_h is the generic external force applied to the body and δ_h is the virtual displacement of the point of application of the *h*-th external force; L_{fi} is the work of possible internal forces. Accordingly, *n* if the number of self-weight forces applied to the bodies of the kinematic chain; *m* is the number of forces not directly applied to the bodies but whose seismic force is applied on the bodies of the kinematic chain; *o* is the number of external forces, not associated to masses, applied to the body.

The seismic spectral acceleration, a^*_0, activating the mechanism is obtained following:

$$a_0^* = \frac{\alpha_0 \sum_{i=1}^{n+m} P_i}{M^* CF} = \frac{\alpha_0 \, g}{e^* CF} \qquad (39)$$

where *g* is the gravity acceleration, e^* is the mass participation factor, and *CF* is the confidence factor, assumed equal to 1.35.

The mass participation factor e^* is computed as:

$$e^* = \frac{g \, M^*}{\sum_{i=1}^{n+m} P_i} \qquad (40)$$

where M^* is evaluated assimilating the virtual displacements of the points of application of the different forces associated to the kinematism, P_i, to a modal shape of vibration:

$$M^* = \frac{\left(\sum_{i=1}^{n+m} P_i \, \delta_{x,i} \right)^2}{g \sum_{i=1}^{n+m} P_i \, \delta_{x,i}^2} \tag{41}$$

As the Italian code assumes to have concentrated masses, the mass participation factor e^* is considered equal to 1.

Following the displacement-based non-linear kinematic analysis, in order to know the displacement capacity of a mechanism up to collapse, the horizontal load multiplier α can be evaluated with reference to any displaced configuration, described by the displacement d_k of a control point of the system. The spectral displacement d^* of the equivalent oscillator can be obtained knowing the displacement of the control point d_k and defining the equivalent spectral displacement with reference to the virtual displacements evaluated with respect to the initial configuration:

$$d^* = d_k \frac{\sum_{i=1}^{n+m} P_i \, \delta_{x,i}}{\delta_{x,k} \sum_{i=1}^{n+m} P_i} \tag{42}$$

where $\delta_{x,k}$ is the horizontal virtual displacement of the point k, assumed as reference for computing the displacement d_k.

The strength and the displacement capacity related to the Damage Limitation Limit State (DLLS) and the Life Safety Limit State (LSLS) are evaluated on the capacity curve, at the following points:

- spectral acceleration, a^*_0, corresponding to the activation of the mechanism, for DLLS;
- spectral displacement, d^*_u, corresponding to the 40% of the displacement that makes $\alpha = 0$, for LSLS.

The safety verifications against the DLLS is satisfied whenever the spectral acceleration of activation of the mechanism, a^*_0, is larger then the seismic demand peak acceleration. When an isolated element or a portion of a construction at ground level is evaluated ($Z = 0$), a^*_0 is compared to the ground acceleration, that is the elastic-spectral ordinate for $T = 0$. On the contrary, if the mechanism involves a portion of the building at a given

height above ground ($Z > 0$), the amplification of the acceleration at the considered height compared to the acceleration of the ground has to be accounted. The seismic demand peak acceleration are reported in Table 5.1.

The verification of the LSLS of local mechanisms, can be developed according to two different procedures:

- simplified verification with behaviour factor q (linear kinematic analysis, strength-based);
- verification by means of capacity spectrum (non-linear kinematic analysis), consisting in the comparison between an ultimate displacement capacity d^*_u of the mechanism and a spectral displacement demand Δ_d.

The spectral displacement demand are reported in Table 5.1.

Table 5.1. Seismic demand peak acceleration and spectral displacement demand according to Damage Limitation Limit State (DLLS) and Life Safety Limit State (LSLS).

	DLLS	**LSLS**	
		linear	**non-linear**
Z=0	$a_0^* \geq a_g(P_{V_R})S$	$a_0^* \geq \frac{a_g(P_{V_R})S}{q}$	$d_u^* \geq S_{De}(T_S)$
Z>0	$a_0^* \geq S_e(T_1)\psi(Z)\gamma$	$a_0^* \geq \frac{S_e(T_1)\psi(Z)\gamma}{q}$	$d_u^* \geq S_{De}(T_1)\psi(Z)\gamma \frac{\left(\frac{T_S}{T_1}\right)^2}{\sqrt{\left(1-\frac{T_S}{T_1}\right)^2 + 0.02\frac{T_S}{T_1}}}$

where a_g is function of the exceedance probability for the assumed limit state and the reference life of the building; S is the coefficient accounting for soil type and topographic conditions; q is the behaviour factor, equal to 2; T_1 is the 1st period of vibration of the whole structure in the direction under consideration; $S_e(T_1)$ is the elastic spectrum ordinate, function of the exceedance probability of the considered limit state and the reference life of the building V_R, calculated for T_1; $\psi(Z)$ is the 1st mode of vibration of the building in the direction under consideration, normalised to unity at the top of the building and generally assumed equal to Z/H, where H is the height above ground of the whole building; γ is equivalent to the modal mass participation factor of the building, assumed equal to $3N/(2N+1)$, with N = number of stories of the building; $S_{De}(T_S)$ is the ordinate of the elastic displacement spectrum, evaluated as a function of the secant period of the mechanism, not of the building; $S_{De}(T_1)$ is the displacement

elastic spectrum ordinate, function of the exceedance probability of the considered limit state and the reference life of the building V_R, calculated for T_1.

In the case of local mechanisms, DLLS corresponds to the appearance of cracks that involve only part of the structure; therefore, in the case of existing masonry buildings, although it is recommended to satisfy this limit state, its verification is not mandatory for conservation issues.

5.3. Operational modal analysis

Ambient excitation testing does not directly lend itself to the frequency response functions (FRFs) in the frequency domain, or impulse response functions (IRFs) in the time domain, because the input forces are not measured. The extraction of modal parameters from the ambient vibration data can be conducted by using several output-only methods, operating both in the frequency and time domain: *Peak Picking*, *Frequency Domain* and *Enhanced Frequency Domain Decomposition*, and *Stochastic Subspace Identification*. According to the methods operating in the frequency domain, namely the first three above-mentioned, the relationship between the input, $x(t)$, and the output, $y(t)$, at a resonant frequency, f, can be written as:

$$G_{yy}(f) = |H(f)|^2 G_{xx}(f) \tag{43}$$

where $G_{yy}(f)$ is the output spectral density function; $G_{xx}(f)$ is the input spectral density function; $H(f)$ is the Frequency Response Function (FRF), a complex number with real and imaginary parts, that in polar notation is equal to:

$$H(f) = |H(f)|\, e^{-i\theta(f)} \tag{44}$$

where $\theta(f)$ is the phase.

Peak Picking (*PP*) method, also known as Basic Frequency Domain technique, is the classical approach that allows identifying the modal parameters of a structure from ambient responses, by processing the signal using the Discrete Fourier Transform. The measured time histories are converted to spectra and the eigenfrequencies are determined as the peaks of the spectra. This method allows to estimate mode shapes directly from the power spectral density matrix at the peak (Bendat and Piersol, 1993), but it gives reliable results only if the modes are well separated and in case of low damping.

Frequency Domain Decomposition (*FDD*) technique has been introduced by Brincker et al. (2000) and is an improvement of the classical approach, overcoming its disadvantages. By decomposing the spectral density function of the output, $G_{yy}(f)$, using the Singular Value Decomposition (SVD), the response is separated into a set of single degree of freedom systems, each corresponding to an individual mode. The SVD of the spectral matrix at each frequency is given by:

$$G_{yy}(f) = U(f)S(f)U^{H}(f) \tag{45}$$

where $U(f)$ is a unitary matrix containing singular vectors and $S(f)$ is a diagonal matrix holding scalar singular values.

If only one mode is dominating at a given frequency, there is only one term in Eq. (45) and the corresponding singular vector is an estimate of the mode shape for that resonant frequency.

Enhanced Frequency Domain Decomposition (*EFDD*) is an extension of the FDD technique (Jacobsen et al., 2007), consisting in taking back to time domain the spectral density function identified around a resonance peak by using the Inverse Discrete Fourier Transform. The function is estimated using the singular vector determined by the basic FDD technique and comparing it to neighbouring vectors by computing the Modal Assurance Criterion (MAC). MAC is a statistical indicator of consistency between mode shapes, being sensitive to large differences between them (Pastor et al. 2012). It is calculated as the normalized scalar product of the two sets of mode shape vectors, ϕ_1 and ϕ_2:

$$MAC(\phi_1, \phi_2) = \frac{\left(\phi_1^T \phi_2\right)^2}{\left(\phi_1^T \phi_1\right)\left(\phi_2^T \phi_2\right)} \tag{46}$$

MAC is a scalar coefficient analogous to the correlation coefficient in statistics and ranges between zero, representing no consistent correspondence, to one. Consequently, if the modal vectors under consideration exhibit a consistent linear relationship, the modal assurance criterion should approach unity. By using the MAC value as a threshold, and generally a value greater than 0.80 is taken into account, only singular values whereby random noise is averaged out are taken into account.

Stochastic Subspace Identification is a method that accounts the stochastic response from a system as a function of time, where the system is considered in a classical formulation as a multi degree of freedom structural system. Moving the classical continuous time formulation to the discrete time domain by introducing the State Space formulation, the classical 2nd order system equation simplifies to a first order equation:

$$\begin{aligned} \dot{x}(t) &= A_c\, x(t) + B\, f(t) \\ y(t) &= C\, x(t) \end{aligned} \tag{47}$$

where $x(t)$ denotes, this time, the system state, $f(t)$ is the system unknown input, A_c is the system matrix in continuous time from which the modal parameters can be calculated, B is the load matrix and C is the observation matrix.

The input term, $B\, f(t)$, which could consist of deterministic and stochastic excitation, can be replaced with a pure stochastic input vector $w(t)$, and the term $v(t)$ is introduced as measurement noise:

$$\begin{aligned} \dot{x}(t) &= A_c\, x(t) + w(t) \\ y(t) &= C\, x(t) + v(t) \end{aligned} \tag{48}$$

Since measurement data is obtained in discrete time samples, the system equations have to be denoted in discrete formulation, and the system matrices can be estimated through the use of a linear regression approach, and modal parameters are found by eigenvalue decomposition:

$$\begin{aligned} x_{t+1} &= A_d\, x_t + w_t \\ y_t &= C\, x_t + v_t \end{aligned} \tag{49}$$

The estimated modes, increasing model dimension, are then plotted on a stabilization diagram, where structural modes should remain “stable” whereas noise modes should be different at any model order and therefore they do not stabilize into a single frequency.

Since the presence of peaks in the spectra of the signals can be due both to the frequency content of the input and to the structural response, it is of paramount importance with any of the accounted methods to look at the phase and at the coherence function. For dominant peaks, in fact, the phase of the cross-spectra is either zero or 180°, as expected for a resonant response of the structure, and is calculated according to:

$$\theta_{xy}(f) = \tan^{-1}\left[\frac{Q_{xy}(f)}{C_{xy}(f)}\right] \tag{50}$$

where $C_{xy}(f)$ and $Q_{xy}(f)$ are, respectively, the real and the imaginary part of the one-sided cross-spectral density function, $G_{xy}(f)$.

On the other hand, for dominant peaks, the coherence function between input force and each response, needed for establishing the random errors in the phase estimates, tend to reach the unity at the identified frequencies. When the coherence function, whose expression is reported in the following Eq. (51), is greater than zero but less than unity, the system relating $y(t)$ to $x(t)$ could be not linear or the output $y(t)$ could be due to other inputs besides $x(t)$:

$$\gamma_{xy}(f) = \frac{\left|G_{xy}(f)\right|^2}{G_{xx}(f)G_{yy}(f)} \tag{51}$$

5.4. Description of the tested churches

The test campaign has been conducted on four churches located in Auckland and deemed to be representative of the New Zealand portfolio, being both in stone and clay brick unreinforced masonry, single- or multiple-nave buildings with or without bell towers, with naves covered by a sloping timber roof or vaults (Figure 5.1).

The church of St Paul's is also known as the Auckland Anglican "Mother Church" as the original St Paul's was the first church to be built in the city. The foundation stone was laid on 1841 and the church also served as Auckland Cathedral for over 40 years. Although it has never been completed, as clearly visible in the unfinished bell tower, St Paul's is nevertheless a particularly fine example of Gothic Revival architecture, with its natural stone facing and finest decorative finishes, with its hammer beam trusses and lancet-shaped openings.

The Church of Our Lady of the Assumption has historical and architectural significance for its striking Gothic Revival design. It is an example of the important work of Thomas Mahoney, major contributor to the ecclesiastical architecture of Auckland, which designed the church in 1887. The brick building presents a steeply-pitched timber roof with arch braces underneath the collar, external buttressing, lancet-shaped openings and broached spire, being thus an expression of Early English Gothic influences. The

addition of the spire completed the church in 1902 and a foyer was added in 1970 along the east side of the nave.

The church of St Matthew's-in-the-City is one of the finest Gothic Revival stone churches throughout New Zealand and is situated on an elevated site at the intersection of two important inner city streets. The cathedral-sized building was designed by a famous firm of English architects, F.L. Pearson, and built in 1902 with Oamaru stone and a considerable use of brick for non-structural walls and for the upper part of the bell tower, externally faced by the same Oamaru stone. The building, unusually wide for its length, presents double aisles with rows of columns in the middle, chancel, chapels, transept and a gallery on the west end. With their finest stone vault ceilings in all roofs except the nave which is timbered, the church is regarded as the finest example of stone vaulting in New Zealand.

Saint Francis and All Sales, built in brick in 1919, is a neo-Gothic Roman Catholic church designed by Thomas Mahoney. Its rectangular floor plan with porches, chapels and sacristies in balance on either side of the rectangular nave, and the two towers topped with octagonal pillars on either side of the front façade, result in a building of almost perfect symmetry. The timber ceiling is a fine example of queen post truss with double hammer beams supported by stone corbels.

5.5. Test setup

An ambient vibration testing campaign was carried out during October 2015 on the four churches reputed representative of the national stock. Tri-axial USB digital accelerometer sensors (Figure 5.2), produced by the Gulf Coast Data Concepts and based on Micro Electro-Mechanical Systems (MEMS) technology were used in the tests. The use of MEMS based accelerometers is an attractive economical alternative to the use of large sensing networks characterized by high costs for both installing and maintaining the extensive wiring system needed in a large structure to connect individual sensors to a central control unit. Moreover, as these accelerometers generally have low energy consumption, they can often operate for an extended period only powered by a battery. Each sensor, and specifically the X6-1A model used in the tests, stores the precise time stamped data on a microSD memory and the real-time data are accessible via USB connectivity. Table 5.2 presents the characteristics of the accelerometer X6-1A.


St Paul’s (1841)


Our Lady of Assumption (1887)


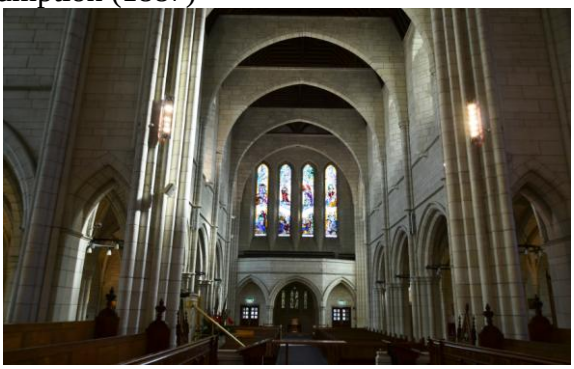

St Matthew in the City (1902)


St Francis de Sales and All Saints (1919)

Figure 5.1. Tested churches, located in Auckland and deemed to be representative of the New Zealand portfolio.

The measurement sensors were placed following both vertical and horizontal alignments and, in each of the setups, the accelerations in *X*, *Y*, and *Z* axes were recorded with a sampling rate of 128 Hz and a sampling time ranging between 60 min and one week. Figure 5.3 shows a schematic representation of the sensors layout in the four different churches, where the different colour of the sensors denotes different testing days. Before installation, all accelerometers were synchronized to a computer clock. The structures were instrumented with twenty accelerometers, on average, lightly glued to the surface of the structural elements under consideration, recording under operational conditions and not interfering with the normal churches activities. Excitation was thus provided only by wind, traffic and human activities. The data processing aimed to the modal identification of the structures has then been carried out using the System Identification Toolbox, a MATLAB-based toolbox for modal parameters identification (Beskhyroun 2011). Figure 5.4 presents an example of the acceleration time series under random excitation and ambient noise relative to one of the test setup.

Table 5.2. Characteristics of the MEMS accelerometer.

Sensor type	X6-1A
Acceleration range (g)	±2.0
Sensitivity (count/g)	2048
Sensitivity Deviation (%)	±1.0
Nonlinearity (%FS)	±0.5
Zero-g Offset Level Accuracy (mg)	±150 (X, Y axis) ±250 (Z axis)
Inter-Axis Alignment Error (Degrees)	±0.1

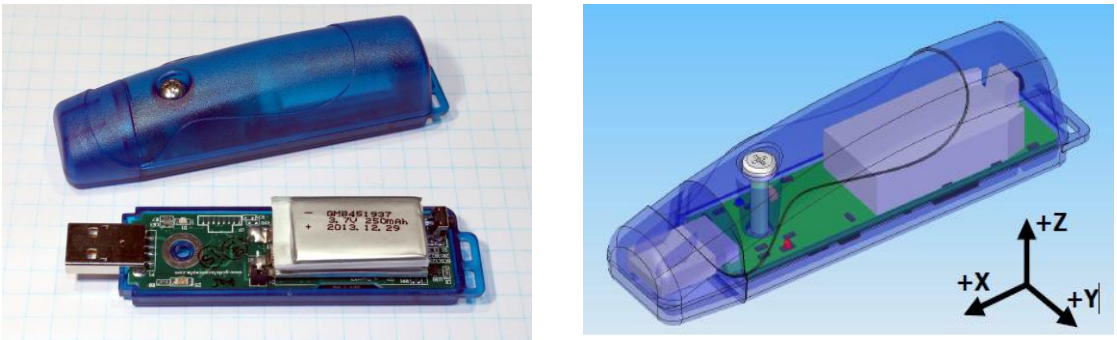

Figure 5.2. Accelerometer X6-1A and Sensor Orientation (www.gcdataconcepts.com).

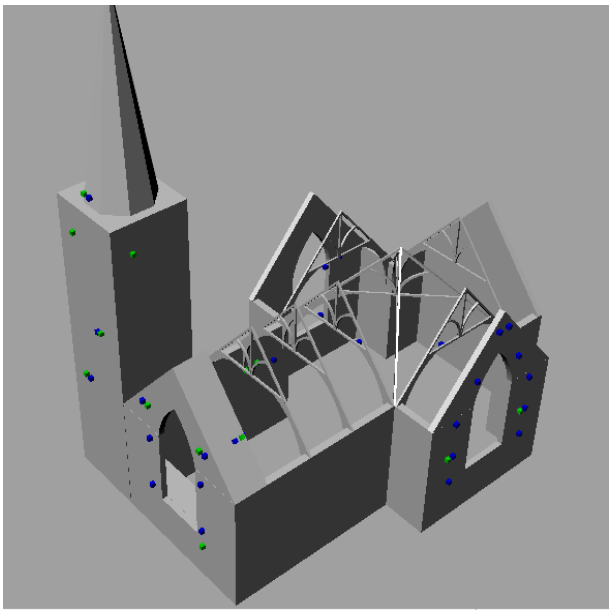

Our Lady of Assumption

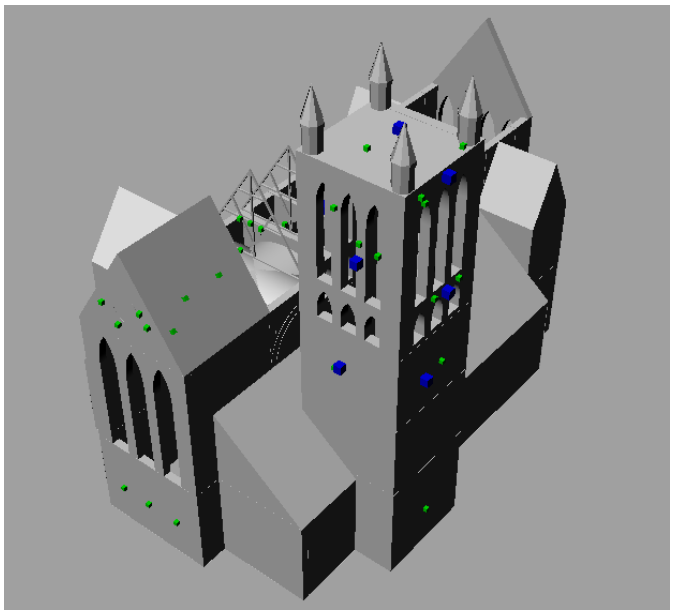

St Matthew in the City

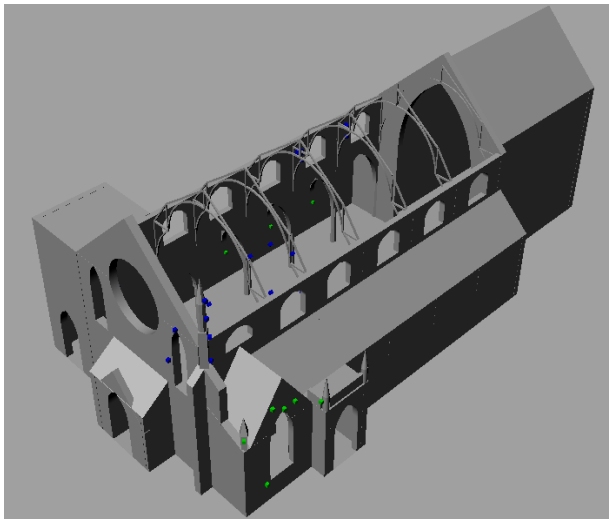

St Paul's

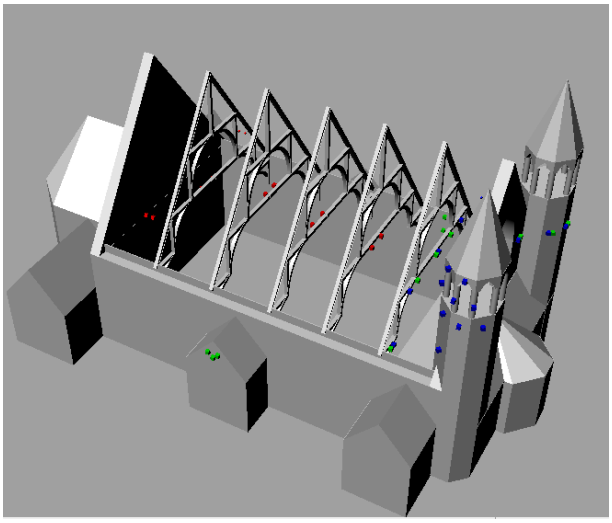

St Francis de Sales and All Saints

Figure 5.3. Layout and distribution of accelerometers in the four tested churches.

5.6. Modal parameter identification

The data processing aimed to the identification of the modal parameters of the structures has been carried out, so far, by using the *Peak Picking* method, thus identifying the potential frequencies of the elements under consideration from the peaks of the Power Spectral Density (PSD) diagrams. For one of the considered test setup, namely the one relative to the façade of the Church of Our Lady of Assumption, the PSD diagrams are shown in Figure 5.5 and Figure 5.6.

A preliminary estimation of the dominant frequencies of some of the structural elements under consideration is summarized in Table 5.3. After further future investigations, involving also a comparison between the results obtained from different output-only identification techniques (§5.3), results of the dynamic tests can be used, as mentioned, to estimate the filter effect that the macro-elements of the building develop on the response of soaring elements, as well as can guide a new empirical formulation for the estimation of the modal participation factors associated to unreinforced masonry churches (refer to Table 5.1).

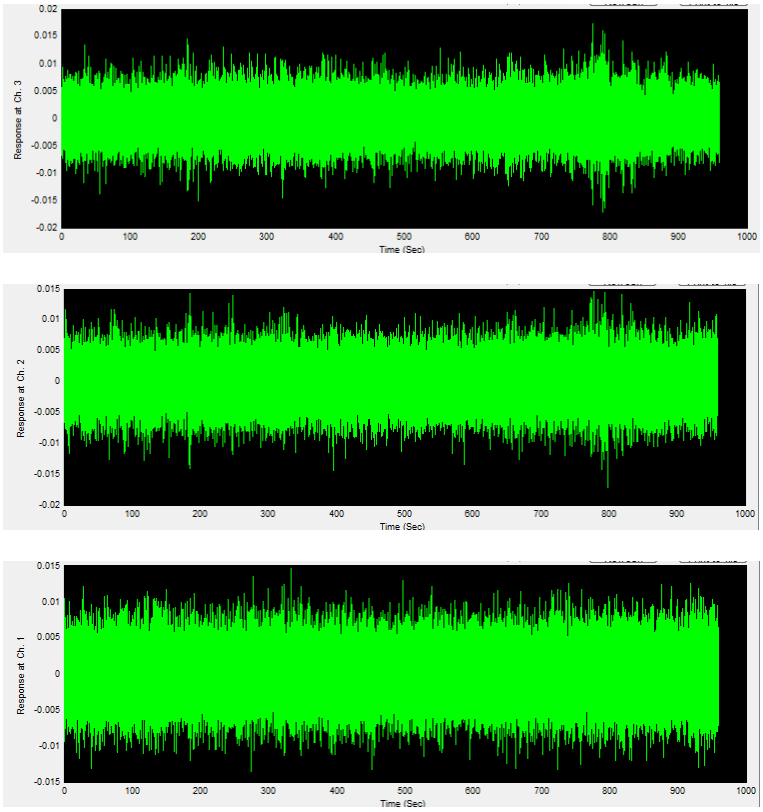

Figure 5.4. Acceleration time series under random excitation and ambient noise of the *Z* (out-of-plane) component of three vertically aligned sensors in the façade of the Church of Our Lady of Assumption (accelerations are measured in m/s^2).

Table 5.3. Natural frequencies identified according to *PP* technique.

Church	Element	*f* (Hz)
St Pauls	Pinnacle	8.6
	Façade	8.8
Our Lady of Assumption	Façade	9.3
	Transept	8.9
St Matthew in the City	Apse	8.1
St Francis de Sales and All Saints	Façade	6.6

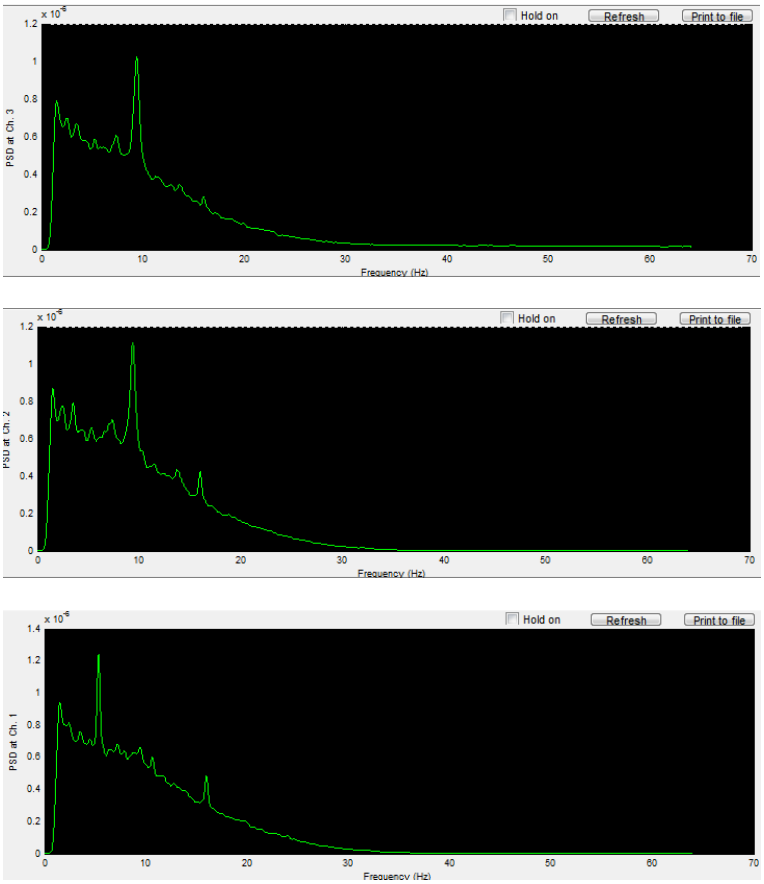

Figure 5.5. Power Spectral Density plot of the *Z* (out-of-plane) component of three vertically aligned sensors in the façade of the Church of Our Lady of Assumption.

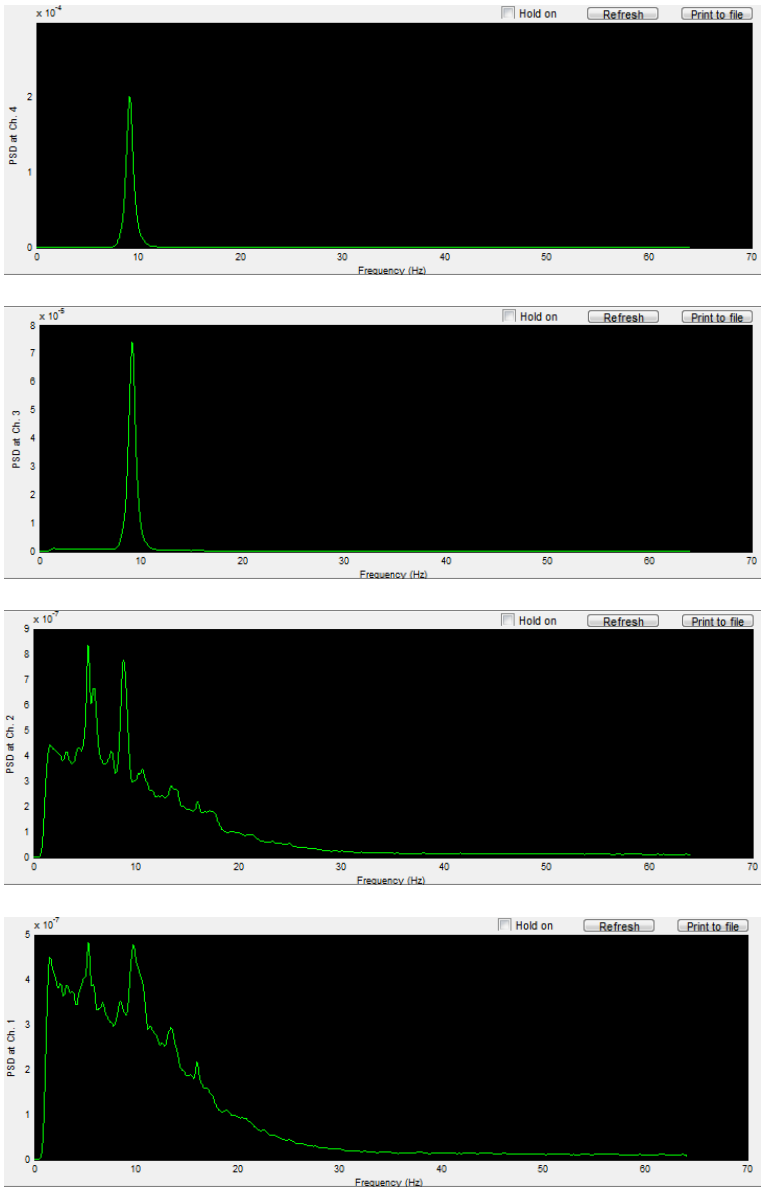

Figure 5.6. Power Spectral Density plot of the *Z* (out-of-plane) component of four vertically aligned sensors in the pinnacle of the Church of St Paul's.

5.7. Preliminary conclusions and future development

The possibility of using natural sources of excitation to define the modal response of an historical structure is very appealing, considering that the procedures used to determine a detectable dynamic response in new structures are mainly unviable for old ones or, eventually, to be carried out with extreme precaution. The use of ambient vibrations as source of excitation is then particularly effective in the assessment of the dynamic behaviour of historical buildings, since it implies a preservation care unlikely reachable with other techniques. Nevertheless, due to the random nature of the excitation used, the

response of the structure includes not only the modal contributions of ambient forces and structural system. For this reason it is fundamental to identify the structural response by decoupling the ambient noise.

Ambient vibration measurements have been conducted on four selected historical churches in Auckland, New Zealand, by means of tri-axis digital accelerometer sensors. The identification of the dynamic parameters (natural frequencies, for the time being) related to some of the structural elements under consideration, has been performed recurring to a classical technique operating in frequency domain, the *Peak Picking*.

Future developments involve the processing of the data relative to all test setups and the use of different output-only methods, operating both in the frequency and time domain.

Results obtained by the in-situ ambient vibration tests can be further used for the estimation of the modal participation factors associated with the soaring elements present in unreinforced masonry churches.

5.8. References

Aras F., Krstevska L., Altay G., Tashkov LJ., 2011. Experimental and numerical modal analyses of a historical masonry palace, *Construction and Building Materials*, 25(1): 81-91.

Baptista M.A., Mendes P., Afilhado A., Agostinho L., Lagomarsino S., Mendes Victor L., 2005. Ambient vibration testing at N. Sra. do Carmo Church, preliminary results, *Proceedings of the 4th International Seminar on Structural Analysis of Historical Constructions*, Padova, Italy, 483-488.

Bayraktar A., Türker T., Sevım B., Altunisik A.C., Yildirim F., 2009. Modal Parameter Identification of Hagia Sophia Bell-Tower via Ambient Vibration Test, *Journal of Nondestructive Evaluation*, 28: 37–47.

Bendat J.S., and Piersol A.G., 1993. *Engineering Applications of Correlation and Spectral Analysis*, John Wiley & Sons, 302 pp.

Beskhyroun S., 2011. Graphical Interface Toolbox for Modal Analysis, *Proceedings of the Ninth Pacific Conference on Earthquake Engineering Building an Earthquake-Resilient Society* 14-16 April, 2011, Auckland, New Zealand.

Brincker R., Zhang L., and Andersen P., 2000. Modal Identification from Ambient Responses using Frequency Domain Decomposition, *Proceedings of the 18th International Modal Analysis Conference (IMAC)*, USA.

Casarin F, Modena C., 2007. Dynamic identification of S. Maria Assunta Cathedral, Reggio Emilia, Italy. *Proceedings of 2nd International Operational Modal Analysis Conference*, 637-644.

CMIT - Circolare del Ministro delle Infrastrutture e dei Tra-sporti del 2 febbraio 2009, n. 617: Circolare contenente le Istruzioni per l'applicazione delle "Nuove norme tec-niche per le costruzioni" di cui al DM 14 gennaio 2008. Gazzetta Ufficiale della Repubblica Italiana n. 47 del 26 febbraio 2009, Supplemento Ordinario n. 27. In Italian.

DMI - Decreto del Ministro delle Infrastrutture del 14 gen-naio 2008: Approvazione delle nuove norme tecniche per le costruzioni. Gazzetta Ufficiale della Repubblica Italia-na, n. 29 del 4 febbraio 2008, Supplemento Ordinario n. 30. In Italian.

Gentile C., Saisi A., 2007. Ambient vibration testing of historic masonry towers for structural identification and damage assessment, *Construction and Building Materials* 21: 1311–1321

Gizzi F.T., Masini N., Sileo M., Zotta C., Scavone M., Liberatore D., Sorrentino L., and Bruno M., 2014. Building features and safeguard of church towers in Basilicata (Southern Italy), in *Science, Tecnology and Cultural Heritage* (M. A. Rogerio-Candelera, ed.), CRC Press, 369-374.

Jacobsen N.J., Andersen P., and Brincker R. 2007. Using EFDD as a Robust Technique to Deterministic Excitation in Operational Modal Analysis. *Proceedings of the 2nd International Operational Modal Analysis Conference (IOMAC)*, Copenhagen, Denmark.

Jaishi B., Ren W., Zong Z., and Maskey P.N., 2003. Dynamic and seismic performance of old multi-tiered temples in Nepal, *Engineering Structures* 25, 1827–1839.

Karatzetzou A., Negulescu C., Manakou M., François B., Seyedi D.M., Pitilakis D., Pitilakis K., 2015. Ambient vibration measurements on monuments in the Medieval City of Rhodes, Greece, *Bulletin of Earthquake Engineering*, 13:331–345.

Marotta, A., Goded, T., Giovinazzi, S., Lagomarsino, S., Liberatore, D., Sorrentino, L., and Ingham, J. M., 2015. An inventory of unreinforced masonry churches in New Zealand, *Bulletin of the New Zealand Society for Earthquake Engineering* 48, 170-189.

Marotta, A., Sorrentino, L., Liberatore, D., and Ingham J. M., 2016. Vulnerability assessment of unreinforced masonry churches following the 2010-2011 Canterbury (New Zealand) earthquake sequence, *Journal of Earthquake Engineering*.

Nohutcu H., Demir A., Ercan A., Hokelekli E., and Altintas G., 2015. Investigation of a historic masonry structure by numerical and operational modal analyses, *The structural design of tall and special buildings*, 24:821–834.

Osmancikli G., Uçak S.,, Turan F.N., Türker T., and Bayraktar A., 2012. Investigation of restoration effects on the dynamic characteristics of the Hagia Sophia bell-tower by ambient vibration test, *Construction and Building Materials* 29: 564–572.

Pastor M., Binda M., Hararik T., 2012. Modal Assurance Criterion, *Procedia Engineering* 48: 543 – 548.

Rainieri, C., and Fabbrocino, G., 2011. Operational modal analysis for the characterization of heritage structures, *Geofizica,* 28: 109-126.

Ramos L.F., Aguilar R., Lourenco P.B., Moreira S., 2013. Dynamic structural health monitoring of Saint Torcato Church, *Mechanical Systems and Signal Processing* 35: 1–15.

Tashkov L., Krstevska L., Naumovski N., De Matteis G., Brando G., 2010. Ambient vibration tests on three religious buildings in Goriano Sicoli damaged during the 2009 L'Aquila earthquake. *COST ACTION C26: Urban Habitat Constructions under Catastrophic Events. In: Proceedings of the final conference,* pp 433–438.

Votsis R.A., Kyriakides N., Chrysostomou C.Z., Tantele E., and Demetriou T., 2012. Ambient vibration testing of two masonry monuments in Cyprus, *Soil Dynamics and Earthquake Engineering,* 43: 58–68.

Young W.C., Budynas R.G., 2002. *Roark's Formulas for Stress and Strain.* McGraw-Hill: New York, 851 pp.

Chapter 6

Conclusions

The 2010-2011 Canterbury earthquake sequence caused extreme disruption, with damage to Christchurch architectural heritage, and specifically to unreinforced masonry churches, being particularly extensive, and thus highlighting the intrinsic structural fragility of this architectural type. Due to the high seismicity of the country, the potential large presence of people in and around religious buildings, and the associated societal relevance for both historical and symbolical reasons, the assessment of the seismic vulnerability of unerinforced churches and the mitigation of their seismic risk are of overriding importance. A detailed inventory of unerinforced churches throughout New Zealand has been compiled from various reference sources, leading to the identification of 297 buildings across the country. Statistics about the occurrence of architectural and structural features have been provided with preliminary evaluation of their role on seismic vulnerability. Detailed analyses have been then performed on a sample of 80 buildings in the affected region of Canterbury, in order to understand the seismic response provided by the ecclesiastic buildings during the earthquake sequence. Because unerinforced churches respond to earthquakes not as a whole, but with a set of macro-elements behaving more or less independently one from the adjacent, damage was surveyed by utilising a form that accounts for 28 possible local collapse mechanisms. In the literature, damage that has occurred to churches has generally been analysed by computing a global damage index, based upon summing up and weighting separate mechanism damage levels. Moreover, correlations with shaking intensity and vulnerability have been attempted only for this parameter. Herein, in addition to established procedures, damage was interpreted mechanism by mechanism, and firstly analysed through damage probability matrices, correlating discrete damage levels with

shaking intensity, and fitted with a binomial distribution. Although reasonable agreements between damage probability matrices and binomial distributions have been observed, and the probabilistic approach has improved compared to the matrices proposed for the global performance, flatness in damage distribution can be found in some cases. This result depends on the base assumption that damage can be explained by the severity of shaking alone, while it is self-evident that this statement is too crude and that the differences in vulnerability need to be addressed. Consequently, additional modifiers that increase/reduce the vulnerability of the macro-elements have been surveyed and introduced, initially, as dichotomous variables in multiple-linear regressions. Results have shown that multiple regression models accounting for vulnerability modifiers, allow far better forecasting of the damage. For this reason, vulnerability indicators are considered essential in the seismic vulnerability assessment of churches, and have been subsequently introduced in regression models also accounting for their structural effectiveness in seismic response. The proposed models, re-calibrated on the Canterbury churches accounting for several other ground motion intensity measures, have then been adopted to develop a quantitative seismic risk assessment for existing unreinforced masonry churches in New Zealand based on the national inventory. An alternative synthetic damage index is also proposed as a ground motion parameter, purely based on observed data and not requiring a conventional estimation of the weights used in previous definitions of a global damage index. Four different indexes expressing the global damage have been computed and then compared through the computation of the total Expected Annual Loss of different regions. The very similar results obtained accounting for the different indexes, guided the selection of the one based on the simple mean as the most straightforward tool when dealing with the assessment of the global damage at territorial scale, supported by the validation provided by the synthetic damage index, that has the advantage of being derived without any a-priori assumption. A method for the expeditious assessment of churches with partial accessibility has also been proposed, by means of the correlation emerged between observed mechanisms.

Findings from the territorial scale assessment of the seismic risk of New Zealand unreinforced masonry churches can be used for emergency management at regional scale in the case of occurrence of an earthquake or to help identifying priorities for more in-depth analysis of individual buildings in a preventive framework. The proposed mechanism-based regression models can be extended to other countries besides New

Zealand and, once calibrated on observed damage and specific structural features, and associated with the relative hazard scenario, can be adopted to support seismic vulnerability mitigation. Alternatively, the proposed models can be used for a rough preliminary assessment in countries with a built heritage similar to New Zealand.

Moving from an empirical approach to an analytical approach, still based on macro-elements, an ambient vibration test campaign has been conducted on four representative New Zealand churches, in order to dynamically characterize the response of religious buildings. The modal identification has been based on the classical operational modal analysis technique, operating in frequency domain, and very preliminary results have been presented, while further processing of the recorded data are ongoing. In this regard, further work on the dynamic assessment of unreinforced masonry churches will be aimed to estimate the filter effect that the macro-elements of the building develop on the response of typical soaring elements present in religious buildings, such as gables, pinnacles and crenellations, for which no calibration is given, and for future identification of the dynamic performance and construction weakness of different structural components, thus guiding the recognition of possible collapse mechanisms.

Appendix A: List of the unreinforced masonry churches in New Zealand, disaggregated for each region

1 –NORTHLAND

Name	Address	HNZ no.
PAIHIA		
Williams Memorial Church of St Paul	36 Marsden Rd	3824

2 –AUCKLAND

Name	Address	HNZ no.
AUCKLAND		
St Patrick's Cathedral	1 St Patricks Square	97
St Andrew's First Presbyterian Church	Cnr of Symonds St and Alten Rd	20
St Matthew in the City	Cnr of Hobson St and Wellesley St	99
Pitt street Methodist Church	78 Pitt St	626
Congregational Church Of Jesus	3 East St	/
Baptist Tabernacle	429 Queen St	7357
St Paul's Church	28 Symonds St	650
Wesleyan Chapel	8A Pitt St	7752
St James' Church	39 Church Rd	689
Church of the Melanesian Mission Building	40-44 Tamaki Drive	111
Dominion Road Methodist Church	426 Dominion Rd	2607
St Alban the Martyr	443 Dominion Rd	511
St Barnabas	283 Mt Eden Rd	516
Holy Trinity	437 Parnell Rd	/
Holy Trinity	18 Mason Ave	2320
St Augustine's Church	95 Calliope Rd	4529
St Francis de Sales, All Souls	2A Albert Rd	/
St Paul's	Cnr of Albert and Victoria Rds	/
St Benedict's Church	1 St Benedicts St	640
St Michaels Church	6 Beatrice Rd	118

Name	Address	HNZ no.
Church of Our Lady of the Assumption	130 Church St	523
St Columba Church	100 Surrey Crescent	2644
King's College Chapel	41 Golf Ave	90
St Paul's Church	14 St Vincent Ave	651
St Saviour's Chapel	80 Wyllie Road	7169
All Hallows	218 Beach Road	/
Calvary Tamil Methodist Church	587 Manukau Road	/
St Vincent de Paul Church	Cnr Fenwick Avenue and Shakespeare Rd,	/
St Joseph and St Joachim	118 Church St,	/
St John's	328 East Tamaki Rd	/
St Thomas	2 Islington Avenue	/
Waikumete Cemetery Chapel	Glenview Rd	2605
St David	70 Khyber Pass Rd	/
Neligan House Chapel	12 St Stephens Ave	/
St Andrews	18 Station Rd	/
New Zealand Chinese Mission Church	161 Trafalgar St	/
St Aidans	90 Onewa Rd	/
?	39 Margan Ave	/
?	40 Margan Ave	/
Selwyn Chapel	105 Great South Rd	693
First Presbyterian Church Papakura	2 Coles Crescent	/
St Johns	120 Great South Rd	/
PUKEKOHE		
St Andrew's	37 Queen Street	/

3 –WAIKATO

Name	Address	HNZ no.
GORDONTON		
St Mary’s Church	974 Gordonton Rd	4303
HAMILTON		
St Mary’s Convent Chapel	47 Clyde St	5460
St Andrews	Cnr River Rd and Te Aroha St	/
HUNTLY		
St Paul's Church	Cnr of William St and Glasgow St	4165
HYDE		
?	9071 Eton St	/
NGARUAWAHIA		
St Paul's Church	128 Thermal Explorer Highway	4246

Name	Address	HNZ no.
RAGLAN		
Raglan District Union Church	3 Stewart St	/
TE AROHA		
St David's Union Church	8 Church St	4288
St Mark's Church	7 Kenrick St	4290
TE AWAMUTU		
Te Awamutu Church	261 Bank St	4295
TIRAU		
Tirau Co-Operating Church	67 Main Rd	/

4 –BAY OF PLENTY

Name	Address	HNZ no.
OPOTIKI		
Former Methodist Church	?	/

5 –GISBORNE

Name	Address	HNZ no.
GISBORNE		
Holy Trinity Church	79 Derby St	3526
St Andrew's Church	176 Cobden St	3525
WAIPIRO		
St Abraham's Memorial Church	12 Marae Rd	3490

6 –HAWKE'S BAY

Name	Address	HNZ no.
PAKIPAKI		
Pakipaki War Memorial church	63 Old Main Rd	/
WAIPUKURAU		
St Mary’s	11 St Mary's Rd	/

7 –TARANAKI

Name	Address	HNZ no.
HAWERA		
St Mary's Church	206 Princes St	861
INGLEWOOD		
St Andrew’s Church	104 Rata Rd	875
NEW PLYMOUTH		
Taranaki Cathedral (St Mary's Church)	37 Vivian St	148

8 –MANAWATU-WANGANUI

Name	Address	HNZ no.
CARTERTON		
St Mary	2 King St	/
DANNEVIRKE		
St John the Baptist	174 High St	4551
LEVIN		
St John's Church	90 Cambridge St	4091
MANAKAU		
Methodist Church (Former)	1104 State Highway 1	4051
MASTERTON		
St. Luke's Union Church	Cnr Worksop Rd and Queen St	/
MOAWHANGO		
Batley Memorial Chapel	32 Wherewhere Rd	3308
PALMERSTON NORTH		
Wesley Broadway	264 Broadway Ave	
All Saints' Church	338 Church St	191
WANGANUI		
Wanganui Collegiate School Chapel	128 Liverpool St	999
WESTMERE		
St Oswald's Church	State highway 3	956
Westmere Memorial Church	110 State Highway 3	2738

9 –WELLINGTON

Name	Address	HNZ no.
LOWER HUTT		
Epuni Baptist Church	304 Waiwhetu Rd	/
Methodist church	Laings Rd	/
WELLINGTON		
Erskine College Chapel	31 Avon Street	7795
All Saints Church	1 Abbot St	/
St Luke's Parish	34 Pitt St	/
St Michael and All Angels	Corner St Michael's Crescent and Upland Rd	/
Karori Crematorium Chapel	Old Karori Road	1399
Congregational Church	45 Cambridge Terrace	/
Miramar Uniting Church	56 Hobart St	/
Our Lady Star of the Sea Convent Chapel	16 Fettes Crescent	1413
St Jude's	68 Freyberg St	/
St Hilda's	311 The Parade	/

Name	Address	HNZ no.
Sacred Heart Cathedral	40 Hill St	214
All Saints Church	94 Hamilton Rd	1331
St Gerard's Church	75 Hawker St	226
St Anne's Church (Former)	77 Northland Rd	3603
Missions to Seamen Building (Former)	7 Stout St	3611

10 –TASMAN

Name	Address	HNZ no.
MOTUEKA		
St Peter Chanel (Former)	31 High St	1671
Former church	207 High St	/
TAKAKA		
Sacred Heart	94 Commercial St	/

11 –NELSON

Name	Address	HNZ no.
NELSON		
Garin Memorial Chapel (Wakapuaka Cemetery)	272 Atawhai Drive	1637
All Saints	30 Vanguard St	/
Christ Church Cathedral	Trafalgar Square	/
STOKE		
St Barnabas’	523 Main Rd	3025

12 –MARLBOROUGH

Name	Address	HNZ no.
BLENHEIM		
The Church of the Nativity	76 Alfred St	/
HAVELOCK		
St Peter's Church	30 Lawrence St	1496
Sacred Heart Church	15 Lawrence St	/
PICTON		
St Joseph’s	119 Wellington Rd	/
WARD		
St Peter’s Chanel	7298 SH1	/
WHARANUI		
St Oswald's Church	8817 State Highway 1	/

13 –WEST COAST

Name	Address	HNZ no.
HOKITIKA		
St Mary’s	71 Sewell St	1705
St Andrew’s United Church	66 Hampden St	5013

14 –CANTERBURY

Name	Address	HNZ no.
AKAROA PENINSULA		
St Paul's Church	850 Old Tai Tapu Rd	4395
St Kentigern	396 Kaituna Valley Rd	/
Church of St John the Evangelist	1131 Okains Bay Rd	1715
St Luke	1280 Chorlton Rd	7094
St Cuthbert's Church	8 Governors Bay Teddington Rd	281
ASHBURTON		
Church of the Holy Name	58 Sealy St	284
St Andrew's Presbyterian Church	130 Havelock St	1809
St Andrew's Presbyterian Church (Former)	130 Havelock St	1804
Ashburton Baptist Church	Corner Havelock St and Cass St	/
CAVE		
St Monica	6 Anne St	/
All Saint's Cave	30 Elizabeth St	/
St David's Memorial Church	Burnetts Rd	312
CHRISTCHURCH		
St Joseph's Parish	133 Main North Rd	/
Christchurch North Methodist	61 Harewood Rd	/
Our Lady of Perpetual Help Church	58 Somme St	/
St John's Church	49 Bryndwr Rd	/
St Barnabas’ Church	145 Fendalton Rd	3681
St Ninians' Church	9 Puriri St	/
St Peter's Church	24 Main South Rd	1792
St Brendan's Church	47 Kirk Rd	/
St John of God Chapel	12 Nash Rd	4393
Cashmere Hills Church	2 Macmillan Ave	1842
St Mark's Church	101 Opawa Rd	/
Opawa Community Church	158 Opawa Rd	/
Church of the All Saints	48 Wakefield Ave	/
St Mary’s Parish	112 Lonsdale St	/
St Faith’s	46 Hawke St	/

Name	Address	HNZ no.
Synagogue	Gloucester St	/
The Rose Historic Chapel	866 Colombo St	7239
Trinity Congregational Church	124 Worcester St	306
Cathedral Church of Christ	100 Cathedral Square	46
Christ`s College Chapel	33 Rolleston Ave	3277
Nurses Memorial Chapel	2 Riccarton Ave	1851
Cathedral of the Blessed Sacrament	136 Barbadoes St	47
St James the Great Riccarton	69 Riccarton Rd	/
St John The Evangelist Church	Christchurch Akaroa Rd	5293
St Mark's Marshland	338 Prestons Rd	/
St John The Evangelist Church	10 St Johns St	/
Prebbleton Community	641 Springs Rd	/
Nazareth House Chapel	220 Brougham St	/
Knox Church	28 Bealey Ave	/
St Columba	88 Petrie St	/
St Andrew's College	347 Papanui Rd	/
Shirley Church	Shirley Rd	/
Ex-St James	?	/
DUNTROON		
St Magnus Presbyterian Church	11 Rees St	3255
St Martin's Church	3487 Kurow - Duntroon Rd	2429
FAIRLIE		
St Patrick and All Saints	7 Gall St	/
GERALDINE		
St Andrew the Apostle	10 Cox St	/
Immaculate Conception	19 Hislop St	/
Church of the Holy Innocents	Rangitata Gorge Rd	1976
HORORATA		
St John’s Hororata	224 Hororata Rd	/
KAIAPOI		
Methodist Church	52 Fuller St	3760
KUROW		
St Alban Chapel	5636 Kurow-Duntroon Rd	/
St Stephen	83 Provincial Highway	2435
LAKE TEKAPO		
Church of the Good Shepherd	Pioneer Drive	311
LEESTON		
St John's The Evangelist	158 High St	/
MAKIKIHI		
St. Mary’s Star of the Sea	1686 Waimate Highway	/

Name	Address	HNZ no.
MAUNGATI		
St James' Maungati	143 Timaunga Rd	/
OTIPUA		
St Marks	High St	/
PLEASANT POINT		
St Mary's Church	29 Afghan St	7697
St Alban's Pleasant Point	20 Harris St	/
SAINT ANDREWS		
St Andrews	8 Thackeray St	/
SEFTON		
St Luke's	Upper Sefton Rd	/
SHEFFIELD		
St Ambrose Sheffield	46 Railway Tce East	/
SOUTHBRIDGE		
St James'	2 Hastings St	/
SOUTHBURN		
Southburn Church	994 Pareora River Rd	/
TEMUKA		
St Peter's Temuka	192 King St	/
St Josephs Catholic Church	28 Wilkin St	2033
Holy Trinity Arowhenua	3 Huirapa St	/
TIMARU		
St Paul	28 Seddon St	/
St Joseph's Church	42 Douglas St	/
Woodlands Road Methodist Church	Cnr Woodlands and North St	/
Bank Street Methodist Church	38 Bank St	3155
St Mary's Church	24 Church St	328
Chalmers Church	4 Elizabeth St	7107
TOTARA VALLEY		
St Paul's Presbyterian Church (Former)	856 Cleland Rd	1995
WAIAU		
All Saints' Church	35 Parnassus St	3690
WAIHAO DOWNS		
St Michael's Church	1115 State Highway 82	/
WAIMATE		
St Pauls Waimate	11 Glasgow St	/
Knox Church	58 Shearman St	/
St Patrick's Church	2 Timaru Rd	7343
WAIPARA		
St Paul's Church	173 Church Rd	7111

Name	Address	HNZ no.
WOODBURY		
St Thomas' Church	6 Church St	/
WOODEND		
Methodist Church	86 Main North Rd	3795

15 –OTAGO

Name	Address	HNZ no.
ALEXANDRA		
St Enoch's church	12 Centennial Ave	/
St Aidan’s	42 Shannon St	/
ARROWTOWN		
St John's Church	26 Berkshire St	2119
St Patrick’s	7 Hertford St	2117
AWAMOKO		
Awamoko Presbyterian Church	1783 Georgetown-Pukeuri Rd	/
BANNOCKBURN		
Bannockburn Presbyterian Church	33 Hall Rd	2385
CLYDE		
St Michael and All Angels Church	8 Matau St	2386
St Dunstan's Church	61 Sunderland St	2387
St Magnus’	60 Sunderland St	/
CROMWELL		
Goldfields Old Church	52 Erris St	/
Mary Immaculate and the Irish Martyrs	3 Sligo St	/
St John's Presbyterian Church	24 Inniscort St	2131
St Andrew's Anglican Church	41 Blyth St	2132
DUNEDIN		
St Davids Church	227 North Rd	4734
Glenaven Church	7 Chambers St	3371
Catholic Church of the Sacred Heart of Jesus	89 North Rd	2214
Opoho Presbyterian Church	50 Signal Hill Rd	/
Dundas Street Methodist Church (Former)	50 Dundas St	3367
All Saints' Church	786 Cumberland St	2136
Knox Church	463 George St	4372
Hanover Street Baptist Church	65 Hanover St	4792
St Paul's Cathedral and Belfry	36 The Octagon	376
Trinity Church (now Fortune Theatre)	231 Stuart St	3378
Moray Place Congregational Church (Former)	81 Moray Place	2218
Synagogue	29 Moray Place	9606
Cathedral Church of St Joseph	288 Rattray St	364

Name	Address	HNZ no.
First Church of Otago	410 Moray Place	60
St Matthew's Church	28 Hope St	2212
St Andrew	64 Melville St	3185
Highgate Presbyterian Church	580 Highgate	/
Kaikorai Presbyterian Church	127 Taieri Rd	/
Roslyn Presbyterian Church	21 Highgate	3377
Caversham Baptist Church	10 Surrey St	/
Caversham Church	61 Thorn St	7319
St Peters Caversham	57 Baker St	9545
Wesley Church	333 Hillside Rd	/
St Patrick's Basilica	32 Macandrew Rd	2213
St James (South Presbyterian)	400 King Edward St	/
Holy Cross	12 Richardson St	/
St Kilda Tongan Fellowship	56 Queens Drive	/
Andersons Bay Presbyterian Church Deacons	76 Silverton St	/
North East Valley Baptist Church	270 North Rd	/
Halfway Bush Union Church	28 Balmain St	/
St Clair	51 Albert St	/
ENFIELD		
Enfield Presbyterian Church	805 Weston-Ngapara Rd	2417
ESK VALLEY		
St Mary's Church	Church Hill Road	319
HAMPDEN		
Presbyterian Church	2 London St	3249
HERBERT		
St John's Presbyterian Church	1 Ord St	2416
HERIOT		
Heriot Community Church	17 Roxburgh St	/
HYDE		
Catholic Church of the Sacred Heart of Jesus	9137 Eton St	2253
KOKONGA		
?	Kyeburn-Hyde Rd	/
KUROW		
Sacred Heart Roman Catholic church	5634 Kurow-Duntroon Rd	/
LAWRENCE		
Lawrence Presbyterian Church (Former)	7 Colonsay St	2243
St Patrick	12 Colonsay St	2243
Holy Trinity Anglican Church	9 Whitehaven St	2245
Lawrence Methodist Church	Corner of Whitehaven St and Colonsay St	/

Name	Address	HNZ no.
LOVELLS FLAT		
?	Station Rd	/
MACRAES FLAT		
St Patrick's Catholic Church (Former)	7 Hyde St	2397
?	1726 Macraes Rd	/
MAHENO		
St Andrew’s	4 Short St	/
MIDDLEMARCH		
St John's Church	4 Aberafon St	/
MILTON		
St John	167 Union St	/
Tokomairiro Church	30 Union St	2250
Immaculate Conception	24 Dryden St	/
MOSGIEL		
East Taieri Presbyterian Church	12A Cemetery Rd	2260
Gospel Hall	75 Gordon Rd	/
Mosgiel Presbyterian Church	11 Church St	/
NASEBY		
St George	46 Derwent St	/
NORTH TAIERI		
North Taieri Presbyterian Church	39 Wairongoa Rd	3234
OAMARU		
Rosary Chapel	70 Reed St	2301
St Patricks Basilica	64 Reed St	58
Reformed Church (Church of Christ)	6 Eden St	/
St Paul's Church	3 Coquet St	2300
St Luke's Anglican Church	2 Tees St	4365
Columba Presbyterian Church	33 Wansbeck St	7313
Wesley Church	22 Eden St	/
PALMERSTON		
St James' Church	80 Tiverton St	3247
St Mary's Church	8 Stromness St	2396
Blessed Sacrament	44 Ronaldsay St	/
PORT CHALMERS		
St Mary's Star of the Sea Church	34 Magnetic St	2328
Holy Trinity Church	1 Scotia St	2320
Iona Church	24 Mount St	7165
QUEENSTOWN		
St Peter's Church	6 Church St	2341
St Joseph's Church	41 Melbourne St	2340

Name	Address	HNZ no.
RANFURLY		
Sacred Heart	4 Stuart Rd	/
ROXBURGH		
Teviot Union Parish Church	75 Scotland St	/
St James' Church	12 Ferry Rd	2345
Our Lady of Peace	5 Liddle St	/
SAINT BATHANS		
St Patrick's Church	Cross St	3210

16 –SOUTHLAND

Name	Address	HNZ no.
CENTRE BUSH		
St Andrew's Presbyterian Church (Former)	1785 Dipton-Winton Highway	7427
GORE		
Holy Trinity	15 Traford Street	/
INVERCARGILL		
First Church	151 Tay St	387
St John's Anglican Church Complex	108 Tay St	391
Central Methodist Church	82 Jed St	2449
St Paul's Church	178 Dee St	2517
Windsor Community Church	19 Windsor St	/
All Saints Anglican Church and Parish Hall	509 Dee St	2440
St Stephen's Church	284 North Rd	2518
Sacred Heart	449 North Rd	/
St Patrick’s	33 Rimu St	/
St Mary’s	54 Eye St	/
MATAURA		
St Savious	127 Main Rd	/
Mataura Presbyterian	?	/
WYNDHAM		
St Kevin’s	45 Inkermann St	/

Appendix B: Damage Probability Matrices and binomial distribution of the 20 considered mechanisms

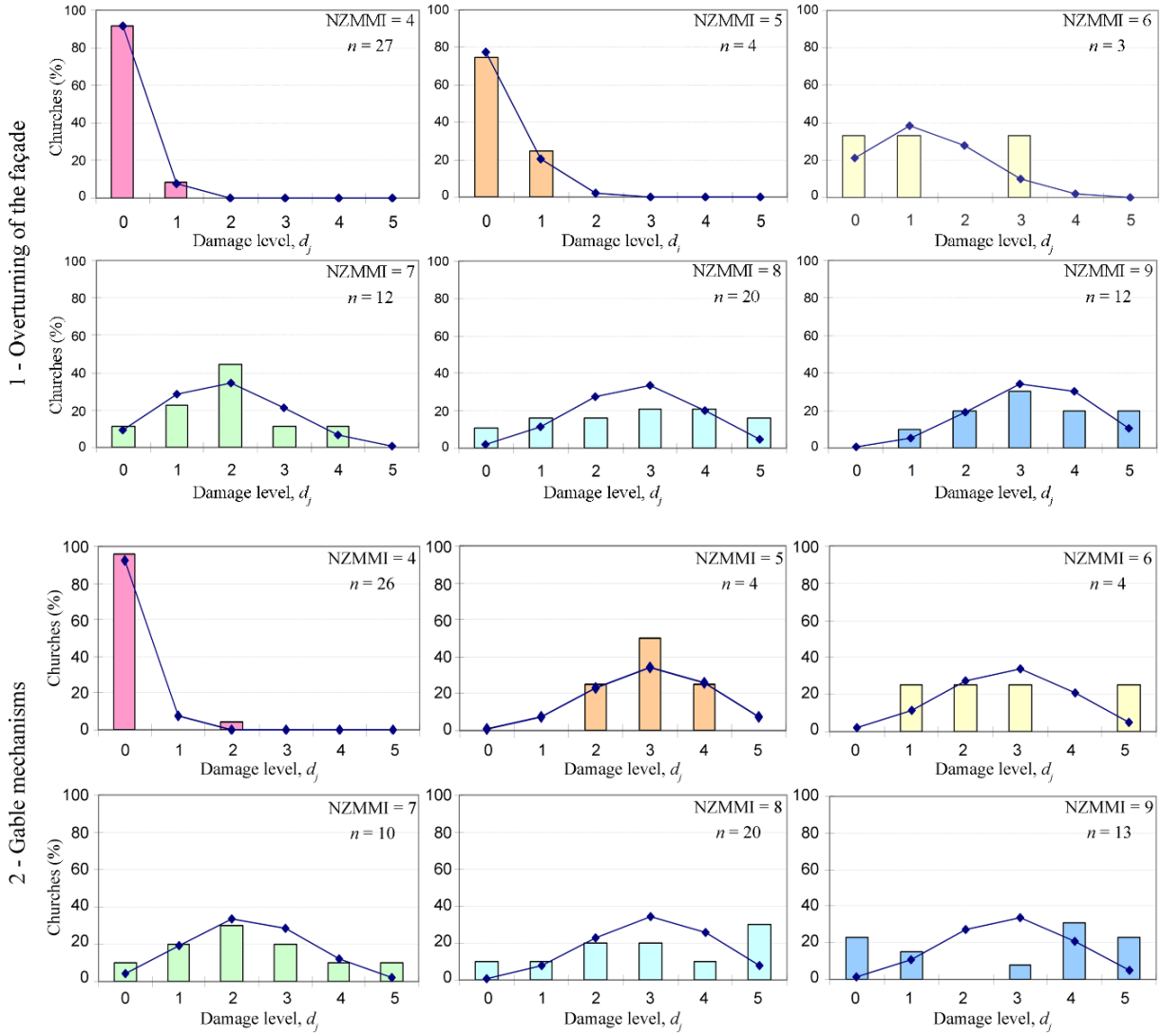

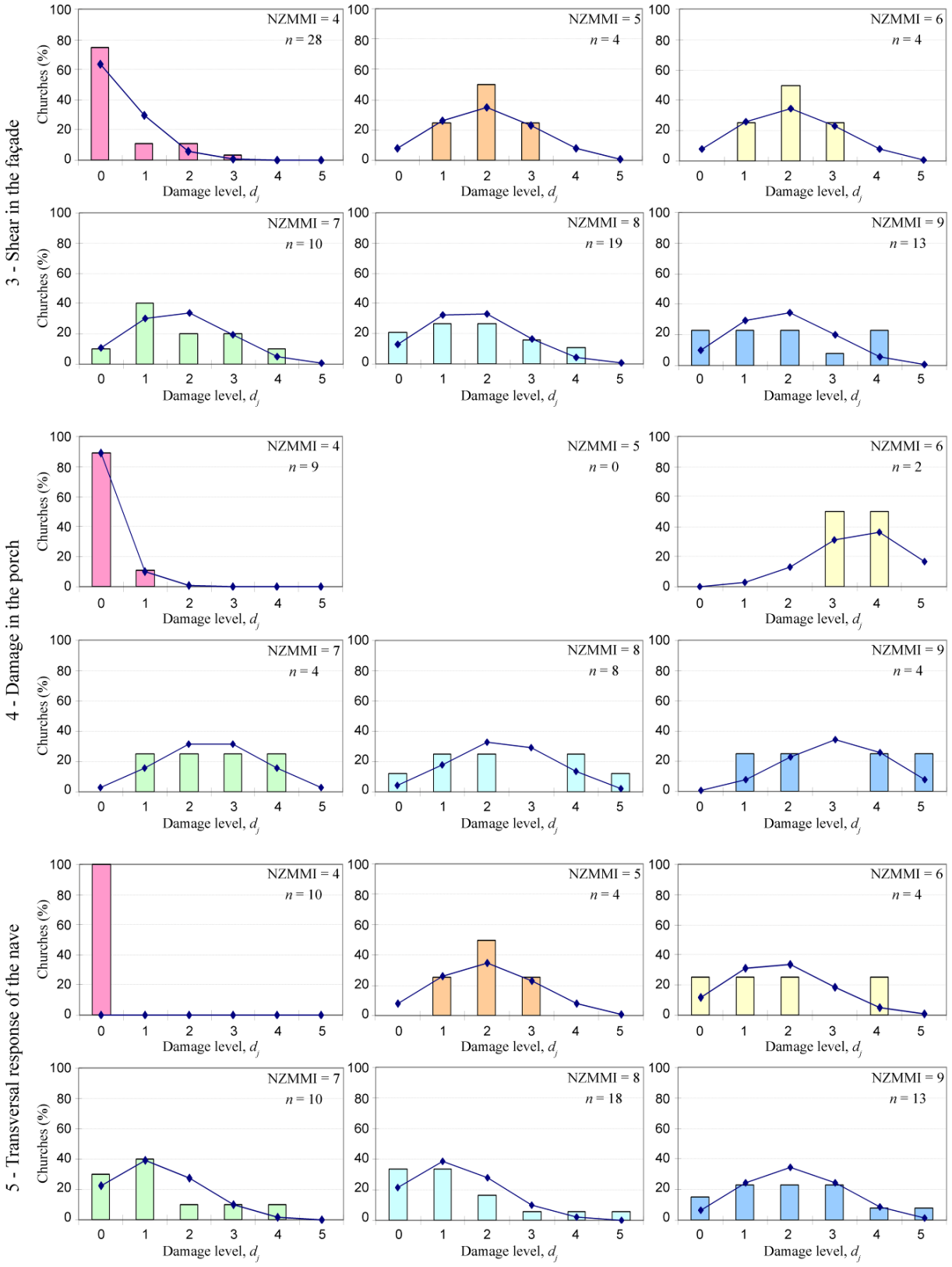
3 - Shear in the façade
4 - Damage in the porch
5 - Transversal response of the nave
Churches (%)
Damage level, d_j
NZMMI = 4
n = 28
NZMMI = 5
n = 4
NZMMI = 6
n = 4
NZMMI = 7
n = 10
NZMMI = 8
n = 19
NZMMI = 9
n = 13
NZMMI = 4
n = 9
NZMMI = 5
n = 0
NZMMI = 6
n = 2
NZMMI = 7
n = 4
NZMMI = 8
n = 8
NZMMI = 9
n = 4
NZMMI = 4
n = 10
NZMMI = 5
n = 4
NZMMI = 6
n = 4
NZMMI = 7
n = 10
NZMMI = 8
n = 18
NZMMI = 9
n = 13

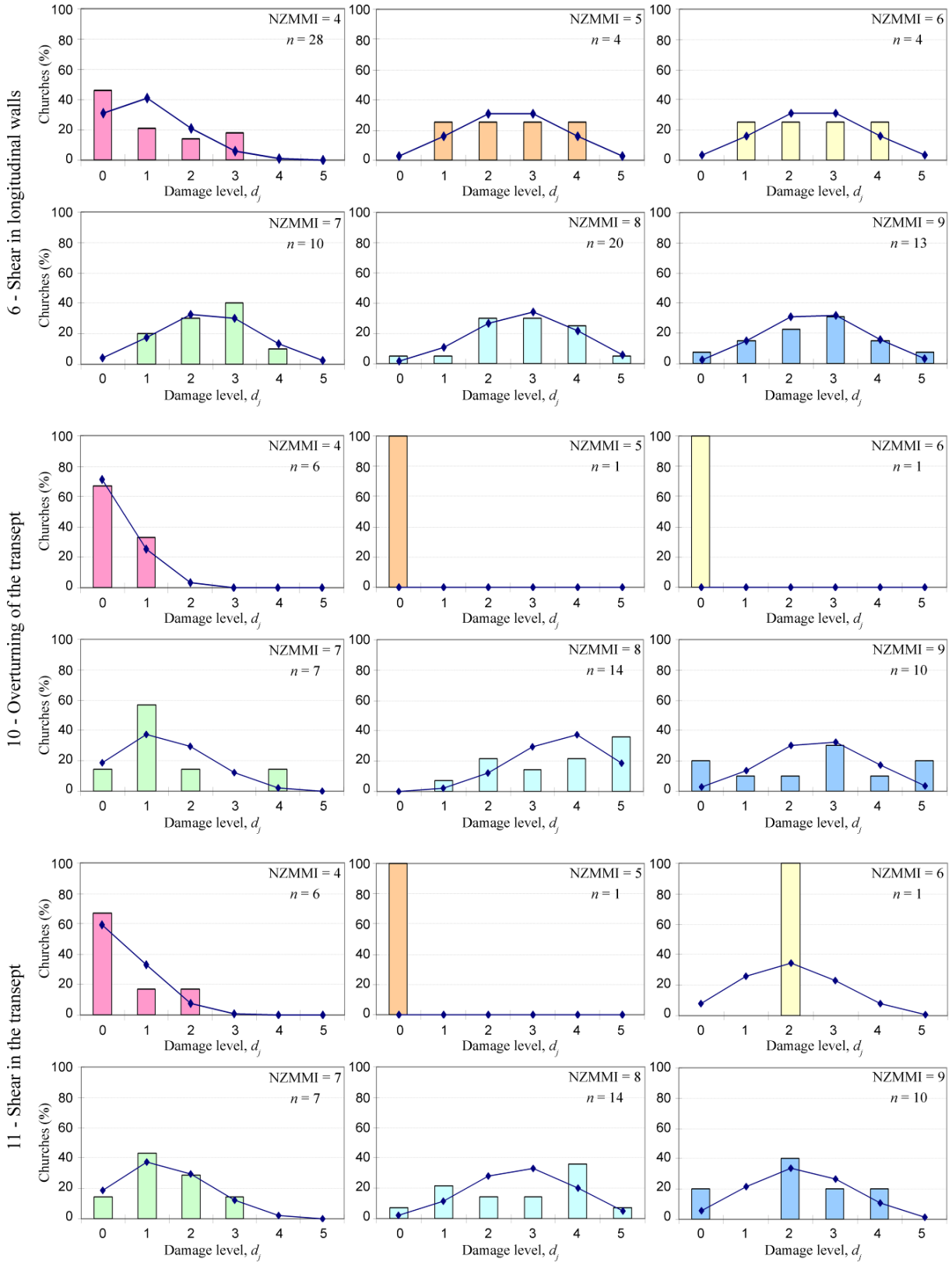
6 - Shear in longitudinal walls
10 - Overturning of the transept
11 - Shear in the transept
Churches (%)
Damage level, d_j
NZMMI = 4
n = 28
NZMMI = 5
n = 4
NZMMI = 6
n = 4
NZMMI = 7
n = 10
NZMMI = 8
n = 20
NZMMI = 9
n = 13
NZMMI = 4
n = 6
NZMMI = 5
n = 1
NZMMI = 6
n = 1
NZMMI = 7
n = 7
NZMMI = 8
n = 14
NZMMI = 9
n = 10
NZMMI = 4
n = 6
NZMMI = 5
n = 1
NZMMI = 6
n = 1
NZMMI = 7
n = 7
NZMMI = 8
n = 14
NZMMI = 9
n = 10

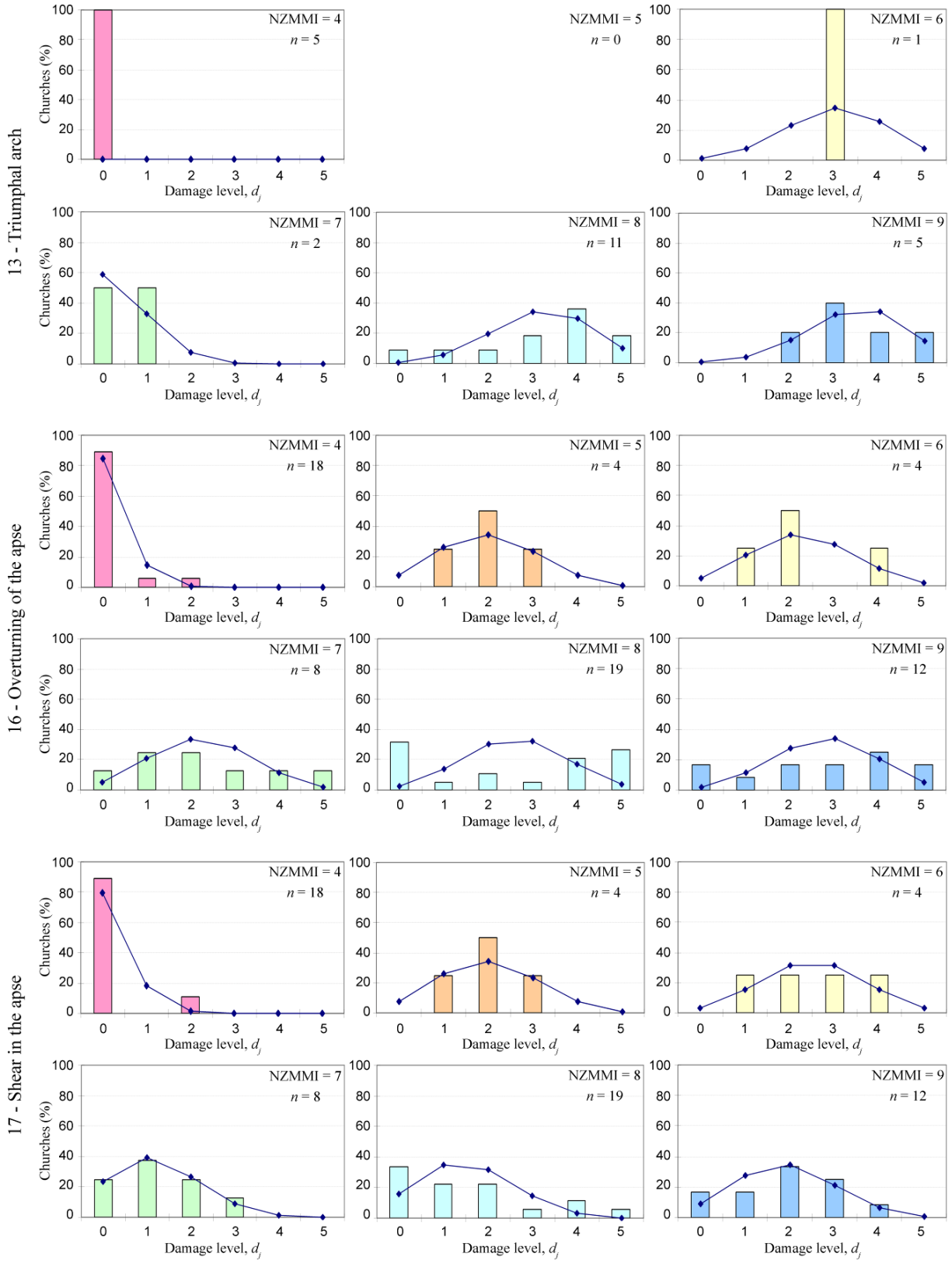
13 - Triumphal arch
16 - Overturning of the apse
17 - Shear in the apse
NZMMI = 4
n = 5
NZMMI = 5
n = 0
NZMMI = 6
n = 1
NZMMI = 7
n = 2
NZMMI = 8
n = 11
NZMMI = 9
n = 5
NZMMI = 4
n = 18
NZMMI = 5
n = 4
NZMMI = 6
n = 4
NZMMI = 7
n = 8
NZMMI = 8
n = 19
NZMMI = 9
n = 12
NZMMI = 4
n = 18
NZMMI = 5
n = 4
NZMMI = 6
n = 4
NZMMI = 7
n = 8
NZMMI = 8
n = 19
NZMMI = 9
n = 12
Churches (%)
Damage level, d_j

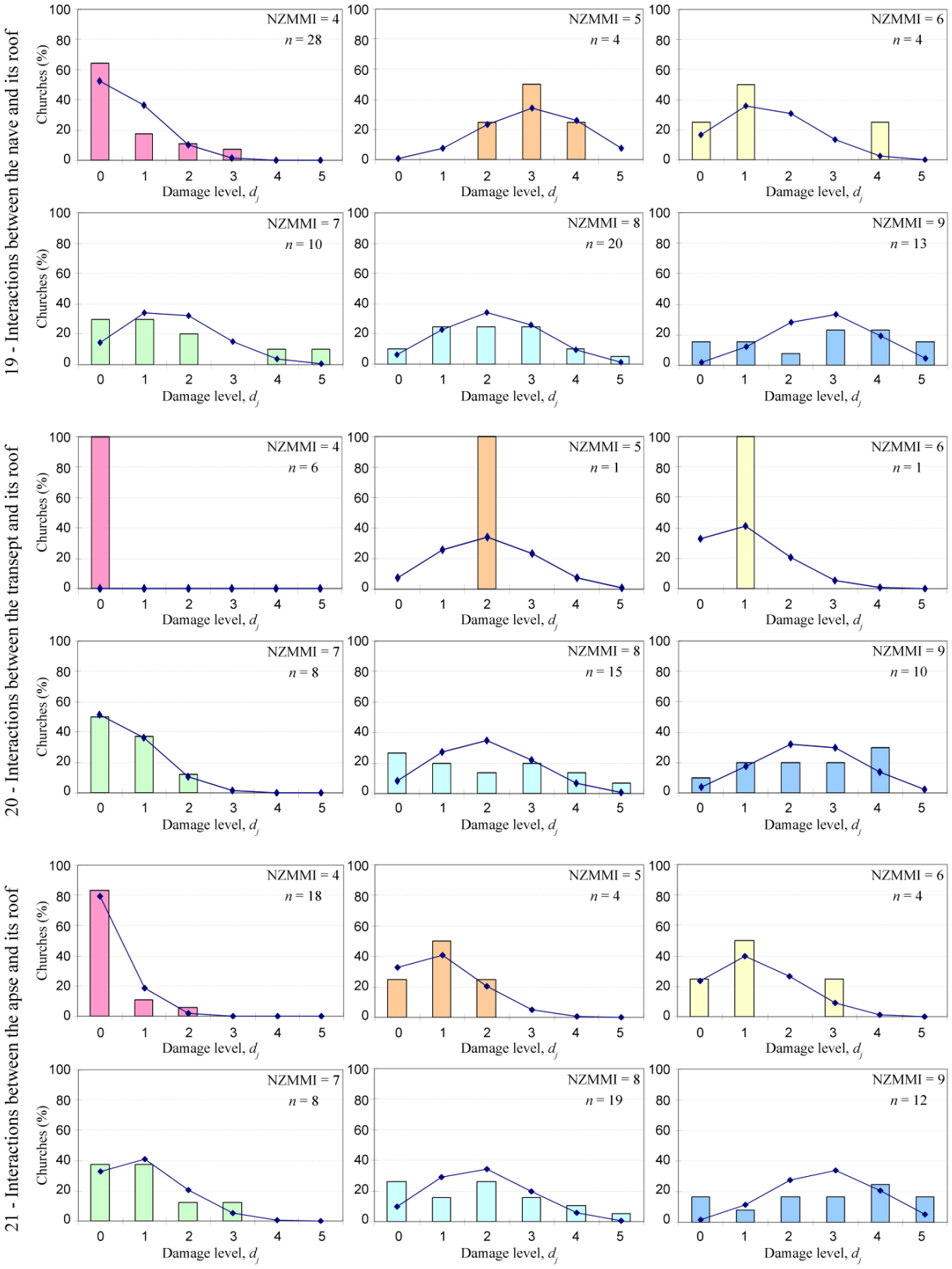
19 - Interactions between the nave and its roof
NZMMI = 4
n = 28
NZMMI = 5
n = 4
NZMMI = 6
n = 4
NZMMI = 7
n = 10
NZMMI = 8
n = 20
NZMMI = 9
n = 13
20 - Interactions between the transept and its roof
NZMMI = 4
n = 6
NZMMI = 5
n = 1
NZMMI = 6
n = 1
NZMMI = 7
n = 8
NZMMI = 8
n = 15
NZMMI = 9
n = 10
21 - Interactions between the apse and its roof
NZMMI = 4
n = 18
NZMMI = 5
n = 4
NZMMI = 6
n = 4
NZMMI = 7
n = 8
NZMMI = 8
n = 19
NZMMI = 9
n = 12
Churches (%)
Damage level, d_j

22 - Overturning of the chapels

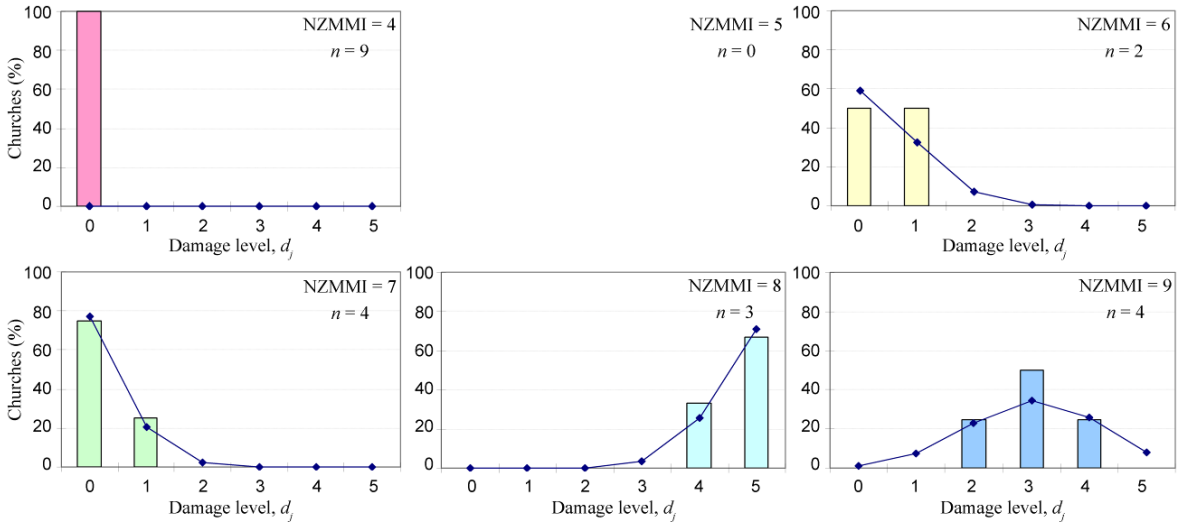

23 - Shear in the chapels

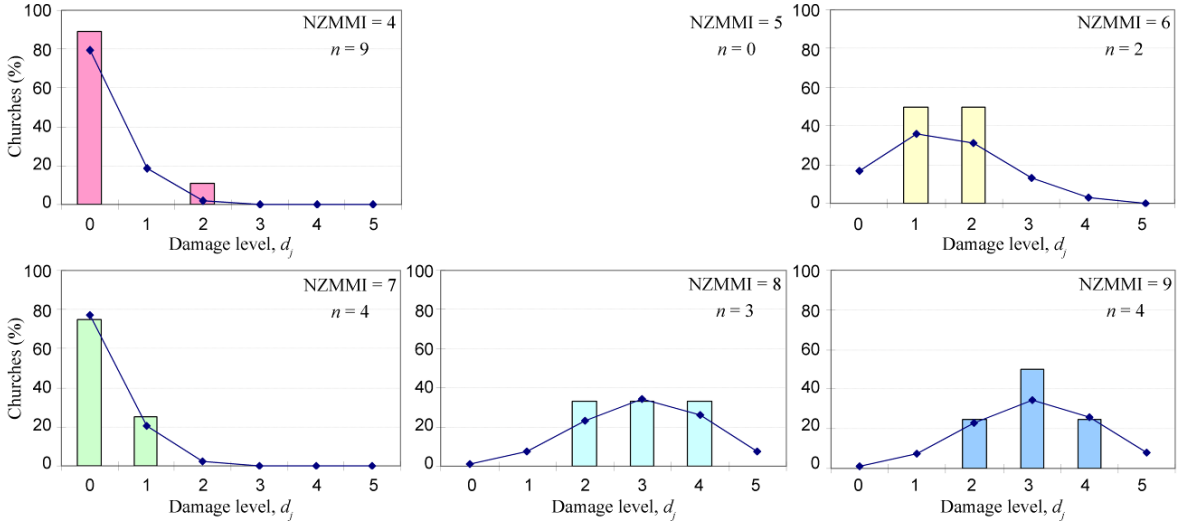

25 - Interactions next to irregularities

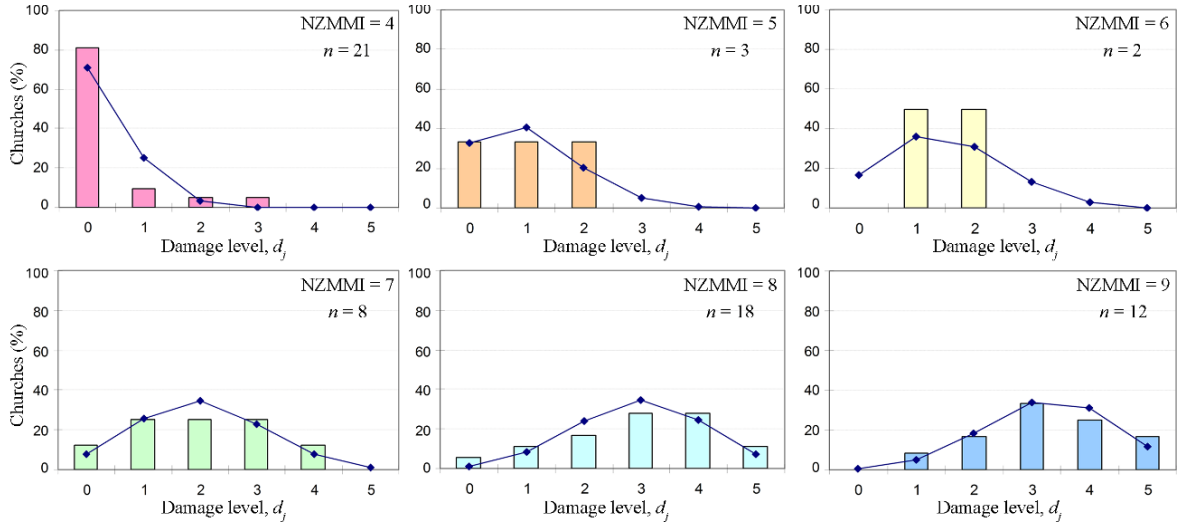

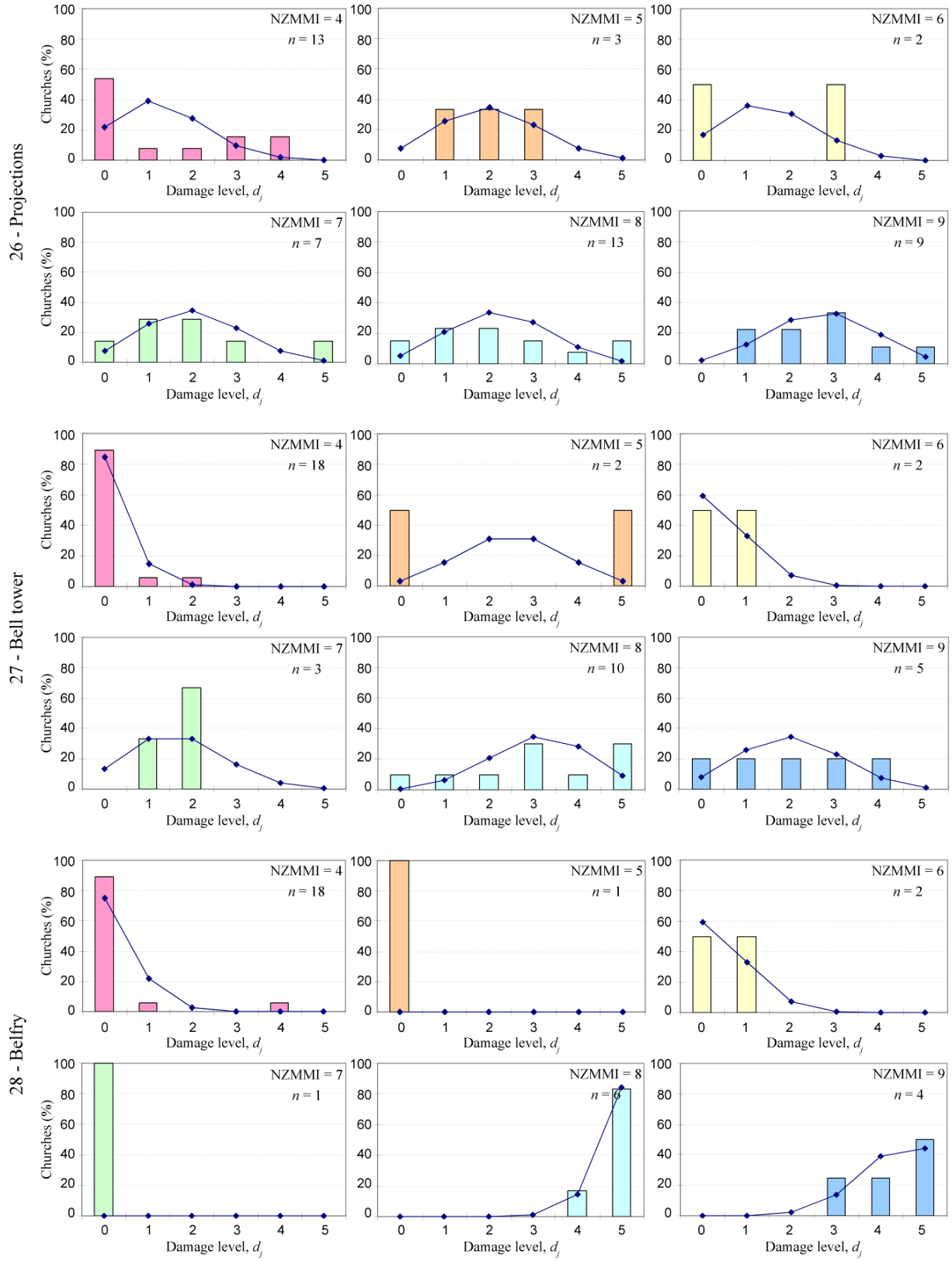
26 - Projections
27 - Bell tower
28 - Belfry
Churches (%)
Damage level, d_j
NZMMI = 4
n = 13
NZMMI = 5
n = 3
NZMMI = 6
n = 2
NZMMI = 7
n = 7
NZMMI = 8
n = 13
NZMMI = 9
n = 9
NZMMI = 4
n = 18
NZMMI = 5
n = 2
NZMMI = 6
n = 2
NZMMI = 7
n = 3
NZMMI = 8
n = 10
NZMMI = 9
n = 5
NZMMI = 4
n = 18
NZMMI = 5
n = 1
NZMMI = 6
n = 2
NZMMI = 7
n = 1
NZMMI = 8
n = 6
NZMMI = 9
n = 4

Appendix C: Goodness-of-fit test of the 20 considered mechanisms

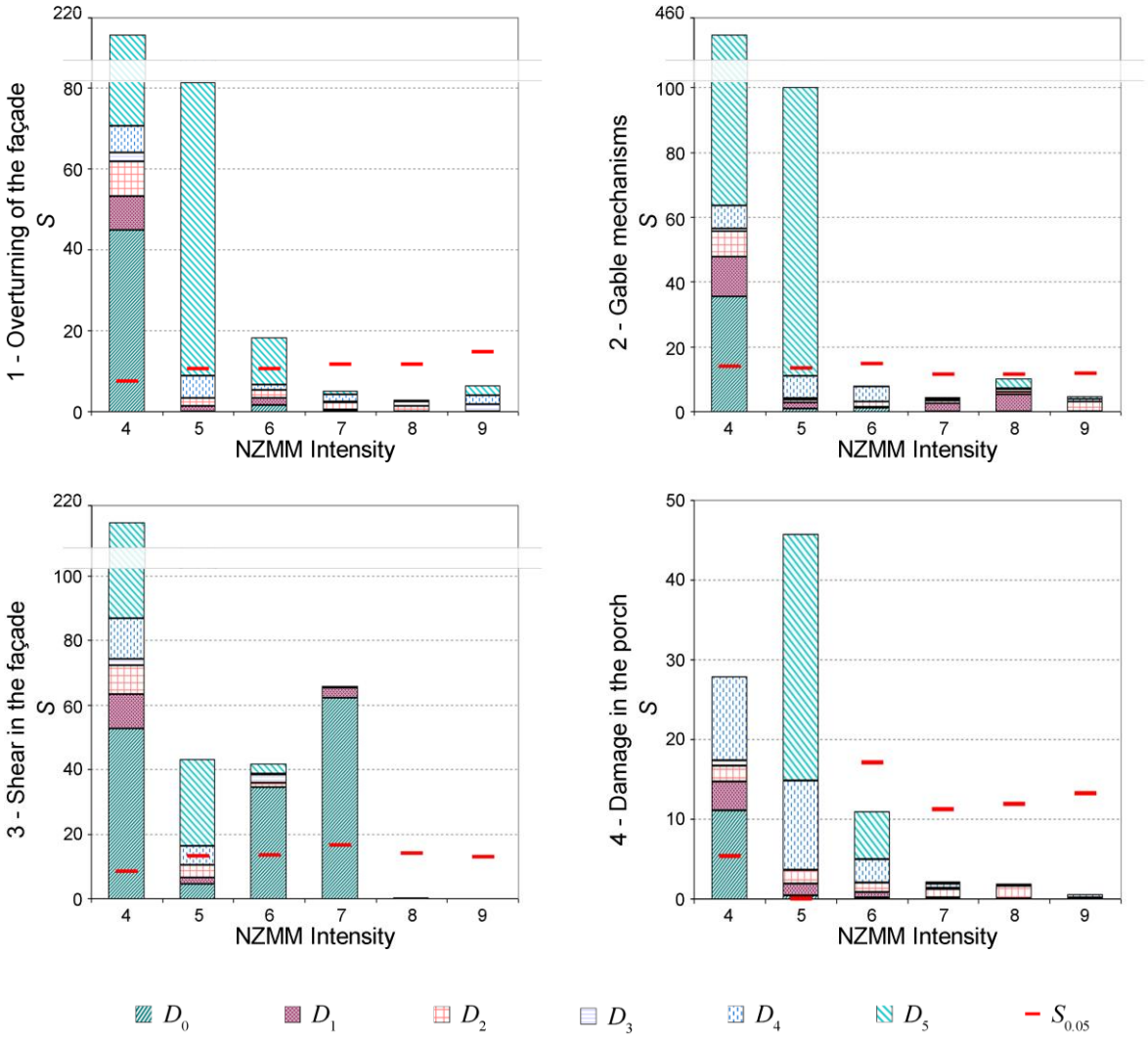

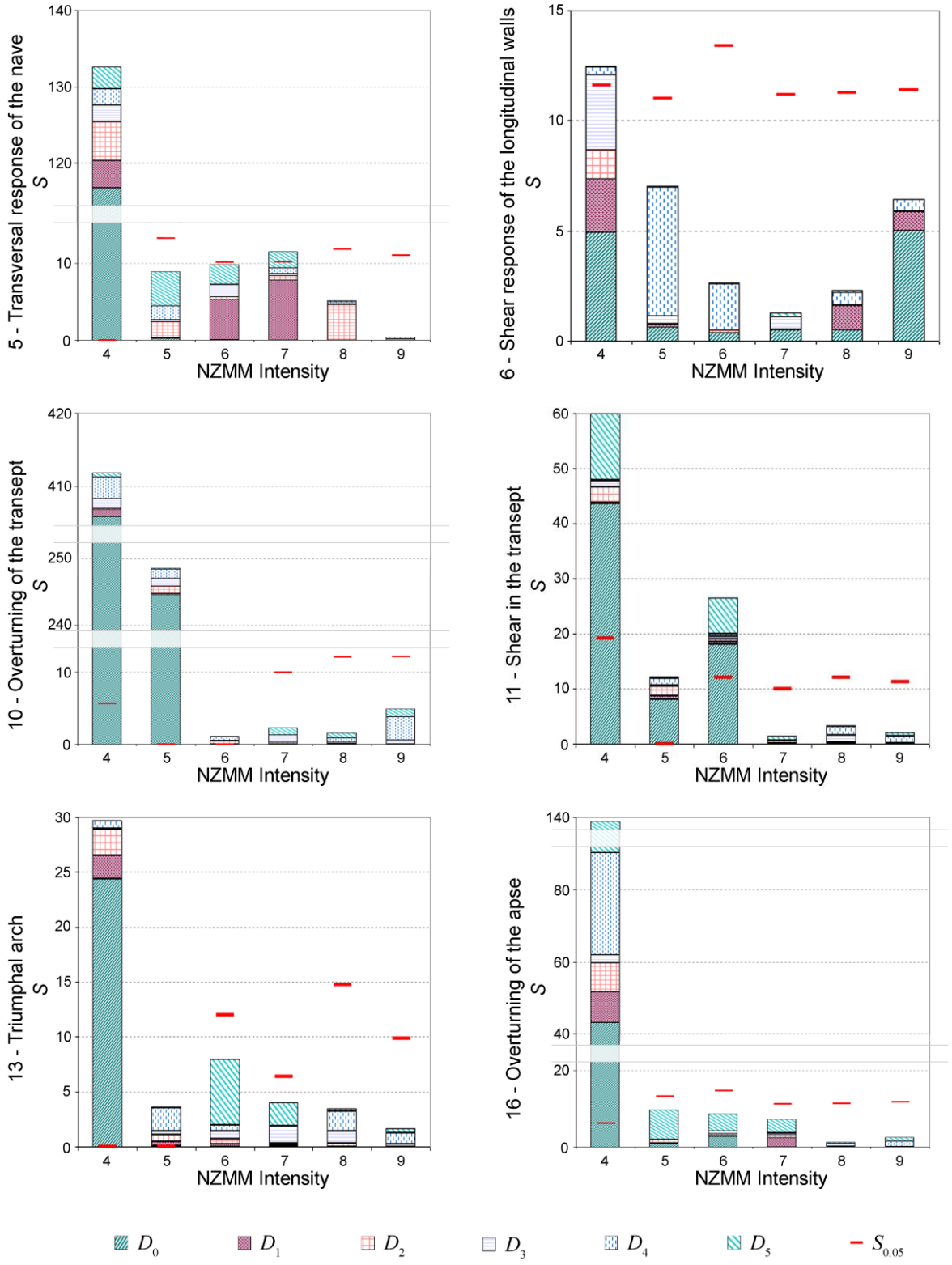
5 - Transversal response of the nave
S
NZMM Intensity
6 - Shear response of the longitudinal walls
S
NZMM Intensity
10 - Overturning of the transept
S
NZMM Intensity
11 - Shear in the transept
S
NZMM Intensity
13 - Triumphal arch
S
NZMM Intensity
16 - Overturning of the apse
S
NZMM Intensity
D_0
D_1
D_2
D_3
D_4
D_5
$S_{0.05}$

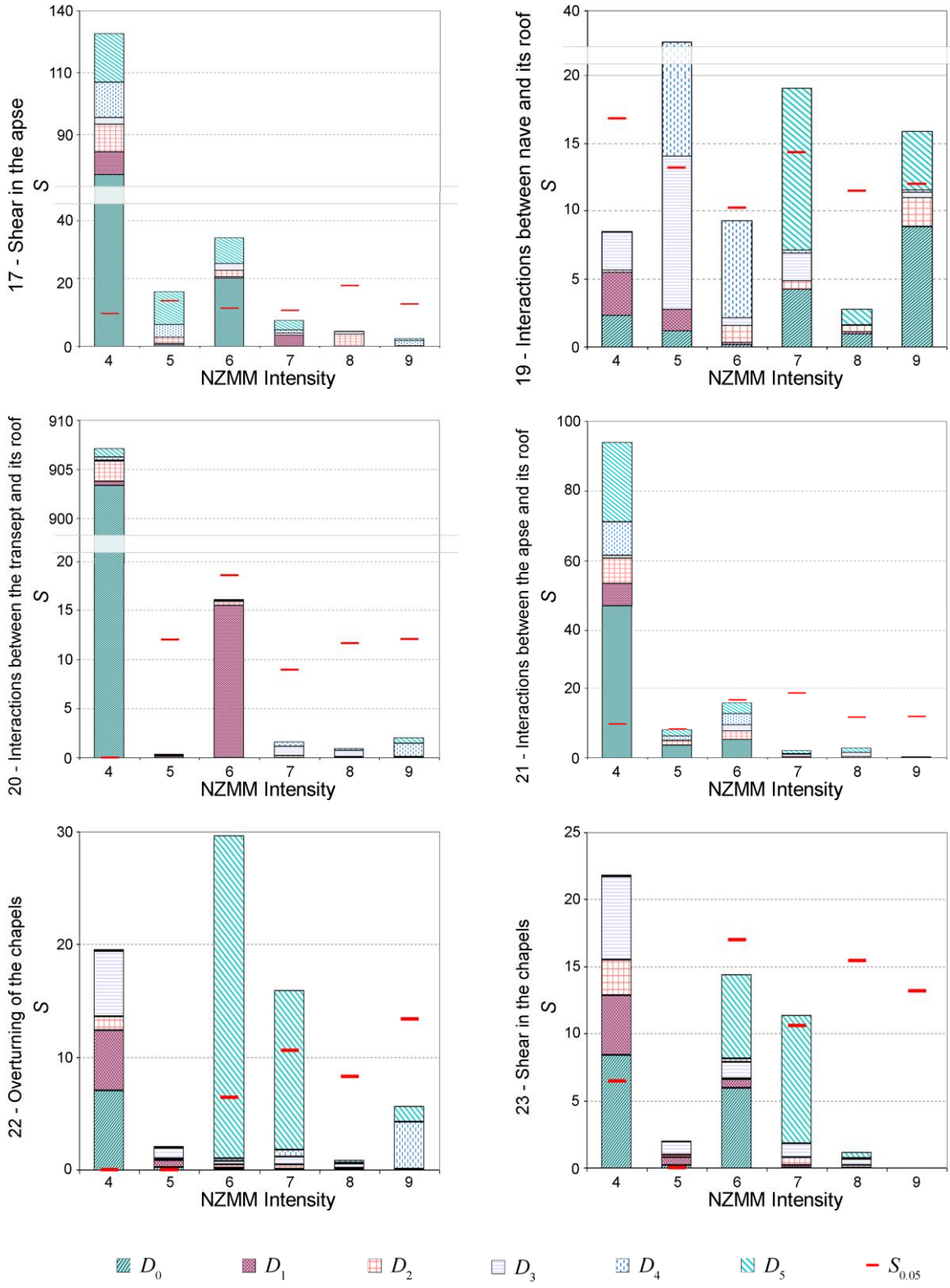
17 - Shear in the apse
S
NZMM Intensity
19 - Interactions between nave and its roof
S
NZMM Intensity
20 - Interactions between the transept and its roof
S
NZMM Intensity
21 - Interactions between the apse and its roof
S
NZMM Intensity
22 - Overturning of the chapels
S
NZMM Intensity
23 - Shear in the chapels
S
NZMM Intensity
D_0
D_1
D_2
D_3
D_4
D_5
$S_{0.05}$

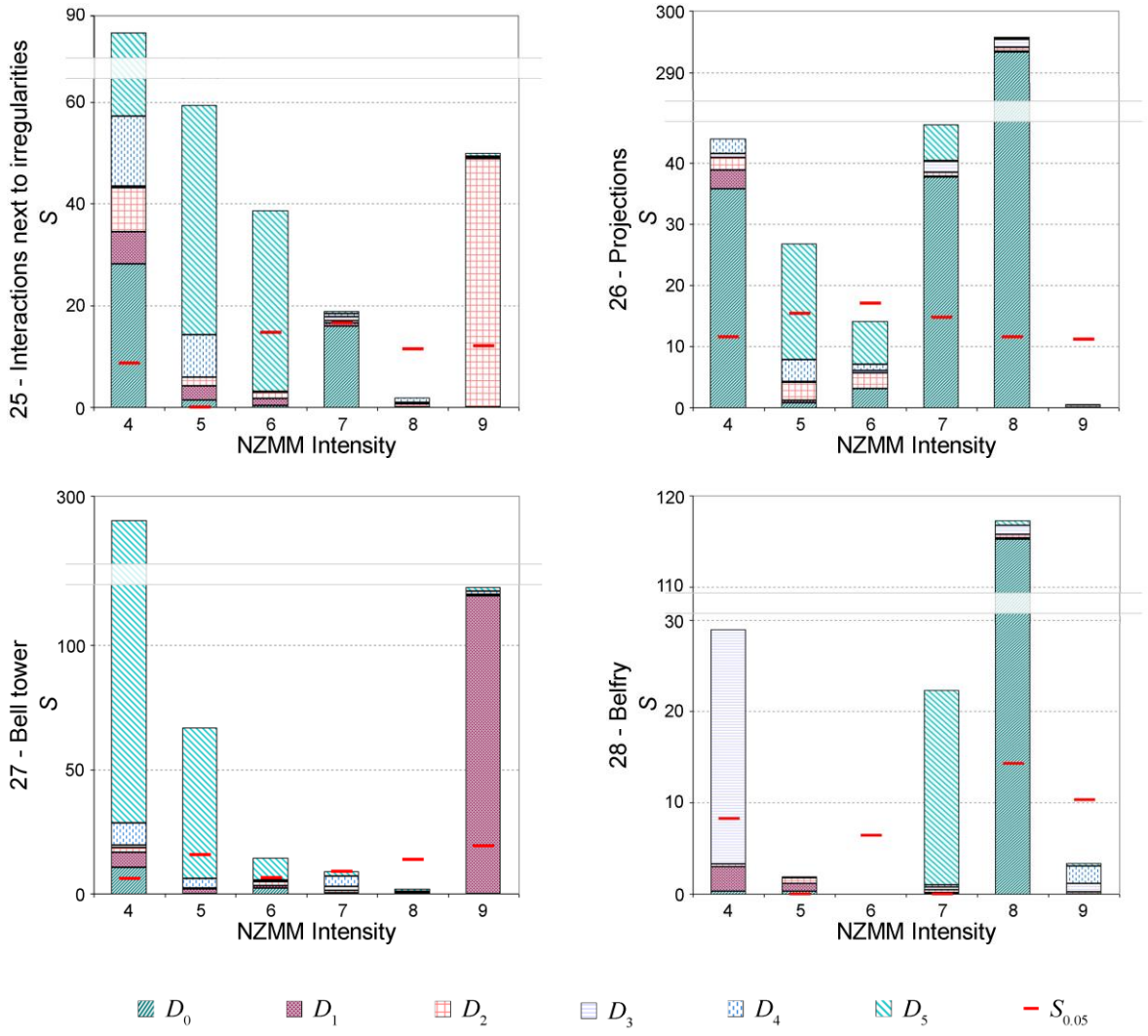
25 - Interactions next to irregularities
S
NZMM Intensity
26 - Projections
S
NZMM Intensity
27 - Bell tower
S
NZMM Intensity
28 - Belfry
S
NZMM Intensity
D_0
D_1
D_2
D_3
D_4
D_5
$S_{0.05}$

Appendix D: Linear regressions between occurred damage levels and macroseismic intensity for the 20 considered mechanisms

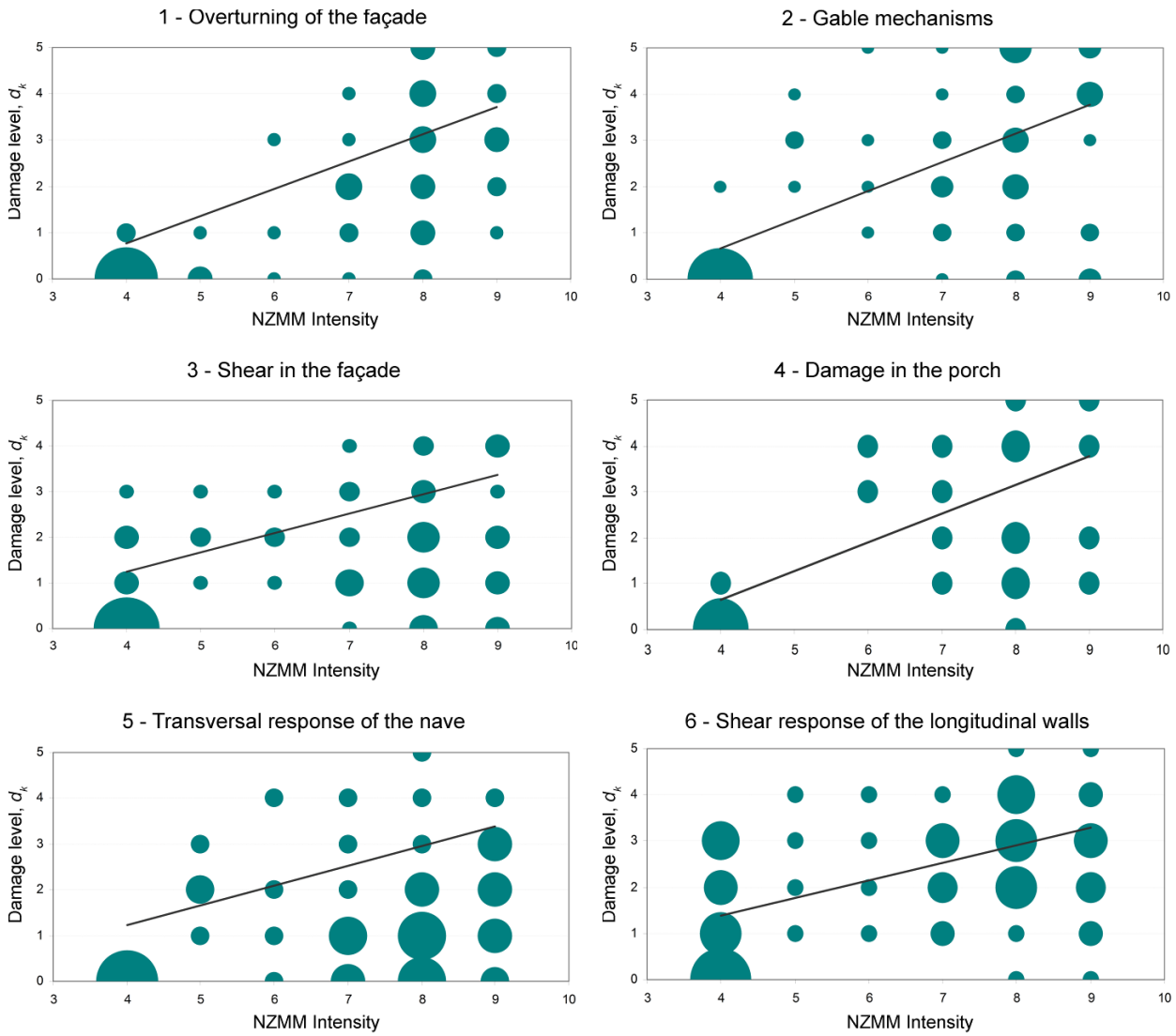

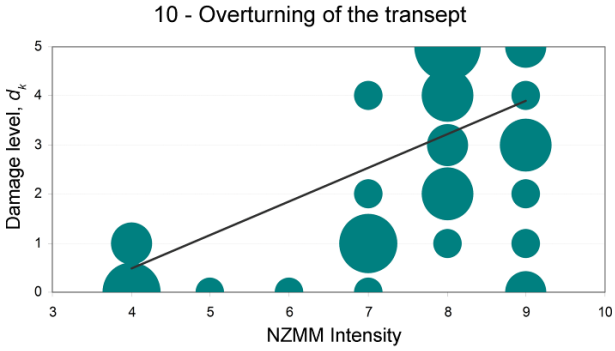
10 - Overturning of the transept
Damage level, d_k
NZMM Intensity

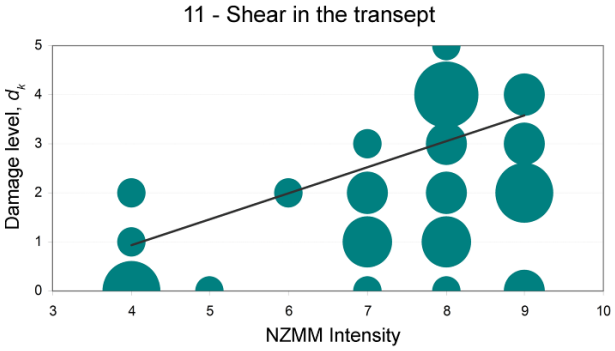
11 - Shear in the transept
Damage level, d_k
NZMM Intensity

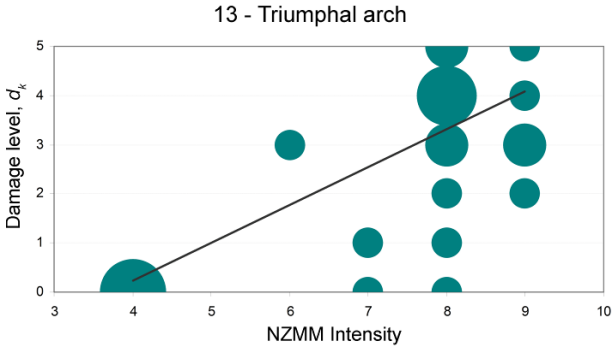
13 - Triumphal arch
Damage level, d_k
NZMM Intensity

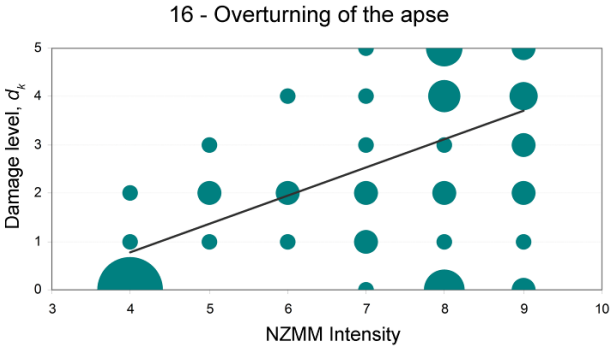
16 - Overturning of the apse
Damage level, d_k
NZMM Intensity

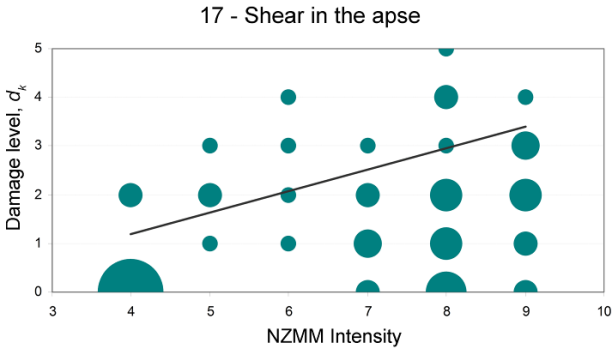
17 - Shear in the apse
Damage level, d_k
NZMM Intensity

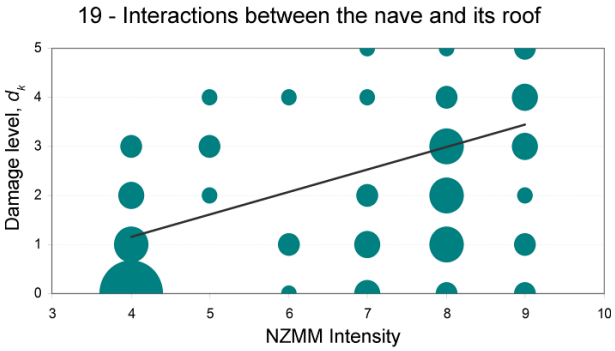
19 - Interactions between the nave and its roof
Damage level, d_k
NZMM Intensity

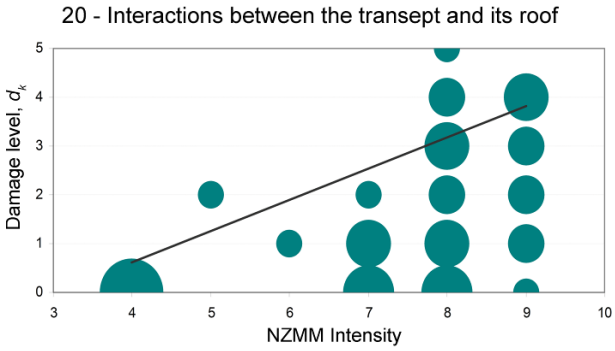
20 - Interactions between the transept and its roof
Damage level, d_k
NZMM Intensity

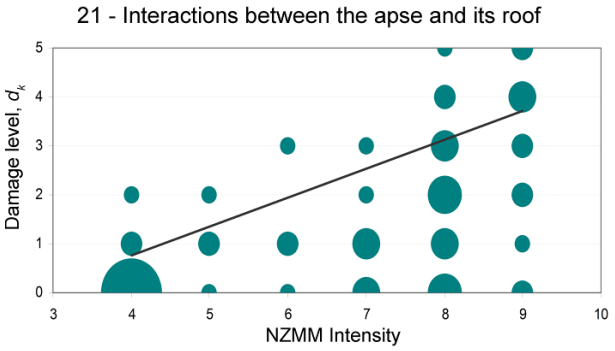
21 - Interactions between the apse and its roof
Damage level, d_k
NZMM Intensity

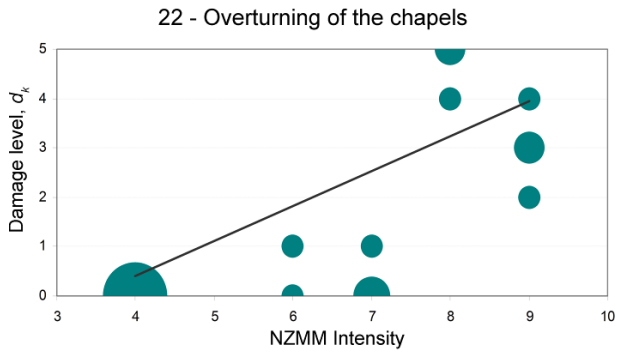
22 - Overturning of the chapels
Damage level, d_k
NZMM Intensity

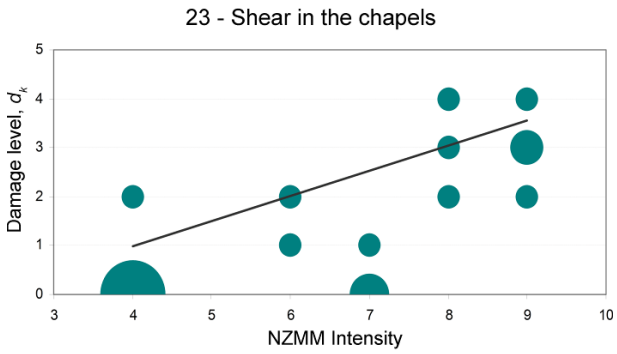
23 - Shear in the chapels
Damage level, d_k
NZMM Intensity

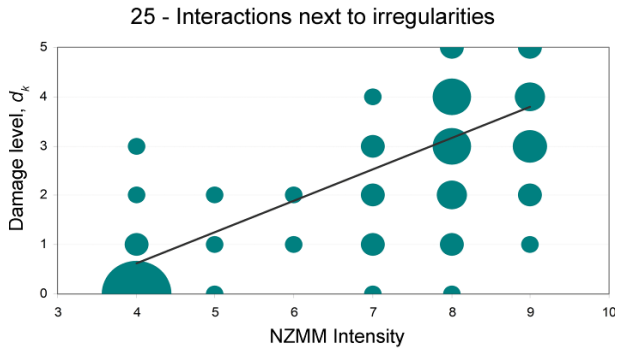
25 - Interactions next to irregularities
Damage level, d_k
NZMM Intensity

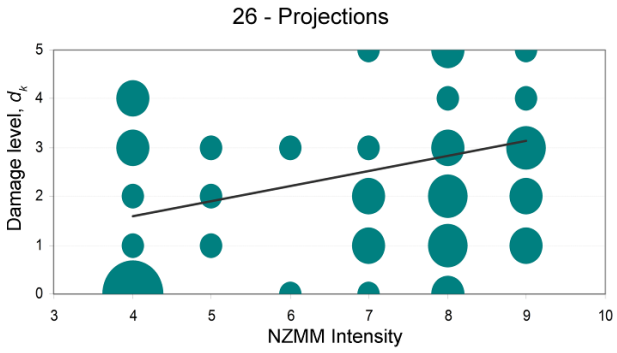
26 - Projections
Damage level, d_k
NZMM Intensity

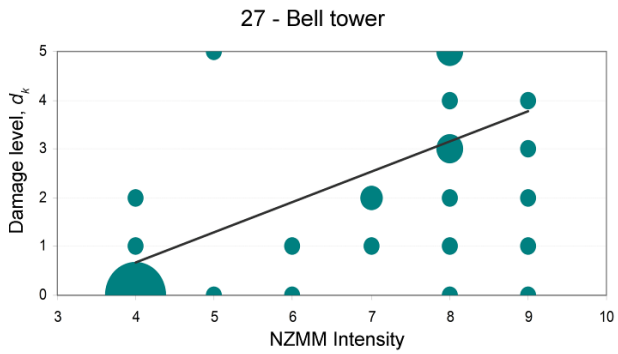
27 - Bell tower
Damage level, d_k
NZMM Intensity

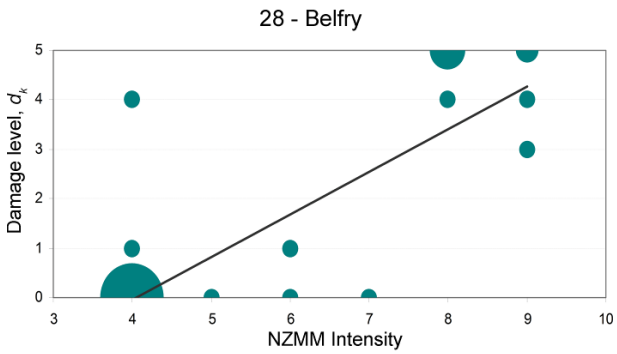
28 - Belfry
Damage level, d_k
NZMM Intensity

Appendix E: Comparison in the correlation between damage observed and damage predicted using simple- or multiple-linear regression models for the 20 considered mechanisms

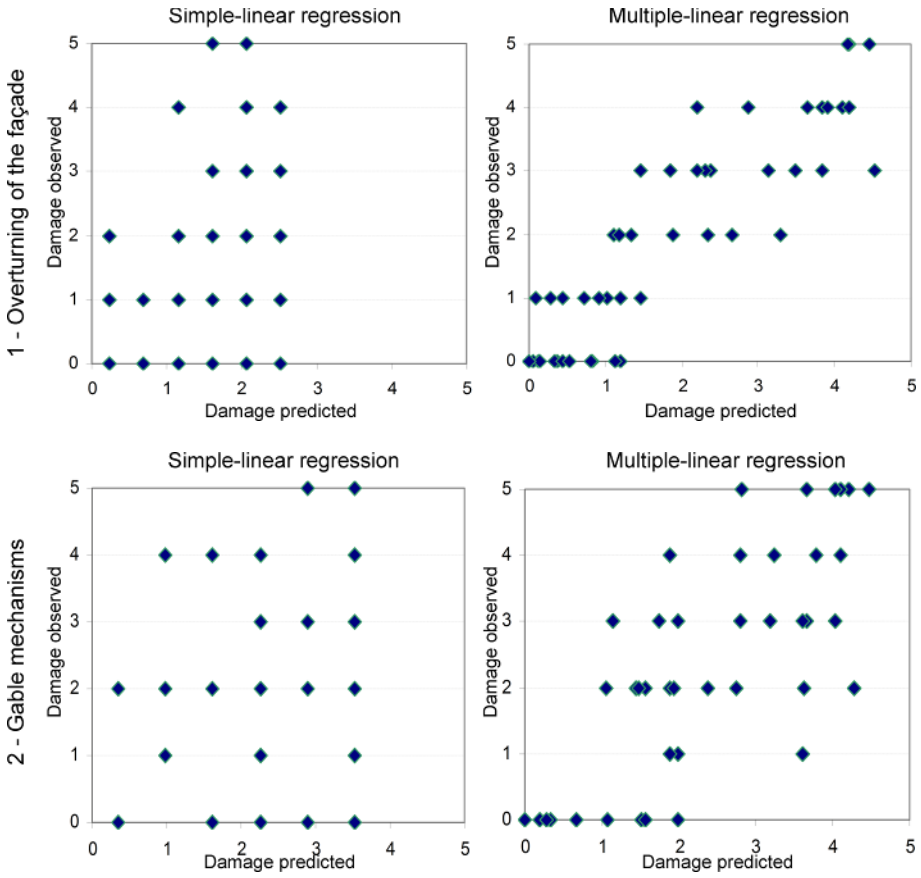

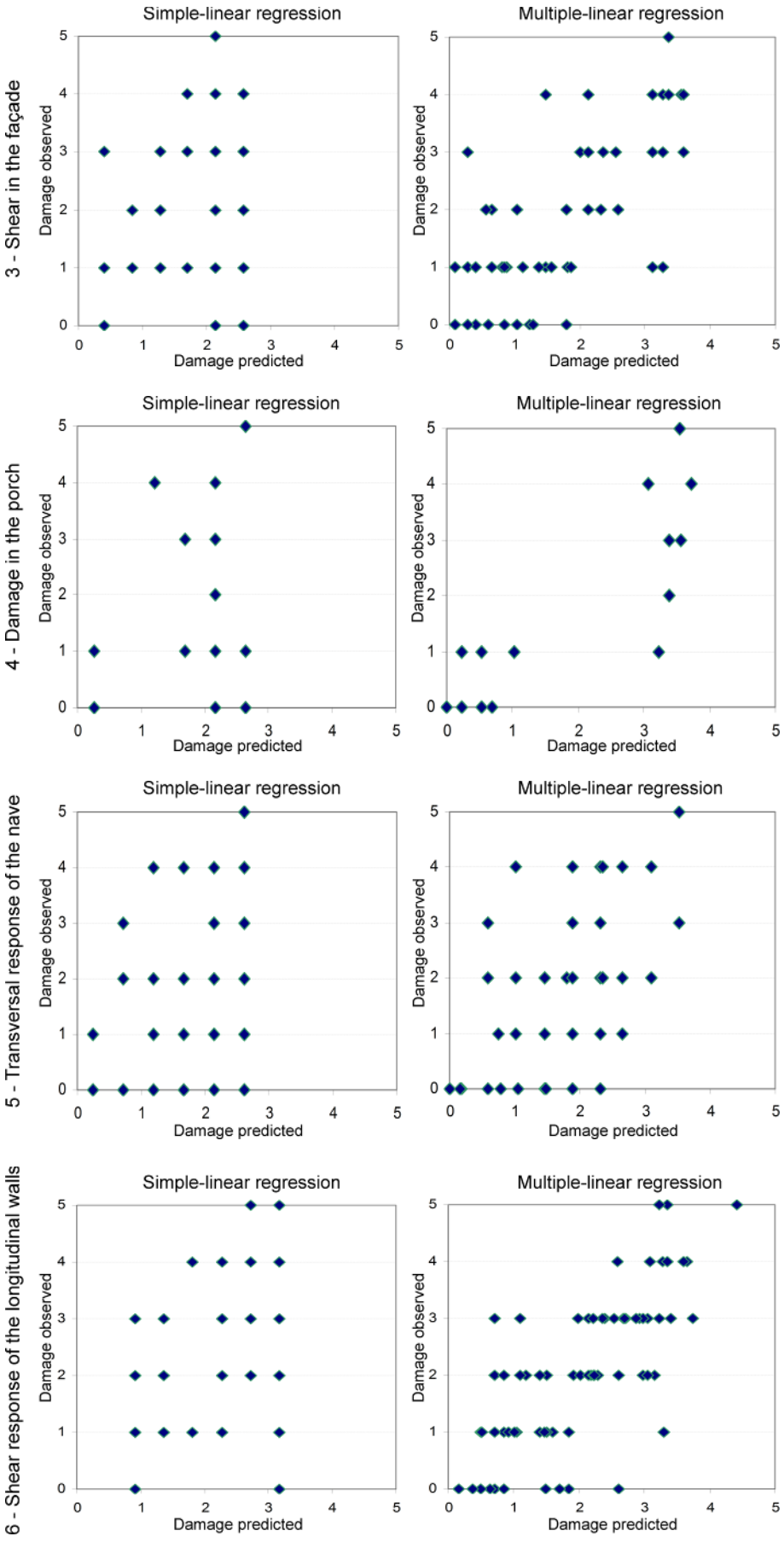
3 - Shear in the façade
Simple-linear regression
Multiple-linear regression
Damage observed
Damage predicted
4 - Damage in the porch
Simple-linear regression
Multiple-linear regression
Damage observed
Damage predicted
5 - Transversal response of the nave
Simple-linear regression
Multiple-linear regression
Damage observed
Damage predicted
6 - Shear response of the longitudinal walls
Simple-linear regression
Multiple-linear regression
Damage observed
Damage predicted

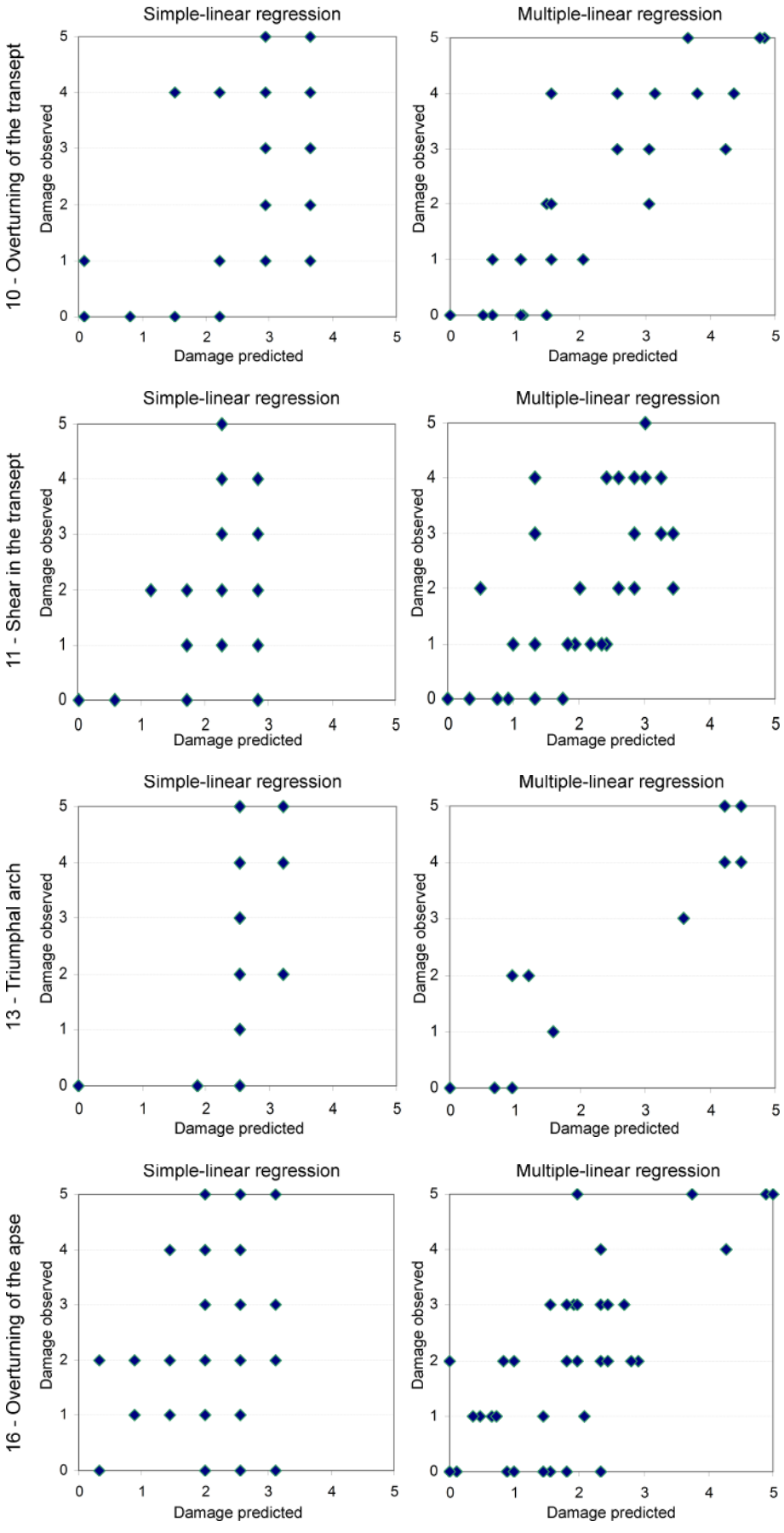
10 - Overturning of the transept
11 - Shear in the transept
13 - Triumphal arch
16 - Overturning of the apse
Simple-linear regression
Multiple-linear regression
Damage observed
Damage predicted
0
1
2
3
4
5

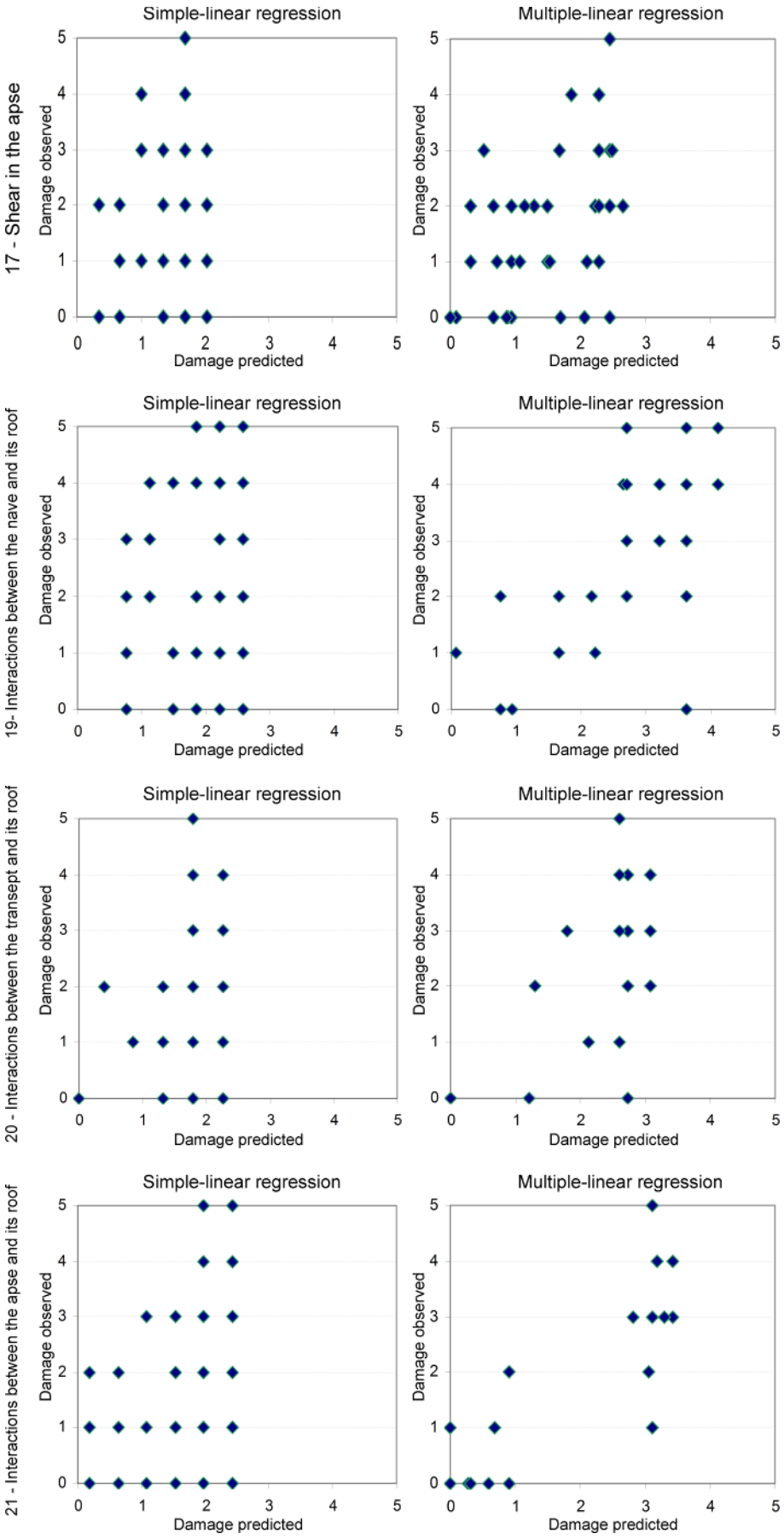
17 - Shear in the apse
Simple-linear regression
Multiple-linear regression
Damage observed
Damage predicted
19- Interactions between the nave and its roof
Simple-linear regression
Multiple-linear regression
Damage observed
Damage predicted
20 - Interactions between the transept and its roof
Simple-linear regression
Multiple-linear regression
Damage observed
Damage predicted
21 - Interactions between the apse and its roof
Simple-linear regression
Multiple-linear regression
Damage observed
Damage predicted

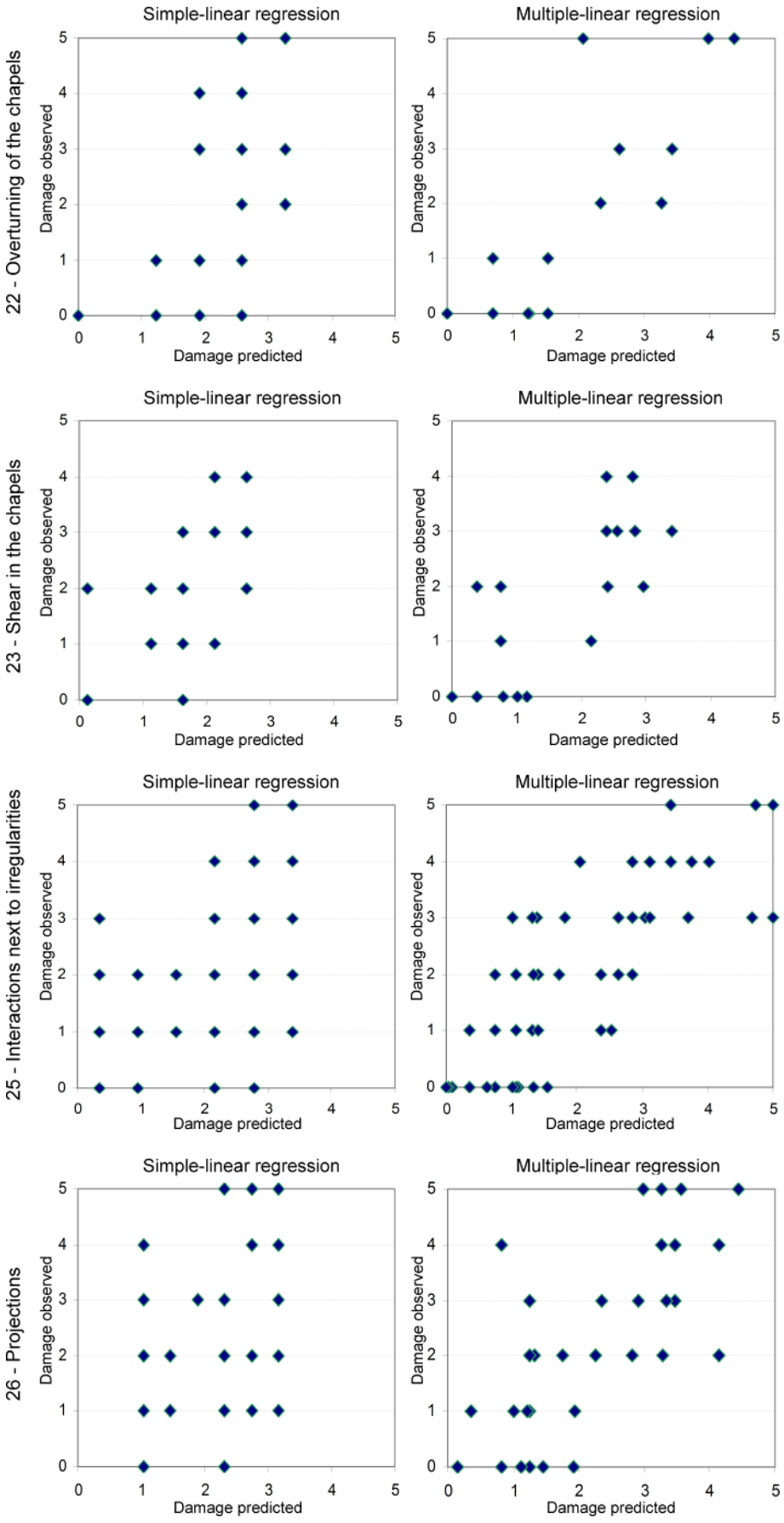
22 - Overturning of the chapels
23 - Shear in the chapels
25 - Interactions next to irregularities
26 - Projections
Simple-linear regression
Multiple-linear regression
Damage observed
Damage predicted
0
1
2
3
4
5

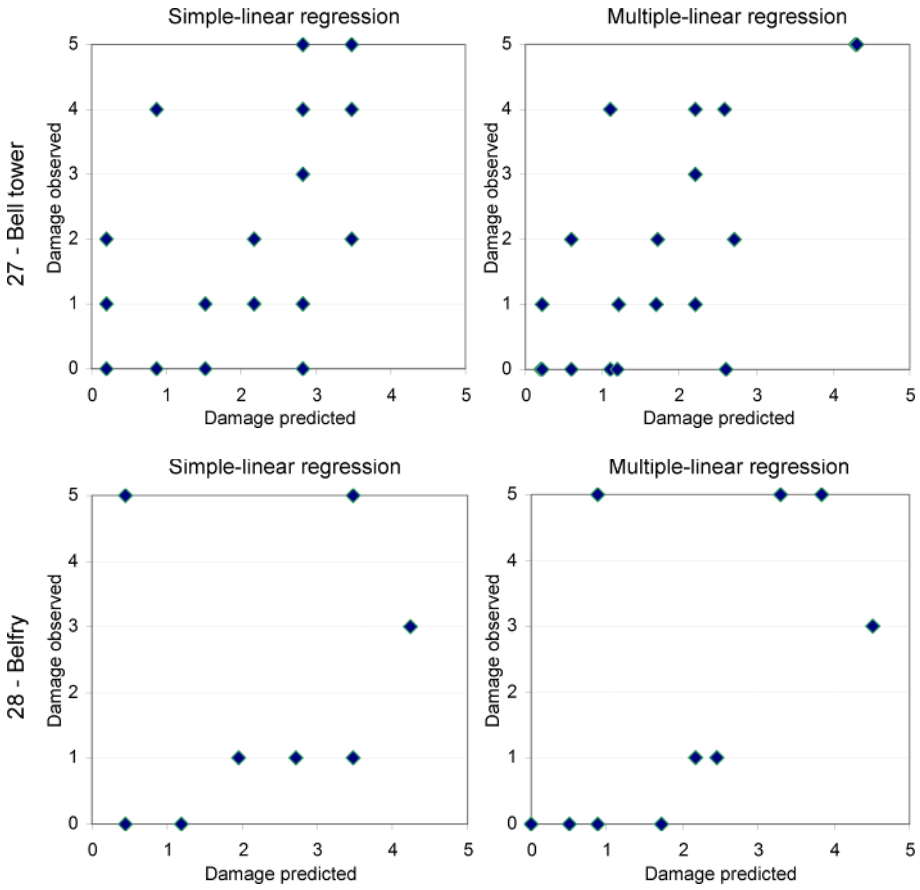
Simple-linear regression
Multiple-linear regression
27 - Bell tower
28 - Belfry
Damage observed
Damage predicted
0
1
2
3
4
5

Appendix F: Regression coefficients for all considered intensity measures

Table 0.1. Computed coefficients of the regression models for NZMMI as intensity measure

Mechanism no. / Variable	*1*	*2*	*3*	*4*	*5*	*6*	*10*	*11*	*13*	*16*
Intensity measure	0.329	0.369	0.255	0.230	0.294	0.407	0.541	0.595	0.066	0.296
Lateral restraint	N/A	N/A	N/A	N/A	N/A	0.590	1.240	N/A	0.359	N/A
Buttresses	N/A	1.088	N/A	0.630	N/A	N/A	N/A	N/A	N/A	N/A
Lintels	N/A	N/A	N/A	1.476	N/A	0.707	N/A	N/A	N/A	N/A
Thrusting elements	1.730	N/A	N/A	N/A	N/A	N/A	N/A	N/A	N/A	N/A
Large openings	0.591	0.521	N/A	N/A	N/A	N/A	1.166	0.964	N/A	N/A
Top beam	N/A	0.669	N/A	N/A	N/A	N/A	4.484	N/A	N/A	N/A
Heterogeneous materials	N/A	N/A	N/A	N/A	N/A	N/A	N/A	N/A	N/A	N/A
Connections	1.425	1.848	N/A	1.703	2.301	N/A	2.044	N/A	N/A	1.610
Slenderness	0.708	0.525	1.398	N/A	0.875	N/A	N/A	1.142	N/A	1.834
Asymmetry conditions	N/A	N/A	N/A	N/A	N/A	N/A	N/A	N/A	N/A	N/A
Poor quality masonry	0.882	N/A	0.486	1.096	N/A	0.696	N/A	N/A	4.118	N/A
b (intercept)	-1.870	-3.108	-0.775	-2.603	-0.973	-2.081	-8.323	-3.280	-0.247	-0.928

Mechanism no. / Variable	*17*	*19*	*20*	*21*	*22*	*23*	*25*	*26*	*27*	*28*
Intensity measure	0.175	0.256	0.299	N/A	0.432	0.441	0.352	0.356	0.420	N/A
Lateral restraint	N/A	N/A	N/A	N/A	N/A	N/A	N/A	N/A	N/A	N/A
Buttresses	N/A	N/A	N/A	N/A	N/A	N/A	N/A	N/A	N/A	N/A
Lintels	N/A	N/A	N/A	N/A	N/A	N/A	N/A	N/A	N/A	N/A
Thrusting elements	N/A	3.327	2.369	N/A	N/A	N/A	N/A	N/A	N/A	N/A
Large openings	N/A	N/A	N/A	N/A	N/A	N/A	N/A	N/A	0.728	N/A
Top beam	N/A	N/A	N/A	N/A	N/A	N/A	N/A	N/A	N/A	N/A
Heterogeneous materials	N/A	N/A	N/A	N/A	N/A	N/A	1.020	N/A	N/A	N/A
Connections	N/A	N/A	N/A	N/A	2.270	N/A	0.946	N/A	2.401	N/A
Slenderness	1.795	N/A	N/A	N/A	N/A	1.740	N/A	1.831	N/A	2.580
Asymmetry conditions	N/A	N/A	N/A	N/A	N/A	N/A	N/A	1.181	1.473	N/A
Poor quality masonry	N/A	1.188	3.337	2.751	1.073	N/A	1.532	0.804	N/A	2.475
b (intercept)	-0.418	-2.910	-4.317	0.152	-2.138	-1.605	-1.914	-1.767	-1.550	0.440

Table 0.2. Computed coefficients of the regression models for PGA as intensity measure

Mechanism no. / Variable	*1*	*2*	*3*	*4*	*5*	*6*	*10*	*11*	*13*	*16*
Intensity measure	1.616	1.497	1.199	1.318	0.997	2.425	1.472	3.227	0.697	1.627
Lateral restraint	N/A	N/A	N/A	N/A	N/A	0.721	N/A	N/A	0.444	N/A
Buttresses	N/A	1.155	N/A	0.764	N/A	N/A	1.019	N/A	N/A	N/A
Lintels	N/A	N/A	N/A	1.437	N/A	0.632	N/A	N/A	N/A	N/A
Thrusting elements	1.886	N/A	N/A	N/A	0.650	N/A	N/A	N/A	N/A	N/A
Large openings	0.588	0.354	N/A	N/A	N/A	N/A	1.476	1.127	N/A	N/A
Top beam	N/A	N/A	N/A	N/A	N/A	N/A	2.540	N/A	N/A	N/A
Heterogeneous materials	N/A	N/A	N/A	N/A	N/A	N/A	N/A	N/A	N/A	N/A
Connections	1.338	2.208	N/A	1.538	2.150	N/A	1.983	N/A	N/A	1.362
Slenderness	0.805	0.539	1.465	N/A	0.855	N/A	N/A	0.885	N/A	2.105
Asymmetry conditions	N/A	N/A	N/A	N/A	N/A	N/A	N/A	N/A	N/A	N/A
Poor quality masonry	1.044	N/A	0.584	1.001	N/A	0.705	N/A	N/A	3.725	N/A
b (intercept)	-0.471	-0.785	0.331	-1.607	0.210	-0.435	-2.890	-0.588	-0.011	0.326

Mechanism no. / Variable	*17*	*19*	*20*	*21*	*22*	*23*	*25*	*26*	*27*	*28*
Intensity measure	1.103	2.407	N/A	N/A	3.377	1.660	1.700	1.648	1.657	7.437
Lateral restraint	N/A	N/A	N/A	N/A	1.730	N/A	N/A	N/A	N/A	N/A
Buttresses	N/A	N/A	N/A	N/A	N/A	N/A	N/A	N/A	N/A	N/A
Lintels	N/A	N/A	N/A	N/A	N/A	N/A	N/A	N/A	N/A	N/A
Thrusting elements	N/A	3.016	N/A	N/A	N/A	N/A	N/A	N/A	N/A	N/A
Large openings	N/A	N/A	N/A	N/A	N/A	0.638	N/A	N/A	N/A	N/A
Top beam	N/A	N/A	N/A	N/A	N/A	N/A	N/A	N/A	N/A	N/A
Heterogeneous materials	N/A	N/A	N/A	N/A	N/A	N/A	1.052	N/A	N/A	N/A
Connections	N/A	N/A	N/A	N/A	1.543	N/A	0.867	N/A	2.914	N/A
Slenderness	1.824	N/A	N/A	N/A	N/A	1.703	N/A	1.936	N/A	N/A
Asymmetry conditions	N/A	N/A	N/A	N/A	N/A	N/A	N/A	0.978	1.669	N/A
Poor quality masonry	N/A	N/A	3.310	2.751	1.299	0.937	1.662	0.825	N/A	N/A
b (intercept)	0.288	-1.287	0.039	0.152	-2.130	-0.011	-0.347	-0.115	0.483	0.029

Table 0.3. Computed coefficients of the regression models for PGV as intensity measure

Mechanism no. / Variable	*1*	*2*	*3*	*4*	*5*	*6*	*10*	*11*	*13*	*16*
Intensity measure	1.546	1.510	1.366	1.162	1.077	2.145	2.409	2.883	0.144	1.421
Lateral restraint	N/A	N/A	N/A	N/A	N/A	0.749	0.767	N/A	0.457	N/A
Buttresses	N/A	1.300	N/A	0.696	N/A	N/A	0.690	N/A	N/A	N/A
Lintels	N/A	N/A	N/A	1.599	N/A	0.670	N/A	N/A	N/A	N/A
Thrusting elements	1.735	N/A	N/A	N/A	0.601	N/A	N/A	N/A	N/A	N/A
Large openings	0.529	0.341	N/A	N/A	N/A	N/A	1.309	N/A	N/A	N/A
Top beam	N/A	0.565	N/A	N/A	N/A	N/A	2.968	N/A	N/A	N/A
Heterogeneous materials	N/A	N/A	N/A	N/A	N/A	N/A	N/A	N/A	N/A	N/A
Connections	1.364	2.038	N/A	1.808	2.282	N/A	1.965	N/A	N/A	1.307
Slenderness	0.839	0.580	1.565	N/A	0.714	N/A	N/A	1.432	N/A	2.044
Asymmetry conditions	N/A	N/A	N/A	N/A	N/A	N/A	N/A	N/A	N/A	N/A
Poor quality masonry	1.019	N/A	0.491	1.110	N/A	0.859	N/A	N/A	4.230	N/A
b (intercept)	-0.498	-1.475	0.246	-1.788	0.173	-0.524	-4.352	-0.163	0.068	0.327

Mechanism no. / Variable	*17*	*19*	*20*	*21*	*22*	*23*	*25*	*26*	*27*	*28*
Intensity measure	0.923	1.996	2.064	N/A	1.926	1.481	1.811	1.913	2.495	3.984
Lateral restraint	N/A	N/A	N/A	N/A	N/A	N/A	N/A	N/A	N/A	N/A
Buttresses	N/A	N/A	N/A	N/A	N/A	N/A	N/A	N/A	N/A	N/A
Lintels	N/A	N/A	N/A	N/A	N/A	N/A	N/A	N/A	N/A	N/A
Thrusting elements	N/A	3.148	1.741	N/A	N/A	N/A	N/A	N/A	N/A	N/A
Large openings	N/A	N/A	N/A	N/A	N/A	0.588	N/A	N/A	N/A	N/A
Top beam	N/A	N/A	N/A	N/A	N/A	N/A	N/A	N/A	N/A	N/A
Heterogeneous materials	N/A	N/A	N/A	N/A	N/A	N/A	0.852	N/A	N/A	N/A
Connections	N/A	N/A	N/A	N/A	2.159	N/A	0.950	N/A	2.084	N/A
Slenderness	1.779	N/A	N/A	N/A	N/A	1.616	N/A	2.262	N/A	N/A
Asymmetry conditions	N/A	N/A	N/A	N/A	N/A	N/A	N/A	1.153	N/A	N/A
Poor quality masonry	N/A	1.003	3.006	2.751	1.341	0.871	1.529	1.008	0.983	2.074
b (intercept)	0.300	-1.955	-2.575	0.152	-0.275	0.026	-0.366	-0.419	-0.039	-0.267

Table 0.4. Computed coefficients of the regression models for I_A as intensity measure

Mechanism no. / Variable	*1*	*2*	*3*	*4*	*5*	*6*	*10*	*11*	*13*	*16*
Intensity measure	0.170	0.141	0.129	0.172	N/A	0.282	0.138	0.382	0.087	0.191
Lateral restraint	N/A	N/A	N/A	N/A	N/A	0.836	N/A	N/A	0.496	N/A
Buttresses	N/A	1.166	N/A	0.813	N/A	N/A	1.113	N/A	N/A	N/A
Lintels	N/A	N/A	N/A	1.436	N/A	N/A	N/A	N/A	N/A	N/A
Thrusting elements	1.989	N/A	N/A	N/A	0.746	N/A	N/A	N/A	N/A	N/A
Large openings	0.541	0.382	N/A	N/A	N/A	N/A	1.490	1.182	N/A	N/A
Top beam	N/A	N/A	N/A	N/A	N/A	N/A	2.724	N/A	N/A	N/A
Heterogeneous materials	N/A	N/A	N/A	N/A	N/A	N/A	N/A	N/A	N/A	N/A
Connections	1.474	2.363	N/A	1.534	2.670	N/A	2.153	N/A	N/A	1.464
Slenderness	0.884	0.664	1.556	N/A	0.864	N/A	N/A	1.050	N/A	2.263
Asymmetry conditions	N/A	N/A	N/A	N/A	N/A	N/A	N/A	N/A	N/A	N/A
Poor quality masonry	1.111	N/A	0.677	1.105	N/A	0.945	N/A	N/A	3.936	N/A
b (intercept)	-0.286	-0.623	0.447	-1.538	-0.247	0.175	-2.831	-0.112	0.014	0.484

Mechanism no. / Variable	*17*	*19*	*20*	*21*	*22*	*23*	*25*	*26*	*27*	*28*
Intensity measure	0.132	0.376	N/A	0.464	0.281	0.202	0.190	0.199	N/A	1.259
Lateral restraint	N/A	N/A	N/A	N/A	N/A	N/A	N/A	N/A	N/A	N/A
Buttresses	N/A	N/A	N/A	N/A	N/A	N/A	N/A	N/A	N/A	N/A
Lintels	N/A	N/A	N/A	N/A	N/A	N/A	N/A	N/A	N/A	N/A
Thrusting elements	N/A	2.761	N/A	N/A	N/A	N/A	N/A	N/A	N/A	N/A
Large openings	N/A	N/A	N/A	N/A	N/A	0.740	N/A	N/A	N/A	N/A
Top beam	N/A	N/A	N/A	N/A	N/A	N/A	N/A	N/A	N/A	N/A
Heterogeneous materials	N/A	N/A	N/A	N/A	N/A	N/A	1.039	N/A	N/A	N/A
Connections	N/A	N/A	N/A	N/A	2.390	N/A	0.924	N/A	3.184	N/A
Slenderness	1.965	N/A	N/A	N/A	N/A	1.819	N/A	1.925	N/A	N/A
Asymmetry conditions	N/A	N/A	N/A	N/A	N/A	N/A	N/A	0.882	1.736	N/A
Poor quality masonry	N/A	N/A	3.310	1.916	1.643	1.059	1.796	0.973	0.942	N/A
b (intercept)	0.394	-0.974	0.039	-0.441	-0.210	0.095	-0.172	0.058	0.512	0.357

Table 0.5. Computed coefficients of the regression models for mI_H as intensity measure

Mechanism no. / Variable	*1*	*2*	*3*	*4*	*5*	*6*	*10*	*11*	*13*	*16*
Intensity measure	3.885	3.826	2.743	4.323	2.695	6.303	4.265	9.109	1.018	4.330
Lateral restraint	N/A	N/A	N/A	N/A	N/A	0.740	N/A	N/A	0.384	N/A
Buttresses	N/A	1.159	N/A	0.778	N/A	N/A	1.008	N/A	N/A	N/A
Lintels	N/A	N/A	N/A	1.594	N/A	0.658	N/A	N/A	N/A	N/A
Thrusting elements	1.976	N/A	N/A	N/A	0.659	N/A	N/A	N/A	N/A	N/A
Large openings	0.582	0.366	N/A	N/A	N/A	N/A	1.487	1.281	N/A	N/A
Top beam	N/A	N/A	N/A	N/A	N/A	N/A	2.742	N/A	N/A	N/A
Heterogeneous materials	N/A	N/A	N/A	N/A	N/A	N/A	N/A	N/A	N/A	N/A
Connections	1.525	2.324	N/A	1.601	2.248	N/A	2.098	N/A	N/A	1.547
Slenderness	0.748	0.534	1.510	N/A	0.825	N/A	N/A	0.921	N/A	2.105
Asymmetry conditions	N/A	N/A	N/A	N/A	N/A	N/A	N/A	N/A	N/A	N/A
Poor quality masonry	1.113	N/A	0.685	0.987	N/A	0.824	N/A	N/A	4.159	N/A
b (intercept)	-0.473	-0.806	0.338	-1.858	0.189	-0.513	-3.191	-0.771	0.024	0.295

Mechanism no. / Variable	*17*	*19*	*20*	*21*	*22*	*23*	*25*	*26*	*27*	*28*
Intensity measure	2.493	7.949	N/A	N/A	6.255	3.994	4.527	4.728	3.903	12.372
Lateral restraint	N/A	N/A	N/A	N/A	N/A	N/A	N/A	N/A	N/A	N/A
Buttresses	N/A	N/A	N/A	N/A	N/A	N/A	N/A	N/A	N/A	N/A
Lintels	N/A	N/A	N/A	N/A	N/A	N/A	N/A	N/A	N/A	N/A
Thrusting elements	N/A	2.816	N/A	N/A	N/A	N/A	N/A	N/A	N/A	N/A
Large openings	N/A	N/A	N/A	N/A	N/A	0.657	N/A	N/A	N/A	N/A
Top beam	N/A	N/A	N/A	N/A	N/A	N/A	N/A	N/A	N/A	N/A
Heterogeneous materials	N/A	N/A	N/A	N/A	N/A	N/A	1.015	N/A	N/A	N/A
Connections	N/A	N/A	N/A	N/A	2.397	N/A	0.947	N/A	2.677	N/A
Slenderness	1.938	N/A	N/A	N/A	N/A	1.710	N/A	1.997	N/A	N/A
Asymmetry conditions	N/A	N/A	N/A	N/A	N/A	N/A	N/A	1.057	1.454	N/A
Poor quality masonry	N/A	N/A	2.751	2.751	1.472	0.986	1.709	0.891	0.866	2.208
b (intercept)	0.314	-1.371	0.039	0.152	-0.409	0.015	-0.382	-0.217	0.183	-0.261

Appendix G: Complete list of references

Anagnostopoulou, M., Bruneau, M. and Gavin, H. P. (2010) Performance of churches during the Darfield earthquake of September 4, 2010, *Bulletin of the New Zealand Society for Earthquake Engineering*, 43(4), 374–381.

Anbazhagan, P., Sreenivas, M., Ketan, B., Moustafa, S.S. and Al-Arifi, N.S.N. (2015) Selection of Ground Motion Prediction Equations for Seismic Hazard Analysis of Peninsular India, *Journal of Earthquake Engineering*, doi: 10.1080/13632469.2015.1104747. In press.

Andreotti, C., Liberatore, D. and Sorrentino L. (2014) Identifying seismic local collapse mechanisms in unreinforced masonry buildings through 3D laser scanning, *Key Engineering Materials* 628, 79-84. doi:10.4028/www.scientific.net/KEM.628.79.

Anonymous. (1979a). *Historic buildings of New Zealand – North Island*. Methuen Publications, Auckland, New Zealand, 271 pp.

Anonymous. (1979b). *Historic buildings of New Zealand – South Island*. Methuen Publications, Auckland, New Zealand, 264 pp.

Aras F., Krstevska L., Altay G., Tashkov LJ. 2011. Experimental and numerical modal analyses of a historical masonry palace, *Construction and Building Materials*, 25(1): 81-91.

Arias, A. 1970. A measure of earthquake intensity. In *Seismic Design for Nuclear Power Plants*. Edited by R. J. Hansen. Cambridge, MA: MIT Press.

ATC - American Technology Council (1985) Earthquake damage evaluation data for California, Report 13, Redwood City, California.

Bannister, S. and Gledhill, K. (2012) Evolution of the 2010–2012 Canterbury earthquake sequence, *New Zealand Journal of Geology and Geophysics* 55(3), 295-304.

Baptista M.A., Mendes P., Afilhado A., Agostinho L., Lagomarsino S., Mendes Victor L., 2005. Ambient vibration testing at N. Sra. do Carmo Church, preliminary results,

Proceedings of the 4th International Seminar on Structural Analysis of Historical Constructions, Padova, Italy, 483-488.

Bayraktar A., Türker T., Sevım B., Altunisik A.C., Yildirim F., 2009. Modal Parameter Identification of Hagia Sophia Bell-Tower via Ambient Vibration Test, *Journal of Nondestructive Evaluation*, 28: 37–47.

Bendat J.S., and Piersol A.G., 1993. *Engineering Applications of Correlation and Spectral Analysis*, John Wiley & Sons, 302 pp.

Benedetti, D. and Petrini, V. (1984) Sulla vulnerabilità sismica degli edifici in muratura: un metodo di valutazione, *L'Industria delle Costruzioni* 149, 66-74. In Italian.

Benedetti, D., Benzoni, G. and Parisi, M.A. (1988) Seismic vulnerability and risk evaluation for old urban nuclei, *Earthquake Engineering & Structural Dynamics* 16, 183–201. doi: 10.1002/eqe.4290160203.

Benjamin, J.R. and Cornell, C.A. (1970) *Probability, statistics and decision for civil engineers*, McGraw-Hill, New York.

Bernardini, A., Gori, R. and Modena, C. (1990) Application of coupled analytical models and experimental knowledge to seismic vulnerability analyses of masonry buildings, in *Engineering Damage Evaluation and Vulnerability Analysis of Building Structures*, ed A. Koridze (Omega Scientific, Oxon, U.K), pp. 161-180.

Beskhyroun S., 2011. Graphical Interface Toolbox for Modal Analysis, *Proceedings of the Ninth Pacific Conference on Earthquake Engineering Building an Earthquake-Resilient Society* 14-16 April, 2011, Auckland, New Zealand.

Bradley, B.A., Quigley, M.C., Van Dissen, R.J. and Litchfield, N.J. (2014) Ground motion and seismic source aspects of the Canterbury earthquake sequence, *Earthquake Spectra* 30(1), 1–15.

Braga, F., Dolce, M. and Liberatore, D. (1982) A statistical study on damaged buildings and an ensuing review of MSK-76 Scale, *Proc of the 7th European Conference on Earthquake Engineering*, Athens, Greece, pp. 431–450.

Brincker R., Zhang L., and Andersen P., 2000. Modal Identification from Ambient Responses using Frequency Domain Decomposition, *Proceedings of the 18th International Modal Analysis Conference (IMAC)*, USA.

Calvi, G.M., Pinho, R., Magenes, G., Bommer, J.J., Restrepo-Vélez, L.F. and Crowley, H. (2006) Development of seismic vulnerability assessment methodologies over the past 30 years, *ISET Journal of Earthquake Technology* 43(3), 75-104.

Canterbury Earthquake Heritage Buildings Fund - CEHBF. http://www.savecanterburyheritage.org.nz/about/. (Accessed during December 2013).

Cardona, O. D., Salgado, M. A., Carreño, M. L., Bernal, G. A., Villegas, C. P., and Barbat, A. H., 2014. Urban seismic risk assessment of Santo Domingo: a probabilistic and holistic approach, in *Proceedings, 10th U.S. National Conference on Earthquake Engineering: Frontiers of Earthquake Engineering*, 21-25 July, 2014, Anchorage, Alaska.

Casarin F, Modena C., 2007. Dynamic identification of S. Maria Assunta Cathedral, Reggio Emilia, Italy. *Proceedings of 2nd International Operational Modal Analysis Conference*, 637-644.

Cattari, S., Ottonelli, D., Pinna, M., Lagomarsino, S., Clark, W., Giovinazzi, S., Ingham, J.M., Marotta, A., Liberatore, D., Sorrentino, L., Leite, J., Lourenco, P.B. and Goded, T. (2015). Preliminary results from damage and vulnerability analysis of URM churches after the Canterbury earthquake sequence 2010-2011. *New Zealand Society for Earthquake Engineering Technical Conference*, Rotorua, NZ, 10-12 April 2015.

CERA - Canterbury Earthquake Recovery Authority (2014) "Demolitions List". http://cera.govt.nz/demolitions/list. Accessed 05 November 2014.

Chaulagain, H., Rodrigues, H., Silva, V., Spacone, E., and Varum, H., 2015. Seismic risk assessment and hazard mapping in Nepal, *Natural Hazards* **78**, 583–602.

Cherif, S., Chourak, M., and Abed, M., 2015. Seismic risk assessment of the city of Al Hoceima (North of Morocco) using the RISK-UE vulnerability index method, in *Proceedings, 50th International Conference on Earthquake Engineering and Seismology*, 12-16 May, 2015, Kiel, Germany.

Chiauzzi, L., Masi, A., Mucciarelli, M., Vona, M., Pacor, F., Cultrera, G., Gallovič, F., and Emolo, A., 2012. Building damage scenarios based on exploitation of Housner intensity derived from finite faults ground motion simulations, *Bulletin of Earthquake Engineering* **10**, 517–545.

Chrysostomou, C. Z, Kyriakides, N., and Çağnan, Z., 2014. Scenario-based seismic risk assessment for the Cyprus region, in *Proceedings, 2th European Conference on Earthquake Engineering and Seismology*, 25-29 August, 2014, Istanbul, Turkey.

Davidson, A. (2004). *Christianity in Aotearoa: A History of Church and Society in New Zealand*. Education for Ministry, Wellington, New Zealand, 16 pp.

da Porto, F., Silva, B., Costa, C. and Modena, C. (2012) Macro-scale analysis of damage to churches after earthquake in Abruzzo (Italy) on April 6, 2009, *Journal of Earthquake Engineering* 16(6), 739-758. doi: 10.1080/13632469.2012.685207.

D'Ayala, D. (1999) Correlation of seismic vulnerability and damage between classes of buildings: Churches and houses, in *Seismic damage to masonry buildings: proceedings of the International Workshop on Measures of Seismic Damage to Masonry Buildings*, ed. A. Bernardini (Taylor & Francis, Balkerna, Rotterdam), pp. 41-58.

D'Ayala, D.F. (2000). Establishing correlation between vulnerability and damage survey for churches, *12th World Conference on Earthquake Engineering*, Auckland, New Zealand, 30 January – 4 February 2000, Paper No 2237.

D'Ayala, D. and Speranza, E. (2003) Definition of Collapse Mechanisms and Seismic Vulnerability of Historic Masonry Buildings, *Earthquake Spectra* 19(3), 479–509. doi: 10.1193/1.1599896.

D'Ayala, D. (2013) Assessing the seismic vulnerability of masonry buildings, in *Handbook of seismic risk analysis and management of civil infrastructure systems*, ed. S. Tesfamariam and K. Goda (Woodhead publishing, Sawston, Cambridge), pp 334-365.

Decanini, L., Mollaioli, F., and Oliveto, G., 2002. Structural and seismological implications of the 1997 seismic sequence in Umbria and Marche, Italy, in *Innovative approaches to earthquake engineering* (G. Oliveto, ed.), WIT Press, Southampton, 229–323.

De Matteis, G., Criber, E. and Brando, G. (2014) Damage Evaluation On Churches Belonging To The Sulmona-Valva Diocese After The 2009 L'Aquila Earthquake, *Proc of the 2nd International Conference on Protection of Historical Constructions*, Antalya, Turkey.

De Matteis, G., Criber, E., and Brando, G., 2016. Damage Probability Matrices for Three-Nave Masonry Churches in Abruzzi After the 2009 L'Aquila Earthquake, *International Journal of Architectural Heritage* **10**, 120–145.

Di Pasquale, G., Orsini, G. and Romeo, R.W. (2005) New developments in seismic risk assessment in Italy, *Bulletin of Earthquake Engineering* 3(1), 101-128. doi: 10.1007/s10518-005-0202-1.

Dizhur, D., Ingham, J.M., Moon, L., Griffith, M., Schultz, A., Senaldi, I., Magenes, G., Dickie, J., Lissel, S., Centeno, J., Ventura, C., Leite, J. and Lourenco, P.B. (2011).

Performance of masonry buildings and churches in the 22 February 2011 Christchurch earthquake. *Bulletin of the New Zealand Society For Earthquake Engineering.* **44**(4): 279-297.

DMI - Decreto del Ministro delle Infrastrutture del 14 gennaio 2008: Approvazione delle nuove norme tecniche per le costruzioni. Gazzetta Ufficiale della Repubblica Italia-na, n. 29 del 4 febbraio 2008, Supplemento Ordinario n. 30. In Italian.

Doglioni, F., Moretti, A. and Petrini, V. (ed) (1994) *Le chiese e il terremoto. Dalla vulnerabilità constatata nel terremoto del Friuli al miglioramento antisismico nel restauro, verso una politica di prevenzione*, Ed. LINT, Trieste. In Italian.

Dolce, M., Masi, A., Marino M. and Vona, M. (2003) Earthquake damage scenarios of the building stock of Potenza (Southern Italy) Including Site Effects, *Bulletin of Earthquake Engineering* 1(1), 115-140. doi: 10.1023/A:1024809511362.

Dolce, M., Kappos, A., Masi, A., Penelis, G., and Vona, M., 2006. Vulnerability assessment and earthquake damage scenarios of the building stock of Potenza (Southern Italy) using Italian and Greek methodologies, *Engineering Structures* **28**, 357–371.

Donovan, D. (2002). *Country churches of New Zealand*. London: New Holland, Auckland, New Zealand, 126 pp.

Dowrick, D.J. (1996) The Modified Mercalli earthquake intensity scale; revisions arising from recent studies of New Zealand earthquakes, *Bulletin of the New Zealand National Society for Earthquake Engineering* 29, 92-106.

Dowrick D.J., 2003. *Earthquake risk reduction*, John Wiley & Sons, Chichester, UK, 506 pp.

Dowsett, M. (1985). *The illusion of permanence: an investigation into 'timber-as-stone' architecture (non-domestic) of the colonial period*. Thesis for the degree of Bachelor of Architecture, University of Auckland.

DPCM (Direttiva del Presidente del Consiglio dei Ministri) 9 febbraio 2011. "Valutazione e riduzione del rischio sismico del patrimonio culturale con riferimento alle Norme tecniche per le costruzioni di cui al DM 14 gennaio 2008," Gazzetta Ufficiale della Repubblica Italiana n. 47 del 26 febbraio 2009, Supplemento Ordinario n. 54. In Italian.

Draper, N. and Smith, H. (1981) *Applied Regression Analysis*, John Wiley & Sons, New York.

Dunand, F., Nicol, J., Moutou Pitti, R., Fournely, E., and Toussaint, E., 2014. Seismic risk quantification in France: probabilistic evaluation, in *Proceedings, 2th European Conference on Earthquake Engineering and Seismology*, 25-29 August, 2014, Istanbul, Turkey.

Eiby, G.A. (1966) The Modified Mercalli scale of earthquake intensity and its use in New Zealand, *New Zealand Journal of Geology and Geophysics* 9, 122-129.

Eleftheriadou, A. K., Baltzopoulou, A. D., and Karabinis, A. I., 2014. Seismic risk assessment of buildings in the extended urban region of Athens and comparison with the repair cost, *Open Journal of Earthquake Research* **3**, 115-134.

Elton, D.J. and Marciano, E.A. (1990) Ground acceleration near St Michael's Church during the 1886 Charleston, SC, Earthquake, *Earthquake Spectra* 6, 81-103. doi: 10.1193/1.1585559.

Erberik, M.A. (2008) Generation of fragility curves for Turkish masonry buildings considering in-plane failure modes, *Earthquake Engineering and Structural Dynamics* 37(3), 387-405. doi: 10.1002/eqe.760.

Erberik, M. A., 2010. Seismic risk assessment of masonry buildings in Istanbul for effective risk mitigation, *Earthquake Spectra* **26**, 967–982.

Faccioli, E., Pessina, V., Calvi, G. M., and Borzi, B., 1999. A study on damage scenarios for residential buildings in Catania city, *Journal of Seismology* **3**, 327–343.

Fearnley, C. (1977). *Early Wellington churches*. Millwood Press, Wellington, New Zealand, 224 pp.

Gentile C., Saisi A., 2007. Ambient vibration testing of historic masonry towers for structural identification and damage assessment, *Construction and Building Materials* 21: 1311–1321.

Giaretton, M., Dizhur, D., da Porto, F. and Ingham, J.M. (2013). An inventory of unreinforced load-bearing stone masonry buildings in New Zealand, *Bulletin of the New Zealand Society for Earthquake Engineering.* **47**(2): 57 -74.

Giovinazzi, S, Lagomarsino, S. (2005). Fuzzy-random approach for a seismic vulnerability model. In *Proc. ICOSSAR2005 safety and reliability of engineering systems and structures*. Rome, Italy, pp 2879–2887.

Giovinazzi, S., Lagomarsino, S., Resemini, S., (2006). Displacement capacity of ancient structures through non-linear kinematic and dynamic analyses. *Proceedings of the 5th International Conference on Structural Analysis of Historical Constructions,* New Dehli, India.

Giuffrè, A. (1988) *Restauro e sicurezza sismica. La cattedrale di S. Angelo dei Lombardi*, Palladio, nuova serie 1, 95-120. In Italian.

Gizzi, F. T., Masini, N., Sileo, M., Zotta, C., Scavone, M., Liberatore, D., Sorrentino, L., and Bruno, M., 2014. Building features and safeguard of church towers in Basilicata (Southern Italy), in *Science, Tecnology and Cultural Heritage* (M. A. Rogerio-Candelera, ed.), CRC Press, 369-374.

Goded, T., Cousins, W.J. and Fenaughty, K.F. (2014a). Analysis of the Severe-Damage Online Felt Reports for the Canterbury (New Zealand) 2011 Aftershocks on 22 February Mw 6.2, 13 June Mw 6.0, and 23 December Mw 6.0, *Seismological Research Letters* 85(3), 678-691. doi: 10.1785/0220130198.

Goded, T., Ingham, J.M., Giovinazzi, S., Lagomarsino, S., Clark, W, Cattari, S., Ottonelli, D., Marotta, A., Lourenço, P.B. and McClean, R. (2014b) *Results on most probable MMI values for Christchurch URM churches*, Report part of the EQC Project 14/660 Vulnerability analysis of unreinforced masonry churches.

González Ballesteros, J.Á., Gallardo Carrillo, J. and López Aguilera, V. (2012) Afecciones ocasionadas por el terremoto en el conjunto de panteones históricos del cementerio de San Clemente, iglesia de Santa María, iglesia de San Pedro y la Fuente del Oro de Lorca, Murcia, *Boletin Geologico y Minero* 123, 537–548. In Spanish.

Goodwin, C.P. (2009). *Architectural considerations in the seismic retrofit of unreinforced masonry heritage buildings in New Zealand*. M.Arch-Thesis, School of Architecture and Planning, The University of Auckland, New Zealand.

Grünthal, G., Musson, R.M.W., Schwartz, J. and Stucky, M. (1998) *European Macroseismic Scale 1998 (EMS-98)*, European Seismological Commission, Working Group Macroseismic Scales, Luxembourg.

Guerreiro, L., Azevedo, J., Proença, J., Bento, R. and Lopes, M. (2000) Damage in ancient churches during the 9th of July 1998 Azores earthquake, *Proc. of the 12th World Conference on Earthquake Engineering*, Auckland, New Zealand, paper 780.

Guevara, P.L.T. and Sanchez-Ramirez, A.R. (2005) Los sismos de Enero y Febrero de 2001 en El Salvador y su impacto en las iglesias del patrimonio cultural, *Boletin Tecnico, Instituto de Materiales y Modelos Estructurales* 43, 28–57. In Spanish.

Hearn, T. (2012). ”English - Religion” *Te Ara - the Encyclopedia of New Zealand*, updated 13rd July 2012. http://www.teara.govt.nz/en/english/page-11. (Accessed during December 2014).

Heritage New Zealand - Pouhere Taonga (2014). "The List - Rārangi Kōrero". http://www.heritage.org.nz/the-list. (Accessed during December 2013 and January 2014).

Housner, G. W., 1959. Behaviour of structures during earthquakes, *Journal of the Engineering Mechanics Division* **85**, 109-129.

Ingham, J.M., Lourenço, P.B., Leite, J., Castelino, S. and Colaco, E. (2012). Using simplified indices to forecast the seismic vulnerability of New Zealand unreinforced masonry churches. *Australian Earthquake Engineering Society 2012 Conference*, Gold Coast, Australia, 7-9 December 2012.

Jacobsen N.J., Andersen P., and Brincker R. 2007. Using EFDD as a Robust Technique to Deterministic Excitation in Operational Modal Analysis. *Proceedings of the 2nd International Operational Modal Analysis Conference (IOMAC)*, Copenhagen, Denmark.

Jaishi B., Ren W., Zong Z., and Maskey P.N., 2003. Dynamic and seismic performance of old multi-tiered temples in Nepal, *Engineering Structures* 25, 1827–1839.

Johnston, D., Standring, S., Ronan, K., Lindell, M., Wilson, T., Cousins, J., Aldridge, E., Ardagh, M.W., Deely, J.M., Jensen, S., Kirsch, T. and Bissell R. (2014). The 2010/2011 Canterbury earthquakes: context and cause of injury. *Natural Hazards*, **73**: 627–637.

Kappos, A. J., Panagopoulos, G., and Penelis, G. G., 2008. Development of a seismic damage and loss scenario for contemporary and historical buildings in Thessaloniki, Greece, *Soil Dynamics and Earthquake Engineering* **28**, 836-850.

Karatzetzou A., Negulescu C., Manakou M., François B., Seyedi D.M., Pitilakis D., Pitilakis K., 2015. Ambient vibration measurements on monuments in the Medieval City of Rhodes, Greece, *Bulletin of Earthquake Engineering*, 13:331–345

Kidd, J.H. (1991). *Some historic churches of Auckland*. The Club, Auckland, New Zealand, 15 pp.

Kircher, C.A., Nassar, A.A., Kustu, O. and Holmes, W.T. (1997) Development of Building Damage Functions for Earthquake Loss Estimation, *Earthquake Spectra* 13(4), 663-682. doi: 10.1193/1.1585974.

Knight, C.R. (1972). *The Selwyn churches of Auckland*. A.H. & A.W. Reed, Wellington, New Zealand, 85 pp.

Knight, H. (1993). *Church building in Otago*. The University of Otago Printing Department, Dunedin, New Zealand, 345 pp.

Kramer, S. L., 1996. *Geothecnical earthquake engineering*, Prentice Hall, Upper Saddle River, NJ, 653 pp.

Lagomarsino, S. (1998) A new methodology for the post-earthquake investigation of ancient churches, *Proc. of the 11th European Conference on Earthquake Engineering*, Paris, France, paper LAGNMF.

Lagomarsino, S. and Podestà, S. (2004a) Damage and vulnerability assessment of churches after the 2002 Molise, Italy, earthquake, *Earthquake Spectra* 20(S1), 271–283. doi: 10.1193/1.1767161.

Lagomarsino, S. and Podestà, S. (2004b) Seismic vulnerability of ancient churches: II. Statistical Analysis of Surveyed Data and Methods for Risk Analysis, *Earthquake Spectra* 20(2), 395-412. doi: 10.1193/1.1737736.

Lagomarsino, S., Podestà, S., Cifani, G. and Lemme, A. (2004) The 31st October 2002 earthquake in Molise (Italy): a new Methodology for the damage and seismic vulnerability survey of churches, *Proc. of the 13th World Conference on Earthquake Engineering*, Vancouver, B.C., Canada, paper 1366.

Lagomarsino, S. (2006) On the vulnerability assessment of monumental buildings, *Bulletin of Earthquake Engineering* 4, 445-463. doi: 10.1007/s10518-006-9025-y.

Lagomarsino, S. (2012) Damage assessment of churches after L'Aquila earthquake (2009), *Bulletin of Earthquake Engineering* 10, 73–92. doi: 10.1007/s10518-011-9307-x.

Lallemant, D., and Kiremidjian, A. (2015) A Beta Distribution Model for Characterizing Earthquake Damage State Distribution, *Earthquake Spectra* 31, 1337-1352.

Lang, K. (2002) *Seismic vulnerability of existing buildings*, Institute of Structural Engineering (IBK), ETH Zurich, Report No. 273, vdf Hochschulverlag, Zurich.

Leite, J., Lourenço, P.B. and Ingham, J.M. (2013) Statistical assessment of damage to churches affected by the 2010–2011 Canterbury (New Zealand) earthquake sequence, *Journal of Earthquake Engineering* 17(1), 73-97. doi: 10.1080/13632469.2012.713562.

Lester, J.R., Brown, A.G. and Ingham, J.M. (2013) Stabilisation of the Cathedral of the Blessed Sacrament following the Canterbury earthquakes, *Engineering Failure Analysis*, 34, 648-669. doi: 10.1016/j.engfailanal.2013.01.041.

Liberatore, D., Spera, G. and Pacifico, S. (2006) Damage probability matrices of the architectural heritage of Basilicata (Italy), *Proc. of the 1st European Conference on Earthquake Engineering and seismology*, Geneva, Switzerland, paper 1550.

Liberatore, D., Martino, D. and D'Orsi, L. (2009) Valutazione della vulnerabilità e stima del danno atteso di edifici ecclesiastici della Basilicata, *XIII Convegno dell'Associazione Nazionale Italiana di Ingegneria Sismica (ANIDIS) L'Ingegneria Sismica in Italia*, Bologna, ref. S14.19. In Italian.

Liberatore, D., Masini, N., Sorrentino, L., Racina, V., Sileo, M., AlShawa, O., Frezza, L., 2016. Static penetration test for historical masonry mortar, *Construction and Building Materials*, in press. DOI:10.1016/j.conbuildmat.2016.07.097.

Lourenço, P.B., Oliveira, D.V., Leite, J.C., Ingham, J.M., Modena, C. and da Porto, F. (2013) Simplified indexes for the seismic assessment of masonry buildings: International database and validation, *Engineering Failure Analysis* 34, 585-605. doi: 10.1016/j.engfailanal.2013.02.014.

Marotta, A., Goded, T., Giovinazzi, S., Lagomarsino, S., Liberatore, D., Sorrentino, L., and Ingham, J. M., 2015. An inventory of unreinforced masonry churches in New Zealand, *Bulletin of the New Zealand Society for Earthquake Engineering* **48**, 170-189.

Marotta, A., Sorrentino, L., Liberatore, D., and Ingham J. M., 2016a. Vulnerability assessment of unreinforced masonry churches following the 2010-2011 Canterbury earthquake sequence, *Journal of Earthquake Engineering*. DOI:10.1080/13632469.2016.1206761.

Marotta, A., Sorrentino, L., Liberatore, D., and Ingham, J. M., 2016b. Statistical seismic vulnerability of New Zealand unreinforced masonry churches, in *Proceedings of the 10th International Conference on Structural Analysis of Historical Constructions*, 13-15 September, 2016, Leuven, Belgium, 1536 - 1543.

Marotta, A., Sorrentino, L., Liberatore, D., and Ingham, J.M., 2017. Seismic risk assessment of New Zealand unreinforced masonry churches through statistical procedures, *International Journal of Architectural Heritage.* Accepted.

Marulanda, M. C., Carreño, M. L., Cardona, O. D., Ordaz, M. G., and Barbat, A. H., 2013. Probabilistic earthquake risk assessment using CAPRA: application to the city of Barcelona, Spain, *Natural Hazards* **69**, 59–84.

Masi, A., Chiauzzi, L., Braga, F., Mucciarelli, M., Vona, M., and Ditommaso, R., 2011. Peak and integral seismic parameters of L'Aquila 2009 ground motions: observed versus code provision values, *Bulletin of Earthquake Engineering* **9**, 139–156.

McSaveney, E. (2012). "Historic earthquakes - The 1929 Arthur's Pass and Murchison earthquakes", *Te Ara - the Encyclopedia of New Zealand*, updated 13rd July 2012. http://www.TeAra.govt.nz/en/historic-earthquakes/page-5. (Accessed during December 2014).

McVerry, G.H., Gerstenberger, M.C., Rhoades, D.A. and Stirling, M.W. (2012). Spectra and Pgas for the Assessment and Reconstruction of Christchurch. *New Zealand Society for Earthquake Engineering Conference,* Paper No 115.

Montilla, P.J., Uzcategui, A.I. and Hernandez, S.M. (1996) Damages occurred to churches due to the earthquake of February 8, 1995 in Pereira, Colombia, *Proc. of the 11th World Conference on Earthquake Engineering*, Acapulco, Mexico, paper 963.

Moon, L., Dizhur, D., Senaldi, I., Derakhshan, H., Griffith, M., Magenes, G. and Ingham, J.M. (2014) The demise of the URM building stock in Christchurch during the 2010/2011 Canterbury earthquake sequence, *Earthquake Spectra*, 30(1), 253-276. doi: 10.1193/022113EQS044M.

Mouyiannou, A., Penna, A., Rota, M., Graziotti, F., Magenes, G., 2014. Implications of cumulated seismic damage on the seismic performance of unreinforced masonry buildings, *Bulletin of the New Zealand Society for Earthquake Engineering* **47**, 157-170.

Nathan, S. and Hayward, B. (2012). "Building stone - Stone buildings in New Zealand". *Te Ara - the Encyclopedia of New Zealand*, updated 13rd July 2012. http://www.TeAra.govt.nz/en/building-stone/page-1. (Accessed during December 2014).

New Zealand Standards Institute - NZSI (1965). "*NZSS 1900:1965. New Zealand Standard Model Building By-Law*". New Zealand Standards Institute, Wellington, New Zealand.

NZS 1170.5 (2004). "*Structural design actions - Part 5: Earthquake actions*". New Zealand Commentary. Wellington, New Zealand.

New Zealand Society for Earthquake Engineering Guidelines - NZSEEG (2013). "*Assessment and Improvement of the Structural Performance of Buildings in Earthquakes - Section 3 revision: Initial seismic assessment*". Wellington, New Zealand.

Nohutcu H., Demir A., Ercan A., Hokelekli E., and Altintas G., 2015. Investigation of a historic masonry structure by numerical and operational modal analyses, *The structural design of tall and special buildings*, 24:821–834.

Orwin, J. (2012). "Kauri forest - How and where kauri grows", *Te Ara - the Encyclopedia of New Zealand*, updated 13rd July 2012, http://www.teara.govt.nz/en/kauri-forest/page-1. (Accessed during February 2015).

Osmancikli G., Uçak S., Turan F.N., Türker T., and Bayraktar A., 2012. Investigation of restoration effects on the dynamic characteristics of the Hagia Sophia bell-tower by ambient vibration test, *Construction and Building Materials* 29: 564–572.

Pastor M., Binda M., Hararik T., 2012. Modal Assurance Criterion, *Procedia Engineering* 48: 543 – 548.

Perrin, N. D., Heron, D., Kaiser, A., and Van Houtte, C., 2015. VS30 and NZS 1170.5 site class maps of New Zealand, Paper No. O-07, in *Proceedings, New Zealand Society for Earthquake Engineering (NZSEE) Annual Technical Conference*, 10-12 April, 2015, Rotorua, New Zealand.

PCM-DPC MiBAC (Presidenza Consiglio dei Ministri—Dipartimento della Protezione Civile Ministero Beni e Attività Culturali) (2006) "Model A-DC Scheda per il rilievo del danno ai beni culturali—Chiese," http://www.protezionecivile.gov.it/resources/cms/documents/MOD_SCHEDA_DANNO_CHIESE_2006.pdf. In Italian.

Ragone, A., Ippolito, A., Liberatore, D., and Sorrentino, L., 2016. Emerging Technologies for the Seismic Assessment of Historical Churches: The Case of the Bell Tower of the Cathedral of Matera, Southern Italy, in *Handbook of Research on Emerging Technologies for Architectural and Archaeological Heritage* (A. Ippolito, ed.), IGI Global, Hershey, Pennsylvania, 163-200. DOI: http://doi.org/10.4018/978-1-5225-0675-1.ch006.

Rainieri, C., and Fabbrocino, G., 2011. Operational modal analysis for the characterization of heritage structures, *Geofizica*, 28: 109-126.

Ramos L.F., Aguilar R., Lourenco P.B., Moreira S., 2013. Dynamic structural health monitoring of Saint Torcato Church, *Mechanical Systems and Signal Processing* 35: 1–15.

Reitherman, R. (2006). Earthquakes that have initiated the development of earthquake engineering. *Bulletin of the New Zealand Society for Earthquake Engineering*, **39**(3): 145-157.

Dowrick, D.J. (1998). Damage and intensities in the magnitude 7.8 1931 Hawke's Bay, New Zealand earthquake. *Bulletin of the New Zealand National Society for Earthquake Engineering*, **31**(3): 139-163.

Rivera De Uzcàtegui, A.I. and Torres B.R.A. (1997) Estudio de danos originados a las iglesias de la ciudad de Merida por la accion de los terremotos de 1812 y 1894, *Boletin Tecnico, Instituto de Materiales y Modelos Estructurales* 35, 10–21. In Spanish.

Rota, M., Penna, A., Strobbia, C., and Magenes G., 2011. Typological seismic risk maps for Italy, *Earthquake Spectra* 27, 907-916.

Russell, A. P., and Ingham, J. M., 2010. Prevalence of New Zealand's unreinforced masonry buildings, *Bulletin of the New Zealand Society for Earthquake Engineering* 43, 182-201.

Sabetta, F., Goretti, A. and Lucantoni, A. (1998) Empirical Fragility Curves from Damage Surveys and Estimated Strong Ground Motion, *Proc. of the 11th European Conference on Earthquake Engineering*, Paris, France.

Schrader, B. (2013). "Housing - Construction and materials", *Te Ara - the Encyclopedia of New Zealand*, updated 8th July 2013. http://www.teara.govt.nz/en/housing/page-5. (Accessed during February 2015).

Sedcole, A.J. and Crookes, S.I. (1930). *Early New Zealand ecclesiastical architecture*. Auckland University College, School of Architecture, Auckland, New Zealand, 17 pp.

Senaldi, I., Magenes, G. and Ingham, J.M. (2014) Damage assessment of unreinforced stone masonry buildings after the 2010-2011 Canterbury earthquakes, *International Journal of Architectural Heritage Conservation, Analysis, and Restoration*, 9(5), 605-627. doi: 10.1080/15583058.2013.840688.

Siddique, M. S., and Schwarz, J., 2015. Elaboration of multi-hazard zoning and qualitative risk maps of Pakistan, *Earthquake Spectra* 31(3), 1371–1395.

Singhal, A. and Kiremidjian, A.S. (1996) Method for probabilistic evaluation of seismic structural damage, *Journal of Structural Engineering* 122(12), 1459-1467. doi: 10.1061/(ASCE)0733-9445(1996)122:12(1459).

Sofronie, R. (1982) Behaviour of eastern churches in earthquakes, *Proc. of the 7th European Conference on Earthquake Engineering*, Vol. 3, Athens, Greece, pp. 287–294.

Sorrentino, L., Bruccoleri, D. and Antonini, M. (2008). Structural interpretation of post-earthquake (19th century) retrofitting on the Santa Maria degli Angeli Basilica, Assisi, Italy. *6th International Conference on Structural Analysis of Historic Construction*, Bath, UK, 2-4 July 2008, 217-225.

Sorrentino, L., Liberatore, D., Penna, A., Magenes, G., Decanini, L.D., Liberatore, L., 2011. Vulnerabilità delle chiese colpite dal sisma del Cile del 2010, *XIV Convegno dell'Associazione Nazionale Italiana di Ingegneria Sismica (ANIDIS) L'Ingegneria Sismica in Italia*, Bari. In Italian.

Sorrentino, L. (2014). Reconstruction plans after the 2009 L'Aquila earthquake. From building performance to historical centre performance. *9th International Conference on Structural Analysis of Historical Constructions*, Mexico City, Mexico, 14–17 October 2015, Paper No 11-006.

Sorrentino, L., Alshawa, O. and Liberatore, D. (2014a) Observations of out-of-plane rocking in the Oratory of San Giuseppe dei Minimi during the 2009 L'Aquila earthquake, *Applied Mechanics and Materials* 621, 101-106. doi: 10.4028/www.scientific.net/AMM.621.101.

Sorrentino, L., Liberatore, L., Decanini, L.D. and Liberatore, D. (2014b). The performance of churches in the 2012 Emilia earthquakes. *Bulletin of Earthquake Engineering*. 12(5): 2299–2331.

Sorrentino, L., Liberatore, L., Liberatore, D. and Masiani, R. (2014c) The behaviour of vernacular buildings in the 2012 Emilia earthquakes, *Bulletin of Earthquake Engineering* 12(5), 2367-2382. doi: 10.1007/s10518-013-9455-2.

Stafford P.J.,·Berrill J.B., Pettinga J.R. 2009. New predictive equations for Arias intensity from crustal earthquakes in New Zealand. *J Seismol* (2009) 13:31–52.

Statistics New Zealand, Tatauranga Aotearoa - STATS (2013). *Digitised copies of Census of Population and Dwellings reports and results, from 1871 to 1911*. Published 21th August 2013. http://www.stats.govt.nz/browse_for_stats/snapshots-of-nz/digitised-collections/census-collection.aspx. (Accessed during February 2015).

Stirling, M.W., McVerry, G.H., Gerstenberger, M.C., Litchfield, N.J., Van Dissen, R.J., Berryman, K.R., Barnes, P., Wallace, L.M., Villamor, P., Langridge, R.M., Lamarche, G., Nodder, S., Reyners, M.E., Bradley, B., Rhoades, D.A., Smith, W.D., Nicol, A., Pettinga, J., Clark, K.J. and Jacobs, K. (2012). National seismic hazard model for New Zealand: 2010 update. *Bulletin of the Seismological Society of America*, **102**(4): 1514-1542.

Stiros, S., Papageorgiou, S., Kontogianni, V. and Psimoulis, P. (2006) Church repair swarms and earthquakes in Rhodes Island, Greece, *Journal of Seismology* 10, 527–537. doi: 10.1007/s10950-006-9035-x.

Study Group of the NZSEE (1992) A revision of the Modified Mercalli seismic intensity scale, *New Zealand National Society for Earthquake Engineering* 25(4), 345-357.

Tashkov L., Krstevska L., Naumovski N., De Matteis G., Brando G., 2010. Ambient vibration tests on three religious buildings in Goriano Sicoli damaged during the 2009 L'Aquila earthquake. *COST ACTION C26: Urban Habitat Constructions under Catastrophic Events. In: Proceedings of the final conference*, pp 433–438.

Toma-Danila, D., Zulfikar, C., Manea, E. F., and Cioflan, C. O., 2015. Improved seismic risk estimation for Bucharest, based on multiple hazard scenarios and analytical methods, *Soil Dynamics and Earthquake Engineering* **73**, 1–16.

Tonks, G. and Chapman, J. (2009). Earthquake performance of historic timber buildings in New Zealand. *New Zealand timber design journal.* **17**(3): 3-9.

Travasarou T, Bray JD, Abrahamson NA (2003) Empirical attenuation relationship for Arias intensity. *Earthq Eng Struct Dyn* 32(7):1133–1155.

Vicente, R., Parodi, S., Lagomarsino, S., Varum, H. and Silva J.A.R.M. (2011) Seismic vulnerability and risk assessment: Case study of the historic city centre of Coimbra, Portugal, *Bulletin of Earthquake Engineering* 9(4), 1067-1096. doi: 10.1007/s10518-010-9233-3.

Vicente, R., Ferreira, T., and Maio, R., 2014. Seismic risk at the urban scale: assessment, mapping and planning, in *Proceedings, 4th International Conference on Building Resilience, Building Resilience*, 8-10 September, 2014, Salford Quays, United kingdom.

Votsis R.A., Kyriakides N., Chrysostomou C.Z., Tantele E., and Demetriou T., 2012. Ambient vibration testing of two masonry monuments in Cyprus, *Soil Dynamics and Earthquake Engineering*, 43: 58–68.

Walden, H.R. (1961). *A Study of Church Architecture*. Thesis for the degree of Bachelor of Architecture, University of New Zealand.

Walden, H.R. (1964). *New Zealand Anglican church architecture, 1814-1963*. Thesis for the degree of Master of Architecture, University of Auckland.

Warren, D. (1957). *Some Canterbury churches*. The Pegasus Press, Christchurch, New Zealand, 48 pp.

Wells, R. and Ward, T. (1987). *In a country churchyard*. The Caxton Press, Christchurch, New Zealand, 108 pp.

Wells, A. (2003). *Nelson historic country churches*. Nikau Press, Nelson, New Zealand, 176 pp.

Whitman, R.V., Reed, J.W. and Hong, S.T. (1973). Earthquake damage probability matrices, *Proc. of the 5th World Conference on Earthquake Engineering*, Vol. 2, Rome, Italy, pp. 2531-2540.

Yeomans, D.T. (1992). *The trussed roof: its history and development*. Scolar Press, Aldershot, England, 221 pp.